FACULTEIT WETENSCHAPPEN

THE IMPACT OF LAND COVER ON THE URBAN HEAT ISLAND AND ITS SIMULATION

A CASE STUDY USING THE MOCCA NETWORK IN GHENT

Aantal woorden: 32 389
Figuren: 44
Kaarten: 5
Tabellen: 36
Annexen: 9

Sara Top
Stamnummer: 01300578

Promotor: Prof. dr. Piet Termonia
Begeleiders: Dr. Steven Caluwaerts en Dr. Rafiq Hamdi

Masterproef voorgelegd voor het behalen van de graad master in de richting Geografie

Academiejaar: 2017 - 2018

UNIVERSITEIT GENT

ACKNOWLEDGEMENT

As this work was not possible without the help of many people, I would like to thank the people who made this work possible. Starting with my supervisors Dr. Steven Caluwaerts and Dr. Rafiq Hamdi, who taught me a lot about the subject and helped me with the content related questions throughout the writing of this thesis. Thanks to my promotor Prof. Piet Termonia for giving me new opportunities with this thesis. I would like to thank my well English speaking friends for correcting my grammar and spelling mistakes. I would like to thank Alexander Vanhulle for helping me out with programming related issues. Special thanks goes to my family who supported me throughout my whole life and told me to never give up on my dreams. Thanks to my friends for taking some time off with me, for never get bored of my talk about the urban heat island and for the interesting discussions we had. Even when I didn't had time for them because I was too busy, they were there for me. I would like to thank family members and friends for their understanding when I could not spend time with them as I needed to finish this thesis.

The moment I decided to start studying Geography I would not have believed that it would one day result in a thesis like this one, but a friend shared me the following quote:

"Most people overestimate what they can do in one year and underestimate what they can do in ten years" (Bill Gates).

This quote could not have been more accurate as if you want to realise a dream some patience is needed and I can finally say that the patience paid off. While this is the end of a year-and-a-half of research for me it is just a beginning, with further research of climate related subjects expected. Throughout my life I have learned to be careful with words like always and never, but I am sure that choosing the Geography studies subject and writing this thesis are two things I will never regret. Weather and climate intrigue me and by choosing the urban heat island subject I wanted to create more awareness for climate problems that are more prevalent than we may think. That said, the climate related subject was not an obvious choice to make as it was not on the thesis proposal list. Therefore, I want to thank once more Dr. Steven Caluwaerts for helping me define the subject and I want to thank the Geography department for their open-mindedness towards the subject I proposed.

It is my hope that my work can be appreciated and that you can learn from reading this thesis. Finally, I wish that it may be a pleasure to read.

ABSTRACT IN LAYMAN'S TERMS

You may already have noticed that the city is warmer than the surrounding rural area on a warm day with clear sky conditions. This phenomenon is called the urban heat island. Different parameters such as artificial construction materials, building height, narrow streets in between buildings and fewer green and water surfaces cause that the city is unable to keep the temperatures as low as nearby rural environments. This thesis investigates which parameter is dominant in the simulation of the urban heat island in Ghent. Is the implementation of accurate land cover in the model more important than the application of the city geometry? The influence of the use of different land cover databases on the model results of the urban heat island is also examined. Additionally, this thesis investigates which area around the station is most responsible for explaining the magnitude of the observed urban heat island.

POPULARISERENDE TEKST

U hebt het waarschijnlijk ook al ondervonden, tijdens een warme heldere dag voelt een stedelijke omgeving warmer aan dan het platteland. Dit fenomeen waarbij de temperatuur hoger oploopt in de stad dan op het platteland, wordt het stedelijk hitte-eiland genoemd. Verschillende factoren zoals artificiële bouwmaterialen, de gebouwhoogte, de smalle ruimten tussen gebouwen en minder aanwezigheid van groen en water zorgen ervoor dat de warmte sterker blijft hangen in de stad. In deze thesis wordt onderzocht welke factor nu eigenlijk het belangrijkst is voor het voorspellen van een stedelijk hitte-eiland in Gent. Is het belangrijker om accurate informatie van bodembedekking te implementeren in het model of is de bouwstijl belangrijker? Daarnaast wordt nagegaan welke invloed verschillende databases met bodembedekking hebben op de modelleerresultaten van het stedelijk hitte-eiland. Tevens wordt onderzocht welk gebied rondom het meetstation in acht moet worden genomen om het geobserveerde hitte-eiland te verklaren.

ABSTRACT

Many people already experienced the annoyance of not being able to sleep due to the prevailing heat. This is due to the phenomenon called heat stress and has negative effects on our health. Heat stress is more frequently observed in cities than at the countryside due to the effect of the urban heat island (UHI) and this is an increasingly-common phenomenon, as urbanisation continues. Therefore, UHI studies gain more and more importance these days. The quality of living in cities can be maintained or improved by using the knowledge of the UHI phenomenon and the mitigation strategies.

The UHI is caused by the fact that urban areas retain more heat than their surrounding rural environments. Different parameters such as artificial construction materials, building height, narrow streets in between buildings and fewer green and water surfaces are presumed to be the cause of the UHI. Observational MOCCA data and SURFEX model simulations for the summer of 2016 were used in order to investigate the UHI of Ghent. It was found that UHI simulations are more sensitive to the land cover changes compared to adaptations in the city geometry parameters building height and building fraction. Therefore, it is important to implement accurate land cover data for the modelling of the UHI. Another finding in this study was that the land cover of the ECOCLIMAP-II database is closer to reality than the ECOCLIMAP-I land cover data. However, it must be noted that the land cover for one out of six locations was poorly estimated with ECOCLIMAP-II, leading towards worse model results for the UHI. Higher resolution land cover data results in better model performance of the UHI, but this improvement is due to errors that are compensated when the rural temperatures are subtracted from the urban temperatures. The temperatures are not better simulated with higher resolution land cover data and this is probably due to the poor model tuning or to the input of poor forcings at 4 km resolution. Additionally, this study revealed that it is important to take into account the right size of the area that influences the UHI to study and model the UHI. For the six measurement locations in Ghent, the micro-environment is important to understand the observed temperatures during daytime and the local environment of about 1 km² is more important during nighttime. Finally, the model could not be optimised sufficiently by implementing a more accurate land cover, building fraction and building height. Therefore, further investigation to improve the model results is needed.

NEDERLANDSTALIGE SAMENVATTING

Heel wat mensen ergerden zich reeds aan het feit dat ze de slaap niet kunnen vatten door de aanhoudende warmte, dit fenomeen heet hittestress. Hittestress wordt vaker geobserveerd in steden dan op het platteland door de aanwezigheid van het stedelijk hitte-eiland. Dit is een steeds vaker voorkomend fenomeen doordat het urbanisatieproces blijft doorgaan. Daarom gaat er op vandaag meer en meer aandacht uit naar stedelijke hitte-eiland studies. De levenskwaliteit in steden kan worden behouden of zelfs verbeterd door gebruik te maken van de kennis die we hebben omtrent het stedelijke hitte-eiland fenomeen en de mitigatie ervan.

Het stedelijk hitte-eiland wordt veroorzaakt door het feit dat stedelijke gebieden warmte langer vasthouden dan hun omgevende rurale gebieden. Verschillende parameters zoals artificiële bouwmaterialen, de hoogte van gebouwen, de smalle ruimten tussen gebouwen en minder aanwezigheid van groen en water worden beschouwd als mogelijke factoren die ervoor zorgen dat de warmte sterker blijft hangen in de stad. Temperatuurmetingen van het MOCCA netwerk en simulaties met het model SURFEX voor de zomer van 2016 werden gebruikt om het stedelijk hitte-eiland in Gent te bestuderen. Uit deze studie volgt dat stedelijke hitte-eiland simulaties gevoeliger zijn aan wijzigingen in de bodembedekking dan veranderingen in de gebouwhoogte of de proportie aan bebouwde oppervlakte. Het is daarom zeer belangrijk om accurate bodembedekkingsgegevens te gebruiken voor de modellering van het stedelijk hitte-eiland. Daarnaast werd vastgesteld dat de bodembedekkingsdata van de ECOCLIMAP-II database sterker aanleunt bij de realiteit dan de ECOCLIMAP-I data. Er moet echter worden opgemerkt dat bodembedekking voor een van de zes locaties volledig verkeerd wordt weergegeven door ECOCLIMAP-II, wat leidt tot een slechtere simulatie van het stedelijk hitte-eiland. Bodembedekkingsgegevens met een hogere resolutie resulteren in een betere modellering van het stedelijk hitte-eiland, maar deze verbetering is te wijten aan afwijkingen in temperaturen van het stedelijke en rurale station die elkaar deels opheffen wanneer de rurale temperaturen worden afgetrokken van de stedelijke. De temperaturen worden niet beter gesimuleerd wanneer hogere resolutie data wordt geïmplementeerd in het model en dit is waarschijnlijk te wijten aan de povere afstemming van het SURFEX model aan de omstandigheden op de rurale locatie of aan de input parameters van de grovere 4 km resolutie die worden meegegeven aan het SURFEX model. Bijkomend werd gevonden dat het belangrijk is om rekening te houden met de grootte van het gebied rondom het meetstation dat het stedelijk hitte-eiland beïnvloed om dit verder te gebruiken voor de modellering. Voor de zes meetlocaties in Gent werd gedetecteerd dat de nabije omgeving met een bufferafstand van 10 m tot 100 m belangrijk is om de geobserveerde temperaturen overdag te begrijpen en dat de lokale omgeving van een 565 m buffer belangrijk is om het stedelijk hitte-eiland tijdens de nacht te verklaren. Uiteindelijk kon het model niet voldoende worden geoptimaliseerd door enkel de accurate bodembedekking, proportie bebouwing en gebouwhoogte te implementeren. Er is dus nog meer onderzoek nodig om de modelleerresultaten van het stedelijk hitte-eiland te verbeteren.

TABLE OF CONTENTS

LIST OF ABBREVIATIONS

ALADIN	*Aire Limitée Adaptation Dynamique Développement INterternational*
ALARO	ALadin-AROme
ARPERGE-IFS	*Action de Recherche Petite Echelle Grande Echelle* Integrated Forecast System
BBK	*Bodembedekkingskaart*
CNRM	National Centre for Meteorological Research
DEM	digital elevation model
FAO	Food and Agriculture Organization of the United Nations
GIS	geographical information system
GRB	*Grootschalig Referentie Bestand*
ISBA	Interaction Soil Biosphere Atmosphere
IV	*Informatie Vlaanderen*
LSM	land surface model
Meso-NH	mesoscale non-hydrostatic model
MOCCA	MOnitoring the City's Climate and Atmosphere
NWP	numerical weather prediction
OSM	OpenStreetMap
RMI	Royal Meteorological Institute of Belgium
RMSE	root mean square error
SURFEX	*SURFace EXternalisée*
SVF	sky view factor
SWI	soil water index
TEB	town energy balance
UBL	urban boundary layer
UCL	urban canopy layer
UHI	urban heat island
USGS	United States Geological Survey
VITO	*Vlaamse Instelling voor Technologisch Onderzoek*

LIST OF FIGURES

LIST OF MAPS

LIST OF TABLES

1. INTRODUCTION

Not being able to fall asleep because of the prevailing heat, many people already experienced this annoyance. This is due to the phenomenon called heat stress and has negative effects on our health (Patz *et al*., 2005; Fischer *et al*., 2012). People suffer from heat stress especially during heat waves and sometimes it might even lead to death (Patz *et al*., 2005). Heat stress is more frequently observed in cities than at the countryside due to the effect of the urban heat island (UHI) (Oke, 1973; Steeneveld *et al*., 2011; Fischer *et al*., 2012). This is caused by the fact urban areas retain more heat than their surrounding rural environments (Arnfield, 2003; EPC, 2008; Stewart, 2011; Best & Grimmond, 2015; Bassett *et al*., 2016). Moreover, a growing number of people over the world live together in expanding cities (Arnfield, 2003; UN-Habitat, 2010). Because of this changing pattern in habitation, natural phenomena have been influenced. Visually, urban areas can be distinguished by the many buildings and artificial surfaces whereas rural areas are shaped by open ground, water and vegetation (Van Hove *et al.*, 2014). In particular, these human changes affect the local climate by influencing the temperature, wind patterns, turbulence and moisture in and near cities (Van Hove *et al.*, 2014; Hamdi *et al*., 2015). This explains the rise of urban climate studies (Arnfield, 2003). These studies on urban climate become more and more important since urbanisation is still going on, leading recently to the fact that the majority of the world population is living in cities (Best & Grimmond, 2015; Hamdi *et al*., 2015).

1.1 Urban heat island (UHI)

One of the affected weather aspects due to the increasing urbanisation is temperature. Urban areas are substantially warmer than their surrounding rural environments (Arnfield, 2003; EPC, 2008; Stewart, 2011; Best & Grimmond, 2015; Bassett *et al*., 2016). This phenomenon is called UHI and UHI intensity is measured as “the difference in temperature between urban areas and rural surroundings” (Van Hove *et al.*, 2014). The intensity of the UHI varies during the diurnal cycle and during the year, as will be discussed further on.

1.1.1 Types of UHI

The broad term UHI includes two types: surface UHI and atmospheric UHI (EPC, 2008). As it is in the name, the first one implies the difference in temperature of the surface or soil between the urban and the rural area and the second one indicates the difference in air temperature (Van Hove *et al.*, 2014). As shown in figure 1, atmospheric temperatures vary less than surface temperatures (EPC, 2008). This is because the thermal diffusivity of air is smaller than the thermal diffusivity of the surface. Consequently, “atmospheric heat islands vary much less in intensity than surface heat islands” (EPC, 2008).

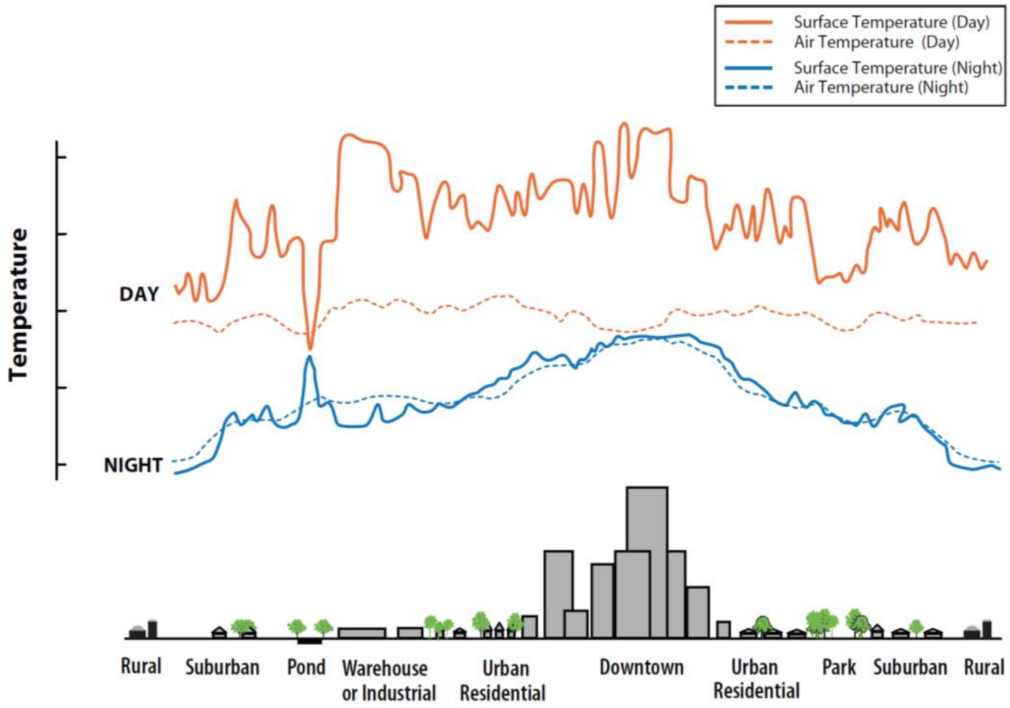

Figure 1: UHI profile variations of surface and atmospheric temperatures above different land covers (Sources: EPC, 2008; adapted from Voogt, 2000).

The atmospheric UHI can be further subdivided since there are different spatial scales at which the interaction between the city and the atmosphere takes place (Caluwaerts *et al*., 2018). There is namely a UHI effect possible at the scale of the urban boundary layer (UBL) and urban canopy layer (UCL) (EPC, 2008; Van Hove *et al.*, 2014). As shown in figure 2, the UBL starts just above the level of rooftops and treetops and goes up until the height where the urban region does no longer affect the atmosphere (EPC, 2008). The UBL has typically a varying vertical scale from a few 100 meters at night up to 1500 m during the day. This is because heat is not dispersed vertically as far from the rooftop level at night as during daytime (EPC, 2008; Bassett *et al*., 2016). For the UBL, the UHI is situated at mesoscale or neighbourhood- to city-scale, while the UHI of the UCL is found at local scale or micro- to neighbourhood-scale (Oke, 1987; Shepherd, 2005; Bassett *et al*., 2016). The UCL can be defined as the layer of air from the ground to the average building roof level (see figure 2) (EPC, 2008; Bassett *et al*., 2016). Because this layer affects the lives of people directly, the canopy layer UHI is the most frequently studied (EPC, 2008; Van Hove *et al.*, 2014). For this reason, the more general term UHI is often used to refer to canopy layer UHI, as will be done in this thesis (EPC, 2008).

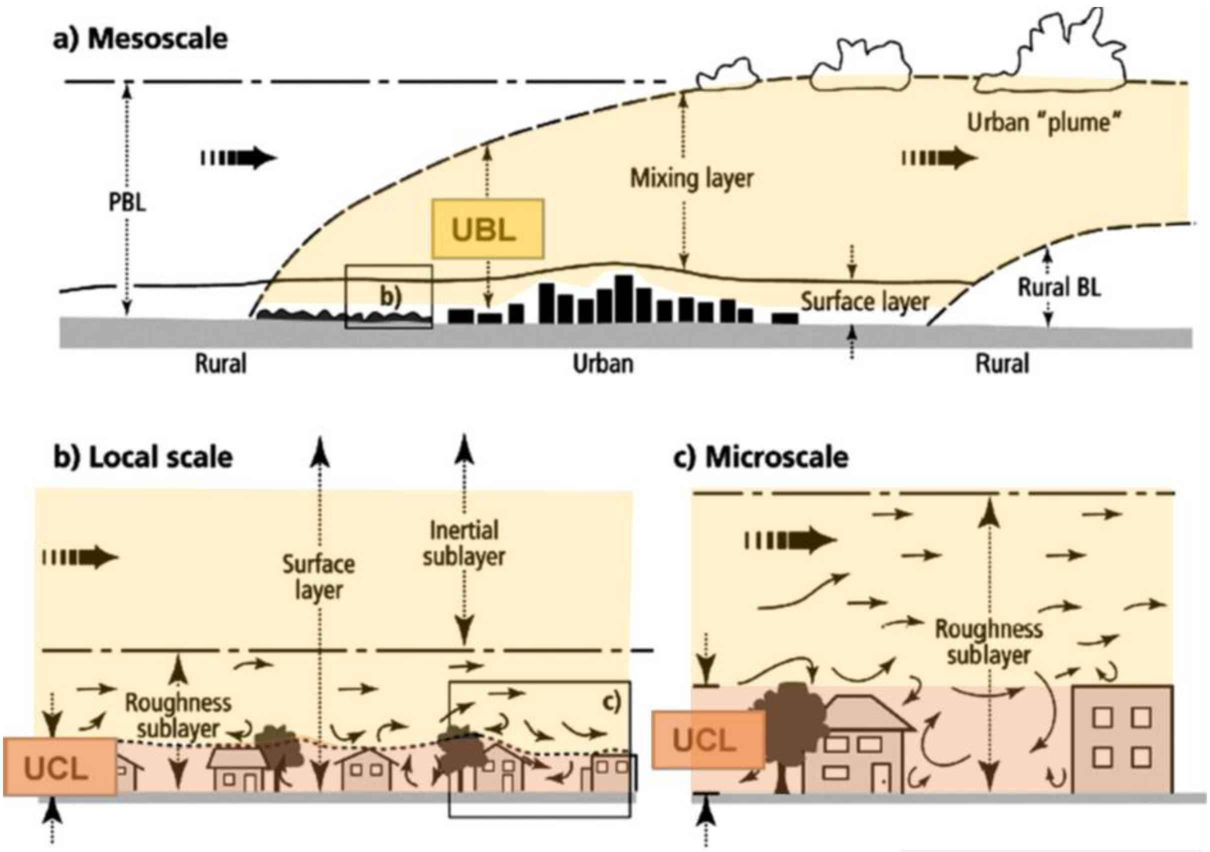

Figure 2: Various scales linking urban environments to the environmental system (Sources: adapted from Shepherd, 2005; Oke, 1987). Yellow indicates the urban boundary layer (UBL) and orange denotes the urban canopy layer (UCL).

1.1.2 Why do UHIs exist?

As it is shown in figure 1, the uneven heating of the different land cover types within a city induces differences in air temperature, especially in the UCL (EPC, 2008). This causes spatial variations in UHI intensity and is known as the intra-urban variability of the UHI (Van Hove *et al.*, 2014). A city can be divided in local climate zones based on different environmental characteristics, as can be seen in figure 1 (Bassett *et al*., 2016). In an urban area the largest UHI intensities are generally found in the downtown area. Van Hove *et al.* (2014) concluded in their case study of the city Rotterdam that local features have an important effect on intra-urban variability of UHI intensity. Factors influencing the UHI intensity significantly are related to two-dimensional plan area characteristics of the site and to the mean building height (Van Hove *et al.*, 2014). The two-dimensional plan area characteristics are determined by the fractions of built area, impervious surfaces, water bodies and green surfaces (Best & Grimmond, 2015).

An increase of dense built-up areas results into higher surface and air temperatures because of a change in the surface energy balance (EPC, 2008; Van Hove *et al.*, 2014). Thus, the reason why an UHI develops in an urban area is because of the fact that urban and rural landscapes differ in their surface energy exchanges (Best & Grimmond, 2015). This involves that UHIs are regulated by the city form and the anthropogenic modifications to the surface energy balance (Oke, 1973; Oke, 1982; Bassett *et al*., 2016). The surface energy balance in a city is altered by artificial construction materials, urban geometry and anthropogenic heat (Van Hove *et al.*, 2014). Each of the previous variables has an influence on the UHI intensity but it is difficult to identify their relative contributions to the UHI from observations (Best & Grimmond, 2015). Therefore a better understanding of the modified surface energy fluxes is needed to clarify the occurrence of UHIs (Best & Grimmond, 2015).

1.1.2.1 Artificial construction materials

The difference in land cover between the urban and rural area is a first aspect that affects the surface energy balance. Building and road materials have different thermal and reflective properties compared to the natural components in rural environments (Bassett *et al*., 2016). Beside these thermal and reflective differences, there is a reduced availability of water due to the large amount of impervious surfaces in the city (Van Hove *et al*., 2014; Best & Grimmond, 2015). In addition, the urban climate is influenced by reduced evapotranspiration due to few vegetation in the urban environment (Bassett *et al*., 2016). Therefore, more of the incoming solar energy is transformed into heat rather than used for photosynthesis and evaporation (Hamdi & Schayes, 2008; Bassett *et al*., 2016). This causes the warmer temperatures in the dense built-up areas like cities (EPC, 2008; Van Hove *et al.*, 2014).

The thermal properties of building materials can be expressed by the parameters thermal diffusivity, heat capacity and surface emissivity (Hamdi & Schayes, 2008). An increase of the thermal diffusivity means construction materials will have lower temperatures and higher temperatures will be found at the air-material interface (Hamdi & Schayes, 2008). The heat capacity of a construction material determines the temperature within the material and affects the air temperature near the surface of the material (Hamdi & Schayes, 2008; Best & Grimmond, 2015). Due to the larger heat capacity of materials in the urban area compared to those in the rural environment, a larger amount of the “energy for heating is held within the fabric of the buildings” (Best & Grimmond, 2015). The surface emissivity is the amount of thermal radiation that a material emits (Hamdi & Schayes, 2008). Construction materials with a higher surface emissivity emit more thermal radiation to space causing an increase in the temperature near the building materials (Hamdi & Schayes, 2008). The increasing emissivity leads to increasing UHI intensities. Thus, thermal diffusivity, heat capacity and surface emissivity affect the diurnal cycle of the urban temperatures by inducing higher UHI intensities at night if their value increases (Hamdi & Schayes, 2008; Best & Grimmond, 2015). The reflective properties of building and road materials can be expressed in terms of surface albedo. This parameter “represents the portion of the incident solar radiation that is reflected by the material” (Hamdi & Schayes, 2008) and has low values in urban areas and higher ones in the rural surroundings (Van Hove *et al.*, 2014). This means that there is more radiation absorbed in a city than in a rural place. Consequently, construction materials with a lower albedo amplify the UHI effect (Hamdi & Schayes, 2008).

1.1.2.2 Urban geometry

Next to the land cover, the urban surface energy balance is altered by the urban geometry. By taking into account the morphology of the city a third dimension is added to the characteristics of the site (Best & Grimmond, 2015). The urban geometry considers the height and spacing of buildings (Van Hove *et al.*, 2014). Van Hove *et al.* (2014) showed that this is an important feature to understand the local climate because it has a significant effect on the radiation budget and air flow. The urban geometry of cities varies in building height, space between the buildings and the impervious area (Van Hove *et al.*, 2014; Best & Grimmond, 2015). The first characteristic, building height is estimated by the mean building height. Secondly, the space between the buildings can be represented by the height-to-width ratio or sky view factor (SVF). The height-to-width ratio is the ratio between mean building height and mean street width, while the SVF quantifies the fraction of sky visible from the ground (Oke, 1981; Masson, 2000; Van Hove *et al.*, 2014; Best & Grimmond, 2015; Bassett *et al*., 2016). The third aspect of the urban geometry, the fraction of impervious surface can be expressed by the surface albedo because built environments cause mostly low albedo values (Van Hove *et al.*, 2014). The urban geometry influences the surface energy budget because higher buildings cause radiative exchanges between the walls (Masson, 2000). These walls increase the absorbed incoming solar radiation and reradiated longwave radiation (Best & Grimmond, 2015). Other differences in radiation are caused by the orientation and the elevation of the sun relative to the buildings. The built environment affects the depth to which the direct sunshine can penetrate and this influences the reflected solar radiation (Best & Grimmond, 2015). In a city the lower SVF will reduce longwave radiation loss at night and buildings cause an increased surface roughness, what results in lower wind speeds (Bassett *et al*., 2016). For these reasons less energy escapes and the heat is captured in the city (Masson, 2000).

1.1.2.3 Anthropogenic heat

An additional and unique aspect in cities is heating by human activities such as: combustion, the internal heating of buildings and the presence of people themselves (Best & Grimmond, 2015). Traffic and industry are two key factors in combustion. Moreover, it is important to take into account the domestic heating or cooling when the UHI is studied, as Ohasi *et al*. (2007) have proven. A method for estimating the seasonal anthropogenic heating was presented by Sailor & Lu (2004).

1.1.3 Variations in UHI intensities

1.1.3.1 Diurnal variation

The intensity of an UHI varies throughout day and night as seen in figure 3. The UHI is often weak in the morning and develops during the day (Van Hove *et al.*, 2014; Bassett *et al*.,2016). This development is caused by the absorption of energy within the built environment of the city (Bassett *et al*., 2016). After sunset subsequent heat release takes place from urban infrastructure and a maximum UHI intensity is reached. Hence, the strongest UHI effect is obtained at night because of the slower cooling down of the city in comparison to the rural surroundings (Van Hove *et al.*, 2014; Bassett *et al.*, 2016). So, intense UHIs are mainly a nocturnal phenomenon (Van Hove *et. al*, 2014). The timing of maximum UHI intensity depends on the characteristics of urban and rural surfaces, the season, and prevailing weather conditions (Morris *et al.*, 2001; EPC, 2008).

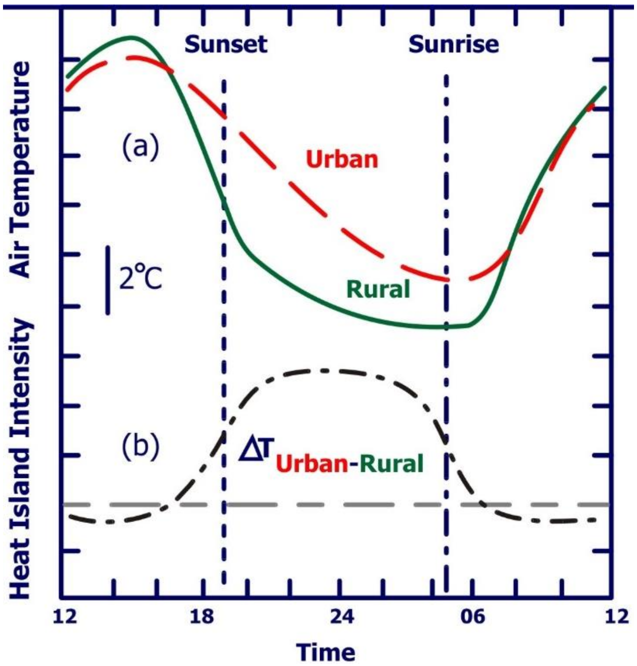

Figure 3: Conceptual graph of the diurnal evolution of the urban and rural air temperatures in section (a) and the consequent development of the UHI in section (b) (Sources: EPC, 2008; adapted from Oke, 1982; Runnalls & Oke, 2000).

1.1.3.2 Climatic variation

UHI intensities are largest during summer under clear skies and calm winds (Oke, 1982; EPC, 2008; Van Hove *et al.*, 2014; Bassett *et al*., 2016). Under a clear sky in summer, the solar heating is largest so the daytime warming in cities increases (Oke, 1982; EPC, 2008). This is why during heatwaves UHIs are very strong and can lead to disastrous consequences (Laaidi *et. al*, 2012; Bassett *et al*., 2016). On the other hand, more turbulent conditions, like strong winds increase atmospheric mixing and weaken UHIs (Oke, 1982; EPC, 2008). If there are clouds during the day, then the incoming radiation is less. This decreases the heating of the surface compared to clear sky circumstances, leading to a less pronounced UHI (Morris *et al*., 2001; EPC, 2008). When there are clouds during the night, the outgoing radiation is radiated back to the surface causing less cooling. Because the rural area does not cool as much as when clear sky conditions prevail, the UHI intensity is lower as well (Morris *et al*., 2001).

1.2 Relevance of studying UHI

As mentioned above, the structure and design of cities does affect the UHI. That is the reason why it is so important to know how the city's characteristics influence the urban climate. If more insight is gained in urban climate, then we can anticipate by sustainable urban planning (Van Hove *et al.*, 2014; Bassett *et al*., 2016). By taking into account the dominant processes of urban warming in new designs of buildings and urban construction, the UHI effect can be reduced (Best & Grimmond, 2015). In this way the quality of living can be maintained or improved in cities (Van Hove *et al.*, 2014; Hamdi *et al*., 2015). However, before the adaptation strategies can be realized, there is a need for more insight in the urban thermal environment (Van Hove *et al.*, 2014; Bassett *et al*., 2016). A second requirement is an improvement in modelling the spatial and temporal variability of the urban climate. In addition the influences of building materials and urban characteristics on the urban climate are needed to be incorporated in those adaptation strategies (Van Hove *et al.*, 2014; Bassett *et al*., 2016). Sustainable planning is needed to overcome the catastrophic consequences of heatwaves in cities, as happened in various European cities in the summer of 2003 (Laaidi *et. al*, 2012). Another remarkable aspect is the local aggravation of global warming in the urban areas (Van Hove *et al.*, 2014). Models state that urbanisation will continue in the next decades, thus such altered processes by cities will become more important (UN-Habitat, 2010; Van Hove *et al.*, 2014; Hamdi *et al*., 2015). Therefore Masson *et al*. (2013) call for climate change scenarios in urban environments. Because of those needs, models are requested that represent the most important features of the UHI (Best & Grimmond, 2015). By doing so, reliable predictions of the city climate could be made (Best & Grimmond, 2015).

1.3 How to study the UHI?

As presented by Mirzaei & Haghighat (2010), there are different approaches to study the UHI. Often the surface temperatures are estimated indirect by remote sensing techniques (EPC; 2008). In the following sections only observations with measurement networks and modelling are discussed because these two methods are relevant for this study.

1.3.1 Observations

Networks of automatic weather stations are a direct measurement method to identify UHIs by measuring the air temperature in urban stations and a rural reference station (Arnfield, 2003; EPC, 2008; Stewart, 2011; Bassett *et al*.,2016). The UHI intensity is then defined as the temperature difference between the urban and rural reference station (Arnfield, 2003; Stewart, 2011; Bassett *et al*.,2016). A network is needed because one measurement point is not representative for the whole city (Van Hove *et al*., 2014). This is due to the spatial variability in local climate (Van Hove *et al*., 2014). Thus, it is important to have monitoring stations at locations with different urban characteristics, in order to cover a range of urban climate zones by the stations (Van Hove *et al*., 2014). This is the case for the MOnitoring the City’s Climate and Atmosphere (MOCCA) network of Ghent University (Caluwaerts *et al.*, 2016). The MOCCA network is installed in the city Ghent by Ghent University in collaboration with Royal Meteorological Institute of Belgium (RMI) and *Vlaamse Instelling voor Technologisch Onderzoek* (VITO) (Caluwaerts *et al.*, 2016; www.observatory.ugent.be, consulted on April 30, 2017).

1.3.2 Modelling

Observational networks are not sufficient since it is the ambition to predict the UHI intensities and how they will develop for a specific urban area. Numerical weather prediction (NWP) models are therefore needed. To study intra-urban variability of temperature, the spatial resolution of the model has to be high. Hence, the atmospheric forcing has to be downscaled to higher resolutions. Hamdi *et al*. (2014) presented a high resolution dynamical downscaling method by using the ALadin-AROme (ALARO) (Termonia *et al*., 2018) model coupled with *SURFace EXternalisée* (SURFEX) (Masson *et al.*, 2013). Another faster method is using the UrbClim model as presented by De Ridder *et al*. (2015). The ALARO-SURFEX strategy will be further explained in the next section because this strategy is used at the RMI for the dynamical downscaling (Berckmans, 2018).

1.4 Models, databases and model configurations to study the UHI

1.4.1 ALARO

ALARO is a NWP model that is used for operational weather forecasts and provides the atmospheric forcing for the land surface model (LSM). This atmospheric forcing includes: different types of precipitation (e.g. convective rain, stratospheric rain, convective snow,…), incoming shortwave radiation and incoming longwave radiation, while the atmospheric state comprises: the temperature of the atmosphere, the humidity, the atmospheric pressure and the wind. ALARO is a model configuration of the *Aire Limitée Adaptation Dynamique Développement INterternational* (ALADIN) model containing an elaborated physics parameterisation (Termonia *et al*., 2018). This ALADIN model is a limited area model version of the global scale *Action de Recherche Petite Echelle Grande Echelle* Integrated Forecast System (ARPERGE-IFS) (Bubnová et al., 1995; ALADIN International Team, 1997). Both atmospheric models, ALADIN and ALARO, were made for NWP at high resolution over a limited area (Termonia *et al*., 2018). Hence, the ALARO model is able to run at a convective permitting resolutions (Termonia *et al*., 2018).

1.4.2 SURFEX

The atmospheric forcing and atmospheric state estimated by the atmospheric model are necessary as the input for the land surface scheme SURFEX, as shown in figure 4. “SURFEX is an […] externalized land and ocean surface platform that describes the surface fluxes and the evolution of four types of surfaces” (Masson *et al.*, 2013). This LSM allows an implicit coupling between the atmosphere and the surface, as represented in figure 4 (Masson *et al.*, 2013; Hamdi *et al.*, 2015). The atmospheric model delivers the atmospheric features to the LSM (Duerinckx *et al.*, 2015). In return, the LSM provides the upward longwave radiation, upward shortwave radiation, momentum flux, heat fluxes and water flux as surface boundary condition for the atmospheric model (Berckmans, 2018). In this way quantities are exchanged between the surface and atmosphere at each model time step (Berckmans, 2018). As illustrated in the right part of figure 4, it is possible to run SURFEX in offline mode. This means the atmospheric forcing is given on a frequent basis to SURFEX, but SURFEX does not return the computed flux (Duerinckx *et al.*, 2015).

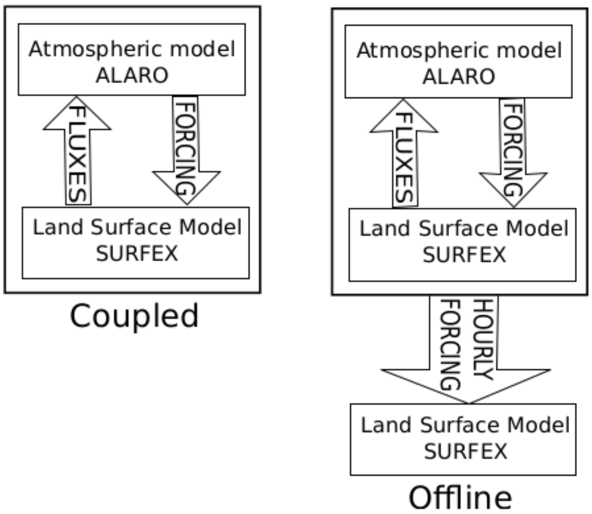

Figure 4: Representation of the implicit coupling between the atmospheric model ALARO and the land surface scheme SURFEX and the difference in coupled and offline mode of ALARO and SURFEX (Source: Duerinckx *et al.*, 2015).

In the SURFEX scheme, one grid cell is divided into tiles of nature, town, inland water and ocean based upon a land cover database to account for subgrid heterogeneities (Masson *et al.*, 2003; Masson *et al.*, 2013; Hamdi *et al.*, 2014). After all surface fluxes are computed for each tile, the fluxes are spatially averaged over the whole grid cell (Berckmans, 2018). ECOCLIMAP-I or ECOCLIMAP-II are often used as land cover database in SURFEX and therefore these databases will be described in more detail in the next section. For each of the four land cover tiles within SURFEX, parameterisations have to be made. The parameterisation for the nature fraction is executed by the Interaction Soil Biosphere Atmosphere (ISBA) scheme (Masson *et al.*, 2013). Additionally, the energy exchanges between the urban surface and the atmosphere are represented by the town energy balance (TEB) urban canopy model (Masson, 2000; Hamdi & Masson, 2008; Masson *et al.*, 2013). Both, TEB and ISBA, are multilayer parameterisation schemes because the substrate and surface are represented by different layers to simulate the transfer of heat and moisture. The possible parameterisation schemes for inland water and oceans are described by Mironov (2008), Gaspar *et al*. (1990) and Le Moigne *et al*. (2018).

It is important to include the TEB scheme for representing the fluxes over the town parts since the UHI will be studied in this thesis (Hamdi *et al.*, 2012). TEB is constructed in such a way it can represent any city in the world, for any time or weather condition, so a simplification of the real city geometry was executed (Masson, 2000). This simplification in the numerical TEB scheme is reached by using the canyon approach to represent a city (Masson, 2000; Masson *et al.*, 2013). In this canyon model, the city is represented by the facets road, roof and two facing walls (Masson, 2000; Best & Grimmond, 2015; Hamdi *et al.*, 2015). In table 1 the parameters to describe the city in a simplified way are represented (Masson, 2000). These parameters depend directly on building shapes and construction materials and some of them are split up in accordance with the division made by the canyon model (Masson, 2000). Thus, the alterations in the surface energy balance by artificial construction materials, urban geometry and human activities can be taken into account by using the TEB scheme in SURFEX.

Table 1: Parameters of the TEB scheme (Source: Masson, 2000).

Symbol	Designation of symbol	Unit
Geometric parameters		
a_{town}	Fractional area occupied by artificial material	–
a_{bld}	Fractional artificial area occupied by buildings	–
$1 - a_{\text{bld}}$	Fractional artificial area occupied by roads	–
h	Building height	m
h/l	Building aspect ratio	–
h/w	Canyon aspect ratio	–
$z_{0_{\text{town}}}$	Dynamic roughness length for the building/canyon system	m
Radiative parameters		
$\alpha_R, \alpha_r, \alpha_w$	Roof, road and wall albedos	–
$\epsilon_R, \epsilon_r, \epsilon_w$	Roof, road and wall emissivities	–
Thermal parameters		
$d_{R_k}, d_{r_k}, d_{w_k}$	Thickness of the kth roof, road or wall layer	m
$\lambda_{R_k}, \lambda_{r_k}, \lambda_{w_k}$	Thermal conductivity of the kth roof, road or wall layer	$\text{W m}^{-1}\text{ K}^{-1}$
$C_{R_k}, C_{r_k}, C_{w_k}$	Heat capacity of the kth roof, road or wall layer	$\text{J m}^{-3}\text{ K}^{-1}$

1.4.3 ECOCLIMAP

ECOCLIMAP is a dual database with an ecosystem classification and a corresponding set of land surface parameters for each ecosystem (Faroux *et al*., 2013). Each land use type is determined by a group of pixels with similar surface characteristics (Berckmans, 2018). The exchange and storage of water and energy in a LSM is based upon the characteristics of the surface. It is therefore important to well estimate the land cover since energy and water budgets are the key for weather and climate prediction models (Prein *et al*., 2015; Berckmans, 2018). ECOCLIMAP-I is a global database that can be used to make a classification of the land cover at 1 km² resolution (Faroux *et al*., 2013). Recently, this database has been updated for Europe to ECOCLIMAP-II/Europe (Faroux *et al*., 2013). The goal of the ECOCLIMAP-II database is to improve the classification into different land cover classes over

Europe (Faroux *et al*., 2013). Therefore, the ECOCLIMAP-II database contains 273 cover types instead of the 215 cover types within the ECOCLIMAP-I database (Faroux *et al*., 2013). Because this study focusses on the UHI, it should be noted that the classification of the urban cover types of ECOCLIMAP-I differs from ECOCLIMAP-II, as can be seen in table 2. In ECOCLIMAP-II not purely urban pixels are classified in functional types, while they were classified based upon the land use within ECOCLIMAP-I (Faroux *et al*., 2013). In contrast to this the town parameters are the same for the two ECOCLIMAP versions (Le Moigne *et al*., 2018).

Table 2: Urban Classes of ECOCLIMAP-I and ECOCLIMAP-II (Source: based on CNRM, *s.d.*, p.103-115).

Urban Classes of ECOCLIMAP-I	Urban Classes of ECOCLIMAP-II
COVER 7 : Urban and built-up COVER 151 : Dense urban COVER 152 : Mediterranean sub-urban COVER 153 : Temperate sub-urban COVER 154 : Cold sub-urban COVER 155 : Industries and commercial areas COVER 156 : Road and rail networks COVER 157 : Port facilities COVER 158 : Airport COVER 159 : Mineral extraction, construction sites COVER 160 : Urban parks COVER 161 : Sport facilities	COVER 561 : Temperate suburban 1 COVER 562 : Temperate suburban 2 COVER 563 : Temperate suburban 3 COVER 564 : Temperate suburban 4 COVER 565 : Temperate suburban 5 COVER 566 : Cold suburban 1 COVER 567 : Warm suburban 1 COVER 568 : Warm suburban 2 COVER 569 : Temperate suburban 6 COVER 570 : Temperate suburban 7 COVER 571 : Warm suburban 3

1.4.4 ERA-Interim

The ERA-Interim dataset contains reanalysis data with a resolution of about 80 km (Berrisford *et al*., 2011). A reanalysis is based upon a data assimilation process that uses a combination of observations and model data to estimate the evolving state of the atmosphere. Such reanalysis data is designed for climate studies and is provided by the European Centre for Medium-Range Weather Forecasts (ECMWF) (Dee *et al*., 2011). The dataset starts from 1979 and is updated once a month, with a delay of two months (www.ecmwf.int, consulted on May 11, 2018).

1.4.5 Downscaling approach

To reach the requested climate model data at 1 km spatial scale ERA-Interim data at global scale must be downscaled, as represented in figure 5. In the downscaling process the ERA-Interim data is used as a boundary condition for the regional climate model ALARO-0 (Hamdi, 2014; Caluwaerts *et al*., 2018). The atmospheric ALARO model is designed to run at high resolution over a limited area (Termonia *et al*., 2018). A domain over Western-Europe is reached by using ALARO, as shown in figure 5 (Berckmans, 2018; Caluwaerts *et al*., 2018). In order to downscale to a smaller spatial scale the ALARO-SURFEX approach is used (Hamdi, 2014; Berckmans, 2018; Caluwaerts *et al*., 2018). This implies that the regional ALARO-0 climate model is coupled inline to the SURFEX scheme. In this way a horizontal resolution of 4 km is obtained over the domain of Belgium (Hamdi, 2014; Caluwaerts *et al*., 2018). In a final step, the output of the regional climate model at 4 km resolution is employed to run the SURFEX scheme in offline mode, so the 1 km horizontal resolution over Ghent is reached (Hamdi, 2014; Caluwaerts *et al*., 2018).

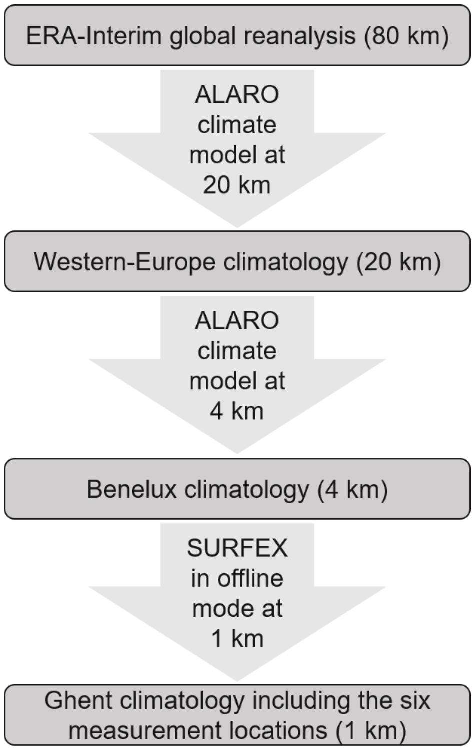

Figure 5: Conceptual model of the downscaling procedure starting from the ERA-Interim reanalysis data going to an atmospheric forcing at 1 km resolution with the ALARO-SURFEX strategy (Sources: adapted from Berckmans, 2018; Caluwaerts *et al*., 2018).

1.5 Problem statement

There is still a lack of knowledge about UHIs today despite the substantial examination that already has been done (Hamdi & Schayes, 2008). Ghent University, RMI and VITO examined the UHI phenomenon in Belgian cities. These institutes and their partners predicted UHI changes for Antwerp (De Ridder *et al.*, 2015; Lauwaet *et al.*, 2015), Brussels (Hamdi *et al.*, 2015; Lauwaet *et al.*, 2016) and Ghent (De Ridder *et al.*, 2015; Caluwaerts *et al.*, 2016). Some questions are still not yet completely answered, for example: How does the UHI exactly influence the climate in cities? Are the differences between the city and rural environment important in terms of weather forecasting and measurements? How can we take UHI into account in weather models? Therefore, we need to enhance the insight in the UHI concept. This should be done in two ways: improve the density of the measurement networks and improve UHI modelling. The MOCCA network is following the first approach and is measuring since July 2016 the microclimate of Ghent by using a high-density measurement network (Caluwaerts *et al.*, 2016). In conjunction with this progress, this thesis will focus on the latter method: How can the modelling of the UHI phenomenon be improved?

1.6 Research objectives

The aim of this thesis is to find out where a LSM can be improved for predicting the UHI, particularly for Ghent. Since ECOCLIMAP-I and ECOCLIMAP-II are physiographical databases that can be implemented, it can be questioned if the LSM output improves by using ECOCLIMAP-II, like Faroux *et al*. (2013) suggested. Therefore, a validation of the model has to be performed with ECOCLIMAP-I, ECOCLIMAP-II and high resolution land cover data over Ghent. The model output can be compared with the measured data of the MOCCA network (www.observatory.ugent.be, consulted on April 30, 2017). Since the UHI intensity is influenced by the environment (Van Hove *et al*., 2014), it is important to take into account the different environments around the measurement stations. Therefore, the environment around the stations will be studied at different spatial scales. To improve the UHI modelling it is essential to know which parameter of the TEB scheme is the most important in studying UHI. When this is determined, only those parameters that affect the UHI the most have to be implemented in numerical models to obtain reliable estimations of the UHI phenomenon. Another argument to investigate this, is to know in which parameter the errors should remain small to get a qualitative good model output. The final question that will be examined is whether the land cover or a parameter of the TEB scheme is dominant for the modelled UHI. Van Hove *et al.* (2014) showed that both the land cover and mean building height influence the UHI intensity significantly, but it is not known which parameter has the biggest influence on modelling the UHI.

1.7 Research questions and hypotheses

1) What is the land cover around the measurement stations of the MOCCA network?
Hypothesis: The MOCCA monitoring stations are sited at locations with different urban characteristics in order to cover a range of urban climate zones (Caluwaerts *et al.*, 2016). A station is situated at the port, another station is located in a suburban neighbourhood, two stations are situated in the densely built city centre, one station is situated in an urban park and the last station is located in a rural environment (Caluwaerts *et al.*, 2016).

2) Which radius around the station is important to take into account the land cover for studying the UHI phenomenon? Is there any scale dependency?
Hypothesis: According to Van Hove *et al*. (2014) the UHI intensity depends on an circular area around the station with a radius that ranges between 250 m and 500 m. This corresponds with an area that is slightly smaller than 1 km². Therefore, the UHI of the UCL is determined by the local or neighbourhood scale. Scale dependency means that a different model result is obtained when a larger or smaller area is taken into account. It is supposed that the model results of the UHI will differ when a different spatial scale is taken into account, since temperature measurements depend on influences over a certain area (Pielke *et al*., 2007).

3) Is ECOCLIMAP-II better in estimating the land cover than ECOCLIMAP-I over the study area in Ghent?
Hypothesis: Faroux *et al*. (2013) suggested that ECOCLIMAP-II will better estimate the land cover than ECOCLIMAP-I. Although, a recent study showed there are some issues for urban areas in the Netherlands (Tijm and de Vries, personal communication, 3 April 2018). The report of Le Moigne *et al*. (2018) notes as well that "ECOCLIMAP-II now needs to be used in order to better qualify the improvements" and shortcomings with respect to ECOCLIMAP-I.

4) Will model output concerning the UHI be more accurate if ECOCLIMAP-II is implemented instead of ECOCLIMAP-I?
Hypothesis: Lemonsu *et al*. (2004) reported that it is important to estimate the land cover well in order to obtain good model results. Since it is assumed that ECOCLIMAP-II represents better the reality, it is expected that the model performance with ECOCLIMAP-II will be better than with ECOCLIMAP-I.

5) Does the model simulate better the UHI when more correct and higher resolution land cover data is used?
Hypothesis: It is expected that the UHI will be represented better if more correct and higher resolution land cover data is implemented in SURFEX.

6) Which parameter of the TEB scheme is the most important in studying the UHI?
Hypothesis: Hamdi & Schayes (2008) found that the urban canyon is an important factor in modelling the UHI during night time in the city of Basel. In this study a linear relationship was found with the SVF. Therefore, it is assumed that the building height and road width will be important parameters when the UHI is modelled.

7) What is the dominant parameter? For which parameter is the model most sensitive: the land cover or a parameter of the TEB scheme?
Hypothesis: Best & Grimmond (2015) concluded that it is important to take into account the vegetation, albedo and geometry of the street canyon in an urban LSM. Van Hove *et al*. (2014) showed that the building surface fraction, building height and impervious and green surfaces are important when the UHI intensity is studied. Therefore, it is expected that the parameters land cover, building fraction and building height will have an influence on the model output of the UHI. Van Hove *et al*. (2014) found that the building fraction is the most important parameter to explain the intra-urban variability of the UHI.

2. STUDY AREA

This study focusses on the agglomeration of Ghent. More precise the observations are done in the municipality of Ghent and Melle. Ghent and Melle are situated in the north of Belgium as represented on map 1. Belgium is characterised by widespread urbanisation, especially in the northern region Flanders (Caluwaerts *et al*., 2018). How to deal with the need for an increase in built-up areas and the shrinking opportunities to save the last open space are subjects in a still ongoing discussion in Flanders. In 2016 about 550 000 people were living within the arrondissement of Ghent whereof just over 250 000 people were living in the city of Ghent (statbel.fgov.be, consulted on April 21, 2018). Therefore the city of Ghent can be considered as a middle-sized European city. The smaller municipality of Melle counts just over 10 000 people (statbel.fgov.be, consulted on April 21, 2018). Ghent is geomorphologically located at the confluence of the rivers Lys and Scheldt and is characterised by a flat topography. Since Ghent is sited about 50 km away from the North Sea, it is not a coastal city (Caluwaerts *et al*., 2016). However, the study area is influenced by the sea-breeze very often (Hertoghs, 2012). Therefore the climate in this area is described as a mild maritime climate with an average minimum and maximum temperature of 13,2°C and 23,0°C in July (Caluwaerts *et al*., 2018; RMI, 2017). From a landscape perspective the study area consists of the densely built and populated historical centre of the city of Ghent. Some parks are present at the border of this core area (Verdonck *et al.*, 2017). Around the urban core there is a concentric growth pattern, known as the urban sprawl (Verdonck *et al.*, 2017). These suburban neighbourhoods are characterised by detached low rise buildings. Further away from the historical centre, the landscape consist of fragmented suburban and rural areas (Verdonck *et al.*, 2017). North of the city Ghent this pattern is not respected as the harbour, characterised by a large industrial zone, is situated there.

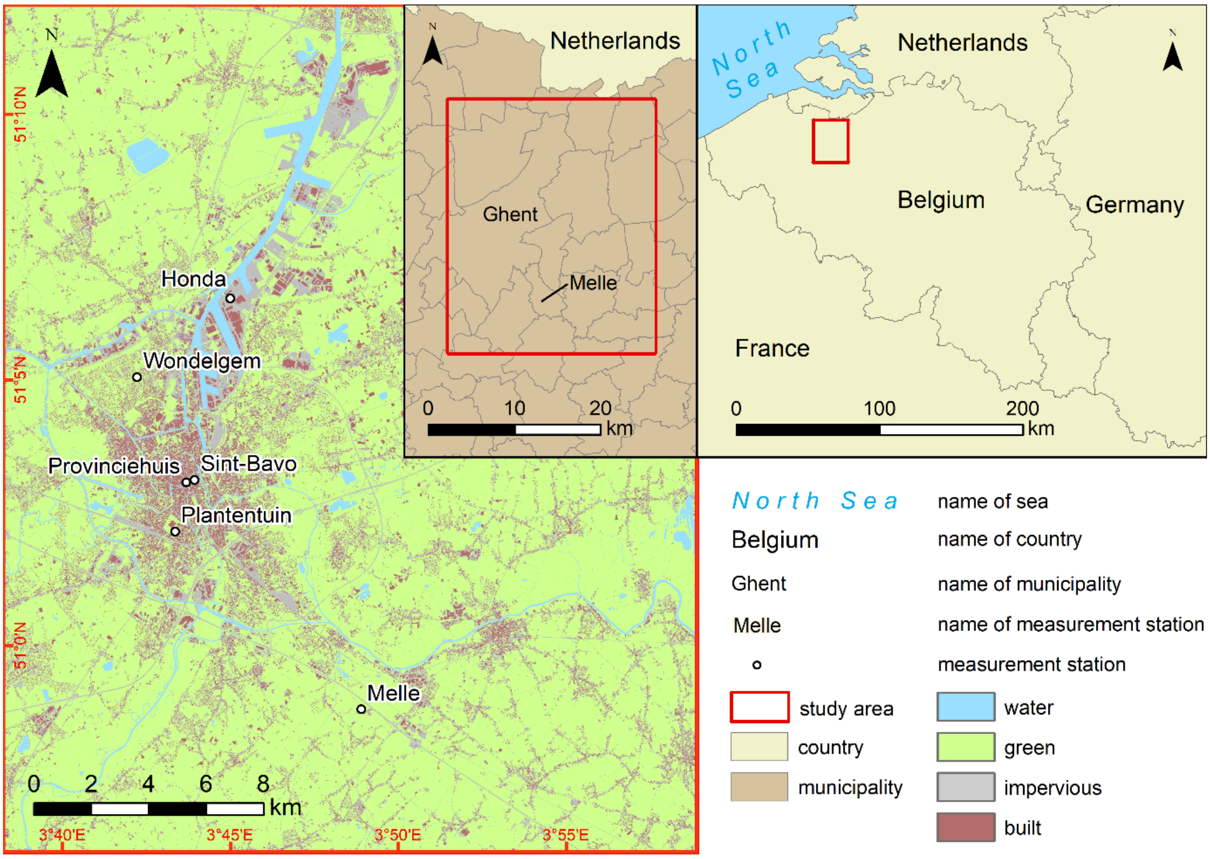

Map 1: Siting of the six weather stations within the agglomeration of Ghent.

For this study temperature measurements of weather stations at different locations within Ghent region are used. On map 1 the locations of those stations are visualised. Here, the six measurement stations are described from north to south. The Honda station is situated at the industrial site of the company Honda in the port of Ghent. The second measurement station is located in the residential Wondelgem district. This neighbourhood is characterised by suburban features such as houses with gardens, less dense built space and lower buildings compared to the city centre. The Sint-Bavo and Provinciehuis stations are both located within the densely built city centre. Those stations are sited only 300 m apart from each other. The station of the Plantentuin is positioned in the botanical garden of Ghent University, southwest of a large public park. This public park is connected to the botanical garden making the Plantentuin station is located in a green spot within the city. The station in Melle is mainly surrounded by fields with low crops and is therefore a rural station.

3. DATA AND MODELS

This section describes the used data and models and motivates why they are chosen. First, the methodology that is applied to extract the temperature model data is explained. The purpose of this study is to look how well the model behaves if different land cover and city geometry data are implemented. Therefore, information about the land cover and building heights is needed. The datasets used to obtain this information are described in section 3.2. Finally, temperature observations are needed to verify the model output. Table 3 shows a summary of all used data and models.

Table 3: Summary of used data and models.

DATA	ADMINISTRATOR	SOURCE	DATE OF ACQUISITION
Forcing data at 4 km resolution	RMI	Dr. Hamdi R. and Duchêne F., RMI	23/11/2017
SURFEX V8.0	CNRM	Dr. Hamdi R., RMI Open version provided on: http://www.umr-cnrm.fr/surfex/spip.php?article387	06/11/2017
gtopo30	USGS	Dr. Hamdi R., RMI Open version provided on: http://mesonh.aero.obs-mip.fr/mesonh52/Download files: gtopo30.hdr.gz gtopo30.dir.gz	23/11/2017
clay_fao	CNRM	Dr. Hamdi R., RMI Open version provided on: https://opensource.umr-cnrm.fr/projects/ecoclimap/files	23/11/2017
sand_fao	CNRM	Dr. Hamdi R., RMI Open version provided on: https://opensource.umr-cnrm.fr/projects/ecoclimap/files	23/11/2017
ECOCLIMAP-I	CNRM	Dr. Hamdi R., RMI Open version provided on: https://opensource.umr-cnrm.fr/projects/ecoclimap/files	23/11/2017
ECOCLIMAP-II	CNRM	http://mesonh.aero.obs-mip.fr/mesonh52/Download files: ECOCLIMAP_II_EUROP_V2.3.hdr.gz ECOCLIMAP_II_EUROP_V2.3.dir.gz	22/02/2018
*Bodem-bedekkings-kaart (*BBK*), 1 m resolutie, opname 2012*	IV	http://www.geopunt.be/download?container=bodembedekkingsbestanden2012\BBK1_12&title=Bodembedekkingskaart%20(BBK%29,%201m%20resolutie,%20opname%202012	08/04/2018
3D GRB	IV	https://download.agiv.be/Producten/Detail?id=971&title=3D_GRB	07/04/2018
MOCCA Temperature data Ghent summer 2016	Ghent University	Dr. Caluwaerts S., Department of Physics and Astronomy (In the future this will be open data provided on www.observatory.ugent.be)	21/03/2018

3.1 Forcing data and model

The downscaling procedure as presented in figure 6 was done by the RMI until the regional level of the Benelux climatology and they provided the downscaled data at 4 km resolution for this thesis (Hamdi *et al*., 2014). How this data was extracted for each station will be discussed in the section method. By doing this the SURFEX scheme can run at 1 km resolution in offline mode. SURFEX needs a Linux environment to be run and the installation of SURFEX is described in Appendix I. The SURFEX scheme can be downloaded for free (www.umr-cnrm.fr, consulted on April 11, 2018), but here an adapted version of SURFEXv8.0 was provided by R. Hamdi (RMI).

3.2 Land cover and building height

Information on the topography and soil texture is needed as input to run SURFEX. The topography is derived from the global gtopo30 dataset. This is a digital elevation model (DEM) that covers the whole world with a spatial resolution of 30” or approximately 1 km resolution (lta.cr.usgs.gov, consulted on April 25, 2018). The arranged dataset to implement in SURFEX was provided by R. Hamdi (RMI), but the general dataset is made available for free by the United States Geological Survey (USGS) (lta.cr.usgs.gov, consulted on April 25, 2018). The datasets clay_fao and sand_fao are used to define the soil texture. These datasets contain percentages of clay and sand and have a horizontal grid spacing of about 10 km. They are acquired via R. Hamdi (RMI), but it is also open data made available by the National Centre for Meteorological Research (CNRM) and the Food and Agriculture Organization of the United Nations (FAO) (opensource.umr-cnrm.fr, consulted on April 25, 2018).

3.2.1 ECOCLIMAP-I and ECOCLIMAP-II

The ECOCLIMAP-I database was provided by R. Hamdi (RMI), but is also freely available at the open source site of CNRM (opensource.umr-cnrm.fr, consulted on April 25, 2018). The ECOCLIMAP-II database is open data as well (opensource.umr-cnrm.fr, consulted on April 25, 2018). Here, the updated version 2.3 is used and this version is acquired via the website of the mesoscale non-hydrostatic model (Meso-NH) (mesonh.aero.obs-mip.fr, consulted on April 25, 2018).

3.2.2 High resolution data for Flanders

To study the environment around each station in detail, very high resolution land cover data is needed. For this the open data from the *Bodembedekkingskaart* (BBK), 1 m resolution, 2012 (www.geopunt.be, consulted on April 8, 2018) is used. This is a spatial dataset maintained by the Flemish administration through the agency *Informatie Vlaanderen* (IV). The advantages of this dataset are the high resolution and the full coverage over Flanders. In addition this dataset contains useful classes and after validation this dataset turned out to be very accurate (AGIV, 2016a). A disadvantage is that the dataset represents the land cover of 2012. However, a fast verification based upon field knowledge did not show remarkable changes in land cover around the measurement stations used for this study. Nevertheless, it would be better to use a land cover dataset that represents the surface at the time the temperature measurements were done. This could be obtained by using the vector data of the *Grootschalig Referentie Bestand* (GRB). On the other hand given the cadastral purposes of this dataset, it is not suited to study the land cover. The dataset has a full coverage over Flanders but the cadastral plots do not contain information about the land cover. As a solution, the land cover of the cadastral plots could be obtained by using OpenStreetMap (OSM) data. However, even by combining the data of both GRB and OSM there is still a limited coverage of the areas around the stations. Remaining gaps could be completed manually based on knowledge of the environment around the stations. Because this method is more time-consuming and no validation of this dataset could be done in the timespan of this thesis, the BBK dataset was used. Another possible dataset to derive the land cover and city geometry around the stations is the local climate zone classification scheme of Verdonck *et al*. (2017). In this dataset the classification is specifically created for climate purposes and gives information about both land cover and city geometry. However, this dataset is not used since the resolution is limited to 30 m, while the BBK has a resolution of 1 m. Still, it could be useful to compare the data extracted for the six stations using both approaches to examine the effect of those datasets on the modelling output.

To obtain the average building height around the measurement stations the open data from 3D GRB is used (www.agiv.be, consulted on April 7, 2018). 3D GRB – *Gebouw LOD1 DHMV II* is a spatial dataset maintained by the Flemish administration and distributed by the agency IV. The dataset covers the region of Flanders without gaps and contains vector data describing each building geometry in three dimensions. The building heights are estimated with an accuracy of 0,14 m and the data has an application scale of 1 : 250 m (AGIV, 2016b).

3.3 Temperature measurements

Observational temperature data was obtained by the six identical measurement stations of the MOCCA network. They were set up to investigate for several years the urban climate of the Ghent region and to validate and improve urban models (Caluwaerts *et al*., 2016). Since these highly-accurate measurement stations are located in neighbourhoods with different environmental characteristics, the spatial variability of meteorological parameters within the city can be studied (Caluwaerts *et al*., 2016). The MOCCA project is still ongoing and this thesis will contribute to this project (Caluwaerts *et al*., 2018). On map 1 the location and the name of the six automatic weather stations are given. The coordinates of each station were obtained with a commercial handheld GPS. The temperature data of the summer 2016 was chosen since large UHIs more often prevail in summer (Oke, 1982; EPC, 2008; Van Hove *et al.*, 2014; Bassett *et al*., 2016). Only one season is investigated to reduce the computing time for the modelling part. The measurement campaign started in July 2016 and at the end of August a heat wave took place over Ghent (Caluwaerts *et al*., 2016). Therefore the temperature data of those two months is used. This data was obtained via S. Caluwaerts and in the future this will be open data provided on www.observatory.ugent.be (consulted on April 30, 2018).

4. METHOD

First, a geographical information system (GIS)-analysis is carried out around the six MOCCA measurement stations incorporating the land cover and building height. This is done for different circular areas around the stations with radii of 10 m, 100 m, 565 m and 1000 m. In a second part the sensitivity of the SURFEX model output for land cover and building height is investigated. In order to make comparisons of different land parameterisations and city geometries, the SURFEX model has to be run with different parameterisations. For this thesis the SURFEX model is used in a so-called offline mode at 1 km resolution. Before the SURFEX model can run in offline mode, it has to get forced by an atmospheric model (Hamdi *et al.*, 2014). Data given by the lowest level of the ALARO-SURFEX limited area model run at 4 km is therefore extracted for each grid point situated closest to the MOCCA observational stations (Hamdi *et al.*, 2014). This data is then used as input for the offline SURFEX runs at 1 km resolution. Such an experiment necessitates the tuning of some parameters (Harshan, 2015). This tuning is done with respect to the MOCCA observations at the rural Melle location. Once the model gives a good model performance compared to the observational data of the Melle station, the model can run with the same tuning for the other stations. The tuning parameters are kept constant during all runs, by doing so the results are not influenced by the tuning of the model. Next, the ECOCLIMAP-I module of the model is replaced by ECOCLIMAP-II and thereafter the same module is replaced by data obtained by the GIS-analysis. After this is done, a statistical comparison is made between the different runs to investigate the sensitivity of SURFEX to the surface and geometry parameters.

4.1 GIS-analysis

In order to see how the land cover and city geometry evolve at different scales, different buffer distances were calculated around each measurement station (Van Hove *et al*., 2014). Therefore, stations are implemented in QGIS using approximated WGS 84 coordinates. These coordinates are transformed to Lambert 72 because a metric coordinate system is necessary to compute the buffer areas. Moreover, Lambert 72 is the standard metric coordinate system used in Belgium. Using OpenStreetMap and aerial photos the points of the stations are dragged onto their real location. Those new, more precise coordinates of the locations are saved and the Lambert 72 and WGS 84 coordinates of these points are added to the attribute table. A detailed overview of the different actions in QGIS is presented in Annex I.

In a next step the buffers were drawn around the stations. A buffer distance of 10 m was chosen to characterise the direct environment of the station. This makes it possible to study the micro-climate of the station. A second radius of 100 m and a third of 1000 m were chosen to represent the wider environment. Since the tiles in SURFEX are at 1 km^2 scale a buffer of the same area was calculated as well, namely a buffer with radius of 565 m. This enables the implementation of land cover data at the same scale level as ECOCLIMAP data in SURFEX.

4.1.1 Land cover

In this section the method of mapping the land cover is described. This is necessary to determine the proportion sea, water, urban and green surface around each measurement station. The data used for this section is the open data from *Bodembedekkingskaart* (BBK), 1 m resolution, 2012 (www.geopunt.be, consulted on April 8, 2018). First the map sheets number 14 and 22, that cover the study area, are merged into one layer. Then the layers impervious surface, green space and water are created based on this data. Classes one to four are assigned as impervious surface, class five is water and class six till fourteen are allocated as green space. Since class eleven to fourteen are green features which are hanging partly above roads, ponds and rivers, there might be an overestimation of the class green spaces at the expense of the classes water and concrete surfaces. This can be seen by comparing figure 6A and 6B. However, this grouping is chosen since the modelling period is during the summer and during this period the green features do cover the other ones. This can be seen by comparing the different pictures in figure 6. Using the zonal statistics tool of QGIS, the amounts of impervious, green space and water raster cells are computed for every buffer area around each station. In the same way the total amount of raster cells in the buffer area is determined. Subsequently, the fraction of concrete, green and water is calculated by dividing the amount of cells of one category by the total amount of cells.

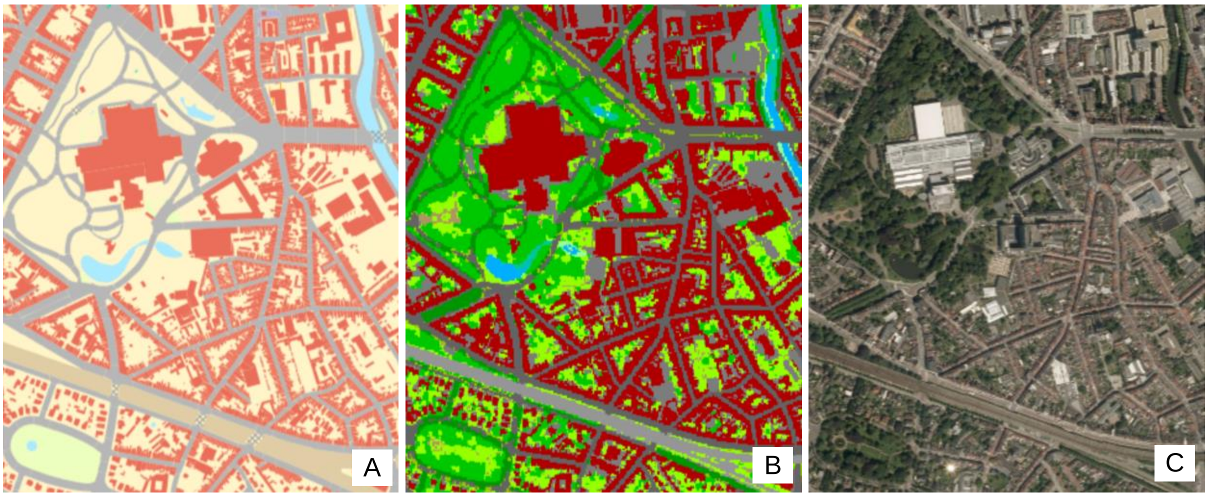

Figure 6: Comparison between the GRB 2016 (A), BBK 2012 (B) and aerial photo summer 2012 (C) (Sources: *Basiskaart* - GRB*: volledige kaart*; *Bodembedekkingskaart (*BBK*), 1 m resolutie, opname 2012*; *Luchtfoto Vlaanderen, zomer 2012 - kleur*, www.geopunt.be; consulted on April 11, 2018).

4.1.2 Fraction of buildings

The built surface is determined in the same way as the different land cover categories from the previous section. Here, the raster cells in the buffer area around the station with value ‘1’ are counted. In SURFEX the parameter XUNIF_BLD represents the fraction of buildings. Since this is a component of the TEB module, the fraction of buildings has to be computed with respect to the area indicated as town. This means that the fraction of buildings is defined as the built area divided by the area of the impervious features in the buffer.

4.1.3 Building height

To determine the average building height around a station, the open data of the 3D GRB is used (www.agiv.be, consulted on April 7, 2018). Beside this layer, the buffer areas with radii 10 m, 100 m, 565 m and 1000 m from the previous section are loaded in the QGIS environment. For each buffer area the spatial intersection is taken with the 3D GRB. In the newly created layers, which contain only the buildings within the buffer distance, the attributes with a poor quality label are removed. This is necessary since these attributes comprise buildings with incorrect characteristics, especially for the building height. Thereafter, the area of each building geometry is added to the attribute table. Subsequently, the attribute table is converted to an Excel file. In this file the weighted average height of the buildings around a measurement station is calculated as follows:

$$weigthed\ average\ height = \frac{\sum(height\ of\ building * area\ of\ building)}{total\ area\ of\ built\ space}$$

The obtained values are then implemented as value for the parameter XUNIF_BLD_HEIGHT in SURFEX.

4.2 SURFEX modelling

4.2.1 Extracting data

To run the SURFEX model at 1 km grid resolution in offline mode, an atmospheric forcing of a regional climate model is needed (Hamdi *et al*., 2014). Here the data downscaled to 4 km for the MOCCA study is reused (Caluwaerts et al., 2018). Data from July till September is extracted with the code of Ghent_extrac.R which is given in Annex II. By searching for the closest grid point the 4 km resolution data is projected on the locations of the stations with this code (Hamdi *et al*., 2014). The variables temperature, pressure, zonal wind, meridional wind, specific humidity, shortwave direct sunlight, total shortwave irradiation, longwave radiation, precipitation as water from stratified type and convective type, and precipitation as snow from stratified type and convective type are extracted. These are values of the atmospheric model at the level closest to the surface boundary layer (SBL), namely at 50 m height. Since the variables of the regional climate model differ from those needed in the SURFEX model, a conversion is necessary. This conversion is done in the SURFEX component.

4.2.2 Set up the SURFEX model

Once SURFEX is installed (see Annex III), an experiment can be defined. To get output for a measurement station, such an experiment has to be set up. Thus, for each measurement station the procedure of making a new experiment must be completed. After this is done, the model can be tuned and validated.

4.2.3 Initialization and validation of the model

After the model is set up for the six stations, the output of the model can be compared with the observational data of the MOCCA network. Since the modelled output is hourly, the observational data on minute scale is reduced to hourly scale by taking the value at every hour. Because Melle is the only rural station, this station is taken as the reference station. Therefore the model should represent the observations in Melle as good as possible. The tuning is done by initializing the parameters of the model. The default parameters in the file OPTIONS.nam of the station Melle can be tuned in such a way the model will perform better. More specifically the parameter XHUG_ROOT is modified, so the model better approaches the observations. This parameter reflects the value of the liquid soil water index (SWI) for the root zone soil layers (CNRM, *s.d.*). By default XHUG_ROOT is set to 1,00 and the parameter ranges between 0,01 and 1,00 (Harshan, 2015). Here, the value 1,00 implies a high humidity, while a value of 0,01 indicates a very dry condition. To get the optimal value, different runs for Melle are done with values 1,00; 0,50; 0,25 and 0,01 for XHUG_ROOT. To verify to what extent the reality differs from the model output, the index of agreement, the root mean square error (RMSE) and bias between the observational and modelled data are calculated. In these experiments the index of agreement, RMSE and bias are only computed for the period of August to avoid influences of the spin-up of the model. The model run with the highest index of agreement and lowest RMSE and bias has the best model performance. Therefore the initialisation of XHUG_ROOT with the lowest error will be used for all following runs. In this way runs for each measurement station are done using the ECOCLIMAP-I database. The tuning parameter XHUG_ROOT is kept constant during all runs, so the results are not influenced by the tuning of the model. Since the aim is to study the UHI, the same analysis is done for the temperature differences between the urban Sint-Bavo station and the reference station Melle.

4.2.4 Replacing ECOCLIMAP

In order to change the parameterisation of the land cover, the module of ECOCLIMAP in SURFEX is adapted. This module is present in the OPTIONS.nam file in the folder of each station. First, ECOCLIMAP-II is implemented instead of ECOCLIMAP-I. Second, ECOCLIMAP-I is replaced by the land cover fractions obtained by the GIS-analysis. Finally, changes in city geometry are studied by modifying some parameters of the TEB scheme. By comparing the model performances, the sensitivity of the UHI simulations to changes in each parameter can be estimated.

4.2.4.1 ECOCLIMAP-II module

The downloaded ECOCLIMAP-II files are moved to the ECOCLIMAP directory of SURFEX. In the folders of the stations the links with ECOCLIMAP-I files in the ECOCLIMAP directory are removed and replaced by the links of the ECOCLIMAP-II files. Thereafter, the parameter of the land cover, named YCOVER, must be replaced with the name of the ECOCLIMAP-II files in the OPTIONS.nam file. Here is checked whether the tuning parameters are kept unchanged. After these modifications the model is run again for each station. For a more detailed explanation, see Annex IV. For obtaining the UHI the values of the Melle station, obtained with the ECOCLIMAP-II run, are subtracted from the temperatures of the urban station.

4.2.4.2 Implementation land cover fractions GIS-analysis

In this case there is no coupling needed with an ECOCLIMAP module. Therefore, the OPTIONS.nam file has to include all the parameters that were assigned by ECOCLIMAP before. This file is standard given as OPTIONS.nam file if SURFEX is downloaded. Annex V shows how this code looks like and how it was exactly adapted. In the module NAM_FRAC the land cover fractions of the GIS-analysis are implemented and the model is run again for each station. This is done for the results of the 100 m, 565 m and 1000 m buffer distances. The model performances of the land cover parameterisation with the 565 m buffer distance, ECOCLIMAP-I and ECOCLIMAP-II can be compared since they are determined on the same scale level, 1 km². Also a comparison of the model performances of 100 m, 565 m and 1000 m buffer distances can be made, to see to what spatial extent of land cover the temperatures measured in one point are influenced.

4.2.4.3 Adapting TEB based on GIS-analysis

In the same OPTIONS.nam file as in the previous section, the parameters fraction of buildings and building height can be adapted in the TEB module called NAM_DATA_TEB. For these runs only the land cover parameterisation of the GIS-analysis for the 565 m buffer is used. The fraction of buildings, named XUNIF_BLD, obtained from the GIS-analysis is implemented, while the other parameters retain their default values. This is done for each station and the model is run again. After these runs are finished, the fraction of buildings is set again to the default value of 0,5. Subsequently, the parameter building height, called XUNIF_BLD_HEIGHT, is adapted. The standard value of 10 m is replaced by the heights around each station obtained by the GIS-analysis. After this is done the model is run again for each station.

4.3 Statistical scores

In order to evaluate the model performance after adapting the parameters of each station, the index of agreement, bias and RMSE are calculated. The index of agreement is a percentage that expresses how well the modelled temperatures agree with the observed values based upon the difference with the average observed temperatures (Willmott, 1982). This is calculated as followed (Willmott, 1982):

$$index\ of\ agreement = 1 - \frac{\sum_{i=1}^{N}(P_i - O_i)^2}{\sum_{i=1}^{N}(|P_i - \bar{O}| + |O_i - \bar{O}|)^2}$$

With: P_i = modelled value i

O_i = observed value i

$\bar{O}$ = average of observed values

An advantage of this score is the possibility to make cross-comparisons between models because of the normalized values (Willmott, 1982). The bias is the difference between the average of modelled and observed temperatures and the RMSE is the square root of the sum of all squared differences between the modelled and observed temperatures. In addition the RMSE is split up in a systematic and an unsystematic fraction to investigate whether the parametrisation of the model is improved or the random errors are lowered by the adaptations in the model. The random errors are induced by the forcing given as input to the SURFEX model. The systematic RMSE comprises the errors caused by physical processes that are not simulated well by the model (Hamdi *et al.*, 2009). The goal is to minimize this error by adapting the land cover and the city geometry parameters to values that are closer to the reality. When the systematic RMSE approaches zero, then the model is good and the unsystematic RMSE will approach the RMSE (Willmott, 1982). Moreover, two-tailed pared T-tests are carried out between the observed and simulated temperatures for the different runs. By doing so, it is examined whether the distributions of the observed and simulated temperatures differ significantly from each other. The null hypothesis states that the observed and simulated temperature series are equal. When this hypothesis is rejected at a significance level of 99%, then it is assumed that the observed and simulated temperature series differ significantly from each other. This p-value is closely linked with the bias, since the T-test investigates if there is a significant difference between the means of the distributions of the observed and simulated temperatures. The same scores are calculated for the simulations of the UHI. Based upon previous statistical values an interpretation is made of how well the model can simulate the observed temperatures.

By comparing the errors of the different runs conclusions can be drawn to which parameter is most sensitive with respect to modelling the temperature. Two-tailed pared T-tests are carried out between the different simulated temperatures to examine whether they differ significantly from each other. Here the null hypothesis states again that the temperature series are equal. If they differ significantly, then the null hypothesis is rejected and the temperature simulations are sensitive to the change in the adjusted parameter. The R-code used for these statistical calculations can be found in Annex VI.

5. RESULTS

5.1 GIS-analysis

In this section the land cover and building characteristics around the stations are discussed. Table 4 represents the coordinates of the six different locations with a measurement station. Since the data of the BBK is at 1 m² resolution it is necessary to use the more precise coordinates. In this study the Lambert reference system is used, but for global applications the more precise WGS 84 coordinates are given in table 4 as well.

Table 4: Given and precise coordinates of the observation stations.

Location	Given x coordinate WGS 84 (°)	Given y coordinate WGS 84 (°)	x coordinate Lambert 72 (m)	y coordinate Lambert 72 (m)	x coordinate WGS 84 (°)	y coordinate WGS 84 (°)
Provinciehuis	3,728	51,051	105057,0	193642,9	3,727799	51,0512
Sint-Bavo	3,732	51,052	105352,4	193729	3,732	51,052
Honda	3,749	51,109	106597,2	200059,9	3,749	51,109
Plantentuin	3,722	51,036	104668,4	191921,7	3,72247	51,0357
Wondelgem	3,703	51,084	103342,2	197307,0	3,702875	51,084
Melle	3,816	50,98	111165,0	185719,9	3,815744	50,98043

5.1.1 Land cover

The land cover around the stations is studied to determine objectively in what environment the measurement stations are located. By using buffers with different radii, the environments at different spatial scales are examined. In the following sections the land cover fractions for each station are discussed starting from the Honda station in the north to the station Melle in the south. On map 2 and graphs 3a, 4a, 5a, 6a, 7a and 8a the proportions of land cover around the stations are given for a radius of 10 m around the station. The land cover within these buffer areas represents the environments at micro scale. It should be noted that the built area on the following maps is taken into account in the fraction of impervious land cover. In map 3 and graphs of figures 7b, 8b, 9b, 10b, 11b and 12b the land cover fractions within a distance of 100 m of the station are presented. This procedure is repeated for a radius of 565 m and 1000 m around the measurement stations. By comparing the land cover fractions at different scales the evolution of going to a more wide area is discussed.

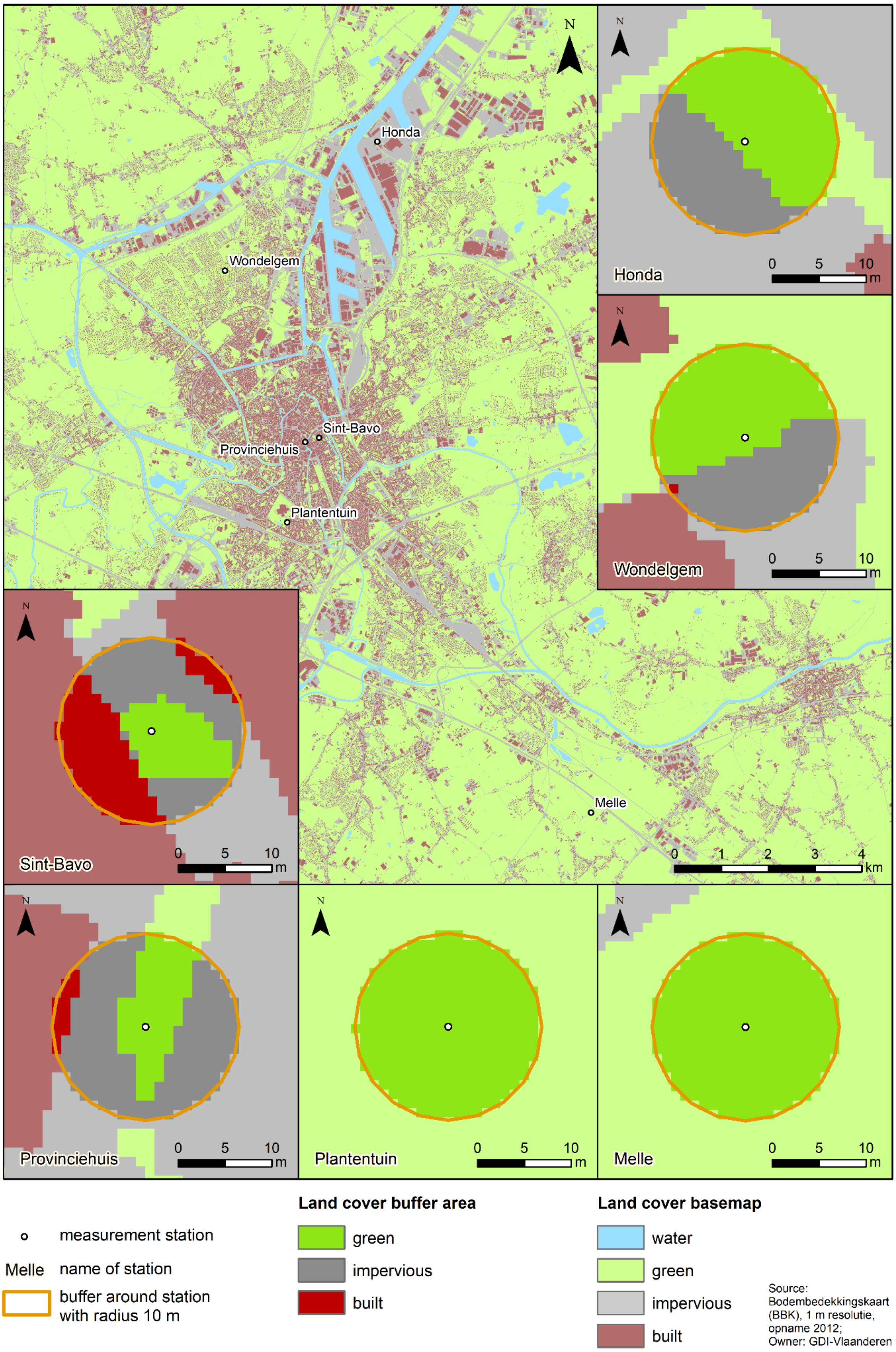

Map 2: Land cover within 10 m radius around the measurement stations.

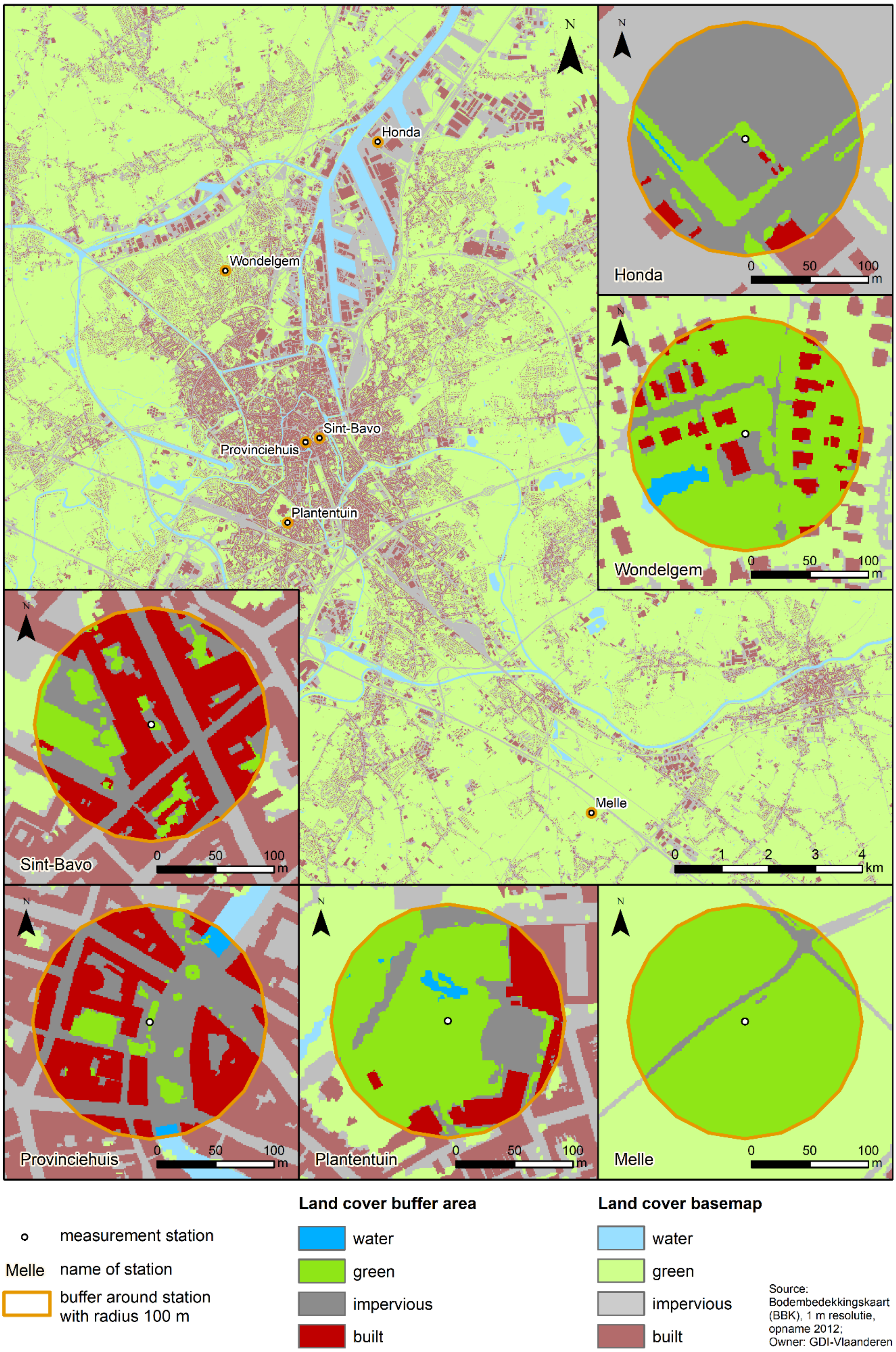

Map 3: Land cover within 100 m radius around the measurement stations.

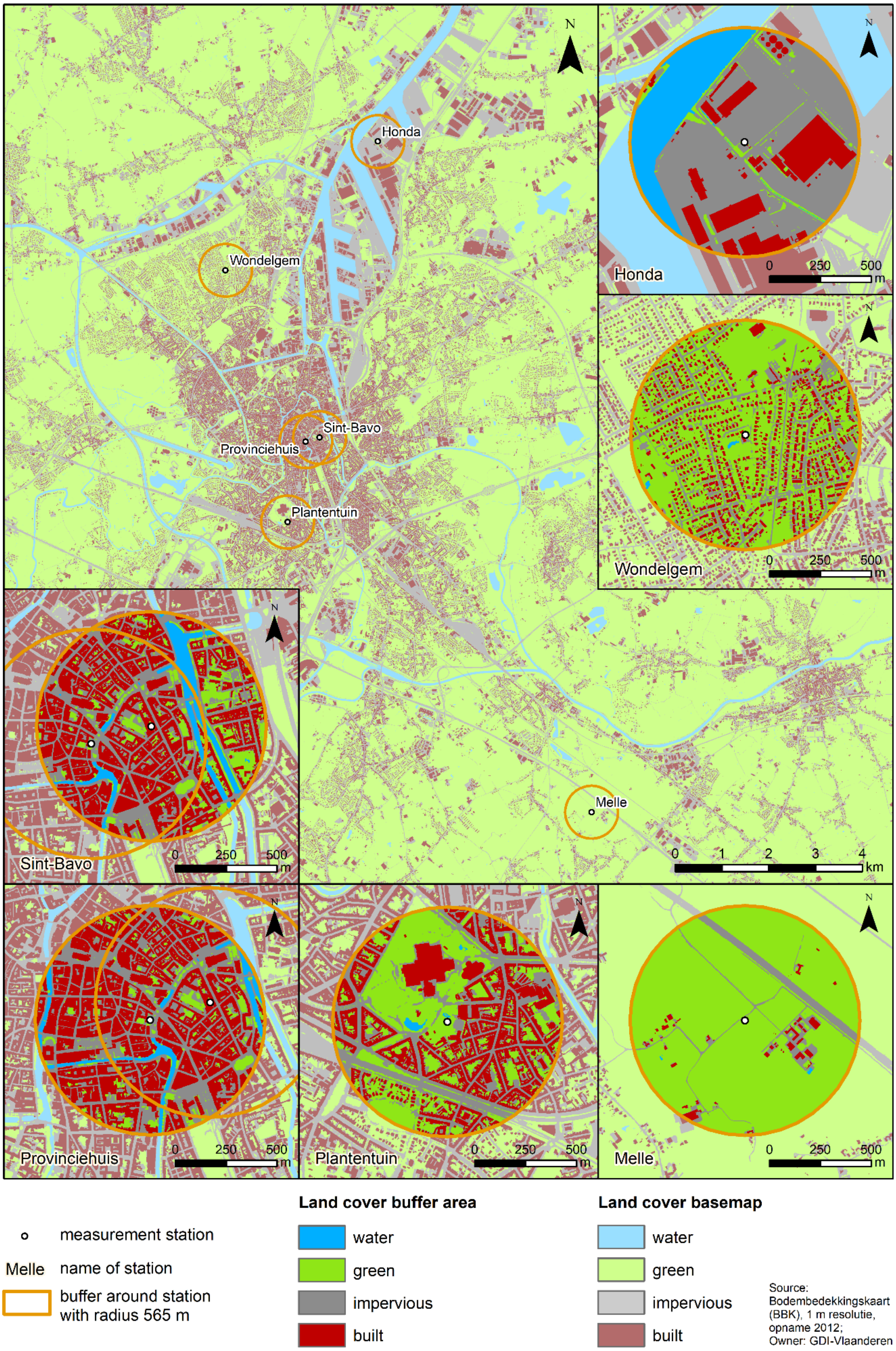

Map 4: Land cover within 565 m radius around the measurement stations.

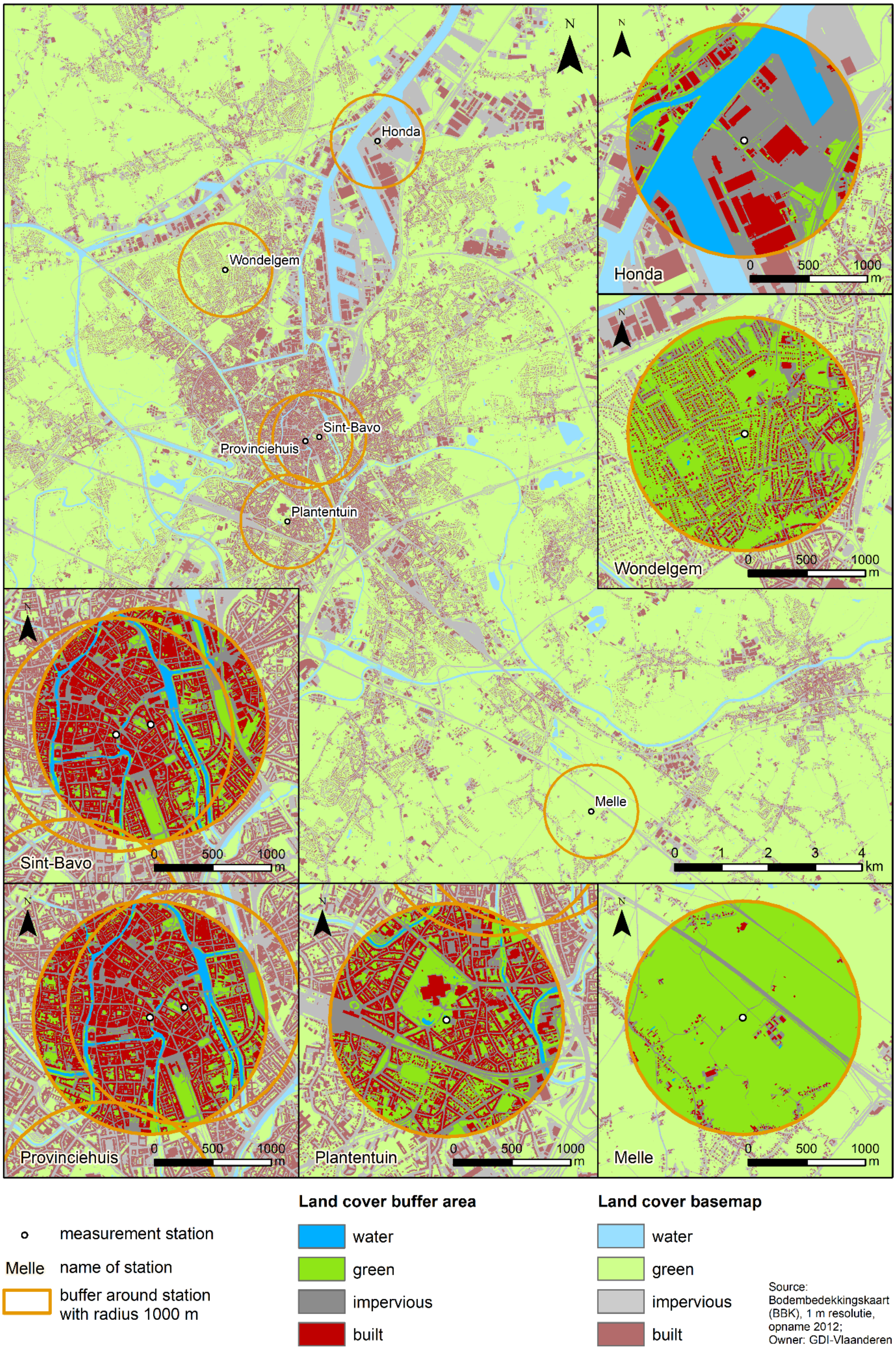

Map 5: Land cover within 1000 m radius around the measurement stations.

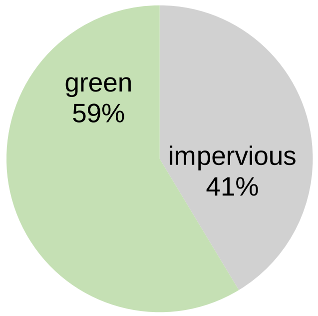

Figure 7a: 10 m buffer Honda.

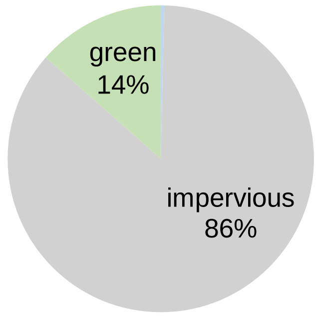

Figure 7b: 100 m buffer Honda.

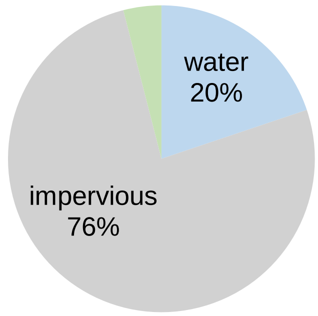

Figure 7c: 565 m buffer Honda.

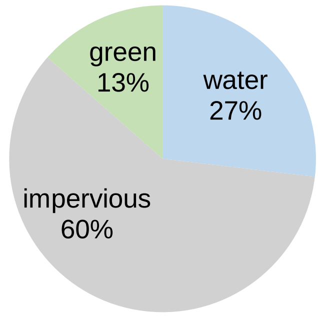

Figure 7d: 1000 m buffer Honda.

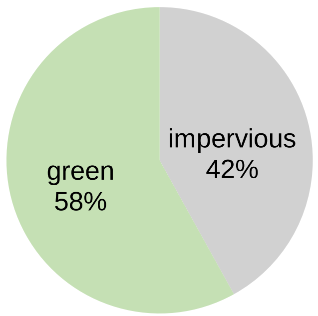

Figure 8a: 10 m buffer Wondelgem.

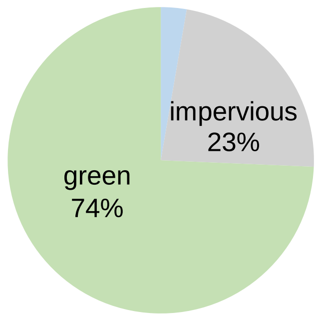

Figure 8b: 100m buffer Wondelgem.

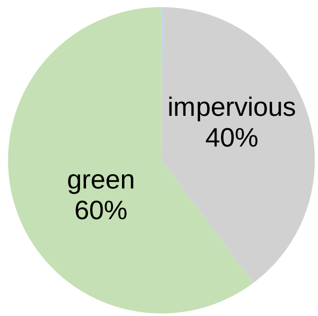

Figure 8c: 565 m buffer Wondelgem.

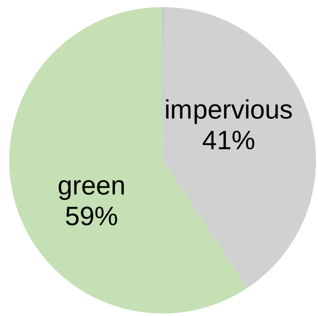

Figure 8d: 1000 m buffer Wondelgem.

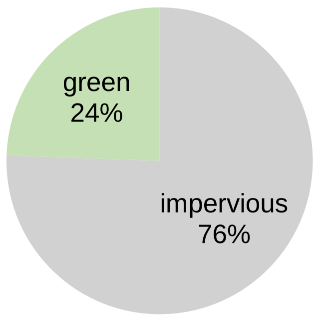

Figure 9a: 10 m buffer Sint-Bavo.

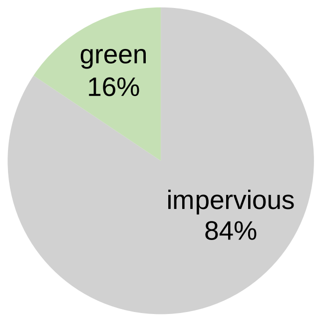

Figure 9b: 100 m buffer Sint-Bavo.

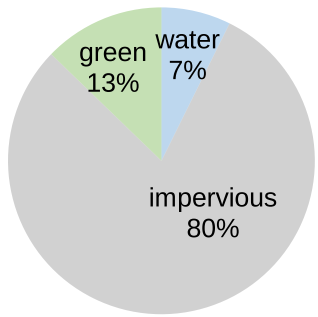

Figure 9c: 565 m buffer Sint-Bavo.

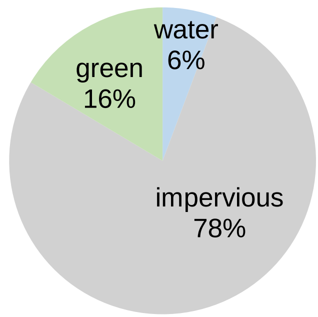

Figure 9d: 1000 m buffer Sint-Bavo.

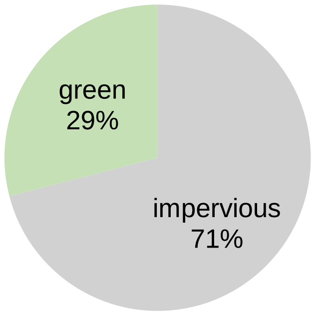

Figure 10a: 10 m buffer Provinciehuis.

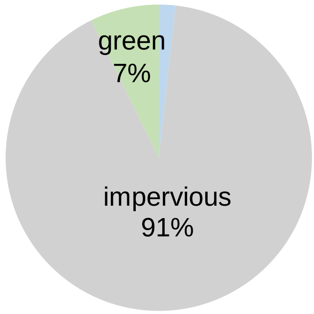

Figure 10b: 100 m buffer Provinciehuis.

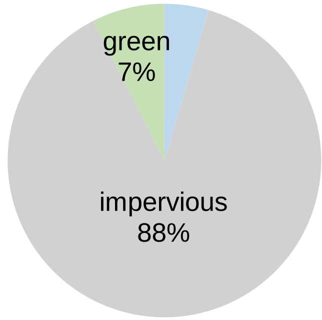

Figure 10c: 565 m buffer Provinciehuis.

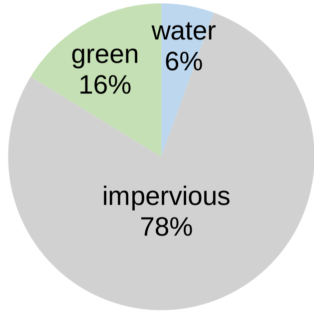

Figure 10d: 1000 m buffer Provinciehuis.

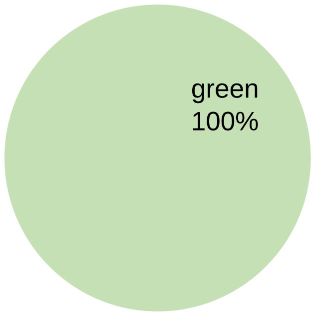

Figure 11a: 10 m buffer Plantentuin.

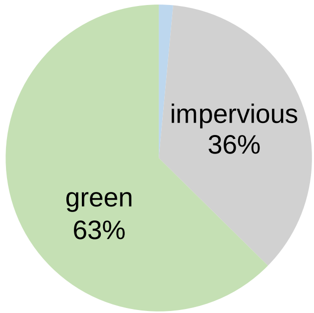

Figure 11b: 100 m buffer Plantentuin.

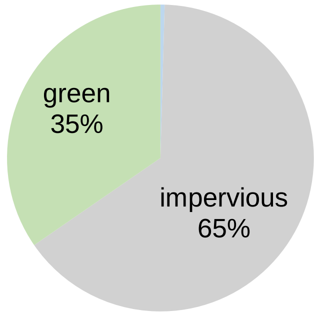

Figure 11c: 565 m buffer Plantentuin.

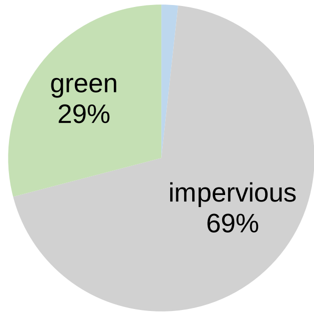

Figure 11d: 1000 m buffer Plantentuin.

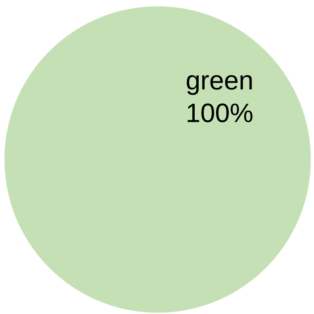

Figure 12a: 10 m buffer Melle.

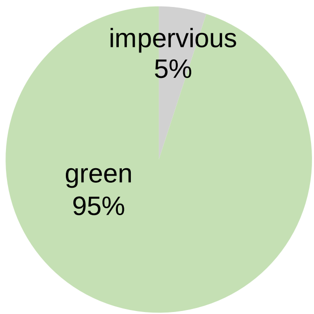

Figure 12b: 100 m buffer Melle.

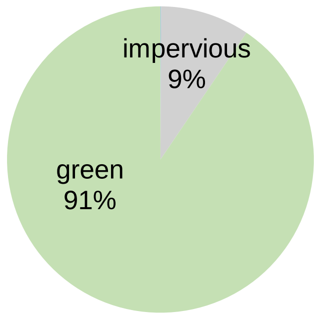

Figure 12c: 565 m buffer Melle.

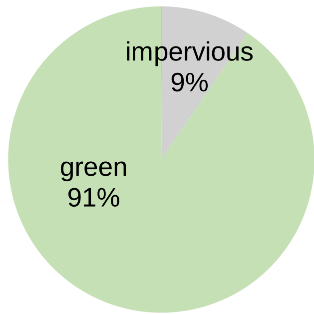

Figure 12d: 1000 m buffer Melle.

5.1.1.1 Honda

The Honda measurement station is located on the lawn next to a sports court and parking, as observed in figure 13. Therefore, the land cover of the micro-environment consists of a green and impervious part, as observed in map 2. Deduced from figure 7a, the micro-environment of the station consists of 59% green and 41% impervious surface. As can be seen in figure 7a and 7b, the impervious fraction increases extremely at the expense of the green space if the buffer area is enlarged to a 100 m radius. This is mainly due to features like car parks and roads as can be observed on figure 13. There are also some buildings within this buffer, but this is a minor fraction of the impervious surface. By going to a buffer distance of 565 m this changes. Deduced from map 3 and 4, there are more buildings that are part of the impervious fraction in the 565 m radius. On this level the environment consists of 20% water which is a new feature. This large fraction of water is due to the characteristics of the port. Thus, the level of 1 km² is the most detailed scale on which the first characteristics of the port can be seen. Going to the larger area of buffer distance 1000 m gives a similar result, as seen on map 5. Here, the impervious surface even still decreases at the expense of the water and green fraction (figure 7d).

Figure 13: Picture of the measurement station at the Honda site (Source: Peter Camps, 25/06/2017).

5.1.1.2 Wondelgem

The micro-environment of the Wondelgem station is similar to the one of Honda based on figure 8a. Here the station is located above lawn next to a car park that is surrounded by green, as depicted in figure 14. The only observed difference on map 2 is that the station of Wondelgem is located closer to some buildings. However, the distribution of the buffer with a 100 m radius differs completely from the one of Honda (figure 7b and 8b). At this scale there is more green space compared to the Honda station. On map 3 different buildings are visible around the station. These are almost all houses of the Wondelgem district and they form the major part of the impervious surface. The large fraction of green is due to a public park, the gardens around the houses and the green infrastructure along the roads. In the public park there is a pond that is responsible for the fraction of water in a radius

Figure 14: Picture of the measurement station in Wondelgem (Source: Peter Camps, 25/06/2017).

of 100 m. At the level of the 565 m buffer, this water fraction has less influence (map 4). Here, the fraction of impervious land cover increases at the expense of the water and green surface, as can be seen on figure 8c. In contrast to the 100 m buffer, the 565 m buffer contains different groups of houses delineated by streets. If figure 8c and 4d are compared, then a similar land cover distribution is observed for the 1000 m buffer. As seen on map 4 and 5, the structure of those two buffers is comparable as well. The only difference between the 565 m and 1000 m radius is the larger area that is taken into account.

5.1.1.3 Sint-Bavo

Figure 15: Picture of the measurement station at Sint-Bavo school (Source: Peter Camps, 25/06/2017).

The Sint-Bavo measurement station is located above a small lawn in between two buildings, as depicted on figure 15 and map 2. On map 2 and figure 9a the impervious fraction is the dominant land cover with 76% for the area of the smallest buffer. Also different from the previous stations is the large portion of built area at micro level. Going to the buffer area with 100 m radius this impervious surface even increases with 8% (figure 9a and 9b). At this level the canyon between the buildings consists of concrete and green spots, as observed on map 3. Here, the distribution green-impervious-water is comparable to the one of the Honda station (figure 9b and 7b). However, on map 3 can be seen there is a huge difference in the proportion built and concrete surface of the impervious fraction for these two stations. At the level of 1 km² (figure 9c), a considerable fraction of water appears at the expense of the impervious and green fraction. As observed on map 4, this water fraction is coming from the rivers flowing through the historical city centre of Ghent. The distributions of figure 9c and 9d are similar. The only difference between the 565 m and 1000 m radius is the slightly larger amount of green fraction. Because of the larger buffer distance, the covered area includes more open spaces, like public parks at the border of the historical city centre. Comparing map 4 and 5 shows that the 565 m buffer represents the densely built centre better.

5.1.1.4 Provinciehuis

The measurement station Provinciehuis is situated in between vegetation surrounded by car parks, as depicted on figure 16 and map 2. The land cover distribution of the micro-environment is similar to the distribution of Sint-Bavo (figure 10a and 10a). On map 2 the difference in built area at micro scale is observed between the stations Provinciehuis and Sint-Bavo. While the measurement station of Sint-Bavo is located in a narrow urban canyon, the station of Provinciehuis is situated near to only one building in the West direction. At the scale of the 100 m buffer the fraction of impervious surface

Figure 16: Measurement station near the building Provinciehuis indicated with yellow circle (Source: Peter Camps, 25/06/2017).

increases considerably and a small fraction of water appears (figure 10b). This water fraction is due to the historical flow of the river Scheldt through the city centre and is artificially maintained today. As seen on map 3 the fraction of built area is less at this scale level compared to the area around the Sint-Bavo station. This is due to the square next to the station Provinciehuis and broader streets within this area. At the level of 1 km² the water fraction increases slightly at the expense of the impervious fraction (figure 10c). There is a large overlap with the buffer of 565 m around the Sint-Bavo station, as observed on map 4. Although the land cover fractions of Provinciehuis and Sint-Bavo do still differ at this scale level (figure 10c and 9c). This is not the case anymore at the level of the 1000 m buffer. Comparing figure 9d and 10d shows the fractions are exactly the same at this level. Also on map 5 it is clear that the 1000 m buffer of Provinciehuis covers almost the same area of the 1000 m buffer of Sint-Bavo. From this observation can be derived that those two stations represent a same environment at this scale level. Both embody the urban environment of the historical centre of Ghent. With a more detailed scale there is still heterogeneity, as showed with the 565 m buffer.

5.1.1.5 Plantentuin

The station Plantentuin is located in between the vegetation of the botanical garden of Ghent University, as illustrated in figure 17. Therefore the land cover in the direct environment of the station consist of 100 % green space, as can be seen in figure 11a and map 2. Because the station is positioned under trees and not above lawn, the observations can be influenced (Pielke *et al*., 2007). On the smaller scale of the 100 m radius the land cover exists of a pond, a square, roads and buildings (map 3). This

Figure 17: Picture of the measurement station Plantentuin (Source: Peter Camps, 25/06/2017).

causes a change from homogeneous to heterogeneous environment though adapting the scale level. Moreover the distribution of the land cover fractions transforms as represented in figure 11b. There appears a small fraction water of 1% and a impervious part of 36% at this scale level. Going to the larger radius of 565 m implies a larger impervious fraction since the station is located in a park of the city. This is observed on figure 11c and map 4, where it is clear the green spaces are surrounded by a dense network of impervious features. At this level there is still a large green fraction due to the public parks in this neighbourhood and the water fraction is even smaller because there are only some small ponds within this area. At the scale level of the 1000 m buffer the land cover fraction distribution is similar to the one of 565 m (figure 11c and 11d). The impervious part and water fraction increased slightly at the expense of the green space. The increase in water is due to the rivers flowing through the city come into focus, while the larger impervious part is due to the more densely built areas in the north and west of this buffer. On map 5 it is observed that the 1000 m buffer around the Plantentuin station intersects the 1000 m buffers of Provinciehuis and Sint-Bavo. Due to the different public parks in the environment of the Plantentuin station, the green fraction is still present with 29%. This stands in contrast with the smaller green fraction of the stations Provinciehuis and Sint-Bavo in the core of the city (figure 11d, 9d and 10d). By looking at figures 11a, 11b, 11c and 11d, it is noticed a larger buffer area around the Plantentuin station implies a larger the impervious fraction. This is due to the fact that this station is located in a green patch of the city. Therefore the completely green micro-environment stands in sharp contrast with the features in the broader area around the station.

5.1.1.6 Melle

Just like the Plantentuin station this station has a complete green coverage at a radius of 10 m (figure 12a and map 2). In contrast to the Plantentuin station this station is placed above lawn, as depicted in figure 18. At the scale level of the 100 m buffer this station has still a large proportion of green coverage (figure 12b). As observed on map 3, the small impervious part consists mainly of linear road segments. In the 1 km² area around the station the land cover fractions are similar to the fractions of the 100 m buffer (figure 12c and 12b). There is a green matrix with some small groups of buildings and linear elements of concrete that represent roads as observed on map 4. Comparing figure 12c and 12d shows the 565 m and the 1000 m buffers have the same land cover fractions. Looking to the land cover distribution at different scales, it is clear this station includes the characteristics of a rural place. This can also be seen on map 5, where the 1000 m buffer is represented.

Figure 18: Picture of the measurement station in Melle (Source: Peter Camps, 25/06/2017).

5.1.1.7 General outcomes land cover

For all stations the land cover fractions do not change a lot going from a 565 m radius to a 1000 m radius (figures 7a - 12d). The land cover around the MOCCA stations is thus quite scale independent when going from the 565 m buffer scale to the 1000 m scale. Therefore, it is expected that model results with implementation of the 100 m radius land cover fractions will differ more from the 565 m data than the 1000 m model results. In addition, similar entities can visually be distinguished at 565 m and 1000 m radius scale, thus from landscape perspective those two radii comprise a similar spatial scale level (map 4 and 5). Besides this, it is not possible to distinguish between the two stations in the historical city centre when using the land cover of the 1000 m buffer. This is only possible when a smaller buffer distance is used.

5.1.2 Fraction of buildings

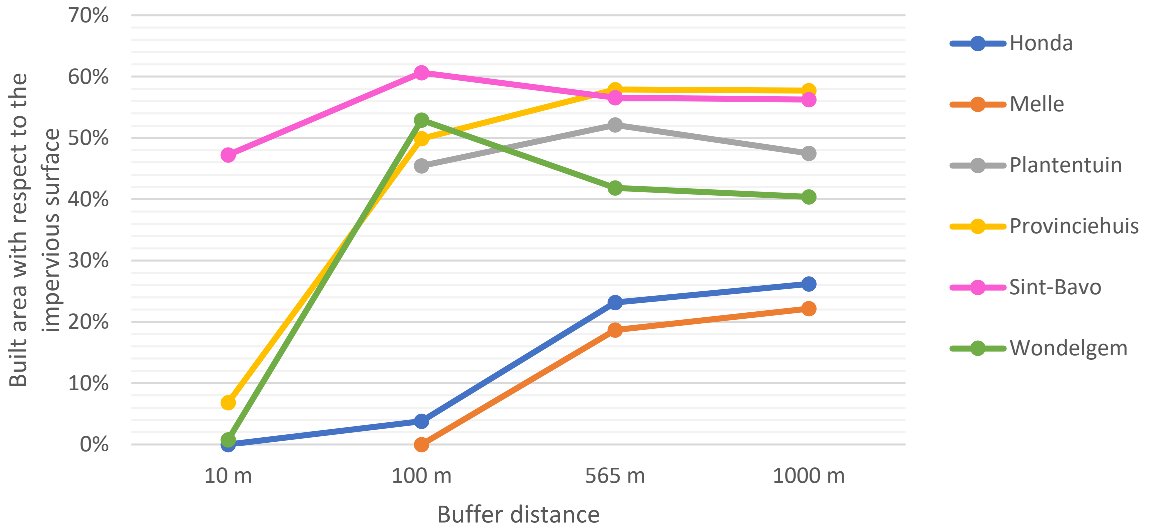

Figure 19: Fraction of buildings for each buffer area around the measurement stations.

In figure 19 the fraction of buildings is given with respect to the total impervious surface. Because the stations Melle and Plantentuin only consist of green features within the 10 m radius, there is no built fraction. Therefore the ratio built-impervious surface cannot be calculated for those stations at this level. At the scale level of the 10 m radius, the built fraction is equal to 0% for the Honda station because there are no buildings. For the Wondelgem station there is almost no built fraction, since only a little part of a building is lying within the buffer distance of 10 m (map 2). Both stations in the city centre have a considerable built fraction at this scale level. The station Provinciehuis has a small fraction of built area, while Sint-Bavo possesses a large fraction of built area. This large fraction is due to the location of the Sint-Bavo station within the narrow urban canyon.

At the scale level of the 100 m buffer, the high built fraction of Wondelgem is remarkable. On map 3 it can be seen that there is little concrete surface coming from roads or squares. This is caused by overhanging trees in this area. Thus, for Wondelgem there is a notable underestimation of the concrete fraction, since it is overlaid with green features. Therefore, the built fraction is lower in reality. Also around the Plantentuin station, the trees do overlap the roads frequently. Thus, also for this station there is an observable overestimation in built fraction. Another striking feature are the low values of the stations Melle and Honda compared to the high values of Plantentuin, Provinciehuis, Sint-Bavo and Wondelgem. The latter stations are located in densely built zone, while the Melle and Honda station are characterised by more open space. This aspect is also observed for the 565 m and 1000 m buffer, however the contrast becomes smaller if the buffer distance increases. Despite Melle and Honda are both stations in a less built environment, there is still a difference in the land cover of the open space as described in the previous sections concerning the land cover. Melle is a rural location with a lot of green space, while Honda is an industrial site with a large amount of concrete used as parking or storing place.

Table 5: Building fractions for the buffer distance of 565 m around the station.

Location	Building fraction (%)
Honda	23
Melle	19
Plantentuin	52
Provinciehuis	58
Sint-Bavo	57
Wondelgem	42

At the scale level of the 565 m radius, the expected order is obtained in terms of characteristics intuitively linked to the locations of the stations. Here, Provinciehuis and Sint-Bavo, the two locations in the city centre, obtain the highest built fraction of respectively 58% and 57% (table 5). Moving further away from the centre the environment is more open around the Plantentuin and Wondelgem stations. The 1 km² area around the Plantentuin station is characterised by a building fraction of 52%, while the area around the Wondelgem station has a building fraction of 42% at this scale level (table 5). As mentioned before the environments around the Honda and Melle stations have a low built fraction. From table 5 is deduced that there are 23% buildings around the Honda station and 19% around the Melle station at the scale level of 1 km². In general, the percental building fractions for each station are almost the same if the 565 m buffer and the 1000 m buffer are compared. Another remarkable thing is the similar evolution of the built fraction over the different radii for the Honda and Melle environments.

5.1.3 Building height

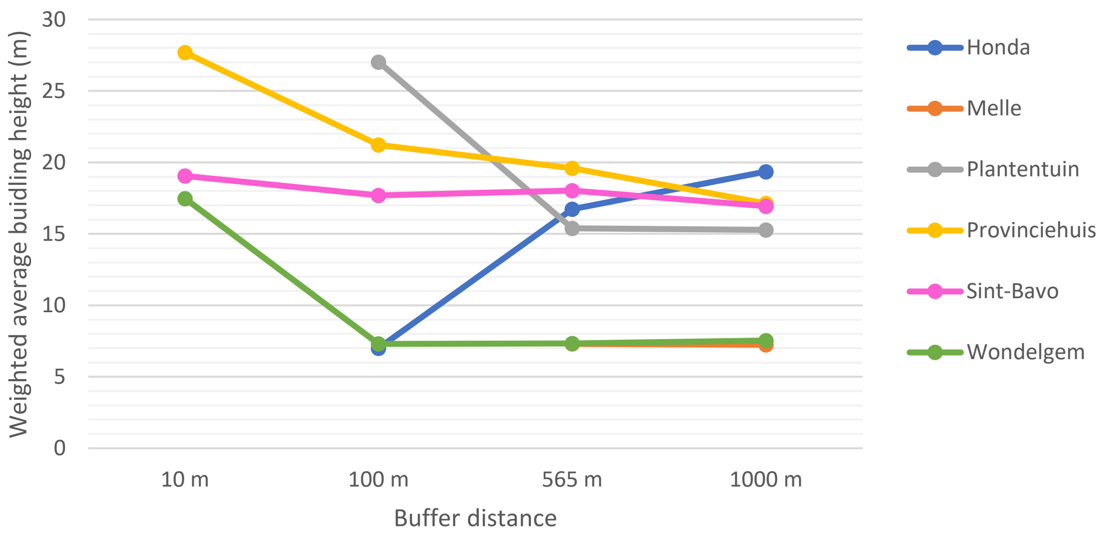

Figure 20: Weighted average building height for each buffer distance around the measurement stations.

In figure 20 the weighted average of the building heights for each station and the different buffer distances are given. The stations Honda, Plantenuin and Melle do not have a value for the radius of 10 m because there are no buildings within this buffers. Also in the 100 m buffer of the Melle station there are no buildings, so no average building height can be calculated. The average building height in the 10 m buffer of the stations Provinciehuis and Wondelgem is the height of only one building lying partly within the buffer (map 2). Thus, the information about the building height in the 10 m buffer is limited.

For a radius of 100 m around the stations the average building height is high for the Plantentuin site compared to the other ones. This is because two large buildings are lying partly within this buffer distance. This creates a wrong picture of this area because the buildings just outside the buffer are much lower. In contrast to this, the buildings within the 100 m radius of the Honda station are small around the sports court. Consequently, this buffer area does not include the height of the industrial buildings. Previous problems do not occur for a buffer distance of 100 m around the Wondelgem, Sint-Bavo and Provinciehuis stations. These buffer areas contain more buildings, so taking an average here makes more sense. The stations Provinciehuis and Sint-Bavo have on average high buildings, while there are on average low buildings situated around the Wondelgem station. This is what is expected since the Provinciehuis and Sint-Bavo stations are located in the densely built city centre, whereas the Wondelgem station is located in a residential neighbourhood. From the 100 m buffer onwards the average building height stays more or less constant for the Sint-Bavo and Wondelgem site. The average building heights around the Sint-Bavo station are even similar to each other for all buffer distances. This does not mean the buildings do have the same height on average in the city centre. There is namely a difference between the average building height around the Provinciehuis and Sint-Bavo station at scale level of the 100 m and 565 m buffer. Since both stations are located in the city centre this indicates there is quite some variation in building height within the historical centre. The more the buffer areas of the Sint-Bavo and Provinciehuis station overlap, the more the average building height of those two stations converges. There is a decrease in the building heights if the buffer area of the Provinciehuis station grows.

Table 6: Weighted average building height for the buffer distance of 565 m around the station.

Location	Weighted average building height (m)
Honda	16,7
Melle	7,3
Plantentuin	15,4
Provinciehuis	19,6
Sint-Bavo	18,0
Wondelgem	7,3

At 565 m and 1000 m buffer distance two groups of stations are distinguished. The stations Provinciehuis, Sint-Bavo, Honda and Plantenuin have rather high buildings, while the stations Wondelgem and Melle comprise more low rise buildings. Melle and Wondelgem have both an average building height of 7,3 m at the scale level of 1 km² (table 6). Over all the buffer distances the values of the weighted average building height of Melle are more or less the same as those of Wondelgem, if buildings are present. At the 565 m scale the highest buildings are on average situated around the Provinciehuis station, followed by the Sint-Bavo station. Those locations have respectively an average building height of 19,6 m and 18,0 m (table 6) at the 1 km² scale. This is in contrast with what is observed at the 1000 m scale level. Here, the buildings around the Honda station are on average higher than those around the Provinciehuis and Sint-Bavo station. This phenomenon is caused by the fact that a larger buffer around the stations in the city centre reduces the influence of some high historical monuments in the centre. In addition the larger buffer area around the Honda station comprises a large, high building that results in an increase of the average of the building height. For the stations Melle, Wondelgem, plantentuin and Sint-Bavo the average building height is similar for the 565 m buffer and the 1000 m buffer. This does not hold for the stations Honda and Provinciehuis, where there is a difference for each scale level.

5.2 Spatial scale and UHI

By comparing the diurnal evolution of the temperature with the land cover fractions at different spatial scales an estimation is made over which area the temperature is influenced by the land cover. In table 7 the rankings of the impervious land cover fractions on different spatial scales are compared with the rank of the temperature for the different locations.

A small fraction of impervious surface is expected to cause lower temperatures. During nighttime the rural Melle location is coldest (figure 21), since there is a only negligible fraction of artificial building materials in the direct environment that can release heat (figures 12a, 12b, 12c and 12d). Based upon the land cover fractions of the 10 m buffer, it is expected that the Plantentuin and Melle station measure continuously the lowest temperatures (figures 11a and 12a). For the Plantentuin location this lower temperatures are the case during daytime but not during nighttime (figure 21). The warmer temperatures during the night indicate that a larger buffer area should be considered to take as well the heat release into account of the buildings that surround the urban park. In contrast to this, the lower temperatures during the day can be related to the shadow and cooling effect of evapotranspiration by the trees around the station. Those low temperatures during daytime, induced by micro-environment features, result in a negative UHI (figure 22).

For the Honda location the observed temperatures neither correspond with what is expected from the land cover of the micro-environment as observed in table 7. For this site there is a lot of green in the 10 m radius, but the measured temperatures at this location are consistently warmer than the temperatures at other locations with a larger impervious fraction for the 10 m buffer. Therefore, it is deduced that the temperature and UHI are influenced by the land cover of the larger 1 km² environment.

Table 7: Ranking of the stations based on the impervious land cover fraction (lowest impervious fraction has value 1) and temperature (lowest temperature has value 1) (For absolute temperature values see Annex VII). Daytime is defined as the period from 5 UTC to 19 UTC and nighttime is defined as the period form 20 UTC till 4 UTC.

Location	10 m	100 m	565 m	1000 m	Daytime temperature (°C)	Nighttime temperature (°C)
Honda	3	5	4	3	4	4
Melle	1/2	1	1	1	2	1
Plantentuin	1/2	3	3	4	1	3
Provinciehuis	5	6	6	5/6	6	5/6
Sint-Bavo	6	4	5	5/6	5	5/6
Wondelgem	4	2	2	2	3	2

From table 7 it is derived that the order of the stations based upon their nighttime temperatures correspond well with the 565 m buffer rank in impervious surface. This is an indication that the observed UHI is influenced by features in a radius of 565 m and thus taking into account the land cover of this radius is important for UHI studies. During daytime a slightly different order is obtained for the temperatures. This order cannot be linked to a specific spatial scale by looking to the different rankings of the land cover. Therefore, other spatial features must be taken into account as well.

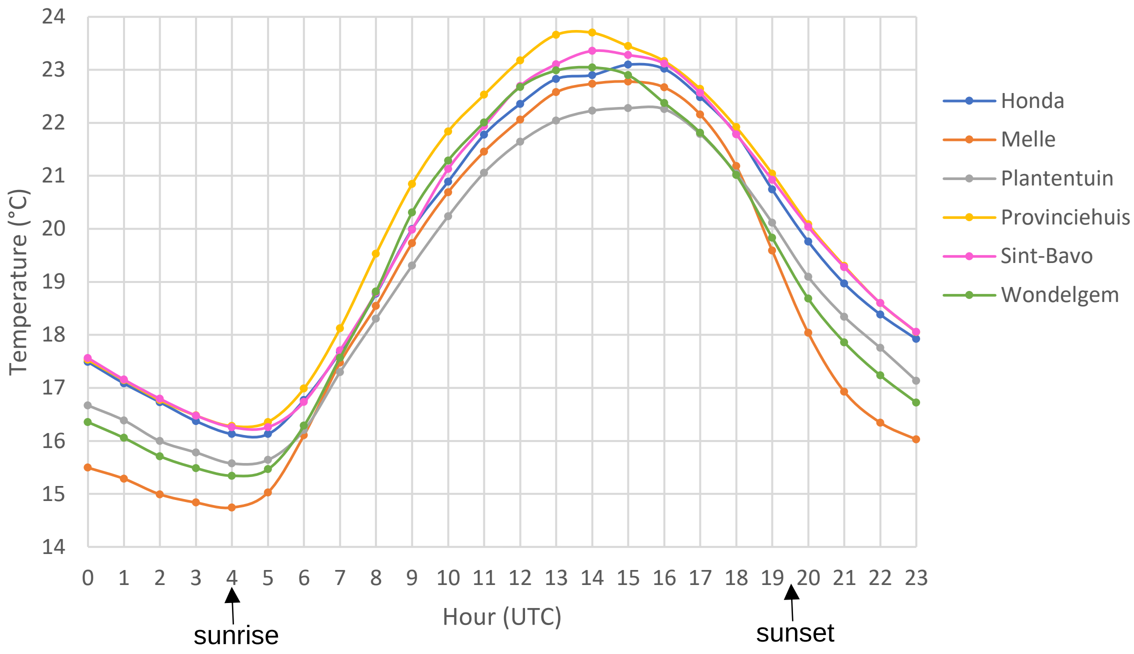

Figure 21: Diurnal evolution of the temperature at the different MOCCA measurement sites over the period of July and August 2016.

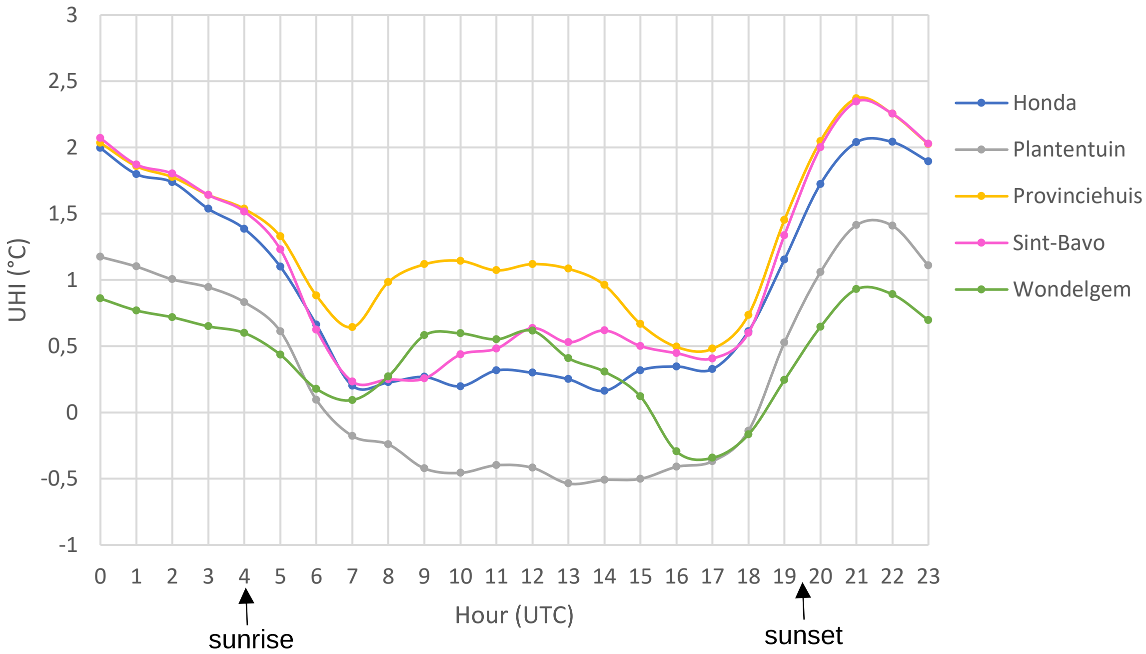

Figure 22: Diurnal evolution of the UHI at the different MOCCA measurement sites over the period of July and August 2016.

On figure 21 it is observed that the temperature increases first at the Melle location just after sunrise. The first urban station that experiences an increase in temperature after sunrise is the Provinciehuis station. This temperature increase in the morning is not that pronounced at the Sint-Bavo location, the other location in the city centre. This difference is due to the difference in exposure to direct sunlight. The Melle station is not surrounded by buildings and thus the first sunlight is heating directly the surface and the air surrounding the station. In contrast to this, the Sint-Bavo station is located in a narrow urban canyon and thus the measurement station is shielded from direct sunlight in the morning. For the Provinciehuis station only a building is sited in the north-east direction, as visible on map 2 and 3. Therefore, the direct radiation of the morning sunlight causes a higher temperature at this location compared to the Sint-Bavo station. Subsequently, the UHI reaches a first small peak in the morning hours at the Provinciehuis location, as can be observed in figure 22. A similar explanation can be given to the lower temperatures at the Wondelgem location in the late afternoon. At this location there is a building located in the south-west of the station that blocks the direct sunlight between 15 UTC and 19 UTC (map 2 and 3). As seen in figure 22, this lower temperatures at the Wondelgem site result in negative values for the UHI.

During daytime there are differences in the temperatures between the two stations in the city centre. In order to explain those differences based upon the land cover, a spatial area smaller than 1000 m radius is needed since from this scale onwards the land cover fractions are the same for both stations in the city centre.

Based upon these case studies the micro-environment seems to be more important to explain the temperature variations during the day. An environment with a scale in between the radius of 10 m and 100 m explains the temperature evolutions during the day. From this can be concluded that the micro-environment is important to understand the observed temperatures and UHI during daytime and the local environment of about 1 km² is more important to understand the temperatures and UHI during nighttime.

5.3 Quality of the land cover data

The quality of land cover data for each station is examined by comparing the land cover data in ECOCLIMAP-I and ECOCLIMAP-II with the data obtained from the GIS-analysis. The fractions obtained for the ECOCLIMAP data are the fractions of the pixel in which the measurement station is located, while the land cover fractions of the GIS analysis are the proportions of a buffer around the station. The land cover fractions of the GIS-analysis are more accurate since the land cover was extracted from the high resolution data from the BBK instead of the coarse land cover data within the ECOCLIMAP modules. Only the data of the 565 m buffer from the BBK is compared with the ECOCLIMAP data. By doing this, data on a scale level of about 1 km² is compared with each other. This is important since the previous section showed that land cover fractions depend on the scale level. In tables 8, 9, 10, 11, 12 and 13 it is observed there is in none of the datasets a sea fraction detected for the studied sites. This is in accordance with the expectations since Ghent is not a coastal city.

5.3.1 Honda

The land cover fractions around the Honda station differ a lot for each data source as shown in table 8. ECOCLIMAP-I and the BBK both give a low value for the green space, while ECOCLIMAP-II gives a very high value. Similar results are obtained for the impervious fraction where the value is high for ECOCLIMAP-I and BBK, while ECOCLIMAP-II gives a very low value. With the considerable amount of water fraction the BBK differs from ECOCLIMAP-I and ECOCLIMAP-II. Thus, only from the BBK dataset can be derived that the Honda measurement station is located in the harbour. Based on the BBK and field knowledge ECOCLIMAP-II is completely wrong in estimating the land cover around the Honda station. ECOCLIMAP-I is doing better, but this dataset neither contains the water fraction as it is expected in the environment of the harbour.

Table 8: Land cover fractions for ECOCLIMAP-I, ECOCLIMAP-II and GIS analysis based upon BBK around the Honda station.

Honda	ECOCLIMAP-I	ECOCLIMAP-II	BBK
Sea	0,0	0,00	0,00
Green space	0,1	0,99	0,04
Water	0,0	0,00	0,20
Concrete	0,9	0,01	0,76

5.3.2 Wondelgem

None of the datasets contain a significant water fraction around the Wondelgem station as observed in table 9. Compared to ECOCLIMAP-I, ECOCLIMAP-II estimates the land cover of the higher resolution BBK data slightly better. However, the difference between the land cover fractions of ECOCLIMAP-I and ECOCLIMAP-II is small. This small difference is solely due to the lower precision of the ECOCLIMAP-I data.

Table 9: Land cover fractions for ECOCLIMAP-I, ECOCLIMAP-II and GIS analysis based upon BBK around the Wondelgem station.

Wondelgem	ECOCLIMAP-I	ECOCLIMAP-II	BBK
Sea	0,0	0,00	0,00
Green space	0,4	0,45	0,60
Water	0,0	0,00	0,00
Concrete	0,6	0,55	0,40

Compared to the land cover fractions derived from the BBK, ECOCLIMAP-I and ECOCLIMAP-II have a lower amount of green space at the expense of the impervious space. As mentioned in the section ‘Method’ a simplification of the categories was made to retain only four classes. Since the measurement station of Wondelgem is located in a suburban area, characterised by trees hanging over roads, there could be a significant overestimation of green surface. Still it is unlikely that the difference in green surface between the BBK data and ECOCLIMAP data is fully due to trees hanging over the asphalt.

5.3.3 Sint-Bavo and Provinciehuis

In table 10 and 11 it is observed that the land cover fractions derived from ECOCLIMAP-I and ECOCLIMAP-II do not differ for the area around the Sint-Bavo and Provinciehuis stations. When the ECOCLIMAP-I and ECOCLIMAP-II land cover fractions of Sint-Bavo and Provinciehuis are compared (table 10 and 11), then it is seen that they are the same. This is because both stations are located at the same pixel in both ECOCLIMAP datasets.

Table 10: Land cover fractions for ECOCLIMAP-I, ECOCLIMAP-II and GIS analysis based upon BBK around the Sint-Bavo station.

Sint-Bavo	ECOCLIMAP-I	ECOCLIMAP-II	BBK
Sea	0,0	0,00	0,00
Green space	0,1	0,10	0,13
Water	0,0	0,00	0,07
Concrete	0,9	0,90	0,80

Table 11: Land cover fractions for ECOCLIMAP-I, ECOCLIMAP-II and GIS analysis based upon BBK around the Provinciehuis station.

Provinciehuis	ECOCLIMAP-I	ECOCLIMAP-II	BBK
Sea	0,0	0,00	0,00
Green space	0,1	0,10	0,07
Water	0,0	0,00	0,05
Concrete	0,9	0,90	0,88

The most striking difference between the BBK and ECOCLIMAP data is the missing water fraction in the ECOCLIMAP datasets for the Sint-Bavo and Provinciehuis locations. Compared to the ECOCLIMAP data, the BBK data contains a larger fraction green at the expense of the concrete fraction for the Sint-Bavo station. This is not the case for the Provinciehuis station, where the BBK land cover shows a lower percentage green than ECOCLIMAP. Since the land cover fractions deviate less between the BBK and ECOCLIMAP for the Provinciehuis station it is assumed that the differences in the modelled temperatures and UHI will be smaller for this station.

5.3.4 Plantentuin

Similar to the Wondegem location, none of the land cover datasets contains a significant amount of water for the area around the Plantentuin station at the scale level of 1 km² (table 12). For the Plantentuin location the difference in land cover fractions between each dataset is small. The difference between ECOCLIMAP-I and ECOCLIMAP-II is again due to the rounding of the values of ECOCLIMAP-I. The land cover fractions of ECOCLIMAP-II are therefore closer to those of the BBK. For the land cover around the Plantentuin station the concrete fraction is highest for the BBK and lowest for ECOCLIMAP-I.

Table 12: Land cover fractions for ECOCLIMAP-I, ECOCLIMAP-II and GIS analysis based upon BBK around the Plantentuin station.

Plantentuin	ECOCLIMAP-I	ECOCLIMAP-II	BBK
Sea	0,0	0,00	0,00
Green space	0,4	0,37	0,35
Water	0,0	0,00	0,00
Concrete	0,6	0,63	0,65

5.3.5 Melle

Similar to the area around the Wondelgem and Plantentuin stations, the datasets do not contain a significant water fraction around the Melle station as observed in table 13. Another similarity to the land cover results of the Wondelgem and Plantentuin stations is that the values of ECOCLIMAP-I and ECOCLIMAP-II do not differ a lot. Also here the small difference is solely due to the lower precision of the ECOCLIMAP-I data. Because of this, the land cover fractions of ECOCLIMAP-II are closer to those of the BBK. Compared to the BBK data, both ECOCLIMAP-I and ECOCLIMAP-II overestimate slightly the green space at the expense of the concrete fraction.

Table 13: Land cover fractions for ECOCLIMAP-I, ECOCLIMAP-II and GIS analysis based upon BBK around the Melle station.

Melle	ECOCLIMAP-I	ECOCLIMAP-II	BBK
Sea	0,0	0,00	0,00
Green space	1,0	0,98	0,91
Water	0,0	0,00	0,00
Concrete	0,0	0,02	0,09

5.3.6 General overview land cover data quality

As observed in tables 9, 12 and 13 the ECOCLIMAP-II database is closer to the values of the high resolution BBK data than the ECOCLIMAP-I database for the stations Melle, Wondelgem and Plantentuin. The land cover around the Honda station is estimated worse by ECOCLIMAP-II than by ECOCLIMAP-I (table 8). From this follows that the ECOCLIMAP-II dataset should be corrected for some areas. Therefore, validation is recommended before ECOCLIMAP-II data is used. For the stations Provinciehuis and Sint-Bavo ECOCLIMAP-I and ECOCLIMAP-II contain the same information, as seen in tables 10 and 11. Since the land cover is estimated better with ECOCLIMAP-II for three out of six locations, it is concluded that ECOCLIMAP-II contains land cover data that is closer to reality than ECOCLIMAP-I.

5.4 SURFEX modelling

In the following sections the model performance for the different parameterisations of each station are examined. This is done by computing the values for the index of agreement, RMSE and bias. The higher the index of agreement, the better the model resembles the observations. Contrary, a high RMSE indicates there is a large difference between temperatures of the model and the observations. A positive bias indicates that the modelled temperatures are gradually warmer than the observed temperatures. A negative bias denotes there is a systematic underestimation by the model. If the bias has value 0, the model has no systematic error. Models often need some tuning and this is also the case for SURFEX (Harshan, 2015). As previously mentioned, this is done with parameter XHUG_ROOT which reflects the value of the liquid SWI in the root zone soil layers (CNRM, *s.d.*). First, the tuning of the model with the parameter XHUG_ROOT is evaluated based on these statistical scores. Subsequently, the model results obtained with different parameterisations for the land cover and city geometry are discussed for each measurement station. For these runs the RMSE is split into a systematic and unsystematic part. This is done in order to examine whether the physical processes are captured better by the model when different land cover data is used or when the default values of the city geometry are replaced by the values obtained from the GIS-analysis. In addition T-tests were carried out between simulated and observed temperatures. When the p-value is smaller than 0,01 then the T-test points out that there is a significant difference between both temperature series with a significance level of 99%. This means that the model is not able to reproduce the observed temperatures well. Also T-tests between the different model outputs of one measurement location are executed to investigate whether the simulated temperatures obtained with the different model parameterisations differ significantly from each other. If they do not differ significantly, then there is no significant improvement or degradation. As seen in table 1 of Annex IX most of the model runs differ significantly from each other.

5.4.1 Model tuning

By changing the parameter XHUG_ROOT the model is tuned in such a way that the modelled temperatures approach the observational temperatures better for the rural station Melle. In table 1 of Annex VIII the different scores for model performance are given for the runs with a different XHUG_ROOT value. The high value 1,00 indicates a wet environment, while a low value 0,01 embodies a dry environment (Harshan, 2015). All the scores indicate that the model gives the best performance for Melle if the parameter XHUG_ROOT is set to 0,01. The following runs are therefore done with this value indicating dry conditions. In table 2 of Annex VIII the values of the UHI of Sint-Bavo are given for runs with a different value of XHUG_ROOT. Here the same conclusion can be drawn since the errors are smallest for the 0,01 run and the index of agreement is largest. Although the scores indicate the best model performance with a small value of XHUG_ROOT, it must be noted that the bias and RMSE are still large and the index of agreement can be improved as well. To improve those scores a better tuning of the model is necessary, thus other tuning parameters should be taken into account to improve the model performance. In other words, SURFEX should be improved in general, so the temperatures are estimated better. Another reason for the bad model results could be a bad forcing that is given as input to the LSM. It should be further investigated, whether it is the forcing or the SURFEX scheme that deteriorates the results.

5.4.2 Land cover

In this section the influence of adapting the land cover input parameters on the modelled temperatures and UHI is studied. This is done by investigating how the model performance changes if different land cover data are implemented in the model. The different model runs are obtained by using the databases ECOCLIMAP-I or ECOCLIMAP-II in SURFEX or by implementing the land cover fractions from the previous analysis of the BBK. First, the modelled temperatures of the reference station Melle are discussed, followed by the modelled temperatures and UHI of the urban stations going from north to south.

5.4.2.1 Melle

In table 14 the results of the model performance of the temperature at 2 m height are represented for the rural station Melle. Although, the differences between the runs seems to be small, the model outputs differ significantly from each other based upon the T-test with a 99% significance level (Table 1 Annex IX). Except for the model runs of the 565 m buffer and the 1000 m buffer there is no significant difference. This is due to the fact that the land cover fractions of those two buffer radii are the same (figures 12c and 12d). Therefore, the simulated temperatures and statistical scores are the same for the 565 m and 1000 m buffer (table 14). The modelled temperatures are in general lower than the observed temperatures that have an average of 18,56°C over the studied period of August. This is reflected as well by the negative bias over all runs with a different land cover parameterisation. Thus, no matter which land cover parameterisation is chosen the model underestimates the observations. Therefore, an overestimation of the modelled UHI is likely, since Melle is used as reference station for the rural environment. The p-values in table 14 are lower than 0,01 in all of the cases. The conclusion that can be drawn from this is that the simulated temperatures do not agree well with the observed temperatures. This might be due to the poor tuning of the model or a bad forcing. From table 14 it can be seen that the model approximates better the observed temperatures when the land cover data of ECOCLIMAP-II is implemented instead of ECOCLIMAP-I. The result in figure 23 shows the systematic RMSE is slightly smaller when ECOCLIMAP-II is used. Compared to the model performance of ECOCLIMAP-I the RMSE, systematic RMSE and bias are smaller if the land cover fractions from the 565 m buffer are used (table 14 and figure 23). These smaller values indicate that the model is doing slightly better by implementing the land cover of the 565 m buffer. Besides this, the RMSE and bias are larger compared to the values of ECOCLIMAP-II. Also the systematic RMSE of the 565 m buffer land cover is slightly larger than the systematic RMSE of ECOCLIMAP-II. Therefore, it can be concluded that the model configuration with ECOCLIMAP-II captures the physical processes better than the land cover implementation of the 565 m buffer.

Table 14: Model performance of temperature at 2 m for runs with ECOCLIMAP-I, ECOCLIMAP-II and BBK land cover data over the period of August for the location Melle. Green indicates the best value for each score, while red indicates the worst results.

MELLE	ECOCLIMAP-I	ECOCLIMAP-II	BBK		
			100 m buffer	565 m buffer	1000 m buffer
AVERAGE TEMPERATURE (°C)	17,48	17,84	17,54	17,64	17,64
P-VALUE	1,90E-18	1,31E-09	1,27E-16	4,04E-14	4,04E-14
INDEX OF AGREEMENT (%)	0,86	0,87	0,86	0,86	0,86
RMSE (°C)	3,23	3,08	3,22	3,19	3,19
BIAS (°C)	-1,08	-0,73	-1,02	-0,93	-0,93

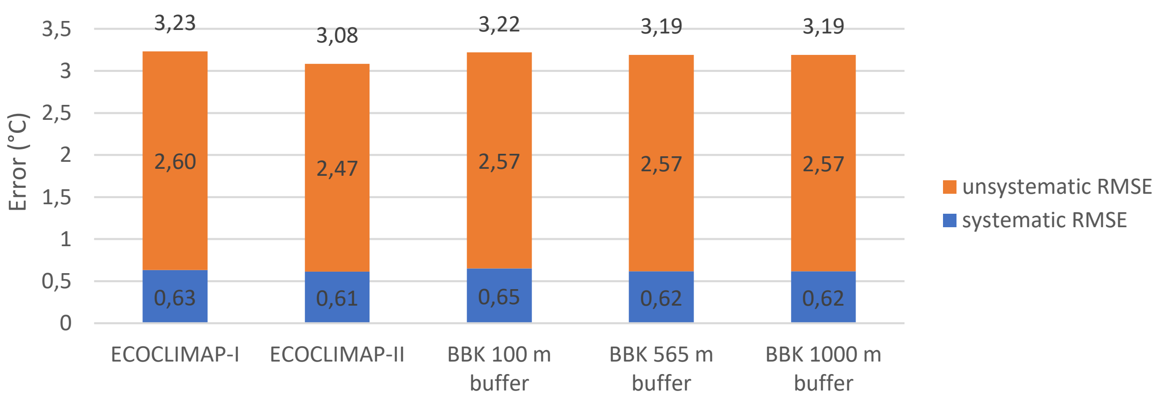

Figure 23: RMSE of the simulated temperatures subdivided into systematic and unsystematic RMSE for the different land cover parametrizations at the Melle location.

The model performance obtained with the implementation of the land cover fractions from the 100 m buffer is worse than the 565 m buffer based upon the scores in table 14 and the larger systematic RMSE (figure 23). As mentioned before, the model performance acquired with the land cover fractions from the 1000 m buffer is the same as the model performance of the 565 m buffer because those two scale levels have the same land cover fractions.

5.4.2.2 Honda

Table 15 presents the results of the model performance of the temperature at 2 m height for the Honda station situated in the harbour. For this location all the model runs with a different land cover parameterisation differ significantly from each other (Annex IX table 1). In contrast to the negative bias for Melle, there is a positive bias obtained for the Honda location with the ECOCLIMAP-I land cover data and the land cover of the 100 m buffer of the GIS-analysis. This means that the temperatures estimated by the model are higher than the observed temperatures and this can be seen when the averages of the modelled temperatures are compared with the average observed temperature of 19,57°C. The on average lower temperatures for the ECOCLIMAP-II, 565 m BBK and 1000 m BBK runs lead to a negative bias. These lower simulated temperatures might be linked to the large fraction green space in the ECOCLIMAP-II dataset and the large fractions of water for the 565 m and 1000 m buffers (figures 7b - 7d and table 8). On the other hand, the higher temperatures might be connected to the larger impervious fraction of ECOCLIMAP-I and 100 m buffer land cover data (figures 7b - 7d and table 8). Those relationships between land cover and temperature should be further investigated with a statistical correlation analysis and a two-tailed T-test should be used for the statistical evaluation of the correlation.

Table 15: Model performance of temperature at 2 m for runs with ECOCLIMAP-I, ECOCLIMAP-II and BBK land cover data over the period of August for the location Honda. Green indicates the best value for each score, while red indicates the worst results.

HONDA	ECOCLIMAP-I	ECOCLIMAP-II	BBK		
			100 m buffer	565 m buffer	1000 m buffer
AVERAGE TEMPERATURE (°C)	19,92	18,03	19,64	18,30	17,55
P-VALUE	0,013	1,41E-34	0,586	1,63E-22	9,45E-52
INDEX OF AGREEMENT (%)	0,79	0,83	0,82	0,78	0,75
RMSE (°C)	3,58	3,37	3,32	3,43	3,70
BIAS (°C)	0,35	-1,54	0,07	-1,27	-2,02

The RMSE of ECOCLIMAP-II is smaller than ECOCLIMAP-I and the index of agreement is larger for ECOCLIMAP-II as observed in table 15. Although, the model has a smaller RMSE when ECOCLIMAP-II is implemented, the systematic RSME is larger than the ECOCLIMAP-I run (figure 24). In addition, the absolute value of the bias is larger for the ECOCLIMAP-II run and the temperature series of the ECOCLIMAP-II run differs significantly from the observed temperatures, while this is not the case for the temperature series of the ECOCLIMAP-I run. Therefore, it can be concluded that the simulated temperatures of the ECOCLIMAP-I run are closer to the observed temperatures than the ECOCLIMAP-II run. The implementation of the 565 m buffer land cover from the GIS analysis gives worse model results compared to ECOCLIMAP-I based upon the p-value of the T-test, the index of agreement, the bias and systematic RMSE (table 15 and figure 24). Thus, the ECOCLIMAP-I land cover parameterisation is better than the ECOCLIMAP-II and the BBK data at 1 km² scale in reproducing the physical processes for the Honda location.

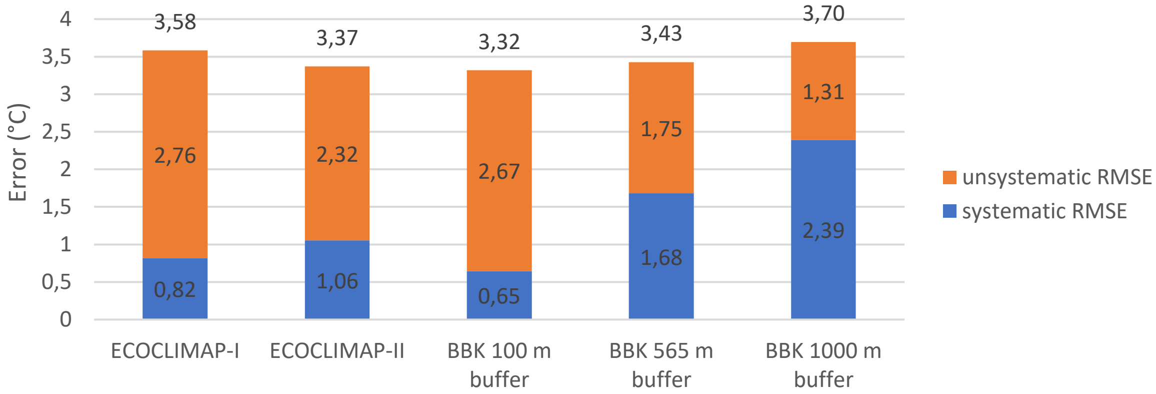

Figure 24: RMSE of the simulated temperatures subdivided into systematic and unsystematic RMSE for the different land cover parametrizations at the Honda location.

Based on the different scores in table 15 the model approaches the temperatures better when the land cover fractions of a radius of 100 m around the station are implemented than when those of the 565 m buffer are implemented (table 15 and figure 24). With the implementation of the 100 m land cover data, the model approaches the observed temperatures even better than the ECOCLIMAP-I parameterisation (table 15). The smallest systematic RSME is achieved for the 100 m buffer land cover parameterisation, as seen in figure 24. This means that the model configuration with the 100 m land cover data captures the physical processes better than a land cover parameterisation at 1 km² scale. If the land cover fractions of a larger area around the station are implemented, the model performance becomes worse. This is seen in table 15 and figure 24 when the statistical scores of the 1000 m buffer are compared with the other land cover parameterisations.

Table 16: Model performance of UHI for runs with ECOCLIMAP-I, ECOCLIMAP-II and BBK land cover data over the period of August for the location Honda. Green indicates the best value for each score, while red indicates the worst results.

HONDA	ECOCLIMAP-I	ECOCLIMAP-II	BBK		
			100 m buffer	565 m buffer	1000 m buffer
AVERAGE UHI (°C)	2,43	0,19	2,10	0,66	-0,09
P-VALUE	8,02E-47	1,84E-43	4,53E-53	3,24E-06	9,41E-44
INDEX OF AGREEMENT (%)	0,50	0,39	0,56	0,60	0,54
RMSE (°C)	2,73	1,60	1,98	1,88	2,15
BIAS (°C)	1,43	-0,81	1,09	-0,34	-1,09

The scores in table 16 represent the model performance of the UHI for the different datasets that determine the land cover fractions. Here, the model performance depends on the modelled temperatures of Melle and Honda, since the UHI is the temperature difference between the urban and rural station. It must be noted that the index of agreement is very small for all different model runs. This indicates that the model does not simulate the UHI well in general. Also the p-values in table 16 denote that the simulated UHIs differ significantly from the observed UHIs with a certainty of 99%. For ECOCLIMAP-I the model overestimates the UHI, because the average simulated UHI is larger than the average observed UHI that amounts to 1,00°C. This overestimation results in a positive bias for the model run with the ECOCLIMAP-I data. On the other hand, the model underestimates the UHI when the land cover fractions of ECOCLIMAP-II and the BBK at 1km² are implemented, resulting in negative biases. These negative biases result from the larger negative biases for the Honda temperatures with respect to the negative biases for the Melle location when the land cover of ECOCLIMAP-II or the 565 m buffer are applied (tables 14 and 15). A lower bias and RMSE is obtained when ECOCLIMAP-II is implemented instead of ECOCLIMAP-I, indicating there is an improvement of the simulated UHI. On the other hand, the lower index of agreement denotes that the model simulates the UHI worse. In figure 25, it is seen that the implementation of the ECOCLIMAP-II land cover makes the model worse, based on the larger systematic RMSE. This very large portion of systematic RMSE might be related to the wrong estimation of the land cover around the Honda station in the ECOCLIMAP-II database (table 8). It is thus concluded that the ECOCLIMAP-II parameterisation is not better in reproducing the UHI at the Honda location with respect to the ECOCLIMAP-I parameterisation. The 565 m buffer land cover parameterisation simulates better the UHI than both ECOCLIMAP parameterisations based upon the scores in table 16 and figure 25. It must be noted that the RMSE for the 565 m buffer is slightly larger than the RMSE obtained with the ECOCLIMAP-II implementation, but this is due to larger unsystematic errors (figure 25). The systematic part of the RMSE is very small for the 565 m land cover parameterisation, which indicates that the model comprises the physical processes well. Another remark that must be made is that the temperature modelling is worse for both locations, Melle and Honda, when the 565 m land cover is implemented. The improved UHI is therefore due to compensating errors of the rural and urban temperatures.

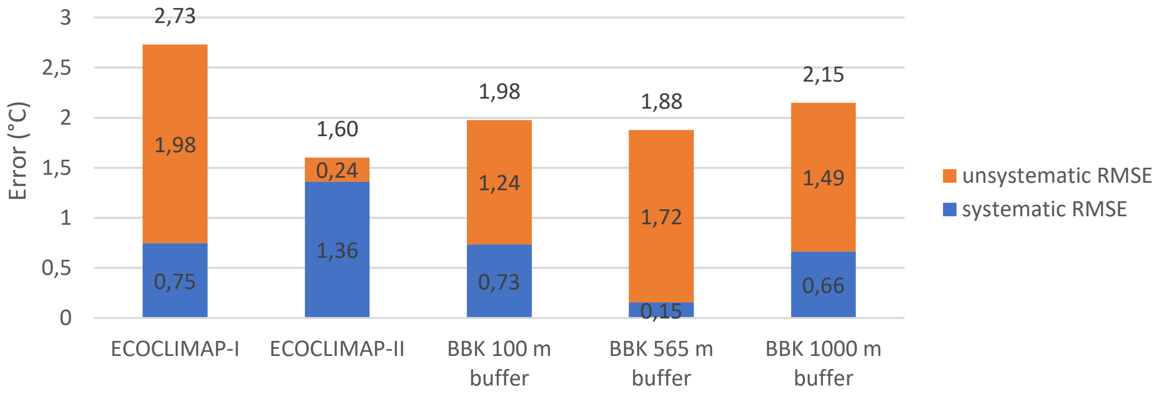

Figure 25: RMSE of the UHI subdivided into systematic and unsystematic RMSE for the different land cover parametrizations at the Honda location.

If the land cover fractions are implemented for an area of 100 m or 1000 m around the station, then the modelled UHI is worse than the simulation with the 565 m buffer (table 16 and figure 25). This worse model performance for the 1000 m buffer is completely due to the worse simulated temperatures for the Honda location, since the parameterisation of the 565 m and 1000 m buffers are the same for Melle (table 14).

5.4.2.3 Wondelgem

In table 17 the model performance of the simulated temperatures at the Wondelgem location are presented. There is a positive bias obtained for the modelled temperatures at Wondelgem with the ECOCLIMAP-I and ECOCLIMAP-II land cover data, since the modelled average temperature is higher than the average observed temperature of 19,08°C. This is not the case for the BBK data, since the biases are negative. Based on the T-tests in table 1 of Annex IX, the model configurations with a different land cover parameterisation differ significantly from each other for the Wondelgem location. The scores for this location differ significantly as well, as seen in tables 2, 3 and 4 of Annex IX. From table 17 is derived that ECOCLIMAP-I and ECOCLIMAP-II do not differ significantly from the observed temperatures at a significance level of 99%. ECOCLIMAP-II has a lower RMSE and bias than ECOCLIMAP-I and the index of agreement is slightly larger for ECOCLIMAP-II. Figure 26 also shows that the systematic RMSE is smaller for the ECOCLIMAP-II run. Because of these reasons it is concluded that the model performance of ECOCLIMAP-II is better than ECOCLIMAP-I. Based upon the RMSE, systematic RMSE and the index of agreement even a better model performance is obtained with the implementation of the land cover fractions from the BBK at 565 m scale (table 17 and figure 26). However, the absolute value of the bias is larger for the model output obtained with the BBK land cover at 1 km² resolution. The larger negative bias means that the model systematically underestimates the temperature if the land cover fractions of the BBK are used. This can be related to the smaller fraction of impervious surface and the larger fraction of green space when the 1 km² BBK land cover parameterisation is used, although this relationship should be still tested statistically. Because of the systematic underestimation, the temperatures simulated with the 565 m land cover parametrization differ significantly from the observed temperatures based upon the p-value in table 17. However, the other scores indicate that the model captures the physical processes better when the BBK land cover is implemented.

Table 17: Model performance of temperature at 2 m for runs with ECOCLIMAP-I, ECOCLIMAP-II and BBK land cover data over the period of August for the location Wondelgem. Green indicates the best value for each score, while red indicates the worst results.

WONDELGEM	ECOCLIMAP-I	ECOCLIMAP-II	BBK		
			100 m buffer	565 m buffer	1000 m buffer
AVERAGE TEMPERATURE (°C)	19,35	19,19	18,01	18,57	18,59
P-VALUE	0,041	0,380	1,43E-18	2,04E-05	4,67E-05
INDEX OF AGREEMENT (%)	0,84	0,85	0,86	0,86	0,86
RMSE (°C)	3,26	3,20	3,18	3,10	3,10
BIAS (°C)	0,26	0,11	-1,07	-0,52	-0,49

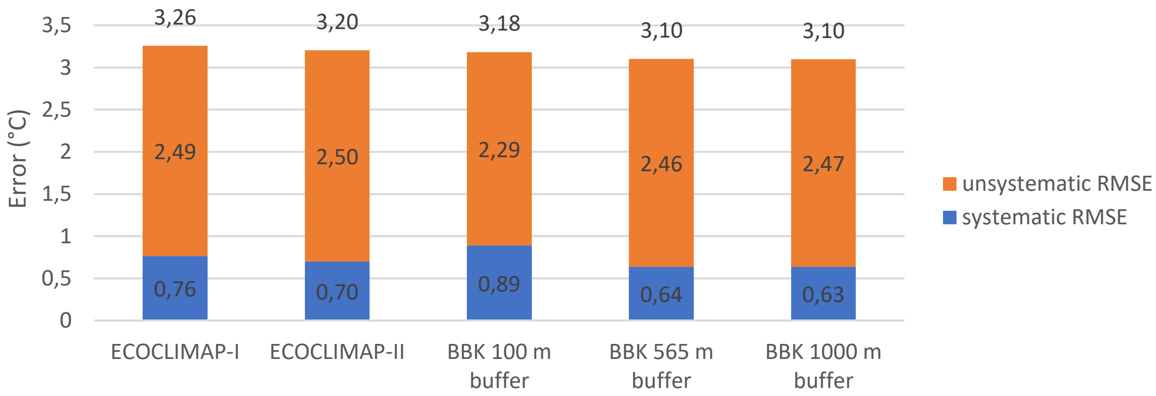

Figure 26: RMSE of the simulated temperatures subdivided into systematic and unsystematic RMSE for the different land cover parametrizations at the Wondelgem location.

When the land cover fractions of a radius of 100 m around the station are implemented, the different scores indicate that the model performance is worse than when the land cover fractions from the 565 m buffer are implemented (table 17 and figure 26). If the land cover fractions of 1000 m around the station are implemented, the model performance is similar to the model performance obtained with land cover fractions of the 565 m radius. The bias and systematic RMSE indicate there is even a small improvement in model performance (table 17 and figure 26). All the modelled temperatures with the different parameterisations of the BBK data differ significantly from the observed temperatures (table 17). This is due to the large negative biases as explained before for the 565 m buffer. These negative biases can be linked to the ratio of the green space and the impervious surface. When the average temperatures are compared with the concrete fractions, then lower average temperatures correspond with lower concrete fractions (tables 17 and 9, and figures 8b, 8c and 8d). A correlation analysis should be performed to confirm this relationship.

For the Wondelgem station there was an average UHI of 0,52°C observed during the studied period of August 2016. Only the model configuration with the 100 m buffer land cover underestimates this value slightly, as seen in table 18. The other land cover implementations overestimate the UHI, resulting in a positive bias. This was expected for ECOCLIMAP-I and ECOCLIMAP-II since the modelled temperatures of Melle and Wondelgem both indicated there would be an overestimation of the UHI (tables 14 and 17). For the BBK data the modelled temperatures of Melle suggested an overestimation, while the modelled temperatures of Wondelgem suggested and underestimation. The smaller biases for the different implementations of the BBK data in table 18 are thus due to the combined effect of overestimation and underestimation.

Table 18: Model performance of UHI for runs with ECOCLIMAP-I, ECOCLIMAP-II and BBK land cover data over the period of August for the location Wondelgem. Green indicates the best value for each score, while red indicates the worst results.

WONDELGEM	ECOCLIMAP-I	ECOCLIMAP-II	BBK		
			100 m buffer	565 m buffer	1000 m buffer
AVERAGE UHI (°C)	1,86	1,36	0,47	0,93	0,95
P-VALUE	1,82E-61	6,76E-43	0,267	3,98E-19	9,90E-21
INDEX OF AGREEMENT (%)	0,38	0,43	0,43	0,48	0,48
RMSE (°C)	2,29	1,66	1,10	1,21	1,22
BIAS (°C)	1,34	0,84	-0,05	0,41	0,43

The values of the RMSE and bias are smallest for the model runs with the BBK data in table 18 and the index of agreement is largest for those runs. Also the systematic RMSEs are lower for the BBK runs (figure 27). Therefore, the model performance for the UHI is better when the land cover data of the BBK is implemented. Based upon the scores in table 18 and figure 27, the ECOCLIMAP-II data is reproducing the UHI better than the ECOCLIMAP-I data. Similar as observed for the Honda station is that the p-values and the indexes of agreement are small for most of the model configurations. The implementation of the 100 m buffer land cover is the only run that does not simulate UHI intensities that differ significantly from the observed UHIs. Except for the 100 m buffer, the scores indicate that the model in general does not simulate well the UHI. A reason for this could be the poor tuning of the model. The SURFEX model should thus be further improved to simulate the UHI better.

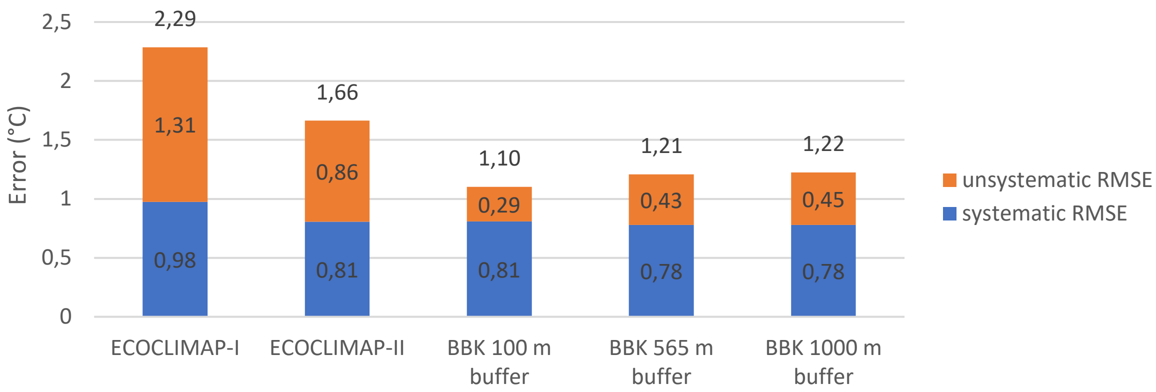

Figure 27: RMSE of the UHI subdivided into systematic and unsystematic RMSE for the different land cover parametrizations at the Wondelgem location.

The scores in table 18 indicate that the UHI is simulated better with the land cover implementation of the 100 m buffer. However, the systematic RMSE becomes larger when the 100 buffer land cover data is used. This is due to the fact that the errors made in the temperature modelling of Melle and the temperature modelling of Wondelgem cancel each other out. This artificial improvement of the scores does not mean that there is some added value by using the land cover of a smaller area. The larger systematic RMSE of the 100 m land cover parameterisation indicates that the model captures the physical processes less with the 100 m parameterisation. Therefore, it is better to use the 565 m parameterisation, although the statistical scores of this land cover parameterisation indicate that the model performs slightly worse. The modelled UHI for the implementation of the land cover 1000 m around the station is slightly worse than the 565 m buffer based upon the scores in table 18, although the systematic RMSE is similar to the one of the 565 m buffer.

5.4.2.4 Sint-Bavo and Povinciehuis

For the stations Sint-Bavo and Provinciehuis, situated in the core of the city, the land cover fractions of ECOCLIMAP-I and ECOCLIMAP-II are the same (table 10 and 11). Because of this, there is no difference in the simulated temperatures with ECOCLIMAP-I and ECOCLIMAP-II (Annex IX table 1). Therefore, the same model performances are obtained with the implementation of ECOCLIMAP-I and ECOCLIMAP-II, as presented in table 19 and 20. In addition, the same simulated temperatures result in a same modelled average temperature of 19,90°C for the Sint-Bavo and Provinciehuis locations (tables 19 and 20). However, the statistical scores of Sint-Bavo differ slightly from those of the Provinciehuis location since their observed temperatures differ. Because of those different temperatures measured in the field they have a different average observed temperature as well. For Sint-Bavo the observed average temperature amounts to 19,70°C and for the Provinciehuis location this is 19,81°C. Except for the temperatures obtained with ECOCLIMAP-I and ECOCLIMAP-II, the simulated temperatures with different land cover parameterisations do differ significantly from each other with a certainty of 99% (Annex IX table 1). In tables 19 and 20 it can be seen that the implementation of the ECOCLIMAP data causes a positive bias, while a negative bias is obtained with the data of the BBK. The negative biases can be linked to a lower amount of impervious surface. As mentioned in the previous sections this should still be tested statistically with a correlation analysis. Also the effect of the water fraction on the simulated temperature could be tested with this method. When the model output of ECOCLIMAP is compared with the model output of the 565 m buffer, then it is observed that the index of agreement and RMSE improve with the 565 m land cover parameterisation (tables 19 and 20). Although, it must be noted that the absolute value of the bias is larger, which may lead to modelled temperatures that differ significantly from the observed temperatures, as it is the case in tables 19 and 20. This is in contrast with the model output obtained with the ECOCLIMAP land cover data that does not differ significantly from the observed temperatures (tables 19 and 20). In addition, the systematic RMSE is similar for the Provinciehuis station and increases for the Sint-Bavo station when the 565 m land cover is implemented (figures 28 and 29). Thus, the physical processes are not better captured with the 565 m land cover parameterisation and it is therefore concluded that this model configuration does not improve the model with respect to the ECOCLIMAP parameterisation.

Table 19: Model performance of temperature at 2 m for runs with ECOCLIMAP-I, ECOCLIMAP-II and BBK land cover data over the period of August for the location Sint-Bavo. Green indicates the best value for each score, while red indicates the worst results.

SINT-BAVO	ECOCLIMAP-I	ECOCLIMAP-II	BBK		
			100 m buffer	565 m buffer	1000 m buffer
AVERAGE TEMPERATURE (°C)	19,90	19,90	19,62	19,14	19,15
P-VALUE	0,154	0,154	0,565	1,14E-05	1,49E-05
INDEX OF AGREEMENT (%)	0,79	0,79	0,83	0,83	0,83
RMSE (°C)	3,58	3,58	3,26	3,24	3,23
BIAS (°C)	0,20	0,20	-0,07	-0,55	-0,55

Table 20: Model performance of temperature at 2 m for runs with ECOCLIMAP-I, ECOCLIMAP-II and BBK land cover data over the period of August for the location Provinciehuis. Green indicates the best value for each score, while red indicates the worst results.

PROVINCIEHUIS	ECOCLIMAP-I	ECOCLIMAP-II	BBK		
			100 m buffer	565 m buffer	1000 m buffer
AVERAGE TEMPERATURE (°C)	19,90	19,90	19,68	19,44	19,15
P-VALUE	0,535	0,535	0,303	0,004	2,24E-07
INDEX OF AGREEMENT (%)	0,79	0,79	0,82	0,82	0,83
RMSE (°C)	3,62	3,62	3,32	3,30	3,27
BIAS (°C)	0,09	0,09	-0,13	-0,37	-0,66

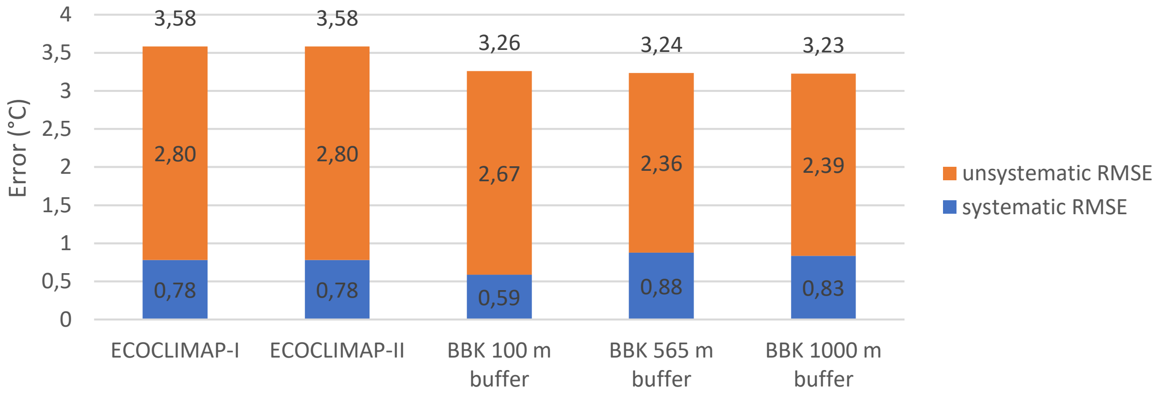

Figure 28: RMSE of the simulated temperatures subdivided into systematic and unsystematic RMSE for the different land cover parametrizations at the Sint-Bavo location.

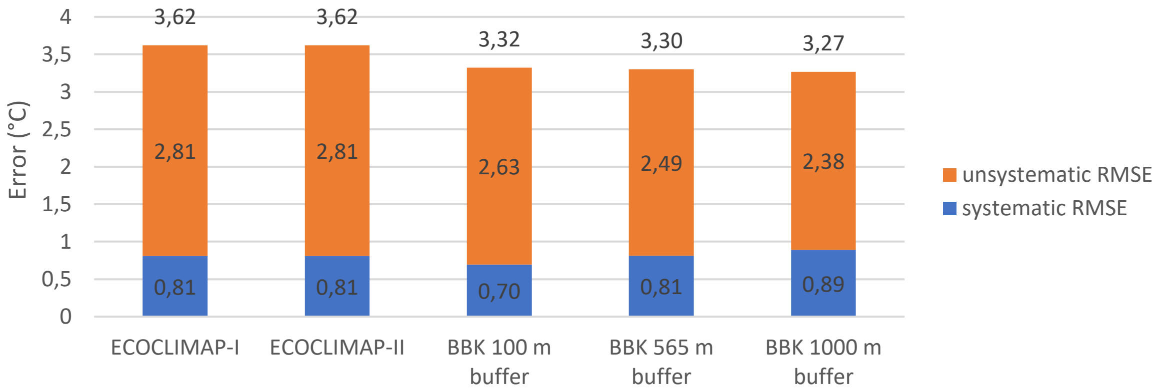

Figure 29: RMSE of the simulated temperatures subdivided into systematic and unsystematic RMSE for the different land cover parametrizations at the Provinciehuis location.

The RMSE of the 100 m buffers displays that the model outputs are slightly worse compared to the 565 m model outputs (tables 19 and 20). However, the absolute value of the bias and the systematic RMSE are smaller, indicating that the model performs better when 100 m land cover data is implemented (tables 19 and 20, and figures 28 and 29). The model performance acquired with the land cover fractions from the 1000 m buffer are similar to those of the 565 m buffer for the Sint-Bavo location (table 19). Based upon the scores in table 19 and the lower systematic RMSE (figure 28), it is derived that the 1000 m land cover parameterisation improves the model slightly compared to the 565 m land cover parameterisation. This is not the case for the Provinciehuis location, where the bias becomes more negative if the 1000 m land cover is implemented (table 20). The RMSE and index of agreement indicate there is a small improvement when the 1000 m land cover is used. Although, the larger negative bias and the systematic RMSE denote that the model is doing worse with the 1000 m land cover parameterisation. In addition, the simulated temperatures with the 100 m land cover parameterisation do not differ significantly from the observed temperatures, while the output with the 565 m buffer and the 1000 m buffer differs significantly from the observed temperatures (tables 19 and 20). Based upon the systematic RMSE, the model captures the physical processes best when the 100 m land cover data is applied. Therefore, the 100 m land cover parameterisation is recommended to simulate the temperatures at both locations in the city centre.

The smaller change in land cover between the ECOCLIMAP and the 565 m land cover data for the Provinciehuis station with respect to the Sint-Bavo station (tables 10 and 11) corresponds as expected to a smaller difference between the simulated temperatures of ECOCLIMAP and the 565 m buffer (table 1 of annex IX). Also a smaller change in the average simulated temperature and the bias of the Provinciehuis station with respect to the Sint-Bavo station is observed in tables 19 and 20 when the scores of ECOCLIMAP and the 565 m buffer are compared. The land cover change is also bigger for the Provinciehuis location between the 565 m buffer and 1000 m buffer (figures 9c, 9d, 10c and 10d). When the average temperatures of those two scale levels are compared then it is observed that the difference in average temperature of the Provinciehuis differs more than the Sint-Bavo station (tables 19 and 20). For going from the 565 m buffer to the 100 m buffer there is a larger land cover change observed for the Sint-Bavo station (figures 9b, 9c, 10b and 10c) and this corresponds with a larger change in average temperature compared to the Provinciehuis station (tables 19 and 20). Since it is likely from this data that a larger land cover change generates a larger temperature difference, it is recommended to investigate to what extent a certain land cover change causes a change in temperature and it should be tested if this correlation is statistically significant.

Table 21: Model performance of UHI for runs with ECOCLIMAP-I, ECOCLIMAP-II and BBK land cover data over the period of August for the location Sint-Bavo. Green indicates the best value for each score, while red indicates the worst results.

SINT-BAVO	ECOCLIMAP-I	ECOCLIMAP-II	BBK		
			100 m buffer	565 m buffer	1000 m buffer
AVERAGE UHI (°C)	2,42	2,06	2,08	1,51	1,52
P-VALUE	1,10E-38	1,18E-28	2,25E-44	4,08E-09	6,23E-10
INDEX OF AGREEMENT (%)	0,52	0,56	0,58	0,63	0,63
RMSE (°C)	2,67	2,22	1,85	1,64	1,60
BIAS (°C)	1,28	0,93	0,95	0,37	0,38

Table 22: Model performance of UHI for runs with ECOCLIMAP-I, ECOCLIMAP-II and BBK land cover data over the period of August for the location Provinciehuis. Green indicates the best value for each score, while red indicates the worst results.

PROVINCIEHUIS	ECOCLIMAP-I	ECOCLIMAP-II	BBK		
			100 m buffer	565 m buffer	1000 m buffer
AVERAGE UHI (°C)	2,42	2,06	2,13	1,80	1,52
P-VALUE	1,70E-31	7,64E-22	3,08E-33	7,99E-16	1,96E-05
INDEX OF AGREEMENT (%)	0,51	0,54	0,56	0,59	0,61
RMSE (°C)	2,68	2,23	1,98	1,80	1,61
BIAS (°C)	1,17	0,81	0,89	0,56	0,27

In table 21 and 22, the model performances for the UHI at the locations of Sint-Bavo and Provinciehuis are given. Again, the different model outputs have low scores for the p-value and index of agreement, which indicates that a better tuning of the SURFEX model is necessary. Similar as for the temperatures, the modelled UHI intensities are the same at the Sint-Bavo and Provinciehuis locations for the ECOCLIMAP-I and ECOCLIMAP-II runs (tables 21 and 22). This is because the land cover fractions of ECOCLIMAP-I and ECOCLIMAP-II are the same for those runs (tables 10 and 11). Therefore, the model performances of ECOCLIMAP-I and ECOCLIMAP-II are quite similar for the Sint-Bavo and Provinciehuis stations. They do differ slightly since the observed UHI intensities differ for each location. For Sint-Bavo the average observed UHI equals 1,13°C and for the Provinciehuis location this amounts to 1,25°C. At the 1 km^2 scale, the RMSE and bias are smallest for the model runs with the BBK data, while the index of agreement is largest (tables 21 and 22). In addition, the systematic RMSE is smallest for this land cover parameterisation (figures 30 and 31). Hence, the UHI is better modelled when the land cover data of the BBK is implemented in SURFEX. However, these improvements might be due to a compensation of the errors by combining the temperature simulations of Melle and the urban stations. The model runs with the ECOCLIMAP-II implementation simulate the UHI better than when the model uses the ECOCLIMAP-I data. This is based upon the statistical scores in tables 21 and 22, and figures 30 and 31. The improvement in modelled UHI for ECOCLIMAP-II with respect to ECOCLIMAP-I is due to the better modelled temperatures at the rural location Melle (table 14). This conclusion can be drawn since the modelled temperatures with ECOCLIMAP-I and ECOCLIMAP-II are the same for the Sint-Bavo and Provinciehuis stations (Annex IX table 1). From table 21 and 22 follows that all model runs with the different datasets overestimate the UHI, since the bias is positive. For the ECOCLIMAP data this is expected since the modelled temperatures of Melle, Sint-Bavo and Provinciehuis indicate an overestimation of the UHI. On the other hand, the temperatures modelled with the BBK data suggest an overestimation based on the temperatures of Melle, while the modelled temperatures of Sint-Bavo and Provinciehuis suggest an underestimation of the UHI. Thus, the same combined effect of overestimation and underestimation as was obtained for Wondelgem is acquired here. Therefore, the biases of the BBK runs are lowered due to this combined effect.

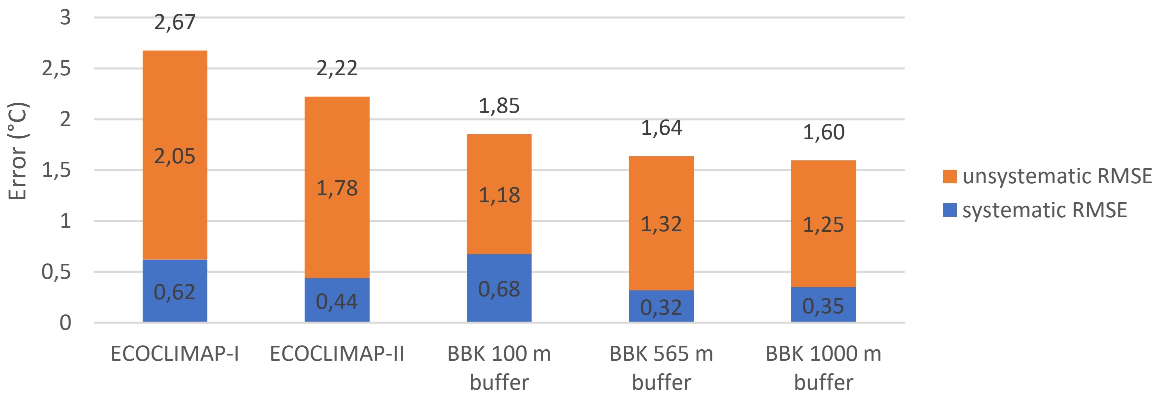

Figure 30: RMSE of the UHI subdivided into systematic and unsystematic RMSE for the different land cover parametrizations at the Sint-Bavo location.

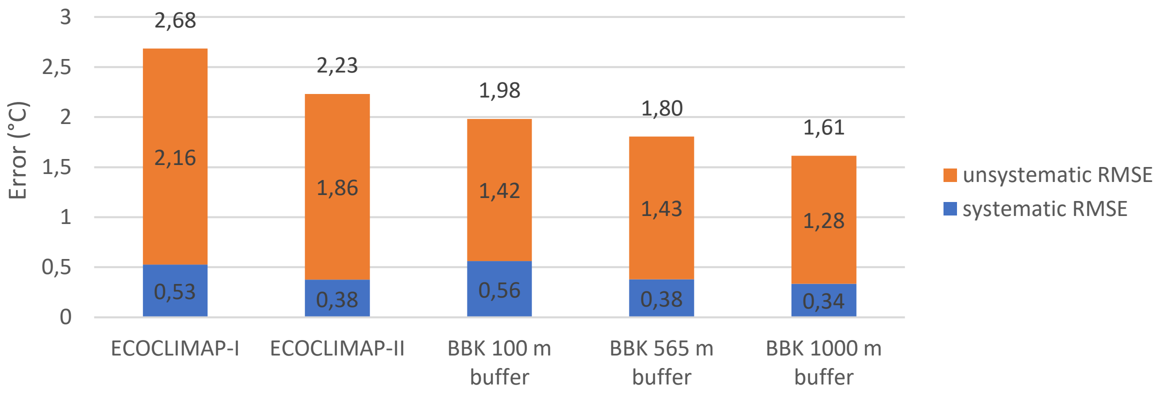

Figure 31: RMSE of the UHI subdivided into systematic and unsystematic RMSE for the different land cover parametrizations at the Provinciehuis location.

If the land cover data of the 100 m buffer is implemented, the model performance for the UHI is worse than the parameterisation with the 565 m buffer for both locations (tables 21 and 22, and figures 30 and 31). There is not a lot of difference between the model performances of the 565 m buffer and 1000 m buffer for the Sint-Bavo station (table 21 and figure 30). This is because the modelled temperatures for Melle are the same at both scale levels and the modelled temperatures for Sint-Bavo do not differ a lot between both scale levels (table 1 Annex IX). For the Provinciehuis station the model performance of the 1000 m buffer differs more from the model performance of the 565 m buffer, than is observed for the Sint-Bavo location (tables 21 and 22). This can be related to the fact that the difference in land cover fractions is smaller at the Sint-Bavo location when going from the 565 m buffer area to the 1000 m buffer area (figures 9c, 9d, 10c and 10d). This smaller difference in land cover between both scale levels seems to induce simulated UHI intensities that are closer to each other, resulting in similar model performances. Thus, similar as was found for the temperatures it would be interesting to investigate to which extent a change in land cover induces a change in UHI. As seen in figure 30, the systematic RMSE is slightly larger when the 1000 m land cover is applied instead of the 565 m buffer for the Sint-Bavo station. This indicates that the model captures the physical processes less with the 1000 m land cover implementation. On the other hand, the systematic RMSE is smallest when the 1000 m land cover is applied for the Provinciehuis station (figure 31). The other statistical scores in table 22 indicate that the model performs better with the 1000 m buffer land cover parameterisation as well. Thus, the model captures the physical processes best with the 1000 m land cover parameterisation for the Provinciehuis and for the Sint-Bavo station this is the 565 m parameterisation. Although, both stations are located close to each other in the city centre. There is thus a difference in area that has to be taken into account to obtain a better model performance for the UHI of the urban stations.

5.4.2.5 Plantentuin

Table 23 presents the model performances of the different land cover parameterisations for the simulated temperatures at the Plantentuin location. There are positive biases observed except for the implementation of the 100 m buffer land cover from the BBK. Thus, except for this model configuration, the simulated temperatures do overestimate on average the average observed temperature of 18,90°C (table 23). The T-tests in table 1 of Annex IX point out that all the different land cover parameterisations for this location differ significantly from each other with a certainty of 99%. From table 23 and figure 32 is derived that ECOCLIMAP-II has a better model performance than ECOCLIMAP-I, since all errors are slightly smaller. The errors become even smaller when the 565 m buffer land cover is used. In contrast to the ECOCLIMAP parameterisations, this parameterisation does not produce temperatures that differ significantly from the observed temperatures. This proves that the model with the 565 m land cover parameterisation simulates the observed temperatures better.

Table 23: Model performance of temperature at 2 m for runs with ECOCLIMAP-I, ECOCLIMAP-II and BBK land cover data over the period of August for the location Plantentuin. Green indicates the best value for each score, while red indicates the worst results.

PLANTENTUIN	ECOCLIMAP-I	ECOCLIMAP-II	BBK		
			100 m buffer	565 m buffer	1000 m buffer
AVERAGE TEMPERATURE (°C)	19,40	19,37	18,45	19,18	19,17
P-VALUE	6,20E-5	1,73E-4	1,87E-4	0,024	0,034
INDEX OF AGREEMENT (%)	0,84	0,84	0,85	0,85	0,84
RMSE (°C)	3,18	3,15	3,09	3,14	3,13
BIAS (°C)	0,50	0,46	-0,45	0,28	0,26

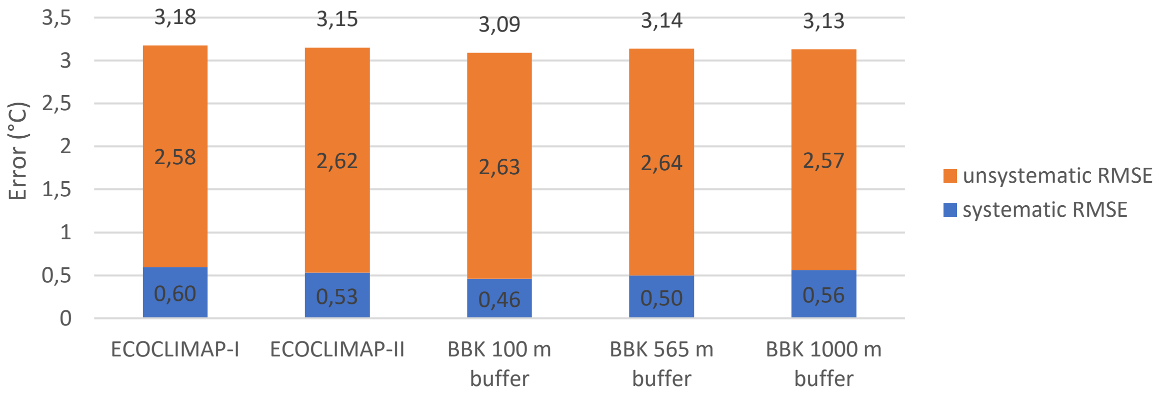

Figure 32: RMSE of the simulated temperatures subdivided into systematic and unsystematic RMSE for the different land cover parametrizations at the Plantentuin location.

The lower systematic RMSE for the 100 m buffer indicates that this model configuration captures the physical processes better (figure 32). However, the absolute value of the bias is larger if the land cover fractions of the 100 m buffer are implemented (table 23). Therefore, the simulated temperatures differ significantly from the observed temperatures. The 1000 m land cover parameterisation approximates the observed temperatures better based on the p-value in table 23. For this model configuration the model output has the smallest bias in absolute value, implying that the simulated temperatures on average deviate less from the observed temperatures. However, the index of agreement indicates that the model performs worse when the 1000 m land cover parameterisation is applied, compared to the 100 m land cover parametrization (table 23). In addition, the model captures the physical processes less based on the systematic RMSE (figure 32). Thus, the 1000 m buffer land cover implementation generates temperatures that are closest to the observed temperatures, although this model configuration does not capture the physical processes as good as the 100 m land cover parameterisation.

Table 24: Model performance of UHI for runs with ECOCLIMAP-I, ECOCLIMAP-II and BBK land cover data over the period of August for the location Plantentuin. Green indicates the best value for each score, while red indicates the worst results.

PLANTENTUIN	ECOCLIMAP-I	ECOCLIMAP-II	BBK		
			100 m buffer	565 m buffer	1000 m buffer
AVERAGE UHI (°C)	1,92	1,53	0,91	1,55	1,53
P-VALUE	5,22E-100	2,91E-83	4,60E-34	1,51E-94	1,18E-86
INDEX OF AGREEMENT (%)	0,53	0,55	0,58	0,57	0,57
RMSE (°C)	2,23	1,79	1,26	1,74	1,77
BIAS (°C)	1,58	1,19	0,57	1,21	1,19

In table 24 the model performances for the UHI obtained with the different land cover parameterisations at the location of the Plantentuin are represented. The p-values and the indexes of agreement are again small for each model run, which indicates that the model should be tuned better. Since the bias is positive for all runs, the average simulated UHI overestimates the average observed UHI of 0,34°C. The smaller bias for the 100 m buffer results from the combined effect of overestimation and underestimation of the temperatures at the rural and urban station (tables 24, 23 and 14). The RMSE, systematic RMSE and bias obtained with ECOCLIMAP-II are smaller compared to the values from ECOCLIMAP-I and the index of agreement is larger (table 24 and figure 33). Therefore, the model performance for the UHI is better when the land cover data of ECOCLIMAP-II is used instead of ECOCLIMAP-I. Compared to the model performance obtained with the ECOCLIMAP-I data, the UHI is also better modelled with the implementation of the BBK data (table 24 and figure 33). The model configuration with the BBK data is reproducing UHI intensities that do not differ significantly from the ECOCLIMAP-II output (table 5 of Annex IX). Although, when the BBK data is implemented the bias and systematic RMSE become slightly larger than those obtained with the ECOCLIMAP-II data. Thus, at a scale level of 1 km², the ECOCLIMAP-II model configuration reproduces slightly better the physical processes that influence the UHI.

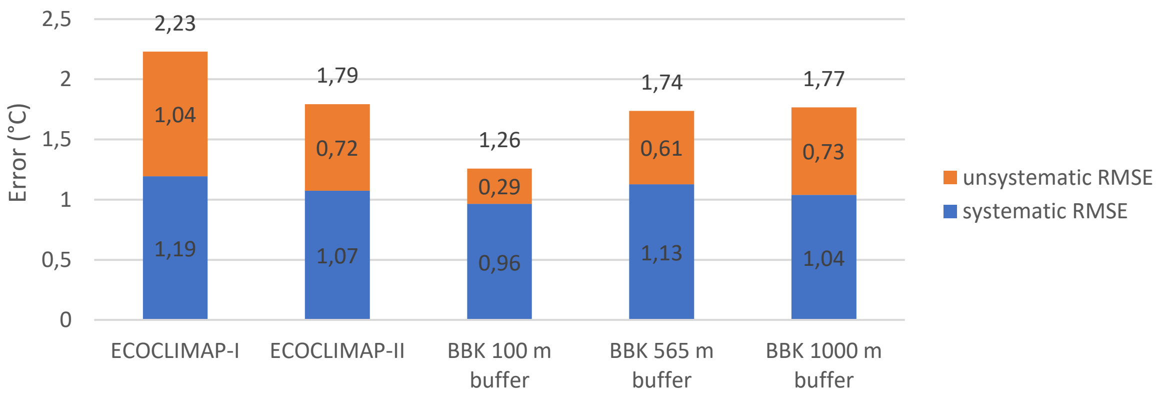

Figure 33: RMSE of the UHI subdivided into systematic and unsystematic RMSE for the different land cover parametrizations at the Plantentuin location.

The scores in table 24 and the lower systematic RMSE in figure 33 indicate that the modelled UHI with the 100 m buffer is closer to the observed UHI than the ECOCLIMAP-II parameterisation. The implementation of the 1000 m buffer land cover produces UHI intensities that do not differ significantly from the ECOCLIMAP-II run (Annex IX table 5). Thus, the model configuration with the 100 m buffer land cover data reproduces the UHI best at the Plantentuin site. Therefore, it is better to look at the land cover of the local environment for the Plantentuin station to estimate the UHI.

5.4.2.6 General impacts of adapting the land cover data

By comparing the results from the different locations, it can be stated that in general the RMSE and bias are large for most of the modelled temperatures and simulated UHIs. The index of agreement and p-values are very low for all simulated UHIs as well. Other than the 100 m buffer land cover implementation of the Wondelgem there is a significant difference with the observed UHI intensities. This indicates that the model tuning must be improved to represent temperatures better in general. When the temperatures are simulated better, the simulation of UHI should improve as well since the UHI is defined as the temperature difference between the urban and rural station. However, the poor tuning of the model or bad forcings cause model results that deviate significant from the observations, there is some sensitivity seen in the different model outputs. Based on this sensitivity some conclusions can be made according to the different land cover implementations.

For the stations of Melle, Wondelgem and Plantentuin there is an enhancement in the simulated temperature when ECOCLIMAP-II is used instead of ECOCLIMAP-I. When ECOCLIMAP-II is applied for the stations Sint-Bavo and Provinciehuis, then the model performance of temperature remains the same and for the Honda station a decrease is observed. These findings can be linked with the improvements and deterioration that were found for land cover data of ECOCLIMAP-II. In addition, a correlation analysis is recommended for each land cover fraction to know to which extent a change in a certain land cover fraction has an influence on the temperature and a statistical T-test should be applied to see whether those relationships are significant. For all the stations except for the Honda station there is an improvement in the simulated UHI observed when ECOCLIMAP-II is implemented instead of ECOCLIMAP-I. The simulated UHI of Provinciehuis and Sint-Bavo undergo the same improvement with the ECOCLIMAP-II parameterisation. For both locations this improvement is completely due to the improvement of the simulated temperatures in Melle since the land cover fractions do not change for the Provinciehuis and Sint-Bavo location by going from ECOCLIMAP-I to ECOCLIMAP-II.

By implementing the land cover fractions derived from the high resolution data of the BBK at 1km², the simulation of the temperature for Melle is better than ECOCLIMAP-I, but worse than ECOCLIMAP-II. The implementation of BBK data causes as well a worse model performance compared to the ECOCLIMAP land cover data implementation for the Honda, Provinciehuis and Sint-Bava locations. In contrast to this, the temperatures are best simulated when the 565 m buffer BBK data is implemented at the locations of the Wondelgem and Plantentuin stations. The latter is in accordance with the expectation that the high resolution data of the BBK data would have the best performance. However, this is not the case for four out of six stations and thus, the more accurate land cover data of the BBK does not induce a better simulation of the temperatures. The reason for this could be the poor model tuning that was based upon the ECOCLIMAP-I land cover data. The modelling of the UHI is best for all locations if the 1 km² BBK data is applied, except for the Plantentuin site. For this site the UHI intensities of ECOCLIMAP-II do not differ significantly from those obtained with the 565 m buffer land cover parameterisation. Nevertheless, the UHI is still better modelled for the Plantentuin location when the

BBK data is used instead of the ECOCLIMAP-I data. Based on the better scores it could be concluded that the observed UHIs are in general approached better when the deduced land cover of the BBK is implemented in SURFEX. However, the improvement in the simulated UHIs seems to be artificial since the simulated temperatures are worse for most of the stations. The better simulation of the UHIs can be explained by errors that cancel each other out when the rural temperatures are subtracted from the urban temperatures. Although, the small systematic RMSEs indicate that there is an added value to the simulation of the physical processes when the UHI is simulated with the BBK data.

If the land cover fractions of 100 m around the station are implemented instead of the 565 m buffer land cover, then the modelled temperatures for Melle and Wondelgem are worse. On the other hand, the temperatures of the Plantentuin, Sint-Bavo, Provinciehuis and Honda locations are better approximated with the 100 m buffer land cover parameterisation (table 25). The modelled UHI is worse for the Honda, Sint-Bavo and Provinciehuis sites with the 100 m buffer land cover parameterisation when compared to the 565 m buffer parameterisation, although the temperatures were simulated better with this parameterisation. For the Wondelgem and Plantentuin stations the UHI is better approximated when the land cover data of the 100 m buffer is implemented in SURFEX. From this can be concluded that it is better for stations in a suburban area or in a large public park to take the land cover of the local environment into account rather than the large area of 1 km².

The model performance of the 1000 m land cover parameterisation is for most of the locations similar to the model performance of the 565 m radius, since the changes in land cover are small. The results of the modelled temperature for Melle are even identical when the 1000 m land cover is implemented. The simulated temperatures for the Wondelgem and Sint-Bavo stations are slightly better when the land cover of the 1000 m buffer is implemented in SURFEX instead of the 565 m buffer. However, the 100 m buffer still gives a better model performance for the Sint-Bavo station than when the 1000 m buffer land cover is implemented (table 25). The model performance obtained with the 1000 m buffer parameterisation is slightly worse than the 565 m parameterisation for the Plantentuin and Provinciehuis stations. The modelled temperatures at the Honda location with the 1000 m buffer parameterisation causes a model performance that is much worse than the other land cover parameterisations. When the land cover of the 1000 m buffer is implemented, the modelled UHI is slightly worse than the modelled UHI obtained with land cover of the 565 m buffer for the Honda, Wondelgem and Sint-Bavo locations. The Provinciehuis and Plantentuin sites are the only cases where the UHI is better approximated with the 1000 m land cover fractions. It must be noted that the UHI with the 100 m land cover parameterisation is still better than the 1000 m parameterisation for the Plantentuin station (table 25). A summary of the land cover parameterisation for each station to obtain the best model performance is given in table 25.

Table 25: Summary of land cover parameterisations that give the best model performance for temperature and UHI.

LOCATION	TEMPERATURE	UHI
HONDA	100 m buffer	565 m buffer
WONDELGEM	1000 m buffer	565 m buffer
SINT-BAVO	100 m buffer	565 m buffer
PROVINCIEHUIS	100 m buffer	1000 m buffer
PLANTENTUIN	100 m buffer	100 m buffer
MELLE	ECOCLIMAP-II	/

5.4.3 Building fraction and building height

In this section the sensitivity of the modelled temperature is examined specifically with respect to the city geometry parameterisation. This is done by investigating how the model performance changes if the built fraction or building height is implemented in the model instead of the default values. The default value for the built fraction amounts to 0,50 and for building height the default value is set to 10 m for all areas around the stations. The different model runs are accomplished by using the built fraction and building height obtained from the previous GIS-analysis for the 1km² area (tables 5 and 6). Although a lot of the scores seem to be the same at the precision level in the following tables, there are some very small but significant differences in model performance. That is why some values are marked with a colour as best value for specific runs even though the numbers seem to be the same at that precision level.

5.4.3.1 Melle

Although the p-values in table 26 denote that all different runs differ significantly from the observed temperatures for the Melle station, some deductions can be drawn concerning to which implementation deviates more or less from the observed temperatures. For Melle, the built fraction is lowered from 0,50 to 0,19 as perceived in table 6. In table 26, a very small change is observed in the p-values when the built fraction is adapted. Although, the averaged simulated temperatures do not differ at the precision level in table 26. The paired T-test between the default run of the BBK data and the run with the adapted built fraction points out that there is no significant difference between both temperature series (table 1 Annex IX). This means that the model is not sensitive to this change of the built fraction. However, there is a small improvement in the RMSE compared to the default 565 m BBK run, but the other scores indicate that the modelled temperatures are slightly worse when the built fraction set to 0,19 (table 26). Therefore, it can be concluded that more accurate information on the built fraction does not improve the simulation of the temperatures at the Melle location.

Table 26: Model performance of temperature at 2 m for runs with 1 km² BBK land cover data: without any changes (default run); built fraction modified to 0,19 or building height changed into 7,3 m over the period of August for the Melle location. Green indicates the best value for each score, while red indicates the worst results.

MELLE	BBK (DEFAULT)	BUILT FRACTION	BUILDING HEIGHT
AVERAGE TEMPERATURE (°C)	17,64	17,64	17,64
P-VALUE	4,04E-14	3,86E-14	4,62E-14
INDEX OF AGREEMENT (%)	0,86	0,86	0,86
RMSE (°C)	3,19	3,19	3,19
BIAS (°C)	-0,93	-0,93	-0,93

When the building height is set to 7,3 m instead of 10 m then there is a very small change in model performance because the temperatures of this run differ significantly from the default run (table 1 Annex IX). The index of agreement is slightly worse, while the p-value, RMSE and bias improve slightly compared to the default BBK run (table 26). From this it can be concluded that the implementation of the building height improves the temperature modelling slightly. Although, the systematic RMSEs obtained with the different city geometry parameterisations are similar (figure 34). This means that the different model configurations capture the physical processes equally. The observed negative biases in table 26 that are obtained for each run of the modelled temperature might influence the modelled UHI by overestimating it.

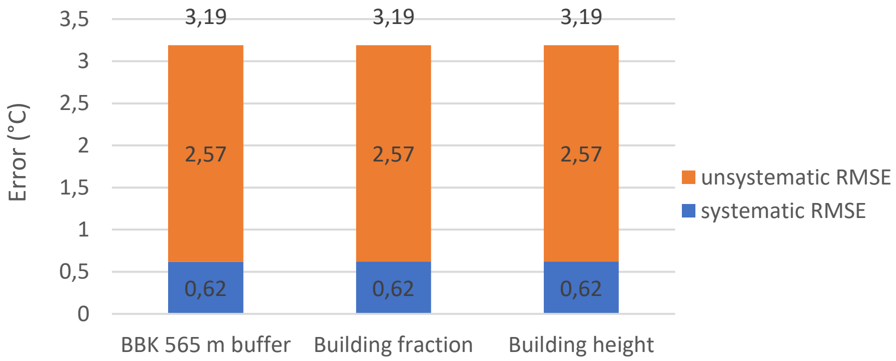

Figure 34: RMSE of the simulated temperatures subdivided into systematic and unsystematic RMSE for the different city geometry parametrizations at the Melle location.

Although, the built fraction is greatly reduced for the Melle location, there is no significant difference in the modelled temperatures. A possible reason for this is the small amount of impervious fraction, namely 9% (figure 12c). Since the impervious fraction is small, the adaptations in the TEB module do not have a large influence on the overall determination of the temperature. On the other hand, the building height parameterisation causes a significant difference for the same amount of impervious fraction, thus from this can be concluded that the model is more sensitive to the building height with respect to the built fraction.

5.4.3.2 Honda

Similar to the Melle station, the p-values in table 27 denote that all different runs differ significantly from the observed temperatures. The same feature is observed for the UHI intensities in table 28. However, some deductions can be drawn concerning to which implementation deviates more or less from the observed temperatures or UHI. When the built fraction or building height is adapted for the Honda location, then there is a visible change in the average temperatures and UHI intensities (tables 27 and 28). However, the temperature series of the built fraction run does not differ significantly from the default BBK run (tables 1 of Annex IX). On the other hand, the model performance scores do differ significantly from each other (tables 2 - 4 and 6 - 8 from Annex IX). The smaller index of agreement, larger RMSE and more negative bias indicate that the temperatures are simulated slightly worse when the built fraction is modified to 0,23 instead of 0,50 (table 27). On the other hand, the p-value indicates that the simulated temperatures with the built fraction parameterisation fit the observed temperatures better. Because the resulting simulated temperatures do not differ significantly from the default run, the model does not improve significantly with this adaptation in built fraction. Another feature that supports this conclusion is the fact that the systematic RMSEs are equally for the three different city geometry parameterisations, as it is seen in figure 35.

Table 27: Model performance of temperature at 2 m for runs with 1 km² BBK land cover data: without any changes (default run); built fraction modified to 0,23 or building height changed into 16,7 m over the period of August for the Honda location. Green indicates the best value for each score, while red indicates the worst results.

HONDA	BBK (DEFAULT)	BUILT FRACTION	BUILDING HEIGHT
AVERAGE TEMPERATURE (°C)	18,30	18,29	18,28
P-VALUE	1,63E-22	1,80E-22	1,52E-23
INDEX OF AGREEMENT (%)	0,78	0,78	0,78
RMSE (°C)	3,43	3,46	3,41
BIAS (°C)	-1,27	-1,28	-1,29

In contrast to the built fraction parameterisation, there is a significant difference between the temperature series of the default BBK and building height parameterisations (table 1 Annex IX). When the building height is set to 16,7 m (table 6), then the index of agreement and RMSE indicate that the model output improves slightly compared to the default run. Contrary, the larger absolute value of the bias and smaller p-value suggest this model configuration produces temperatures that differ more from the observed temperatures. Thus, based upon the different scores it cannot be concluded that the building height parameterisation improves the temperature modelling completely. Since the bias is negative for all runs, it is expected that the UHI will be underestimated by using these simulated temperatures.

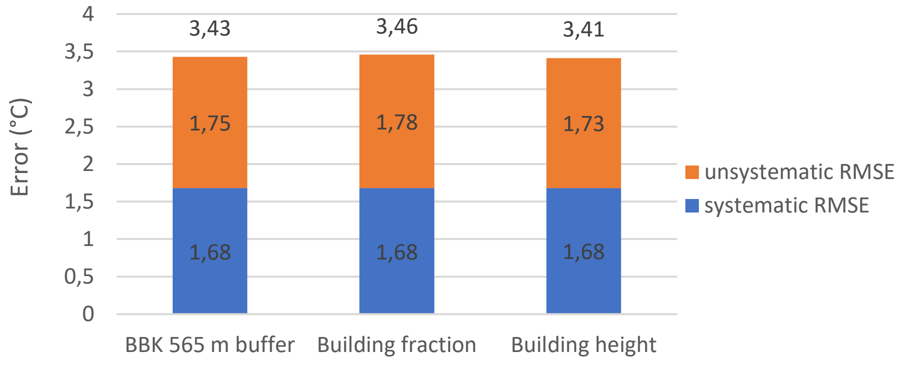

Figure 35: RMSE of the simulated temperatures subdivided into systematic and unsystematic RMSE for the different city geometry parametrizations at the Honda location.

In table 28, it is observed that the model performance of the UHI decreases when the built fraction is applied. However, the adaptation of the built fraction causes a lower systematic RMSE (figure 36), meaning the physical processes are better integrated. Even with those observations, the UHI intensity series of the built fraction run does not differ significantly from the default BBK run and thus there is no significant improvement by applying the more detailed information about the build fraction (table 5 of Annex IX).

Table 28: Model performance of the UHI at the Honda location for the runs with 1 km² BBK land cover data: without any changes (default run); built fraction modified or building height adjusted over the period of August. Green indicates the best value for each score, while red indicates the worst results.

HONDA	BBK (DEFAULT)	BUILT FRACTION	BUILDING HEIGHT
AVERAGE UHI (°C)	0,66	0,65	0,64
P-VALUE	3,24E-06	3,07E-06	2,80E-07
INDEX OF AGREEMENT (%)	0,60	0,60	0,60
RMSE (°C)	1,88	1,93	1,83
BIAS (°C)	-0,34	-0,35	-0,37

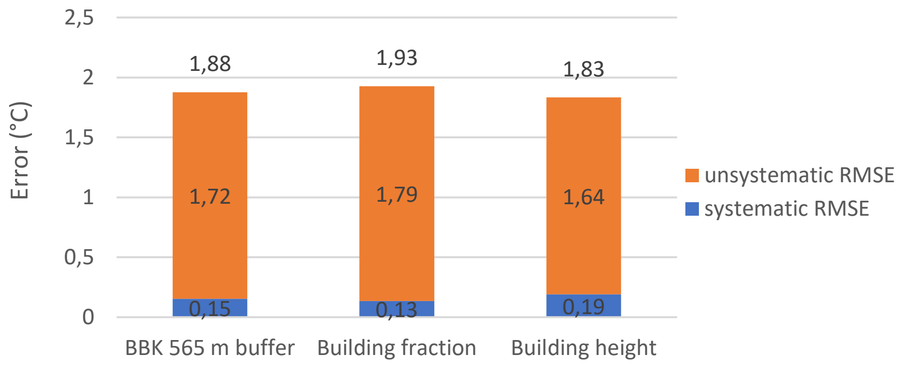

Figure 36: RMSE of the simulated UHI subdivided into systematic and unsystematic RMSE for the different city geometry parametrizations at the Honda location.

Contrary to the built fraction adjustment, the building height adjustment produces UHI intensities that are significant different from the default run (table 5 Annex IX). When the building height is adjusted in the model, the systematic RMSE and absolute value of the bias become larger, while the index of agreement and p-value decrease slightly (table 28). This indicates that the model performance is worse compared to the default run. In table 28 it is seen that the bias of the modelled UHI is negative for all runs. This means the UHI is underestimated and this is caused by the larger absolute value of the negative biases of the modelled Honda temperatures (table 27) compared to the biases of the simulated temperatures at Melle (table 26).

For this station the building height has thus a larger influence than the built fraction on the simulated temperatures and UHI, since the building height causes significant different temperature and UHI series and the built fraction does not. It is not clear why the built fraction parameterisation does not differ significant from the default run since the impervious fraction amounts to 76% for this station (figure 7c) and the value of the built fraction is lowered a lot.

5.4.3.3 Wondelgem

The p-values of the model runs at the Wondelgem location indicate that the model output differs significantly for the different city geometry parameterisations (tables 29 and 30). Although, some deductions can be made on the model performance of the simulated temperatures and UHIs by comparing the statistical scores of the different runs. For the Wondelgem site there is no significant change in simulated temperatures when the built fraction is set to 0,42 (table 1 Annex IX). However, the Wondelgem station is surrounded by 40% impervious surface (figure 8c). A possible reason for this insignificant small change could be the very small change in the built fraction with respect to the default setting of 0,50. From table 29 it is seen that the RMSE is slightly smaller for the modelled temperatures when the built fraction is adapted to 0,42. However, the smaller p-value, smaller index of agreement and the larger absolute value of the bias are indicating a slightly worse result for the simulated temperatures by implementing the more precise built fraction obtained with the GIS-analysis. Thus, a more precise parameterisation of the building fraction does not improve the model at the Wondelgem site because there is a decrease in model performance and an insignificant difference between the temperatures of the default run. From figure 37 it is also observed that the systematic RMSE is similar for all runs. This means that the different parameterisations resemble the physical processes equally.

Table 29: Model performance of temperature at 2 m for runs with 1 km² BBK land cover data: without any changes (default run); built fraction modified to 0,42 or building height changed into 7,3 m over the period of August for the Wondelgem location. Green indicates the best value for each score, while red indicates the worst results.

WONDELGEM	BBK (DEFAULT)	BUILT FRACTION	BUILDING HEIGHT
AVERAGE TEMPERATURE (°C)	18,57	18,57	18,58
P-VALUE	2,04E-05	1,93E-05	3,00E-05
INDEX OF AGREEMENT (%)	0,86	0,86	0,86
RMSE (°C)	3,10	3,10	3,10
BIAS (°C)	-0,52	-0,52	-0,51

When the building height is set to 7,3 m instead of 10 m (table 6), then the temperature series differ significantly (table 1 Annex IX). The model is thus more sensitive to the change in the building height than a change in the built fraction. Therefore, the parameterisation of the building height is more important to take into account if the temperatures are simulated at the Wondelgem location. In table 29, the RMSE and index of agreement are worse compared to the default run when the building height is set to 7,3 m. Although these values indicate a worse model performance, the absolute value of the bias is smaller than the default setting and the p-value is larger. This suggests that the model produces temperatures that are closer to the observations when the more precise building height is implemented. The negative biases in table 29 indicate that the model underestimates the temperature systematically when those parameterisations are used. Therefore, it is likely that the UHI might be underestimated as well.

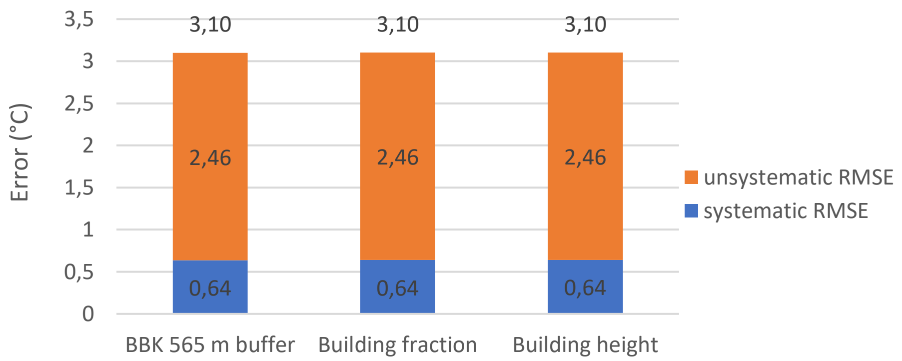

Figure 37: RMSE of the simulated temperatures subdivided into systematic and unsystematic RMSE for the different city geometry parametrizations at the Wondelgem location.

In table 30 there is no visible distinction between the modelled UHI if the built fraction is changed into the value obtained with the GIS-analysis (table 5). However, the T-test points out that the UHI series of the default run and the run with the modification of the built fraction differ significantly (table 5 Annex IX). Except for the p-value, there is no visible difference observed in the scores for the precision level represented in table 30. If a higher precision is taken into account, then the model output has a slightly larger index of agreement and a lower bias (table 30). This means the model performance is slightly better if the more precise built fractions are implemented. In addition, the systematic RMSE is slightly lower (figure 38), indicating a better representation of the physical processes in the model. These small improvements are significant and therefore it is concluded that the implementation of more accurate built fraction leads towards a better simulation of the UHI (tables 6 and 8 Annex IX).

Table 30: Model performance of the UHI at the Wondelgem location for the runs with 1 km² BBK land cover data: without any changes (default run); built fraction modified to 0,42 or building height changed into 7,3 m over the period of August. Green indicates the best value for each score, while red indicates the worst results.

WONDELGEM	BBK (DEFAULT)	BUILT FRACTION	BUILDING HEIGHT
AVERAGE UHI (°C)	0,93	0,93	0,94
P-VALUE	3,98E-19	5,68E-19	1,66E-19
INDEX OF AGREEMENT (%)	0,48	0,48	0,48
RMSE (°C)	1,21	1,21	1,22
BIAS (°C)	0,41	0,41	0,42

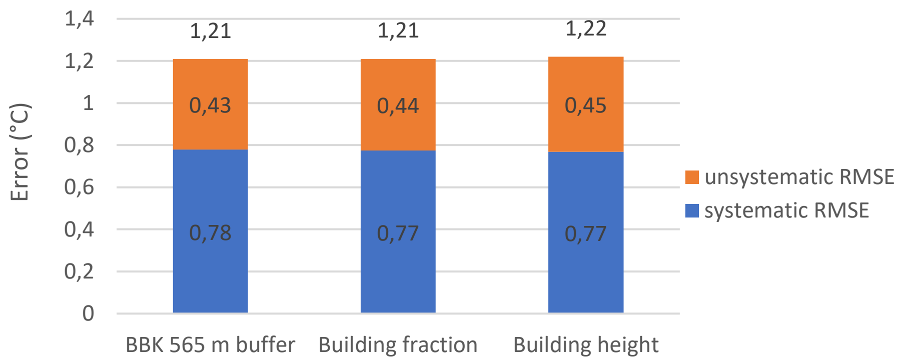

Figure 38: RMSE of the simulated UHI subdivided into systematic and unsystematic RMSE for the different city geometry parametrizations at the Wondelgem location.

Changing the building height to 7,3 m decreases the model performance of the UHI slightly since the RMSE and bias are larger and the p-value is lower. However, the index of agreement and systematic RMSE indicate that the model simulates slightly better the temperatures than the default run. There is thus a small improvement in capturing the physical processes, but the UHI intensities are not simulated better in general. The bias of all runs is positive what indicates that the UHI is overestimated with all the different model settings in table 30.

5.4.3.4 Sint-Bavo and Provinciehuis

For the Sint-Bavo and Provinciehuis stations there is a significant change in modelled temperatures and UHI intensities when the built fraction or the building height is modified into the values obtained with the GIS-analysis (table 1 Annex IX). The model performance of the simulated temperatures and UHI can be investigated, although the p-values in tables 31, 32, 33 and 34 denote that all different runs differ significantly from the observed temperatures or UHI intensities. The larger p-value for the runs with the built fraction indicates that the modelled temperatures are closer to the observed ones (tables 31 and 32). However, the indexes of agreement indicate that the temperatures are simulated slightly worse than the default run (tables 31 and 32). The better fit is thus linked with the smaller RMSE and smaller absolute value of the bias (tables 31 and 32). These listed statistical scores differ significant form each other (tables 2 - 4 of Annex IX), although the precision level in tables 31 and 32 does not reveal this difference. When the systematic RMSE is studied (figure 39), then there is no improvement observed with respect to the default run for the Sint-Bavo station when the built fraction is set to 0,57 (table 5). When the built fraction is adjusted into 0,58 for the Provinciehuis station (table 5), then the systematic RMSE indicates that the model captures the physical processes less good with the implementation of the more accurate built fraction (figure 40). Thus, the implementation of the built fraction does not lead to a fundamental improvement of the simulated temperatures for the Sint-Bavo and Provinciehuis locations.

When the building height is adjusted to 18,0 m for the Sint-Bavo station and 19,6 m for the Provinciehuis station, then a lower RMSE is obtained with respect to the default run (tables 6, 31 and 32). In addition, the indexes of agreement are slightly higher for both stations, implying the model performance is better with the more accurate building height (tables 31 and 32). On the other hand, the absolute values of the bias are noticeably larger, which denotes that the model simulates the temperatures worse than when the default building height is used (tables 31 and 32). The systematic RMSEs are slightly smaller with the modified building height, indicating the model captures the physical processes slightly better (figures 39 and 40). Thus, although the p-values indicate that the simulated temperatures deviate more from the observed temperatures, the model captures the physical processes better with the implementation of the more accurate building heights.

Table 31: Model performance of temperature at 2 m for runs with 1 km² BBK land cover data: without any changes (default run); built fraction modified to 0,57 or building height changed into 18,0 m over the period of August for the Sint-Bavo location. Green indicates the best value for each score, while red indicates the worst results.

SINT-BAVO	BBK (DEFAULT)	BUILT FRACTION	BUILDING HEIGHT
AVERAGE TEMPERATURE (°C)	19,14	19,17	19,12
P-VALUE	1,14E-05	2,50E-05	3,76E-06
INDEX OF AGREEMENT (%)	0,83	0,83	0,83
RMSE (°C)	3,24	3,24	3,22
BIAS (°C)	-0,55	-0,53	-0,58

Table 32: Model performance of temperature at 2 m for runs with 1 km² BBK land cover data: without any changes (default run); built fraction modified to 0,58 or building height changed into 19,6 m over the period of August for the Provinciehuis location. Green indicates the best value for each score, while red indicates the worst results.

PROVINCIEHUIS	BBK (DEFAULT)	BUILT FRACTION	BUILDING HEIGHT
AVERAGE TEMPERATURE (°C)	19,44	19,47	19,41
P-VALUE	0,004	0,008	0,002
INDEX OF AGREEMENT (%)	0,82	0,82	0,83
RMSE (°C)	3,30	3,30	3,27
BIAS (°C)	-0,37	-0,34	-0,40

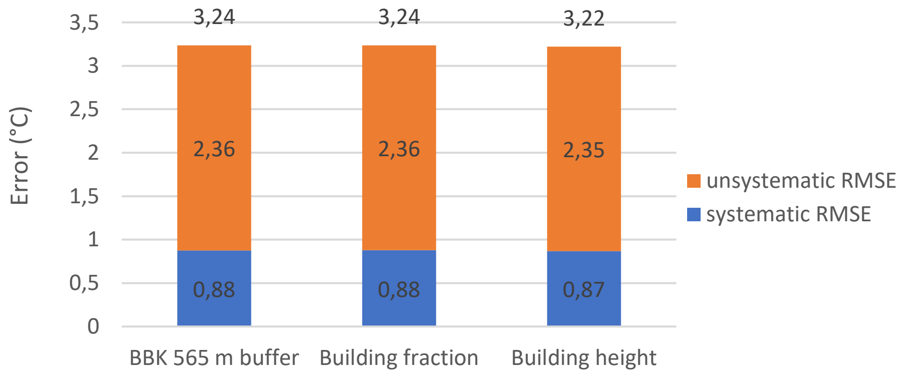

Figure 39: RMSE of the simulated temperatures subdivided into systematic and unsystematic RMSE for the different city geometry parametrizations at the Sint-Bavo location.

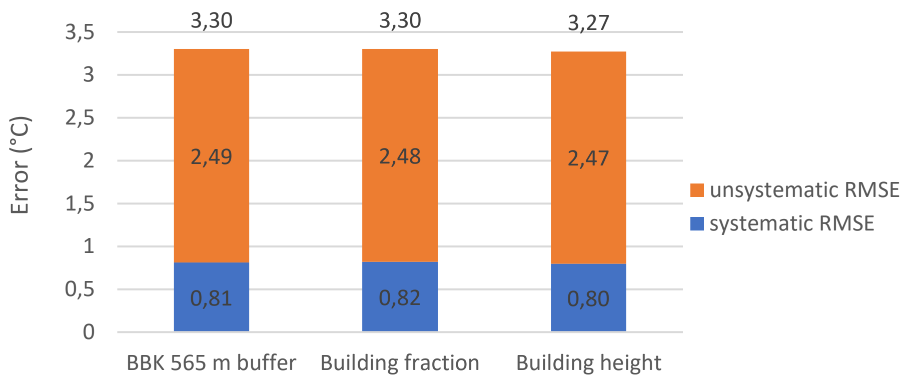

Figure 40: RMSE of the simulated temperatures subdivided into systematic and unsystematic RMSE for the different city geometry parametrizations at the Provinciehuis location.

In addition, it would be interesting to examine to what extent a higher building height leads towards higher temperatures since a larger change in building height seems to have a larger impact on the simulated temperatures. A similar experiment could be examined for the built fraction, since a small change in built fraction seems to have a smaller influence on the simulated temperatures than a large change. A correlation analysis is suggested to be executed for investigating this.

From tables 33 and 34 is derived that the UHI is overestimated with all the different model settings, since the biases of all runs are positive. This is due to the underestimation of the modelled temperatures at the rural location Melle (table 26) and is slightly compensated by the underestimation of the temperatures simulated for the Sint-Bavo and Provinciehuis locations (tables 31 and 32). The smaller RMSE obtained by changing the built fractions of Melle and Sint-Bavo is significant and points towards an improvement of the model (table 33 and table 7 Annex IX). This is not the case for the Provinciehuis station, where the RSME is larger and thus indicates that the model is doing worse when the more accurate built fractions are implemented (tables 5 and 34). The larger biases, smaller indexes of agreement and lower p-values indicate that the model simulates the UHI slightly worse when the built fraction is adapted for both locations. In addition, the larger systematic RMSE of both stations shows that the more accurate built fraction does not capture the physical processes as well as the default run does (figures 41 and 42). The implementation of the accurate built fraction thus causes a model that is not as good at simulating the UHI compared to the model with the default settings. Therefore, it is discouraged to use the more accurate built fraction for simulations of the UHI in the core of the city.

When the building height is adapted for the Sint-Bavo and Provinciehuis station, then the model simulates the UHI better based upon all the statistical scores in tables 33 and 34 that are better. However, the larger systematic RMSEs in figures 41 and 42 reveal that the model captures the physical processes less when the more accurate building height is implemented. Thus, the model approximates the observed UHI better, but this is due to the compensation of errors in the temperatures of the rural and urban stations when the UHI is calculated. Therefore, the underlying physical processes are not better represented and the improvement of the model output is artificial without physical meaning.

Table 33: Model performance of the UHI at the Sint-Bavo location for the runs with 1 km² BBK land cover data: without any changes (default run); built fraction modified to 0,57 or building height changed into 18,0 m over the period of August. Green indicates the best value for each score, while red indicates the worst results.

SINT-BAVO	BBK (DEFAULT)	BUILT FRACTION	BUILDING HEIGHT
AVERAGE UHI (°C)	1,51	1,53	1,48
P-VALUE	4,08E-09	4,34E-10	2,00E-08
INDEX OF AGREEMENT (%)	0,63	0,62	0,63
RMSE (°C)	1,64	1,64	1,58
BIAS (°C)	0,37	0,40	0,34

Table 34: Model performance of the UHI at the Provinciehuis location for the runs with 1 km² BBK land cover data: without any changes (default run); built fraction modified to 0,58 or building height changed into 19,6 m over the period of August. Green indicates the best value for each score, while red indicates the worst results.

PROVINCIEHUIS	BBK (DEFAULT)	BUILT FRACTION	BUILDING HEIGHT
AVERAGE UHI (°C)	1,80	1,83	1,77
P-VALUE	7,99E-16	2,18E-17	2,99E-15
INDEX OF AGREEMENT (%)	0,59	0,58	0,59
RMSE (°C)	1,80	1,81	1,73
BIAS (°C)	0,56	0,59	0,52

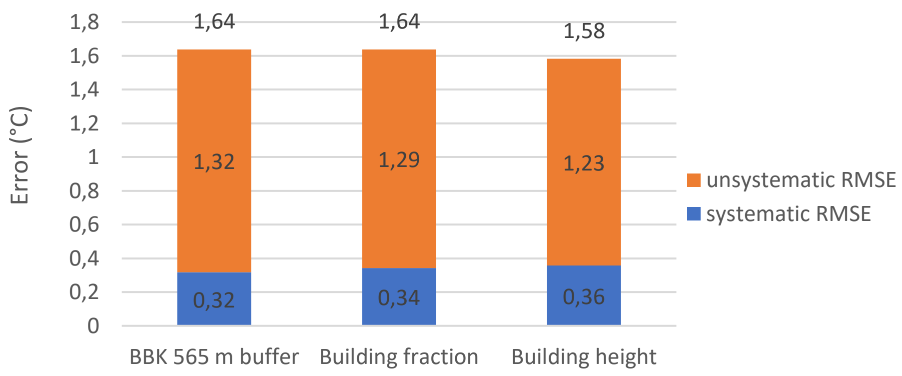

Figure 41: RMSE of the simulated UHI subdivided into systematic and unsystematic RMSE for the different city geometry parametrizations at the Sint-Bavo location.

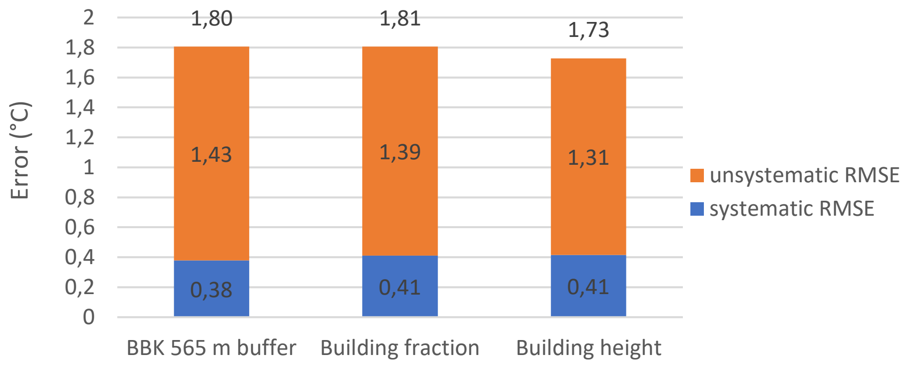

Figure 42: RMSE of the simulated UHI subdivided into systematic and unsystematic RMSE for the different city geometry parametrizations at the Provinciehuis location.

5.4.3.5 Plantentuin

In contrast with the previous stations, the simulated temperatures for the Plantentuin location do not differ significantly from the observed ones with the different city geometry parameterisations (table 35). When the built fraction of 0,52 is implemented for the Plantentuin site (table 5), then there is a slightly higher average temperature obtained that differs significantly from the default run (table 35 and table 1 of Annex IX). Although, there is almost no change in model performance when the built fraction is adapted (table 35). When the higher precision level is taken into account, the model is simulating the temperatures worse based on the slightly larger RMSE and bias (table 35). In addition the lower p-value displays that the simulated temperatures differ more from the observed temperatures than it is the case with the default settings (table 35). However, the index of agreement is indicating that the model performs better than the default run (table 35). The systematic RMSE is similar to the systematic RMSE of the default run (figure 43). There is thus no significant added value when the more accurate built fraction is used to model the temperatures of the Plantentuin station.

Based upon all the different scores in table 35, there is a noticeable improvement in the model performance when the building height is adapted to 15,4 m. The lower systematic RMSE denotes as well that the more accurate parameterisation of the building height improves the model (figure 43). Therefore, it can be concluded that the model captures the physical processes better and simulates the temperatures better when the building height of the GIS-analysis is implemented for the Planetentuin station. The bias is positive for all runs in table 35 and therefore the modelled UHI might be overestimated.

Table 35: Model performance of temperature at 2 m for runs with 1 km² BBK land cover data: without any changes (default run); built fraction modified to 0,52 or building height changed into 15,4 m over the period of August for the Plantentuin location. Green indicates the best value for each score, while red indicates the worst results.

PLANTENTUIN	BBK (DEFAULT)	BUILT FRACTION	BUILDING HEIGHT
AVERAGE TEMPERATURE (°C)	19,18	19,19	19,17
P-VALUE	0,024	0,022	0,033
INDEX OF AGREEMENT (%)	0,85	0,85	0,85
RMSE (°C)	3,14	3,14	3,13
BIAS (°C)	0,28	0,28	0,26

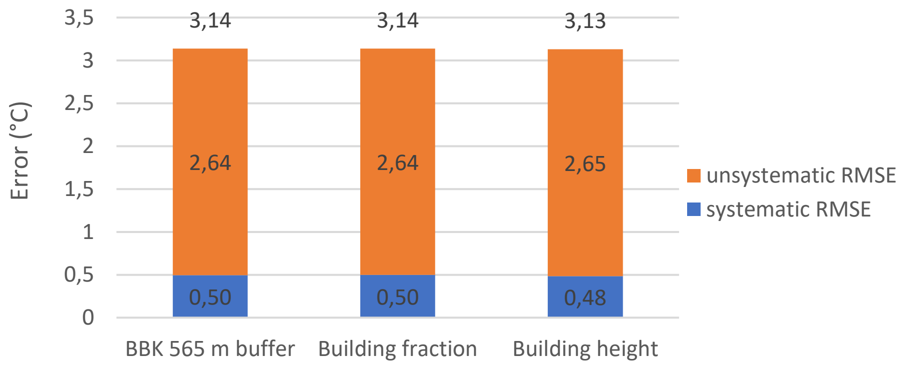

Figure 43: RMSE of the simulated temperatures subdivided into systematic and unsystematic RMSE for the different city geometry parametrizations at the Plantentuin location.

In table 36, it is observed that all the different city geometry parameterisations overestimate the UHI, since the bias is positive. This was expected since the bias of the temperature simulations of Melle and Plantentuin both indicated that the model would overestimate the UHI. Based upon the statistical scores in table 36 it is derived that the model performance of the UHI decreases slightly when the more accurate built fractions are applied. The systematic RMSE in figure 44 indicates also that the implementation of the built fraction from the GIS-analysis deteriorates the simulation of the UHI.

When the building heights are adjusted, the value of the RMSE and bias lowers as observed in table 36. This indicates a small improvement of the modelled UHI at the Plantentuin site. On the other hand the p-value, index of agreement and the systematic RMSE indicate that the model is doing slightly worse when the more accurate building heights are implemented (table 36 and figure 44). Therefore, it is concluded that the more accurate implementation of the building height does not improve the modelled UHI completely for the Plantentuin station.

Table 36: Model performance of the UHI at the Plantentuin location for the runs with 1 km² BBK land cover data: without any changes (default run); built fraction modified to 0,52 or building height changed into 15,4 m over the period of August. Green indicates the best value for each score, while red indicates the worst results.

PLANTENTUIN	BBK (DEFAULT)	BUILT FRACTION	BUILDING HEIGHT
AVERAGE UHI (°C)	1,55	1,55	1,53
P-VALUE	1,51E-94	1,29E-95	1,18E-94
INDEX OF AGREEMENT (%)	0,57	0,56	0,57
RMSE (°C)	1,74	1,74	1,71
BIAS (°C)	1,21	1,21	1,19

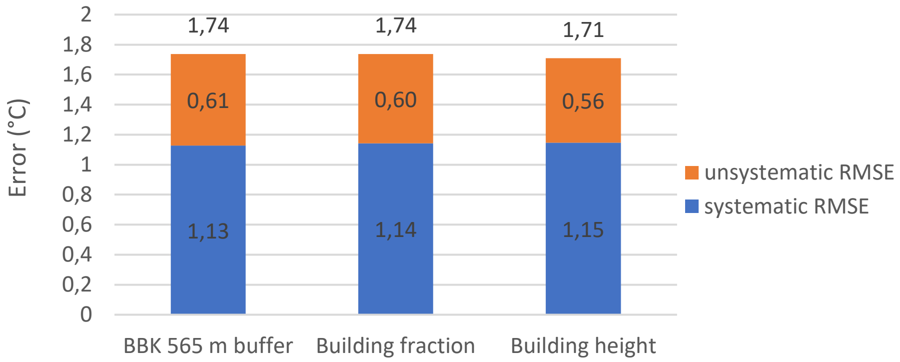

Figure 44: RMSE of the simulated UHI subdivided into systematic and unsystematic RMSE for the different city geometry parametrizations at the Plantentuin location.

5.4.3.6 General impact of changing city geometry

From the previous sections it can be deduced that none of the stations experience a transition of p-values under the threshold of 0,01 towards p-values above 0,01 when the city geometry parameters are adapted and vice versa. This means that the model output, which differs significantly from the observed temperatures and UHI does not shift towards a model output that is similar to the observed values and vice versa. However, some model outputs deviate less from the observed temperatures when the city geometry is adapted based on the different scores that reflect the model performance. From this it can be concluded that a modification in the city geometry results in only small changes in the model output. Except for the simulations of the temperatures at the Plantentuin location, the model simulates temperatures and UHI intensities that differ significantly from the observed ones with the different city geometry implementations. This indicates that the model should be improved in general.

Implementing the more detailed built fraction generally does not lead towards a notable positive influence on the modelled temperatures. For the Melle, Honda and Wondelgem locations there is no significant difference between the default run and the run with the built fraction of the GIS-analysis.

From this it can be concluded that the model is not very sensitive to the adaptations in the built fraction. These three stations that do not differ significantly from the default run have a built fraction that is lower than the default value of 0,50. The other stations with a significant difference have a built fraction that is slightly larger than 0,50. It is thus likely that the value of 0,50 for the built fraction functions as a threshold value for the simulation of the temperatures. When the building height is adjusted to the values of the GIS-analysis, then the modelled temperatures improves slightly for the Melle, Sint-Bavo, Provinciehuis and Plantentuin locations. In contrast to this, the model performance is slightly worse for Honda and Wondelgem when the building height is adapted. For the Honda station the decrease in model performance might be due to the spatial scale that is used for the modelling, since the building height is inhomogeneous at different scale levels (figure 20).

The modelled UHI intensities differ significantly from each other when the city geometry is modified. Except for the Wondelgem station, there is no improvement of the modelled UHI when the detailed building fractions of the GIS-analysis are implemented. Therefore, it is not worth it to implement the more accurate built fractions into the model because the model performance of the simulated temperatures and UHI intensities decrease slightly in most of the cases. Implementing the building height has a positive effect on the model performance of the UHI for the Sint-Bavo and Provinciehuis locations, but this is an artificial improvement without a physical meaning. For the Wondelgem station there is a slight decrease in model performance when the building height is adapted to the value obtained with the GIS-analysis. However, the physical processes are slightly better captured when the more accurate building heights are implemented for this station. The use of more detailed building heights causes worse model results for UHI at the Honda and Plantentuin sites. Therefore, it is concluded that the more accurate building height does not improve the model sufficiently to apply it.

5.4.4 Comparison of changes in land cover and city geometry

Since adapting the built fraction has no noticeable influence on the modelled temperatures of the Melle, Honda and Wondelgem stations (table 1 Annex IX), it can be concluded that the model is not sensitive to changes of the built fractions for those stations. However, the model is sensitive to the adjustments of the built fraction when the UHI is determined for those stations (table 5 Annex IX). For the other stations both temperature and UHI are slightly influenced by the adaptations in the built fraction. The model output undergoes slightly larger changes for every station when the building height is adapted. Therefore, it can be concluded that the model is more sensitive to changes in the building height than changes in the built fraction. Thus, it is more important to improve the parameterisation of the building height because the building height has more influence on the model results than the built fraction.

When the land cover is adapted much larger changes in model performance are obtained compared to the changes that arise when the parameters of the city geometry are adapted. From this it is concluded that the model is more sensitive to changes in land cover. Therefore, it is more important to define the land cover correct to get better model results than implementing the detailed information of the city geometry.

In the previous sections with the modelling results, the biases are not directed towards a specific direction since they variate in positive and negative directions. This indicates that there is no systematic error in the model, but that the error is rather due to the application of different land cover and city geometry parameterisations. Hence, the errors depend mainly on the characteristics of the area that is taken into account. Therefore, it is important to estimate these features correct to improve the model.

6. DISCUSSION

6.1 Land cover MOCCA stations

The land cover around the MOCCA stations corresponds with the description of Caluwaerts *et al.* (2016). The monitoring stations are sited at locations with different land cover characteristics and comprises a range of urban climate zones. This study revealed more details about the different locations of the measurement stations. Going from north to south, the Honda station is situated in the port surrounded by a large fraction of concrete and a very small fraction of taller buildings with an average height of 16,7 m (map 5, figures 19 and 20, and table 5). At this location there is a large body of water where the docks of the port can be found and it becomes visible when going from the 100 m radius towards the 565 m radius (maps 3 and 4, and figures 7b and 7c). The Wondelgem station is located in a suburban neighbourhood that is characterised by a large fraction of green space and impervious space that is occupied by a large fraction of buildings. These buildings are on average low rise buildings with an average height of 7,3 m (table 5). The Sint-Bavo and Provinciehuis stations are both situated in the densely built city centre, but their local and micro-environments differ slightly. The Sint-Bavo station is located in an urban canyon, while the Provinciehuis station is sited at a square with a building in the east direction within a radius of 10 m (map 2). However, both stations are characterised by a large fraction of buildings and tall buildings with almost an average height of 20 m (figures 19 and 20). The Plantentuin station is situated in the botanical garden of Ghent University, which is located next to a large urban park. Therefore, the land cover consists of a large amount of green space when a small radius is taken into account, but when a larger radius is taken into account the impervious fraction dominates. For this station, the fraction of buildings and building height are quite high as well, since the environment around the green lung encloses urban characteristics. The last station Melle is located in a rural environment with a very large amount of green surface and a very small amount of low rise buildings (figures 12a -12d, 19 and 20).

6.2 Appropriate scale to study the UHI effect

During nighttime the observed UHI is linked with land cover features in a radius of 565 m around the stations. The local 1 km² scale is thus important for UHI studies during nighttime. On the other hand, the UHI observed during daytime depends more on micro-environment features around the stations which influence the temperature measurements. This is proved with the two stations in the city centre. During nighttime the Sint-Bavo and Provinciehuis stations measure similar temperatures, resulting in a similar UHI and during daytime the temperatures of those two stations deviate. These differences can only be explained by the difference in the micro-environment, since both stations are located in the city centre. Similar to the findings of Pielke *et al*. (2007), the importance of the siting of the stations is emphasised in this study with some specific cases like the observations of the Wondelgem and Provinciehuis stations that are influenced by a building close to the station positioned in a certain wind direction. For the Plantentuin station, it is observed that the surrounding trees influence the observations. An area with a scale ranging from a 10 m to 100 m buffer radius explains the temperature evolutions during the day. This is in contrast to the findings of Van Hove *et al*. (2014), who stated that the UHI of the UCL is determined by a buffer distance between 250 m and 500 m. However, it must be noted that they focus on the nighttime UHI since they use the maximum UHI values to determine the area of influence. Based on these outcomes, it can be concluded that it is better to split up into daytime and nighttime measurements. In order to substantiate the findings according to the appropriate scale more scientifically, it is recommended to do a linear regression and see which buffer area has statistically the highest correlation coefficient with respect to the observed UHI (Van Hove *et al*., 2014). The modelling results in this study show that the UHI is best simulated with the 565 m land cover parameterisation, since this parameterisation is best for three out of five stations. Thus, compared to the Rotterdam study of Van Hove *et al*. (2014) a slightly wider area affects the UHI in Ghent.

Since the composition of the land cover changes slightly when the buffer area is modified, there is a scale dependency in the land cover. SURFEX generates a different model output when the land cover changes. The temperature and UHI modelling are therefore scale dependent as well. This is in accordance with Pielke *et al*. (2007), who stated that temperature measurements are influenced by land cover features over a certain area. It is thus important to take into account the right size of the area that influences the UHI to study and model the UHI.

In this study for Ghent, it is additionally found that the land cover fractions and city geometry parameters are more or less scale independent when going from a 565 m radius to a 1000 m radius (figures 7a-12d). Therefore, the temperature and UHI distributions with implementation of the 565 m radius land cover fractions differ more from the 100 m model results than from the 1000 m model results, except for the Honda location (table 1 Annex IXI). This indicates there is a correlation between the land cover and the simulated temperature and UHI, as it was stated by Van Hove *et al*. (2014).

6.3 ECOCLIMAP-I versus ECOCLIMAP-II

For the locations Melle, Wondelgem and Plantentuin the land cover is estimated more correct with ECOCLIMAP-II with respect to ECOCLIMAP-I (tables 9, 12 and 13). Both ECOCLIMAP datasets contain the same information for the Provinciehuis and Sint-Bavo locations (tables 10 and 11), so the land cover data is not always improved when ECOCLIMAP-II is used. The land cover around the Honda station is even estimated worse by ECOCLIMAP-II (table 8). The suggestion of Faroux *et al*. (2013) that ECOCLIMAP-II would be better than ECOCLIMAP-I to estimate the land cover is thus not always true. The issue that the land cover at the Honda location is poorly estimated with the ECOCLIMAP-II database corresponds to the findings of Tijm and de Vries (personal communication, 3 April 2018) who obtained similar results for urban areas in the Netherlands. Thus, the shortcomings of ECOCLIMAP-II with respect to ECOCLIMAP-I should be investigated and solved, as Le Moigne *et al*. (2018) advised.

Most of the model results deviate still significant from the observations when the land cover of a different database is implemented. This could be caused by the poor tuning of the model or the input of bad forcings. Although the poor model performances, there is some sensitivity seen in the model outputs of the different land cover parameterisations. Based on this sensitivity some conclusions can be drawn according the model performance obtained with ECOCLIMAP-I and ECOCLIMAP-II. For the simulated temperatures the model performance with ECOCLIMAP-II is better for three out of six stations (tables 14, 17 and 23). For the Sint-Bavo and Provinciehuis stations the model performance of temperature remains the same when ECOCLIMAP-II is implemented (tables 19 and 20) and the model performance becomes worse for the Honda station (table 15). These resulting model performances can be linked with the improvements and deterioration that were found for land cover data of ECOCLIMAP-II. This finding supports Lemonsu *et al*. (2004) who declared that it is important to estimate the land cover well in order to obtain good model results. These improvements in the simulation of the temperatures cause an improvement in the simulated UHI for all the stations except for the Honda station when ECOCLIMAP-II is implemented instead of ECOCLIMAP-I. Honda is an exception to this since it is the only station with a worse estimation of the land cover when ECOCLIMAP-II is implemented. For the Provinciehuis and Sint-Bavo locations the improvement is however completely due to the improvement of the simulated temperatures in Melle, since their land cover fractions do not differ between ECOCLIMAP-I and ECOCLIMAP-II.

6.4 Effect of higher resolution data

The different land cover datasets are compared at the same scale level of 1 km², since it is proved that land cover fractions depend on the scale level. It is expected that the UHI will be better represented if more accurate and higher resolution land cover data is implemented in SURFEX. However, the model performances show that the temperatures are better simulated when the land cover fractions of the high resolution BBK land cover data are implemented for only the Wondelgem and Plantentuin locations. The implementation of the higher resolution data does not result in a better simulation of the temperatures in general, since the model performance is worse for four out of six stations. A possible explanation could be the poor model tuning and the fact that the model tuning was based upon the ECOCLIMAP-I land cover data. It would have been better to tune the model based upon the BBK data of Melle, since it is assumed that this land cover data is the most accurate land cover data.

Based upon the scores of the UHI modelling the model should undergo a general improvement as well. The simulated UHI intensities are best for all locations if the 1 km² BBK data is applied, except for the Plantentuin site. However, the simulated temperatures and UHI of Plantentuin site obtain the best model performance when the 100 m buffer BBK land cover data is implemented. Hence, it is better to look at the land cover of a smaller environment for the Plantentuin station to estimate the UHI and that is why the Plantentuin is an exception for the UHI modelling at 1 km² scale. In general, it can be concluded that the UHI is better approached when the land cover fractions of the BBK are implemented in SURFEX. The UHI is thus better represented when more accurate and higher resolution land cover data is implemented in SURFEX. However, this better simulation of the UHI is contradictory to the temperatures that are simulated worse for most of the stations, with the only exception being Wondelgem. The better simulation of the UHI can be explained by compensating errors of the rural and urban temperatures. Although, there is some added value to the physical processes by simulating the UHI with the BBK data, since the systematic RMSE is small for the simulated UHI intensities.

6.5 Sensitivity of different model parameters

Only very small changes are observed in the model output when a modification is made in one of two TEB parameters that were investigated. The city geometry parameters that were taken into account are the building fraction and building height. Except for the small improvement at Wondelgem station, there is no improvement of the modelled UHI when the detailed building fractions of the GIS-analysis are implemented in SURFEX. Implementing the building height has a positive effect on the model performance of the UHI for the Sint-Bavo and Provinciehuis locations, but this is an artificial improvement without a physical meaning. Therefore, it is concluded that more accurate building heights and built fractions do not improve the model sufficiently to implement them. Compared to the built fraction, the model output undergoes slightly larger changes for every station when the building height is adapted. Therefore, it can be concluded that the model is more sensitive to changes in the building height. Hence, it is more important to improve the building height parameterisation because this city geometry parameter has more influence on the model results than the built fraction. In addition, it must be noted that in this study for Ghent the building height does not influence the simulated temperatures and UHI intensities as much as was highlighted for the city of Basel by Hamdi & Schayes (2008). To know whether other aspects of the urban canyon play a crucial role in estimating the UHI, the sensitivity of the model to the wall-to-horizontal-surface ratio could be investigated for example.

Modifications of the land cover cause much larger changes in the model performance of the UHI compared to the city geometry parameters. From this it is concluded that the model is more sensitive to changes in land cover. Therefore, it is important to correctly define the land cover to improve the model results. Hence, the land cover is the most dominant parameter in the SURFEX scheme out of the parameters that were investigated in this study. This is in contrast with the outcome of Van Hove *et al*. (2014) that the building fraction is the strongest predictor for the UHI. Moreover, Van Hove *et al*. (2014) stated that the land cover, built fraction and building height have a significant influence on the UHI in Rotterdam. In contrast with these findings, the building fraction does not always have a significant influence on the UHI in this study for Ghent.

Finally, none of the parameters that were adapted are able to improve the model sufficiently. Therefore, it is concluded that the SURFEX scheme and the forcing at 4 km resolution should be further investigated to improve the model results.

6.6 Outlook

In the near future the atmospheric forcings at 4 km resolution that are given as input to the SURFEX model should be examined. The model performance of the temperature and UHI at the 4 km scale should be compared with the results of the 1 km scale to see whether there is added value by using SURFEX. The 4 km resolution temperature forcing at the Melle location should approximate the observations well, since this is a rural location. For such an environments the regional model should be able to capture the physical processes well, resulting in temperatures that are reproduced well. On the other hand, the performance of forcings of grid points at urban locations could be worse compared to the performance in Melle, since the urban features are not implemented in the 4 km resolution model. When the forcings of the urban locations are worse than the forcing for Melle then it makes sense to implement the downscaling of 1 km with the urban features. If there are in general large errors in these forcings, then it would explain why the statistical scores of the simulated temperatures and UHIs are poor in general.

On the other hand, the SURFEX model should be improved to obtain model results that are more in line with the observations. In order to improve the parameterisations of the model, more parameters could be investigated in a similar way as was done in this study. The wall-to-horizontal-surface ratio is a city geometry parameter that could be examined easily by adapting the default value in the model. This parameter could be retrieved approximately with a GIS-analysis and might have some influence on the UHI, since this is a characteristic of the urban canyon (Hamdi & Schayes, 2008). Other parameters that might be important to consider when studying the temperatures and UHI are the albedo and emissivity of the roofs, roads and to a lesser extend the albedo of the walls. Also the impact of anthropogenic features would be interesting to investigate, although it is more difficult to quantify this. In the SURFEX model this is quantified by latent and sensible heat produced by industries and traffic. The numbers of these parameters are not directly available. To solve this problem measurements could be taken or proxies could be used. Besides the parameterisations in the model, the physics package of the model should be revised and be improved if possible. It is likely that the physics which represent the land-surface processes can be improved, since the bias and RMSE remain large overall when some parameterisations are improved. However, the variating biases also indicate that the model errors depend mainly on the characteristics of the area that is taken into account. When these issues are solved, the method of this study can be repeated to investigate the new model results and to compare them with the output obtained with the current version of SURFEX.

The method that was applied for this study could be improved by splitting the resulting scores into daytime and nighttime scores. This is recommended since it was found that the areas which influence the UHI differ during the day and night. In addition, different physical processes take place during day and night. Moreover, this splitting could even be expanded to a comparison of hourly results averaged over one season to see how the model performances of the temperatures and UHI change during the diurnal cycle. In this way it could be examined if there is a relationship between the model errors and the evolution of temperatures during the diurnal cycle. For example, do higher temperatures during the afternoon cause larger model errors or is it more difficult to simulate the low temperatures that appear in the morning?

It would be interesting as well to study the energy balance in more detail. In reality, the sensible, latent and ground heat fluxes and radiative balance are connected with each other and with the prevailing temperature. Therefore, it would be interesting to see whether the model incorporates these energy exchanges well. If there are any issues with one of the variables of the energy balance, then this could explain the poor model performances that were obtained.

In this study it was found that the land cover is a very important parameter to comprehend and investigate the UHI, since a more accurate land cover results in better model results. Moreover, some relationships between the land cover around the stations and average temperatures and UHI intensities were observed. From the scores it can be deduced that the impervious surface seems to lead towards average higher temperatures and the water and green fraction seem to cause lower temperatures. In addition, it was observed that a larger change in land cover leads to a larger change in the average simulated temperature. To prove these assumptions, a statistical correlation analysis is recommended for each land cover fraction to quantify the impact of a certain land cover on the resulting average temperatures and UHI. Subsequently, a statistical T-test should be applied to see whether those relationships are significant. Besides this, a linear regression is needed to substantiate the findings of the appropriate scale that should be used to study the UHI.

Another feature that still should be investigated scientifically is the homogeneity of the land cover in the different buffer areas around the stations. It is important that the land cover around the investigated stations is quite homogeneous, since homogeneity is a requirement to compute reliable fluxes with SURFEX (Lemonsu *et al*., 2004). This could be done with landscape metrics that can be computed with the program Fragstats. Zhou *et al*. (2011) reported that the composition of the land cover is more important than the land cover pattern. However, they found as well that the spatial configuration has a significant influence on the UHI and must be taken into account to mitigate the UHI. Therefore, it is advised to do a similar study for Ghent.

There is observational MOCCA data available over the period starting from July 2016 until August 2018 with more data expected for at least another year. Therefore, it would be interesting to expand this UHI study over different seasons and years. In this way the seasonal variations in the observed and modelled UHI can be studied by comparing the results of the different periods. Evolutions in the UHI on long term might be revealed by studying the data of the different years.

7. CONCLUSION

Heat stress that is amplified by the occurrence of an UHI is an increasingly-common phenomenon, since urbanisation continues. Therefore, UHI studies gain more and more importance these days. The quality of living in cities can be maintained or improved by using the knowledge of the UHI phenomenon.

To enhance the insight of the UHI concept, this study focussed on observational and modelled temperatures for the six measurement stations of the MOCCA network in Ghent for the summer period of 2016. Each area around the stations has its own land cover and city geometry characteristics. The Honda station is situated at the port, the Wondelgem station is located in a suburban neighbourhood, the Sint-Bavo and Provinciehuis stations are situated in the historical city centre, the Plantentuin station is situated in a public park and the Melle station is located in a rural environment. The micro-environments of the stations in the city centre differ slightly, since the Sint-Bavo station is located in an urban canyon and the Provinciehuis station is situated on a square close to a building in the east direction.

This study revealed that the micro-environment is important to understand the observed temperatures during daytime and the local environment of about 1 km² is more important during nighttime. Therefore, daytime and nighttime should be investigated separately. In addition, the temperature and UHI modelling are scale dependent. Therefore, it is important to take into account the right size of the area that influences the UHI to study and model the UHI. In order to know the exact area that has statistically the highest correlation coefficient with respect to the observed UHI, it is recommended to do a linear regression.

A validation of the model performed with ECOCLIMAP-I, ECOCLIMAP-II and high resolution land cover data over Ghent suggested that the implementation of more accurate land cover of the ECOCLIMAP-II database improves the model performance compared to ECOCLIMAP-I. However, the land cover around the Honda station is poorly estimated by ECOCLIMAP-II compared to ECOCLIMAP-I, leading towards worse model results for the UHI. Hence, shortcomings of ECOCLIMAP-II with respect to ECOCLIMAP-I should be further investigated and solved. In contrast to the worse modelled temperatures with the higher resolution BBK data, it can be concluded that the UHI is better simulated on average when the land cover fractions of the BBK are implemented in SURFEX. The better simulation of the UHI is due to compensation of the errors in the rural and urban temperatures. This better model performance is thus an artificial way of improvement. The poor simulation of the temperatures with the BBK data could be due to the poor tuning of the model that was based on ECOCLIMAP-I data. When the land cover is improved, most of the model results still deviate significant from the observations. This could be caused by the poor tuning of the model or by the input of poor forcings. Therefore, further research on the SURFEX scheme and the forcing at 4 km resolution is needed.

Another outcome of this study is that the SURFEX model is more sensitive to changes in building height than modifications in building fraction. In contrast to the building height, the building fraction does not always have a significant influence on the UHI. Modifications in the land cover result in more significant changes for the model performance of the UHI compared to the city geometry parameters. Hence, the land cover is the most dominant parameter in the SURFEX scheme out of the parameters that were investigated in this study. Therefore, it is important to define the land cover correctly, since the model is very sensitive to this. Moreover, the model results indicated that there is a positive correlation between the impervious fraction and UHI, and there is a possible negative relationship observed for the green and water fraction. Therefore, it is recommended to execute as statistical correlation analysis for each land cover fraction to quantify the impact of a certain land cover on the resulting average temperatures and UHI. In this way it is possible to examine to what extent a change in land cover can mitigate the UHI. This could also be done for the building height, but a smaller impact is expected since the building height influences the UHI to a smaller extent. In the end, the model could not be optimised sufficiently by implementing a more accurate land cover, building fraction and building height. Therefore, further investigation to improve the model results is needed.

REFERENCE LIST

AGIV (2016a) “Operationele aanmaak Bodembedekkingsbestanden Vlaanderen 2012”. *Report*.

AGIV (2016b) “3D GRB; Vectoriële bestanden van het GRB in 3D; Versie 2”. *Report*.

ALADIN International Team (1997) “The ALADIN project: Mesoscale modelling seen as a basic tool for weather forecasting and atmospheric research”. *WMO Bulletin*, 46, 317-324.

Arnfield, A. J. (2003) “Two decades of urban climate research: a review of turbulence, exchanges of energy and water, and the urban heat island”. *International journal of climatology*, 23 (1), 1-26.

Bassett, R., Cai, X., Chapman, L., Heaviside, C., Thornes, J. E., Muller, C. L., Young, D. T., Warren, E. L. (2016) “Observations of urban heat island advection from a high-density monitoring network”. *Quarterly Journal of the Royal Meteorological Society*, 142 (699), 2434-2441.

Berckmans, J. (2018) “Modelling land-atmosphere interactions: impact of near future land use and climate change over Western Europe”. (Doctoral dissertation, University of Antwerp).

Berrisford, P., Dee, D., Poli, P., Brugge, R., Fielding, K., Fuentes, M., Kallberg, P., Kobayashi, S., Uppala, S., Simmons, A. J. (2011) “The ERA-Interim archive version 2.0”. *Report*.

Best, M. J., Grimmond, C. S. B. (2015) “Key conclusions of the first international urban land surface model comparison project”. *Bulletin of the American Meteorological Society*, 96 (5), 805-819.

Blankenstein, S., Kuttler, W. (2004) “Impact of street geometry on downward longwave radiation and air temperature in an urban environment”. *Meteorologische Zeitschrift*. 13 (5), 373-379.

Bubnová, R., Hello, G., Bénard, P., Geleyn, J. F. (1995) “Integration of the fully elastic equations cast in the hydrostatic pressure terrain-following coordinate in the framework of the ARPEGE/Aladin NWP system”. *Monthly Weather Review*. 123 (2), 515-535.

Caluwaerts S., Termonia P., Hamdi, R., Duchêne, F., Berckmans, J., Degrauwe, D., Wauters, G. (2016) “Monitoring the urban climate of the city of Ghent, Belgium”. *Urban Climate News.* 61, 15-20.

Caluwaerts, S., Hamdi, R., Lauwaet, D., Berckmans, J., Degrauwe, D., De Ridder, K., Duchêne, F., Maiheu, B., Verdonck, M.-L., Wauters, G., Termonia, P. (2018) “Design of MOCCA monitoring network in the city of Ghent based on high-resolution urban modelling”. *International Journal of Climatology.* under revision.

CNRM (*s.d.*) “The externalized surface user’s guide V8.0”. *user’s guide*. Download available at: http://www.umr-cnrm.fr/surfex/spip.php?rubrique10. 17/02/2018.

De Ridder, K., Lauwaet, D., Maiheu, B. (2015) “UrbClim - A fast urban boundary layer climate model”. *Urban Climate*. 12, 21-48.

Dee, D. P., Uppala, S. M., Simmons, A. J., Berrisford, P., Poli, P., Kobayashi, S., Andrae, U., Balmaseda, M. A., Balsamo, G., Bauer, P., Bechtold, P., Beljaars, A. C. M., van den Berg, L., Bidlot, J., Bormann, N., Delsol, C., Dragani, R., Fuentes, M., Geer, A. J., Haimberger, L., Healy, S.B., Hersbach, H., Hólm, E. V., Isaksen, L., Kallberg, P., Köhler, M., Matricardi, M., McNally, A. P., Monge-Sanz, B. M., Morcrette, J.-J., Park, B.-K., Peubey, C., de Rosney, P., Tavolato, C., Thépaut, J.-N., Vitart, F. (2011). “The ERA-Interim reanalysis: Configuration and performance of the data assimilation system”. *Quarterly Journal of the royal meteorological society*. 137 (656), 553-597.

Duerinckx, A., Hamdi, R., Mahfouf, J. F., Termonia, P. (2015) “Study of the Jacobian of an extended Kalman filter for soil analysis in SURFEXv5”. *Geoscientific Model Development*, 8 (3), 845-863.

Faroux, S., Kaptué Tchuenté, A. T., Roujean, J. L., Masson, V., Martin, E., Moigne, P. L. (2013) “ECOCLIMAP-II/Europe: a twofold database of ecosystems and surface parameters at 1 km resolution based on satellite information for use in land surface, meteorological and climate models”. *Geoscientific Model Development*. 6 (2), 563-582.

Fischer, E. M., Oleson, K. W., Lawrence, D. M. (2012) “Contrasting urban and rural heat stress responses to climate change”. *Geophysical research letters*, 39(3).

Gaspar, P., Grégoris, Y., Lefevre, J. M. (1990) “A simple eddy kinetic energy model for simulations of the oceanic vertical mixing: Tests at station Papa and Long-Term Upper Ocean Study site”. *Journal of Geophysical Research: Oceans*, 95 (C9), 16179-16193.

Gerard, L., Piriou, J. M., Brožková, R., Geleyn, J. F., Banciu, D. (2009) “Cloud and precipitation parameterization in a meso-gamma-scale operational weather prediction model”. *Monthly Weather Review*. 137 (11), 3960-3977.

Hamdi, R., Deckmyn, A., Termonia, P., Demarée, G. R., Baguis, P., Vanhuysse, S., Wolff, E. (2009) “Effects of historical urbanization in the Brussels Capital Region on surface air temperature time series: a model study”. *Journal of Applied Meteorology and Climatology*, 48(10), 2181-2196.

Hamdi, R., Degrauwe, D., Termonia, P. (2012) “Coupling the Town Energy Balance (TEB) scheme to an operational limited-area NWP model: evaluation for a highly urbanized area in Belgium”. *Weather and Forecasting*. 27 (2), 323-344.

Hamdi, R., Masson, V. (2008) “Inclusion of a drag approach in the Town Energy Balance (TEB) scheme: Offline 1D evaluation in a street canyon”. *Journal of Applied Meteorology and Climatology*, 47 (10), 2627-2644.

Hamdi, R., Schayes, G. (2008) “Sensitivity study of the urban heat island intensity to urban characteristics”. *International Journal of Climatology*. 28 (7), 973-982.

Hamdi, R., Vyver, H., Troch, R., Termonia, P. (2014). “Assessment of three dynamical urban climate downscaling methods: Brussels's future urban heat island under an A1B emission scenario”. *International Journal of Climatology*. 34 (4), 978-999.

Hamdi, R., Giot, O., De Troch, R., Deckmyn, A., Termonia, P. (2015). “Future climate of Brussels and Paris for the 2050s under the A1B scenario”. *Urban Climate*, 12, 160-182.

Harshan, S. (2015) “Adaptation of an urban land surface model to a tropical suburban area: Offline evaluation, sensitivity analysis, and optimization of TEB/ISBA (SURFEX)”. (Doctoral dissertation, M.S. Texas Tech University).

Hertoghs, R. (2012) “De zeebries in belgië en de interactie ervan met urbanisatie: een modelstudie”. (Master thesis, Ghent University).

Laaidi, K., Zeghnoun, A., Dousset, B., Bretin, P., Vandentorren, S., Giraudet, E., Beaudeau, P. (2012) “The impact of heat islands on mortality in Paris during the August 2003 heat wave”. *Environmental health perspectives*. 120 (2), 254-259.

Lauwaet, D., De Ridder, K., Saeed, S., Brisson, E., Chatterjee, F., van Lipzig, N. P. M., Maiheu, B., Hooyberghs, H. (2016) “Assessing the current and future urban heat island of Brussels”. *Urban Climate*. 15, 1-15.

Lauwaet, D., Hooyberghs, H., Maiheu, B., Lefebvre, W., Driesen, G., Van Looy, S., De Ridder, K. (2015) “Detailed Urban Heat Island projections for cities worldwide: dynamical downscaling CMIP5 global climate models”. *Climate*. 3 (2), 391-415.

Le Moigne, P., Boone, A., Belamari, S., Brun, E., Calvet, J.-C., Decharme, B., Faroux, S., Gibelin, A.-L., Giordani, H., Lafont, S., Lebeaupin, C., Mahfouf, J.-F., Martin, E., Masson, V., Mironov, D., Morin, S., Noilhan, J., Tulet, P., Van Den Hurk, B., Vionnet, V. (2018) “SURFEX scientific documentation”. *Note de centre (CNRM/GMME), Météo-France, Toulouse, France*.

Lemonsu, A., Grimmond, C. S. B., Masson, V. (2004) "Modeling the surface energy balance of the core of an old Mediterranean city: Marseille". *Journal of Applied Meteorology*. 43 (2), 312-327.

Masson, V. (2000) "A physically-based scheme for the urban energy budget in atmospheric models". *Boundary-layer meteorology*. 94 (3), 357-397.

Masson, V., Champeaux, J. L., Chauvin, F., Meriguet, C., Lacaze, R. (2003) "A global database of land surface parameters at 1-km resolution in meteorological and climate models". *Journal of climate*. 16 (9), 1261-1282.

Masson, V., Grimmond, C. S. B., Oke, T. R. (2002) "Evaluation of the Town Energy Balance (TEB) scheme with direct measurements from dry districts in two cities". *Journal of applied meteorology*, 41(10), 1011-1026.

Masson, V., Le Moigne, P., Martin, E., Faroux, S., Alias, A., Alkama, R., Belamari, S., Barbu, A., Boone, A., Bouyssel, F., Brousseau, P., Brun, E., Calvet, J.-C., Carrer, D., Decharme, B., Delire, C., Donier, S., Essaouini, K., Gibelin, A.-L., Giordani, H., Habets, F., Jidane, M., Kerdraon, G., Kourzeneva, E., Lafaysse, M., Lafont, S., Lebeaupin Brossier, C., Lemonsu, A., Mahfouf, J.-F., Marguinaud, P., Mokhtari, M., Morin, S., Pigeon, G., Salgado, R., Seity, Y., Taillefer, F., Tanguy, G., Tulet, P., Vincendon, B., Vionnet, V., Voldoire, A. (2013) "The SURFEXv7.2 land and ocean surface platform for coupled or offline simulation of earth surface variables and fluxes". *Geoscientific Model Development*. 6, 929-960.

Mironov, D. V. (2008). "Parameterization of lakes in numerical weather prediction". *Deutscher Wetterdienst, COSMO Technical Report 11*.

Mirzaei, P. A., Haghighat, F. (2010) "Approaches to study urban heat island–abilities and limitations". *Building and environment*. 45 (10), 2192-2201.

Morris, C. J. G., Simmonds, I., Plummer, N. (2001) "Quantification of the influences of wind and cloud on the nocturnal urban heat island of a large city". *Journal of Applied Meteorology*. 40 (2), 169-182.

Ohashi, Y., Genchi, Y., Kondo, H., Kikegawa, Y., Yoshikado, H., Hirano, Y. (2007) "Influence of air-conditioning waste heat on air temperature in Tokyo during summer: numerical experiments using an urban canopy model coupled with a building energy model". *Journal of Applied Meteorology and climatology*. 46 (1), 66-81.

Oke, T. R. (1973) "City size and the urban heat island". *Atmospheric Environment (1967)*. 7 (8), 769-779.

Oke, T. R. (1981) "Canyon geometry and the nocturnal urban heat island: comparison of scale model and field observations". *Journal of climatology*. 1 (3), 237-254.

Oke, T. R. (1982) "The energetic basis of the urban heat island". *Quarterly Journal of the Royal Meteorological Society*. 108 (455), 1-24.

Oke, T. R. (1987) "Boundary layer climates". 2nd. *Methuen*. 289p.

Patz, J. A., Campbell-Lendrum, D., Holloway, T., Foley, J. A. (2005) "Impact of regional climate change on human health". *Nature*, 438 (7066), 310-317.

Pielke, R. A., Davey, C. A., Niyogi, D., Fall, S., Steinweg-Woods, J., Hubbard, K., Lin, X., Cai, M., Lim, Y.-K., Li, H., Nielsen-Gammon, J., Gallo, K., Hale, R., Mahmood, R., Foster, S., McNider, R. T., Blanken, P. (2007) "Unresolved issues with the assessment of multidecadal global land surface temperature trends". *Journal of Geophysical Research: Atmospheres*. 112(D24).

Prein, A. F., Langhans, W., Fosser, G., Ferrone, A., Ban, N., Goergen, K., Keller, M., Tölle, M., Gutjahr, O., Feser, F., Brisson, E., Kollet, S., Schmidli, J., van Lipzig, N. P. M., Leung, R. (2015) "A review on regional convection-permitting climate modeling: Demonstrations, prospects, and challenges". *Reviews of geophysics*, 53 (2), 323-361.

Sailor, D. J., Lu, L. (2004) "A top–down methodology for developing diurnal and seasonal anthropogenic heating profiles for urban areas". *Atmospheric environment*. 38 (17), 2737-2748.

Shepherd, J. M. (2005) "A review of current investigations of urban-induced rainfall and recommendations for the future". *Earth Interactions*. 9 (12), 1-27.

Steeneveld, G. J., Koopmans, S., Heusinkveld, B. G., Van Hove, L. W. A., Holtslag, A. A. M. (2011) "Quantifying urban heat island effects and human comfort for cities of variable size and urban morphology in the Netherlands." *Journal of Geophysical Research: Atmospheres*. 116 (D20).

Termonia, P., Fischer, C., Bazile, E., Bouyssel, F., Brozková, R., Bénard, P., Bochenek, B., Degrauwe, D., Derková, M., El Khatib, R., Hamdi, R., Masek, J., Pottier, P., Pristov, N., Seity, Y., Smolíková, P., Spaniel, O., Tudor, M., Wang, Y., Wittmann, C., Joly, A. (2018). "The ALADIN System and its canonical model configurations AROME CY41T1 and ALARO CY40T1". *Geoscientific Model Development*. 11 (1), 257.

United Nations Human Settlements Programme (UN-Habitat) (2010) "State of the World's Cities 2008/2009".

U.S. Environmental Protection Agency. (2008) "Reducing urban heat islands: Compendium of strategies". Draft. https://www.epa.gov/heat-islands/heat-island-compendium.

Van Hove, L. W. A., Jacobs, C. M. J., Heusinkveld, B. G., Elbers, J. A., Van Driel, B. L., Holtslag, A. A. M. (2014) "Temporal and spatial variability of urban heat island and thermal comfort within the Rotterdam agglomeration". *Building and environment*. 83, 91-103.

Voogt, J. A. (2000) "Urban heat island". *Encyclopedia of Global Environmental Change*. 3, 660-666.

Zhou, W., Huang, G., Cadenasso, M. L. (2011) "Does spatial configuration matter? Understanding the effects of land cover pattern on land surface temperature in urban landscapes". *Landscape and urban planning*. 102 (1), 54-63.

Internet sources

Agentschap Informatie Vlaanderen (2016) *Bodembedekkingskaart (BBK), 1 m resolutie, opname 2012*. http://www.geopunt.be/catalogus/datasetfolder/b15fec52-6f04-4758-bef7-1b9063629aec. 08/04/2018.

AGIV (*s.d.*) *3D GRB*. https://download.agiv.be/Producten/Detail?id=971&title=3D_GRB. 07/04/2018.

CNRM (2018) *How to get the SURFEX code*. http://www.umr-cnrm.fr/surfex/spip.php?article387. 11/04/2018.

CNRS (2014) *Ecoclimap*. https://opensource.umr-cnrm.fr/projects/ecoclimap/files. 25/04/2018.

Department of Physics and Astronomy Ghent University (*s.d.*) *MOCCA project: Ghent University studies urban microclimate in Ghent*. www.observatory.ugent.be. 30/04/2017.

ECMWF (*s.d.*) *ERA-Interim*. https://www.ecmwf.int/en/forecasts/datasets/archive-datasets/reanalysis-datasets/era-interim. 11/05/2018.

Meso-NH (2015) *Download Meso-NH*. http://mesonh.aero.obs-mip.fr/mesonh52/Download. 25/04/2018.

Statbel (2016) *Loop van de bevolking per gemeente 2010-2016*. https://statbel.fgov.be/nl/themas/bevolking/loop-van-de-bevolking#figures. 21/04/2018.

USGS (2015) *Global 30 Arc-Second Elevation (GTOPO30)*. https://lta.cr.usgs.gov/GTOPO30. 25/04/2018.

Vlaamse overheid (*s.d.*) *Geopunt-kaart*. http://www.geopunt.be/. 11/04/2018.

ANNEXES

Annex I: Actions in QGIS

1. Creating a shapefile with a given set of coordinates

Save the coordinates as below in Excel as a CSV file.

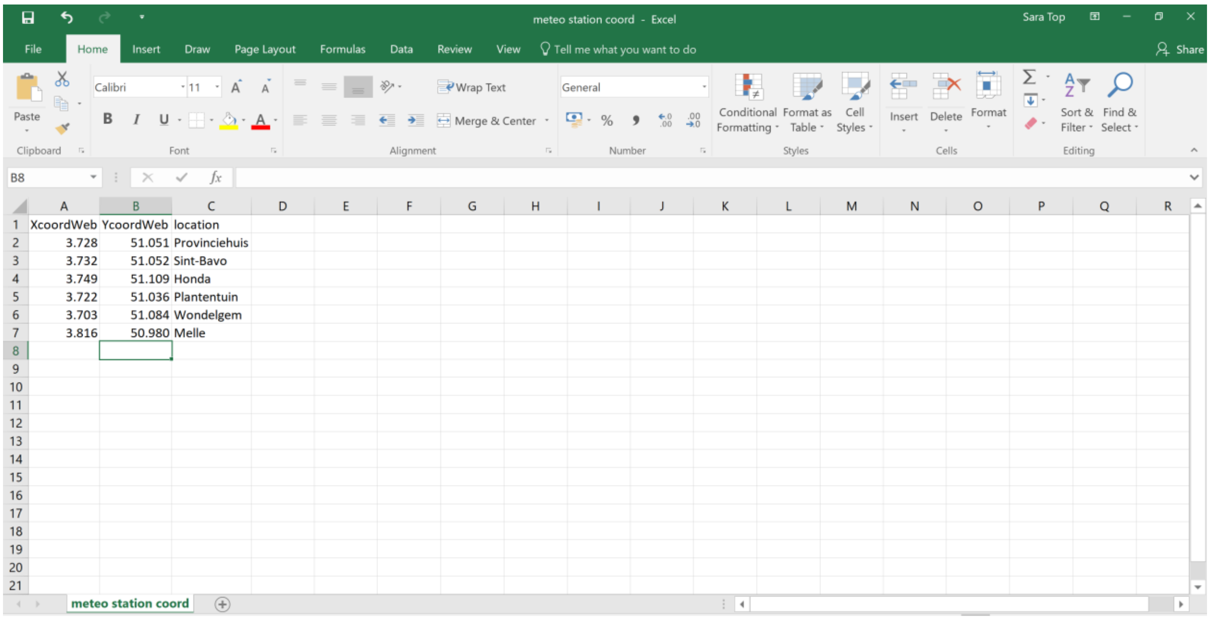

XcoordWeb	YcoordWeb	location
3.728	51.051	Provinciehuis
3.732	51.052	Sint-Bavo
3.749	51.109	Honda
3.722	51.036	Plantentuin
3.703	51.084	Wondelgem
3.816	50.980	Melle

Open QGIS by clicking on the icon of QGIS:

Start a new project by clicking on sheet sign:

Click on the comma sign to load the data of the CSV file:

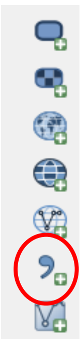

Fill in the window that appears:

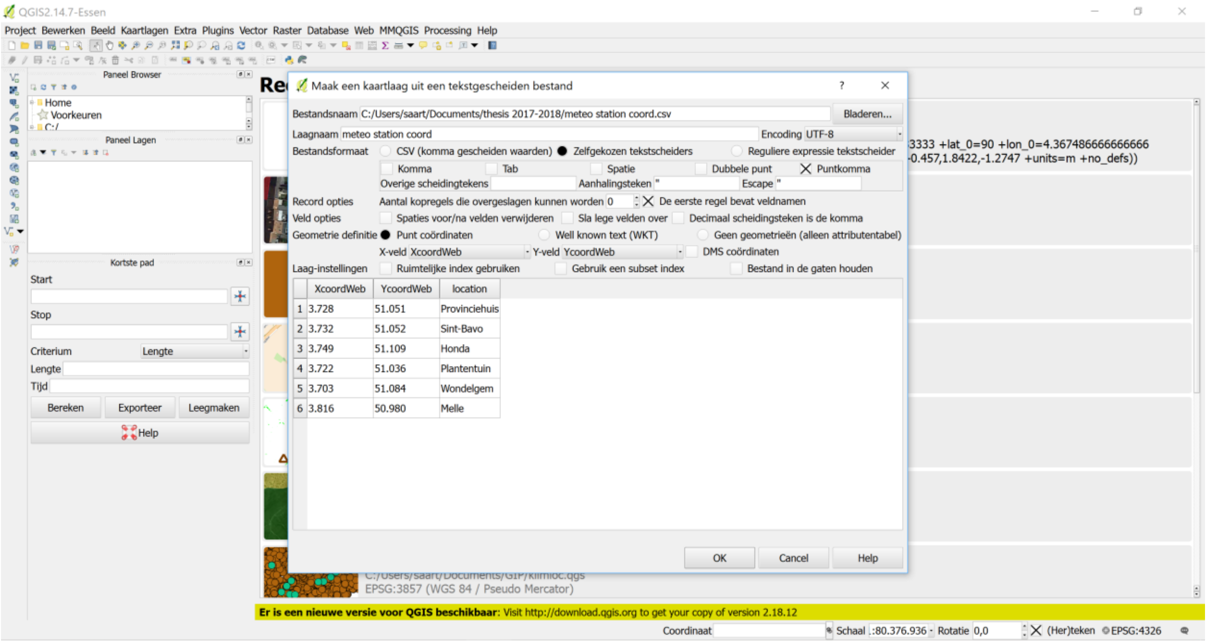

Click on the 'OK' button and choose the right coordinate system for the point you want to create. Here, the coordinates are taken from a handheld GPS that uses WGS 84 as coordinate reference system (CRS). To find this CRS easily you can use the EPSG code, which is 4326 for WGS 84.

Click on the 'OK' button and then you get some points.

Add a basemap, for example OpenstreetMap (OSM), to know if the created points are located correctly. First, install the OSM plugin:

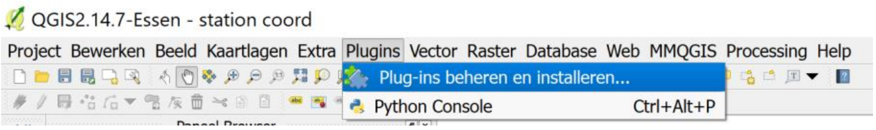

Search for 'OSM' and click on 'OpenLayers Plugin' to install.

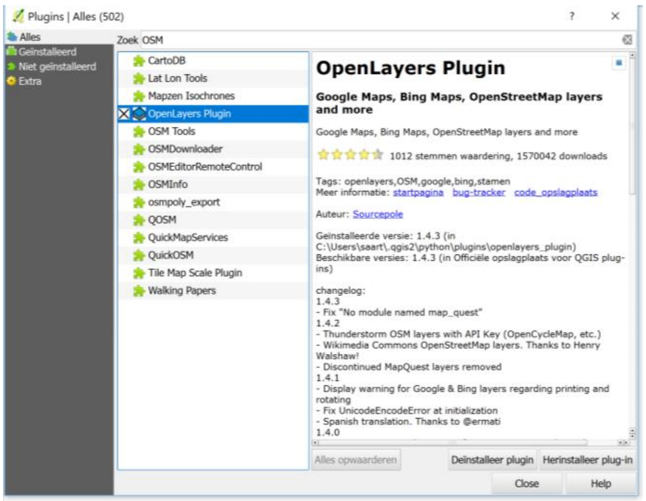

Visualize the OSM map by following the path: Web → OpenLayers plugin → OpenStreetMap → OpenStreetMap.

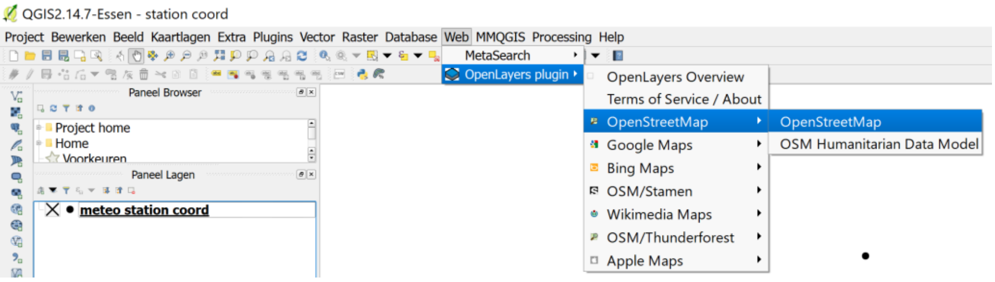

Click on the OSM layer and drag it under the layer with points.

Result:

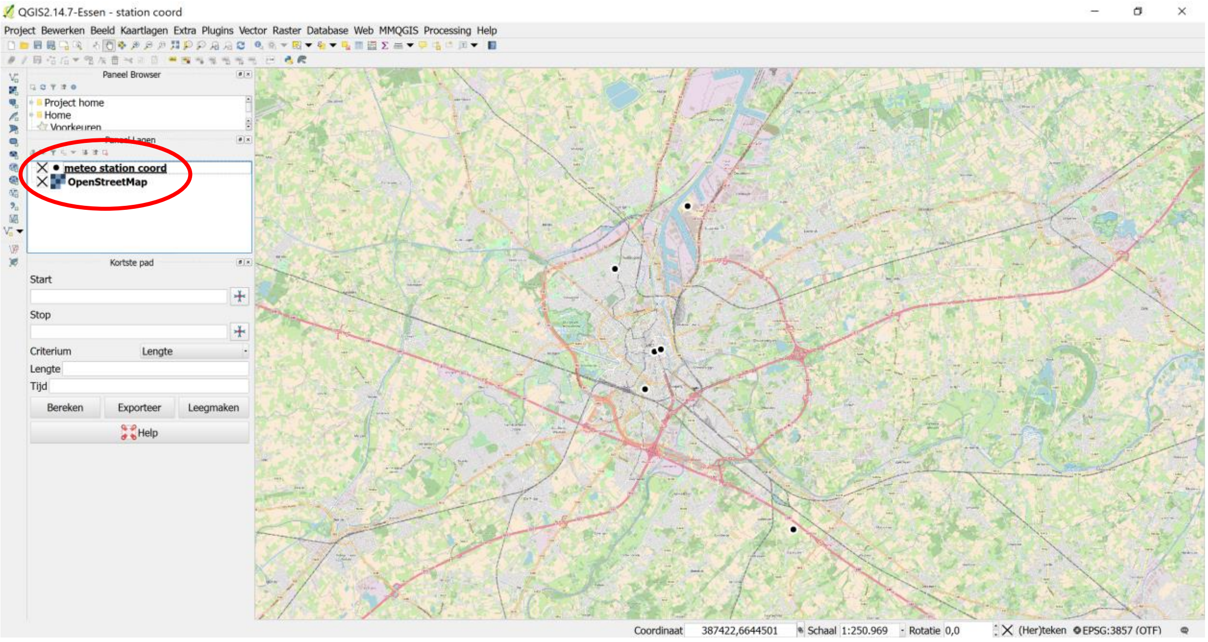

Make sure the project is projected in Lambert72 (EPSG: 31370). This is the national reference system in Belgium. To check this you can go to 'Project Properties'.

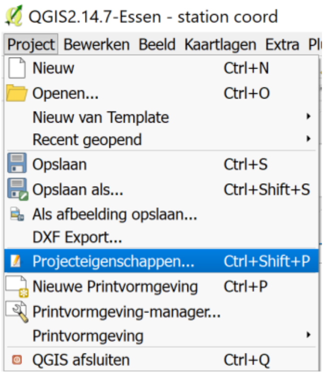

Select the ‘CRS’ option from the left-side menu if necessary.

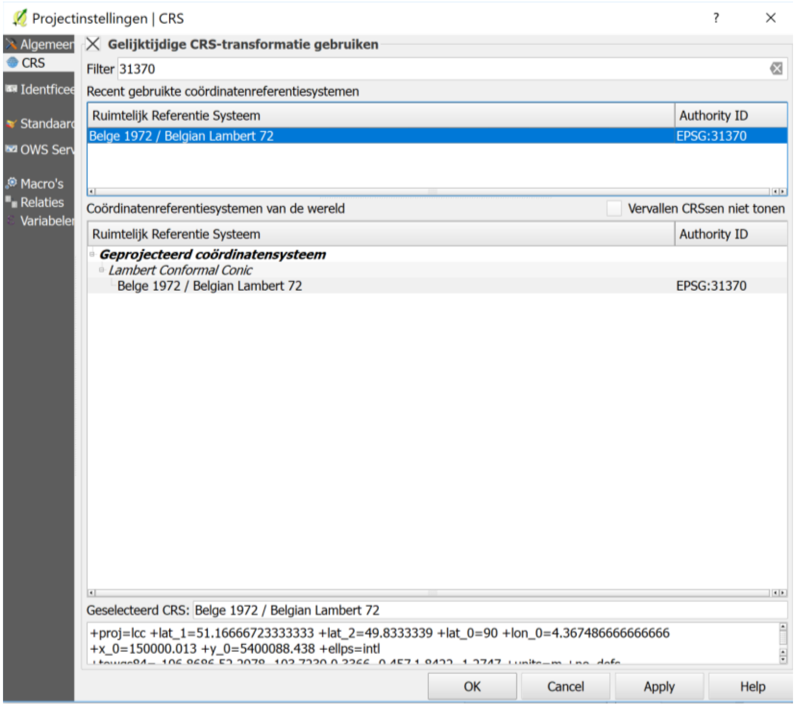

Save the points as a shapefile (.shp). Right click on the layer you want to save and click on the option ‘Save As…’.

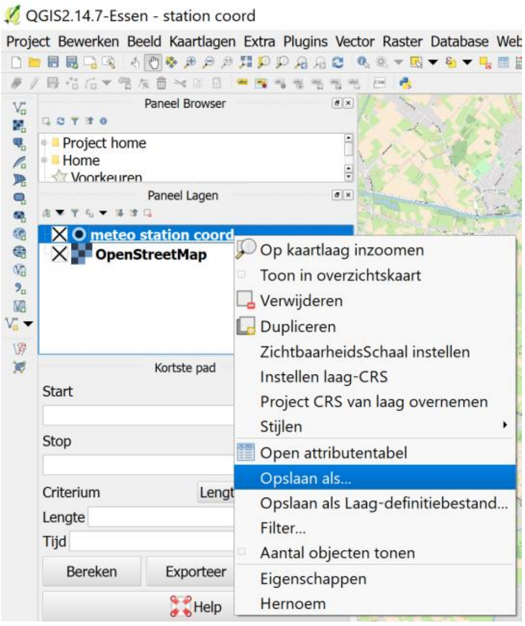

It is handy to put these points in a metric coordinate system, because the goal is to make buffer zones with a radius in metres around these points. The Belgian coordinate system Lambert72 (EPSG: 31370) is metric. That is an additional reason why the points are saved in this coordinate reference system (CRS).

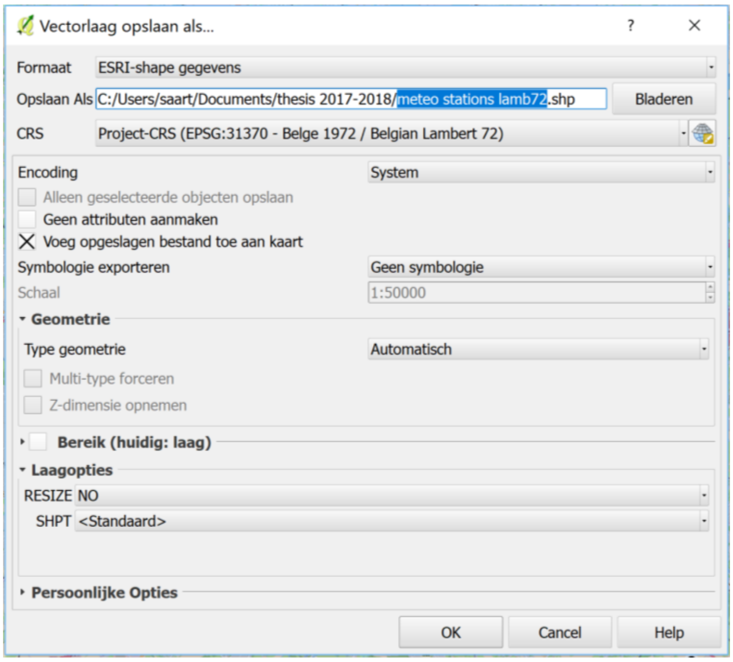

Result: The new points are located at the same spots as the points that were implemented with the CSV file, but now they have a shapefile extension.

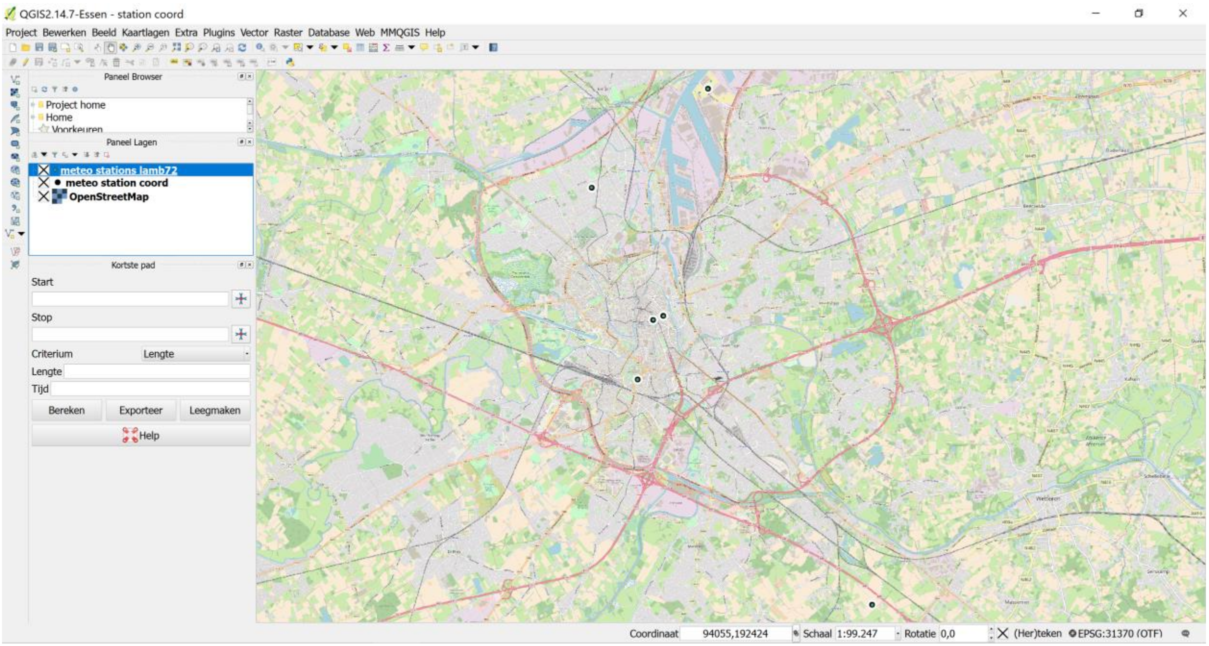

Because the given coordinates are rounded, the points differ a bit from the real location of the measurement stations. Therefore, points are manual replaced to the exact location. This is done as followed:

Select the layer and click on the editing button:

Now, the shapefile can be edited by dragging the points to their exact location.

This adjusted layer is saved as a new shapefile layer. The old (green) and new (red) point layers differ slightly in location.

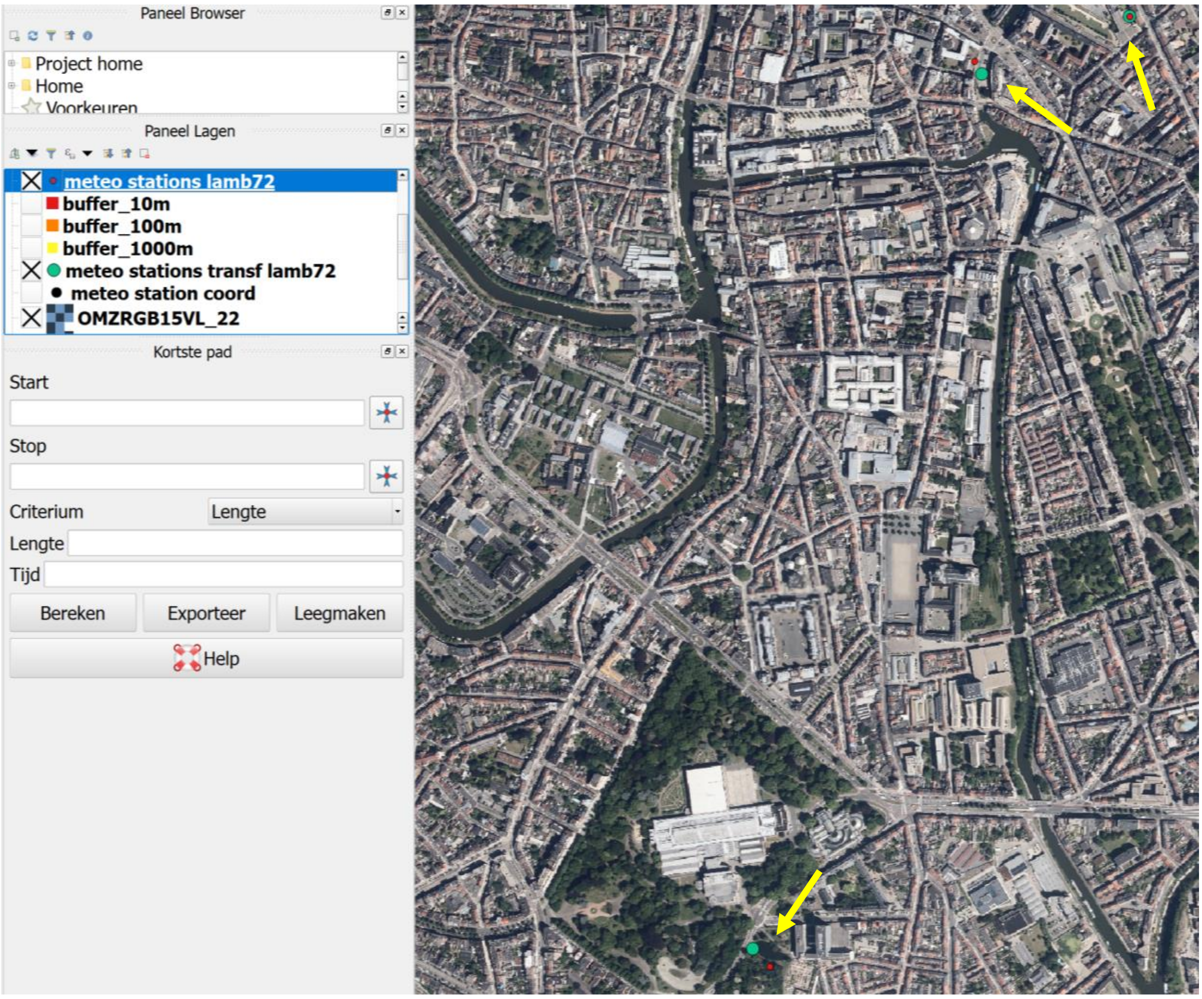

From these exact points the exact coordinates can be derived as followed:

Open the attribute table.

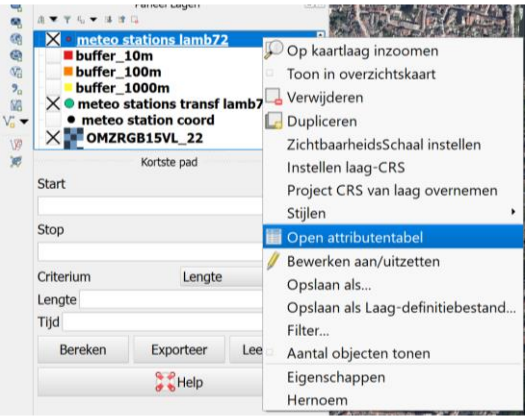

Start editing.

Open the raster calculator.

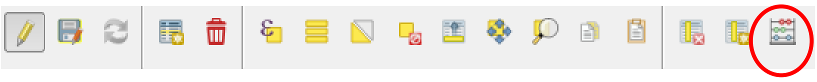

Add a new field for the x-coordinate by clicking on ‘$x’ in the search field.

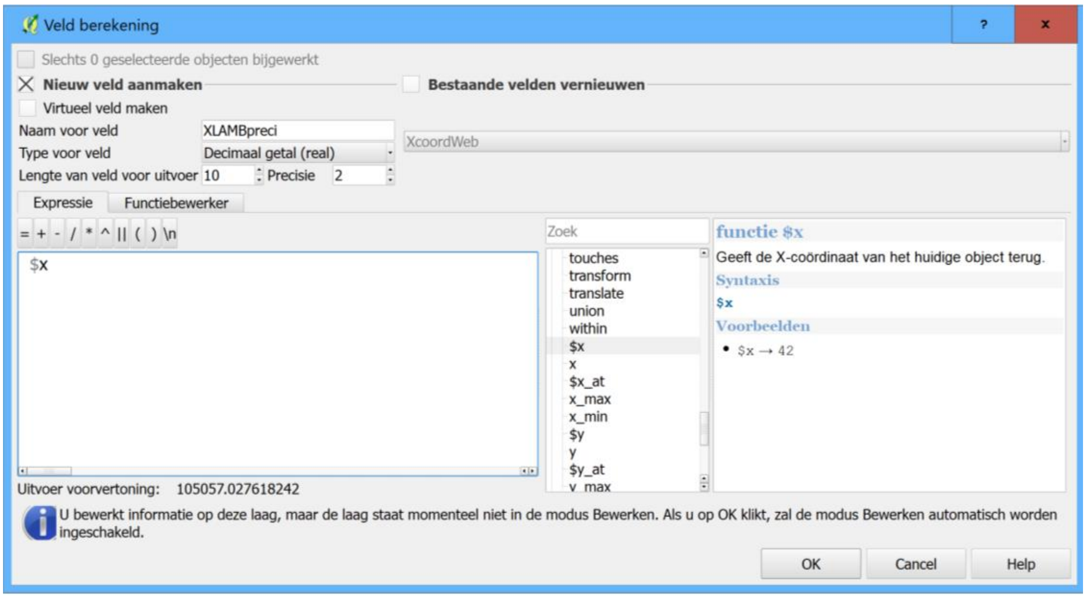

Add a new field for the y-coordinate.

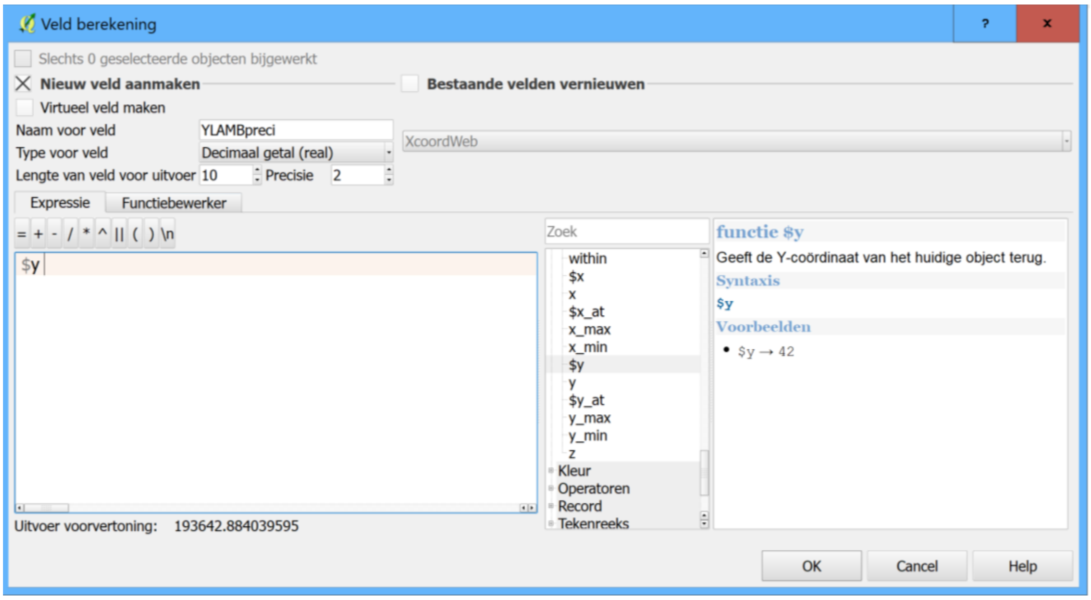

To also obtain the coordinates in WGS 84, the coordinate system of the layer has to be changed. Therefore, the layer must be saved as a WGS 84 layer.

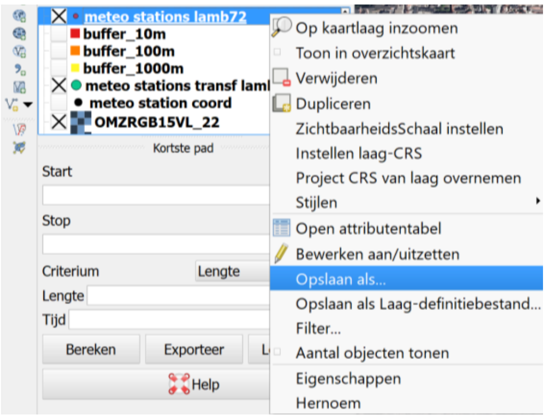

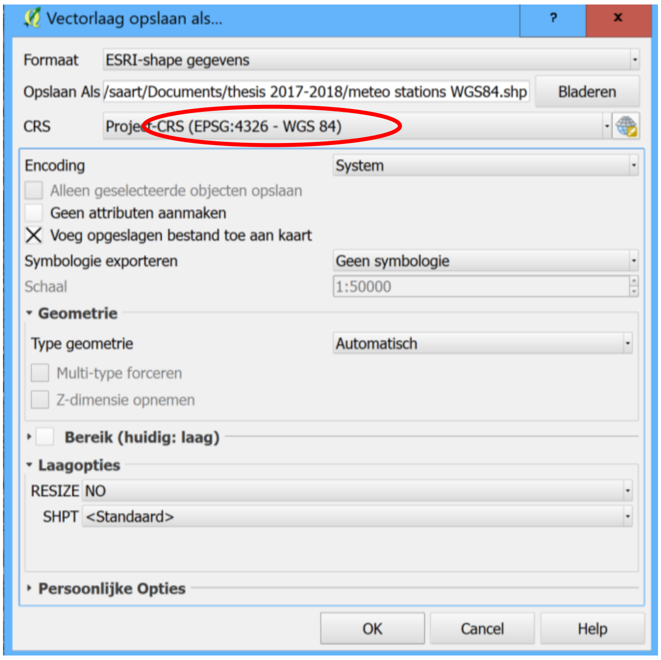

The new layer in WGS 84 coordinates is added to the project and the coordinates are added to the layer similar as was done for the point layer in Lambert72 coordinates.

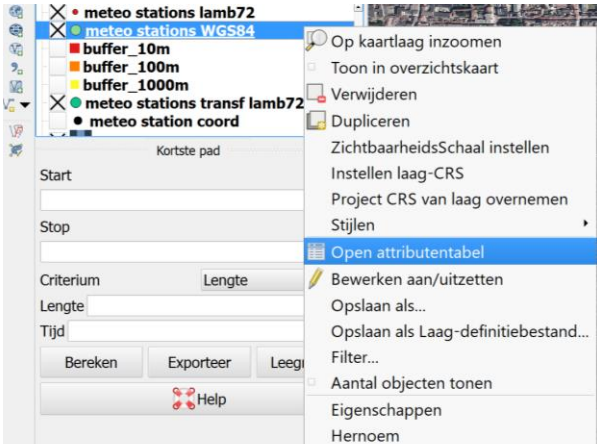

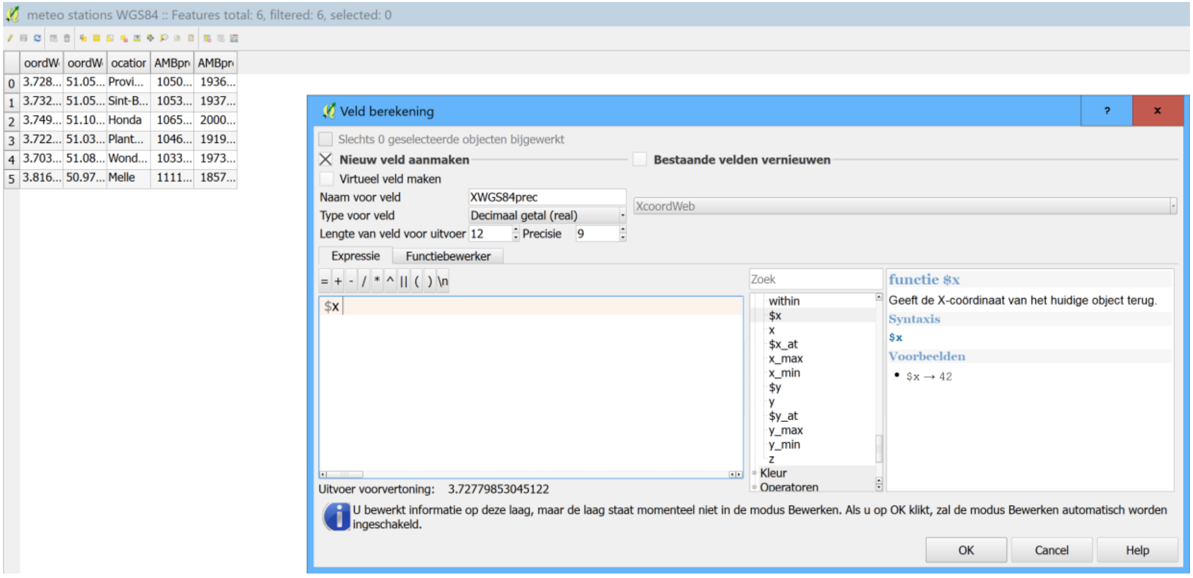

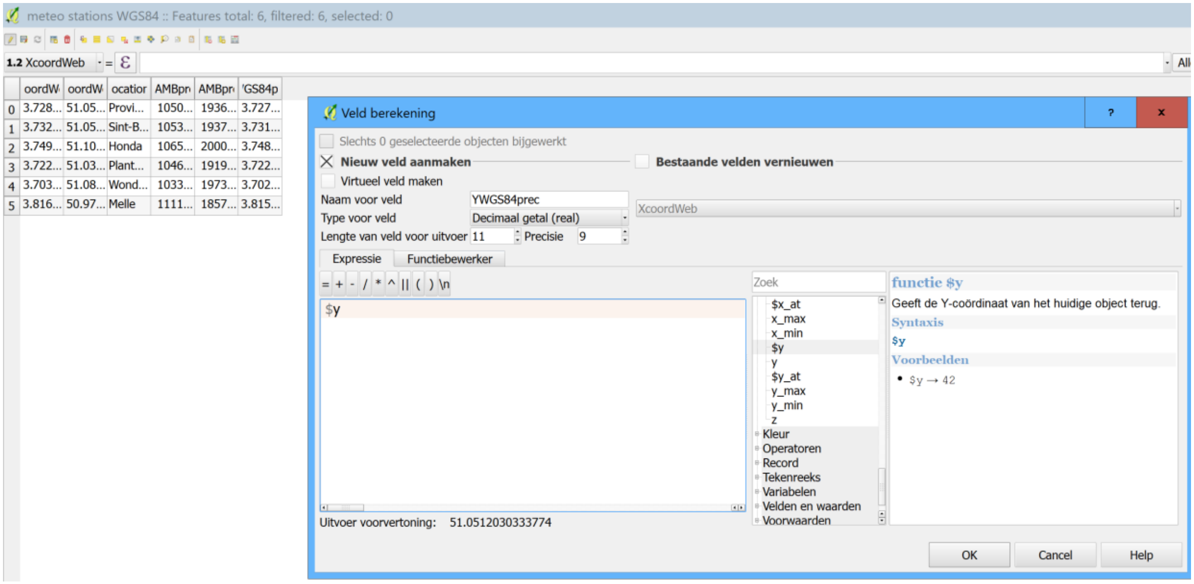

Result:

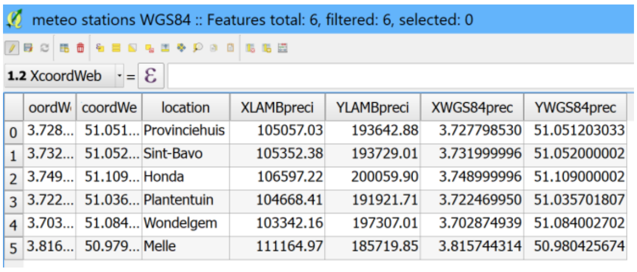

	oordW	coordWe	location	XLAMBpreci	YLAMBpreci	XWGS84prec	YWGS84prec
0	3.728...	51.051...	Provinciehuis	105057.03	193642.88	3.727798530	51.051203033
1	3.732...	51.052...	Sint-Bavo	105352.38	193729.01	3.731999996	51.052000002
2	3.749...	51.109...	Honda	106597.22	200059.90	3.748999996	51.109000002
3	3.722...	51.036...	Plantentuin	104668.41	191921.71	3.722469950	51.035701807
4	3.703...	51.084...	Wondelgem	103342.16	197307.01	3.702874939	51.084002702
5	3.816...	50.979...	Melle	111164.97	185719.85	3.815744314	50.980425674

Save the resulting values as CSV file:

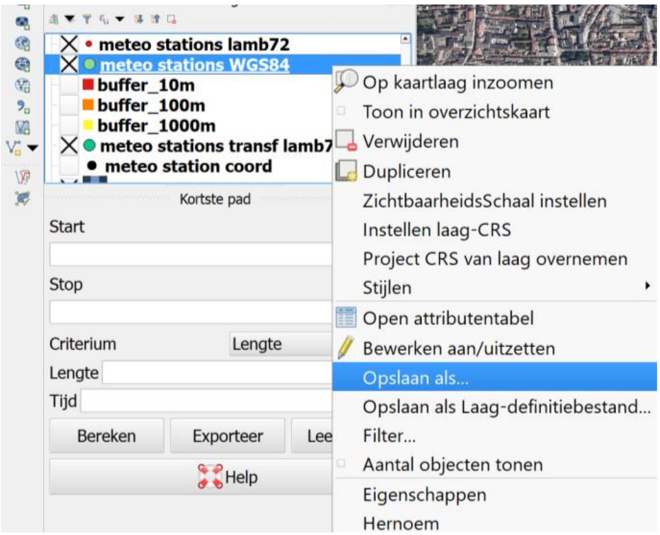

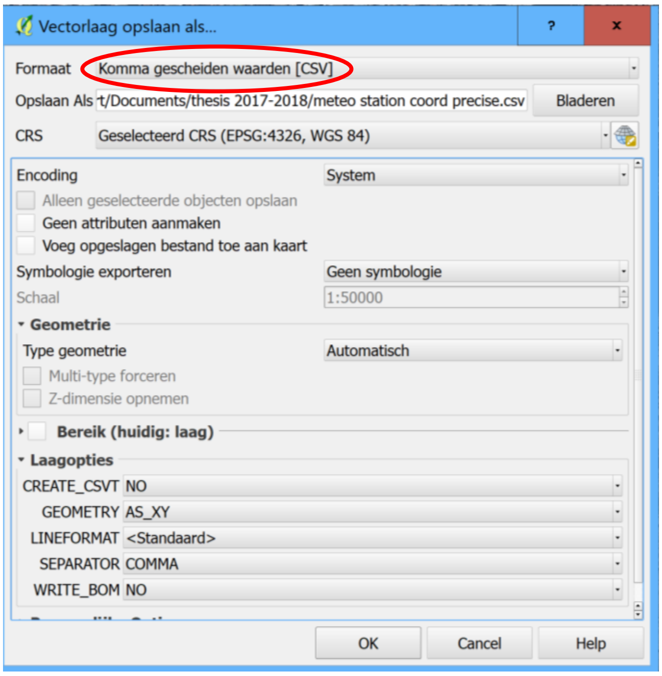

The result is a CSV file with the coordinates saved in the folder that was chosen.

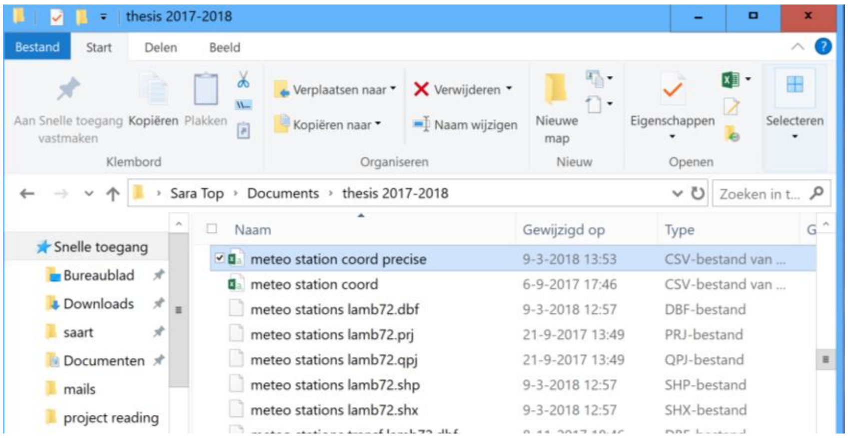

Save the project file of QGIS, so that it is possible to resume the project later on without having to reopen all the different files from the previous session.

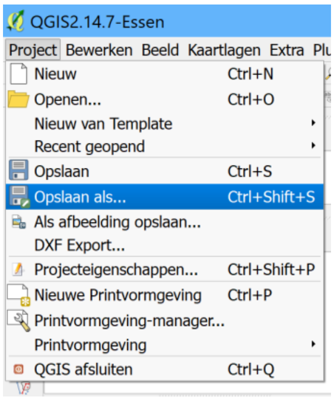

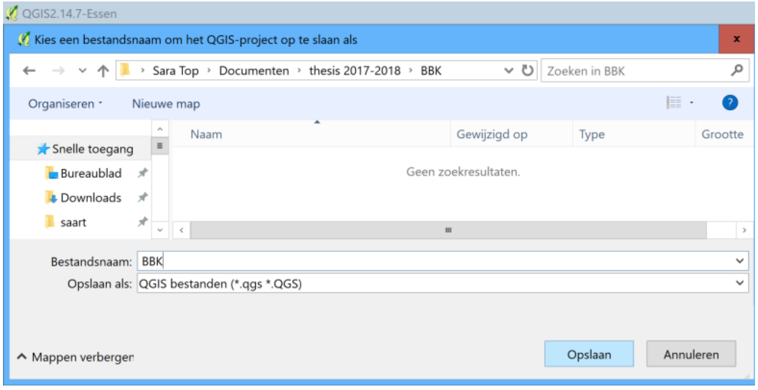

The name changes in the bar above when the project is saved.

2. Create a buffer zone

Go to the ‘Buffer(s)…’ tool.

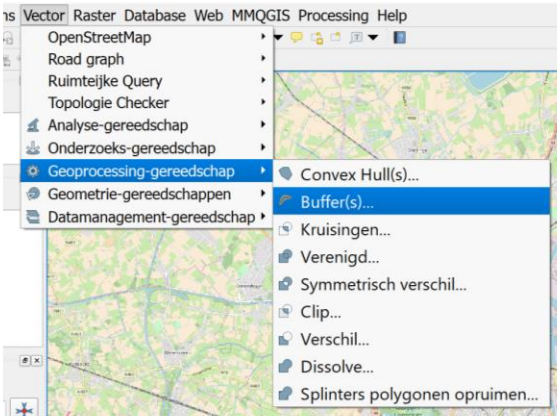

Set the characteristics of the buffer you want to create.

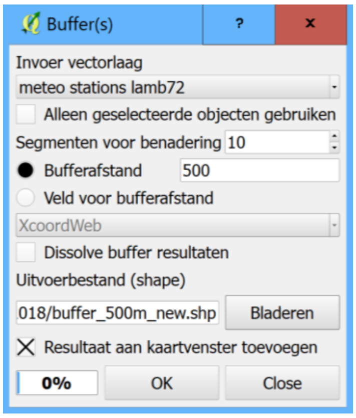

Add the point layer with the points in the Lambert72 coordinate system. The number 500 represents a radius of 500 m because of the metric coordinate system that is used. Repeat this process for buffers with a radius of 10 m, 100 m, 565 m and 1000 m.

The following screenshot shows the result.

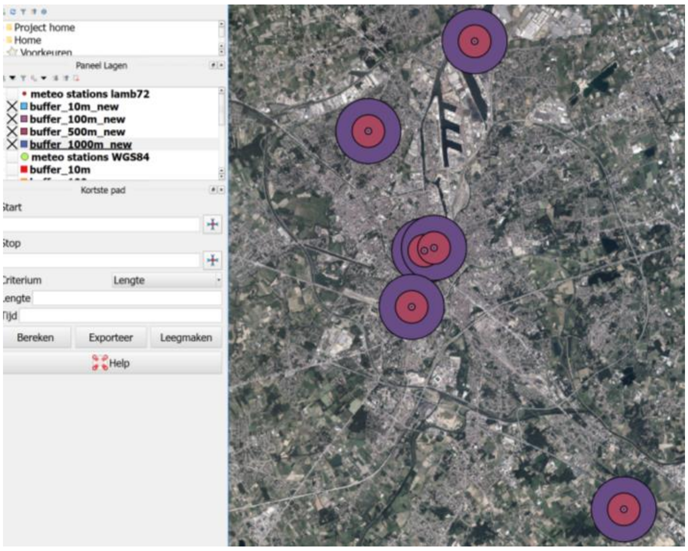

Zoom in with the magnifying glass.

Then select the area of interest by drawing a rectangle.

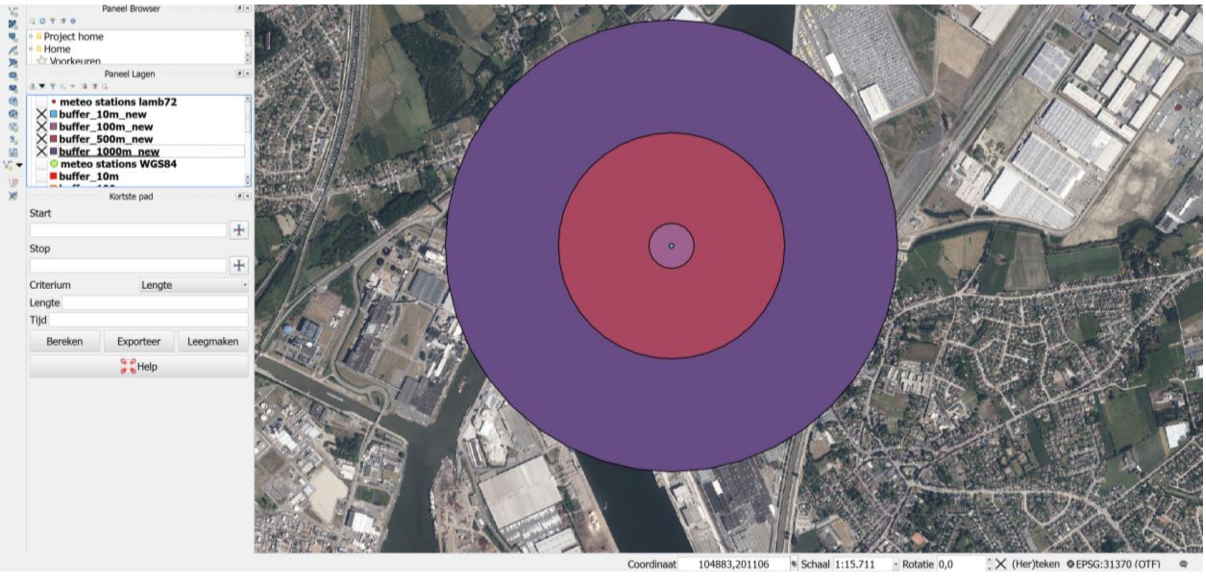

3. Calculating the amount of water, impervious and green surface in the different buffers

Open a new project, if necessary.

Import the raster layers with the land cover information by clicking on ‘Add raster layer’.

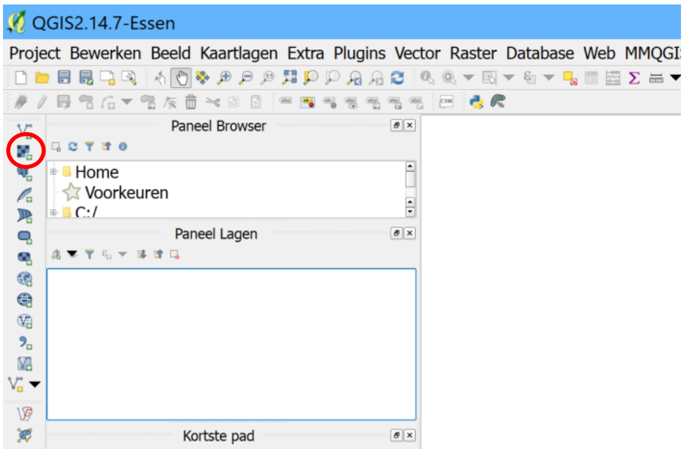

Select the file you want to open and open it.

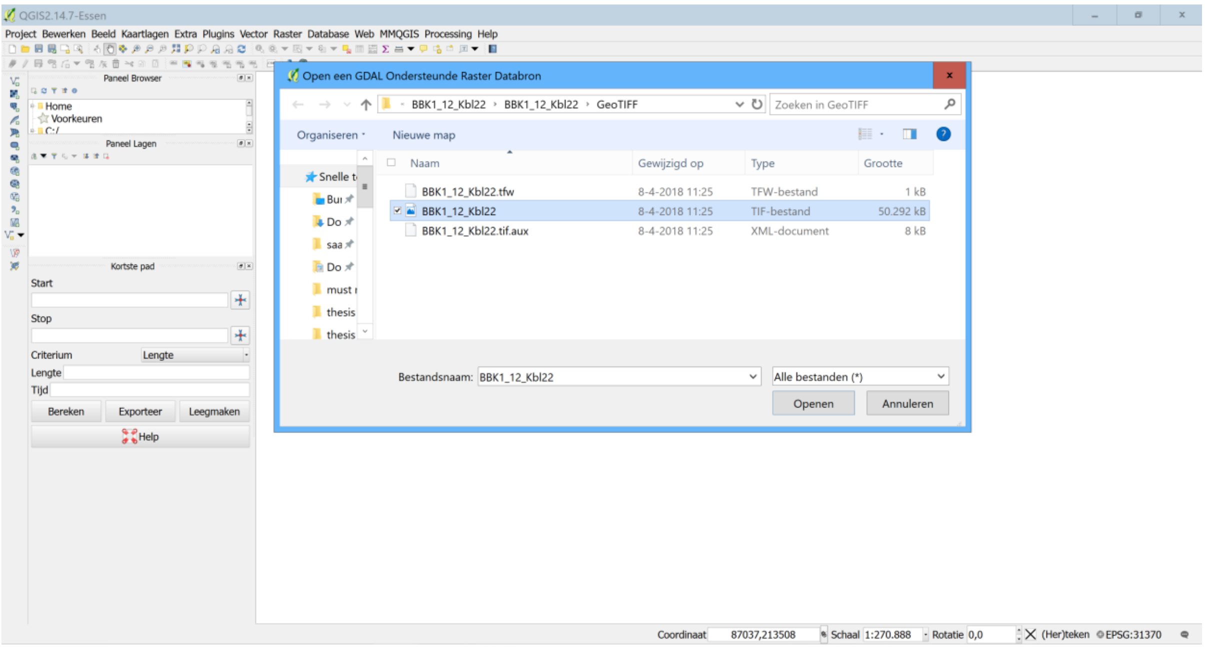

Result:

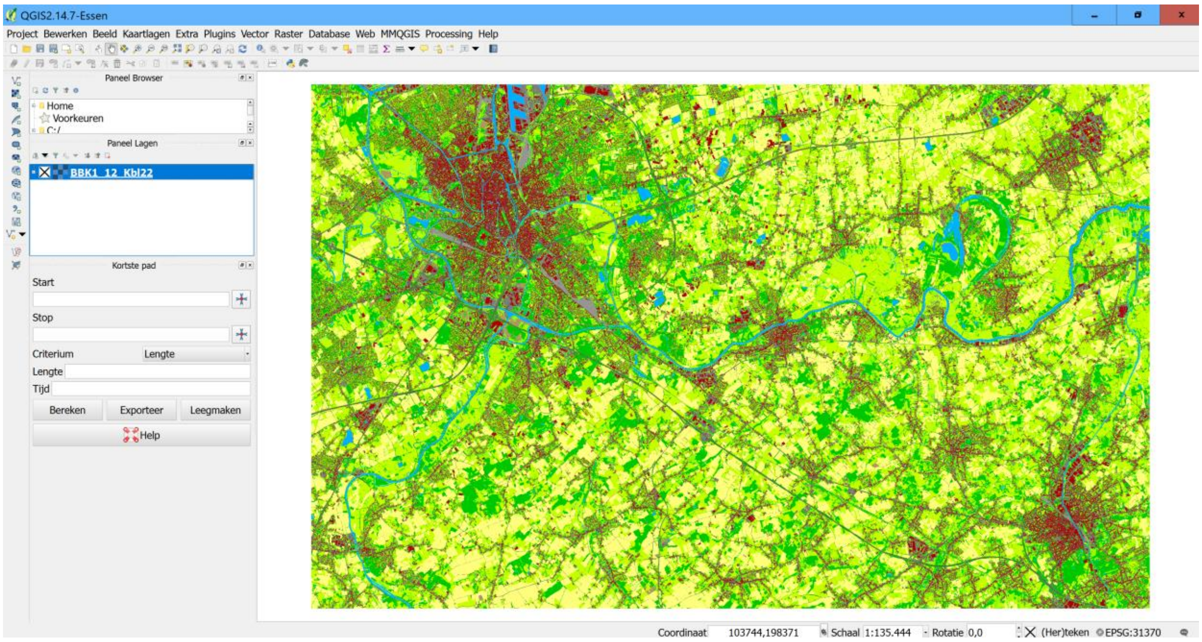

Do the same for the other layers you need. If the layers are in one folder, then you can select them all at once and open them in one click. Also for the next steps it is easier if all the needed files are located in the same folder.

Remember to save the QGIS project file to ensure that your progress is not lost if the program becomes unresponsive.

When there are multiple files but only one layer is desired to do calculations, then the merge tool should be used. Merging the two raster layers is done by following the path: Raster → Miscellaneous → Merge.

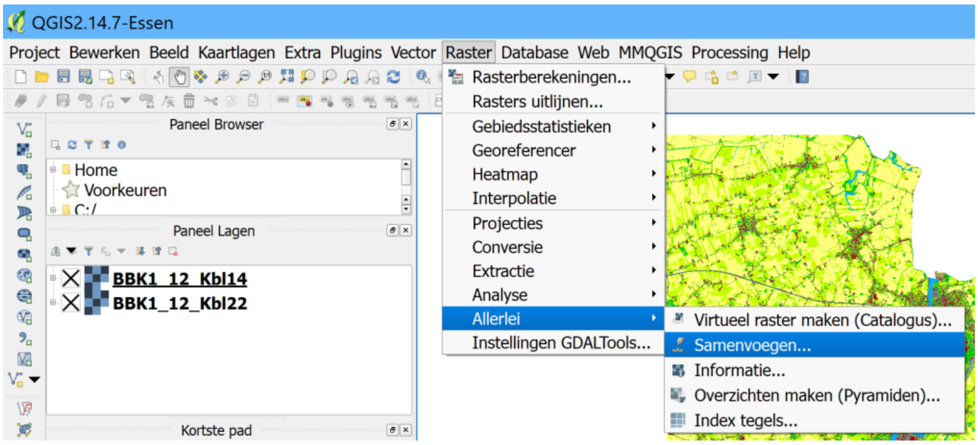

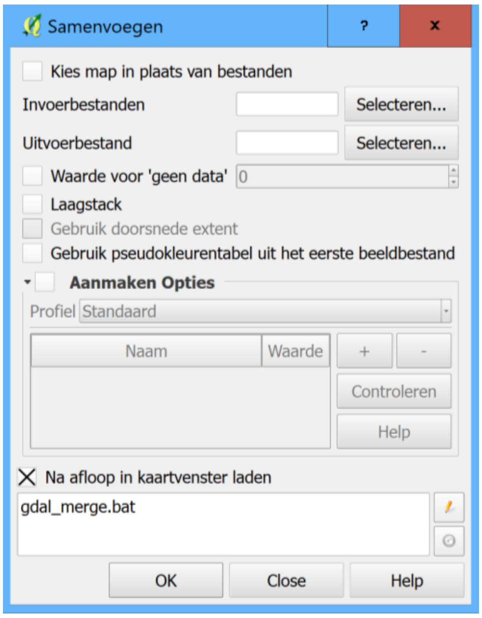

Press ‘Select…’ and add the input files you want to merge.

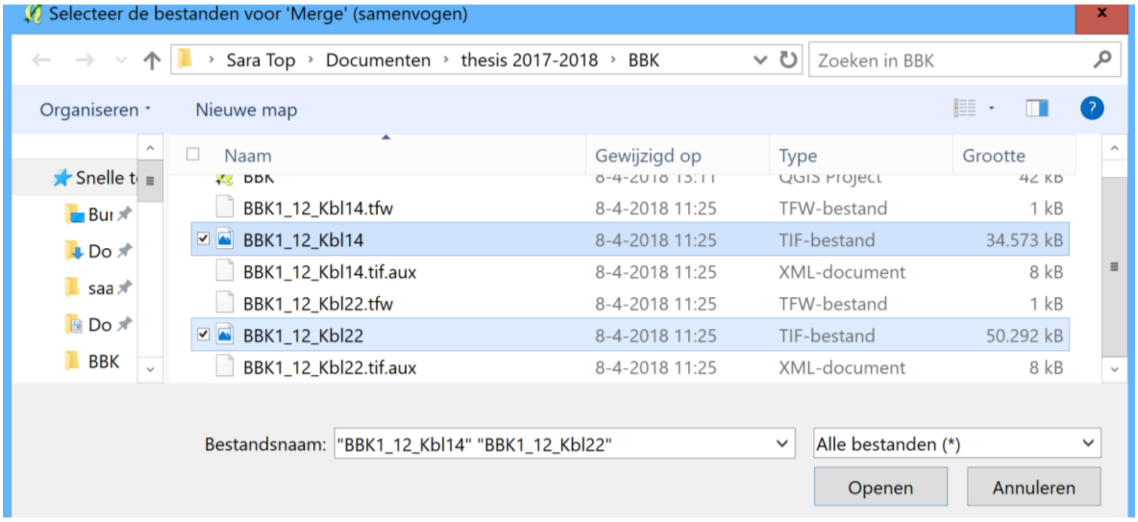

Press select and choose the locations where the output file has to be saved and give a name.

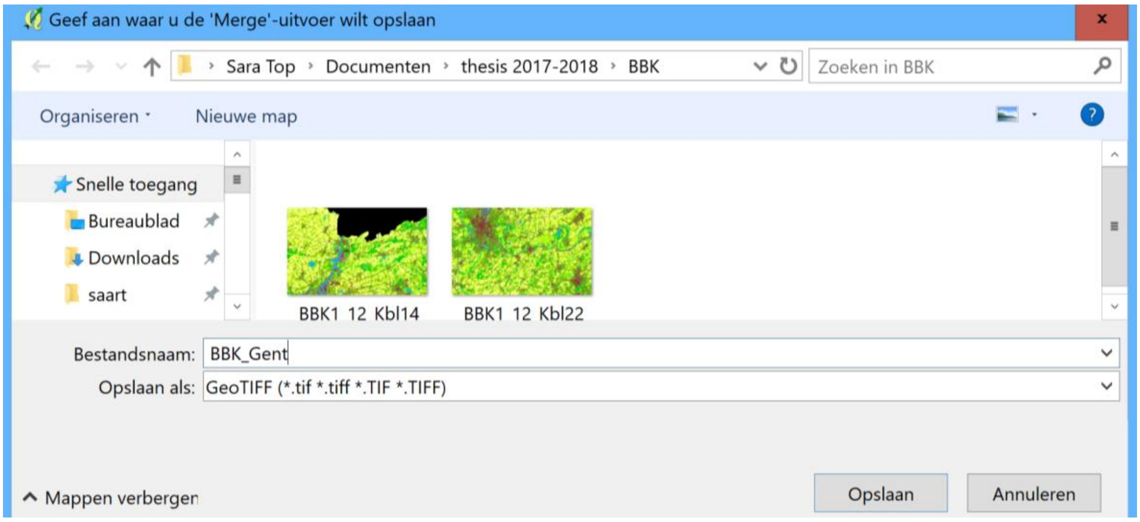

Tick the options ‘No data value’ = 0 and ‘Grab pseudocolor table from the first image’. By doing so, the colours of the original file are preserved.

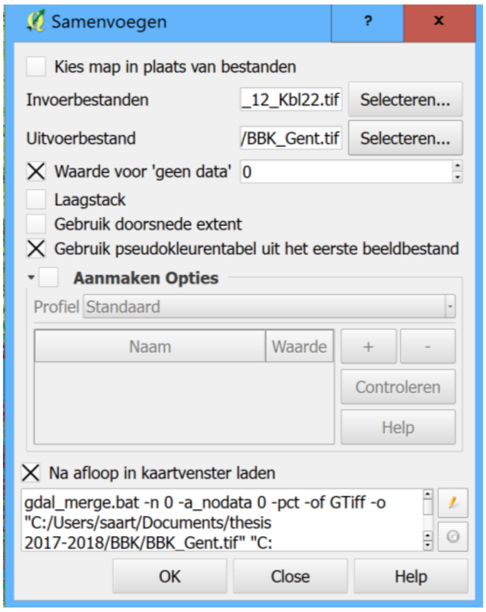

Click ‘ok’. It might take a while to merge the layers.

Result:

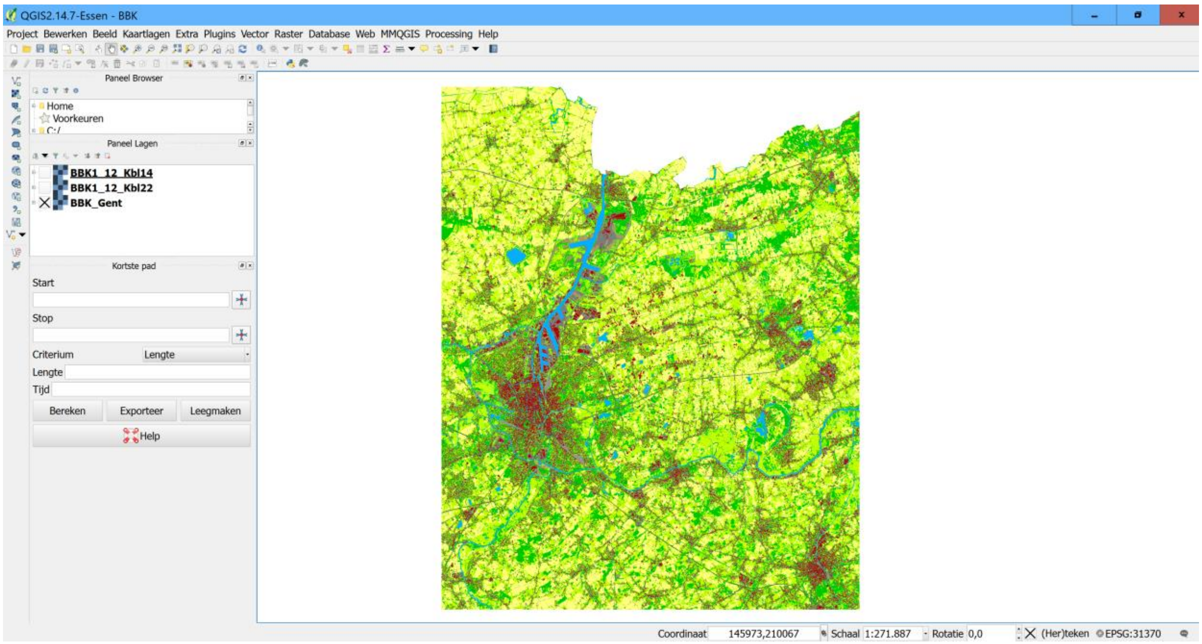

Open the ‘raster calculator’ to create new layers with only impervious, green or water as land cover.

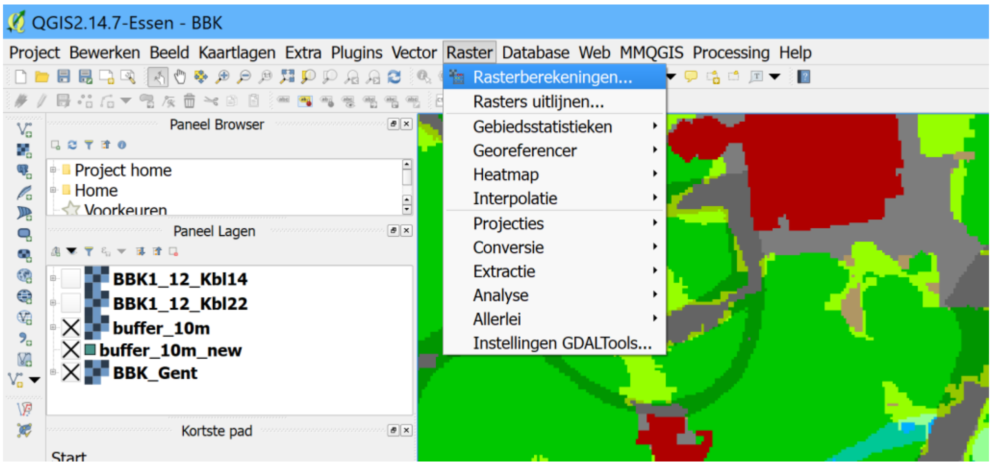

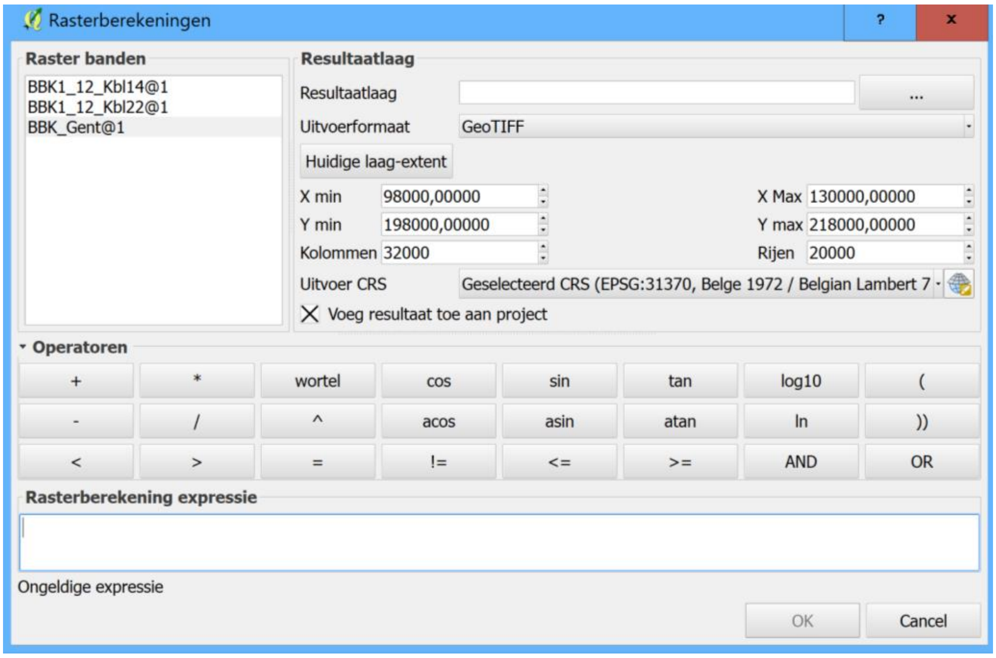

Click on the button with ‘…’ to save the resulting layer of the raster calculation. Choose a name and the folder where you want to save the result.

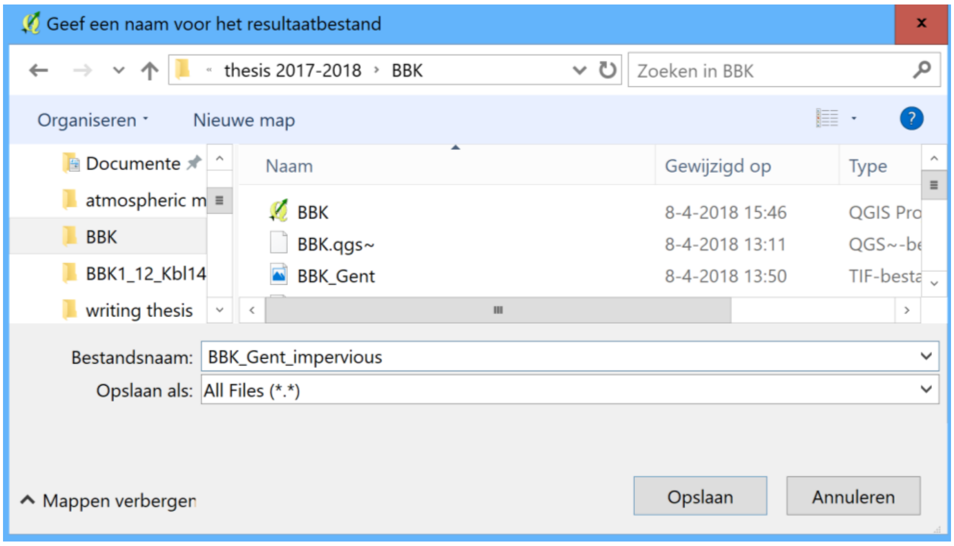

Select the layer to be modified and click on 'Current layer extent' to execute the raster calculation over the specific spatial extent. Thereafter, enter the formula in the box with the expression for the raster calculation, so the impervious features get value 1 instead of values ranging from 1 to 4 (AGIV, 2016a).

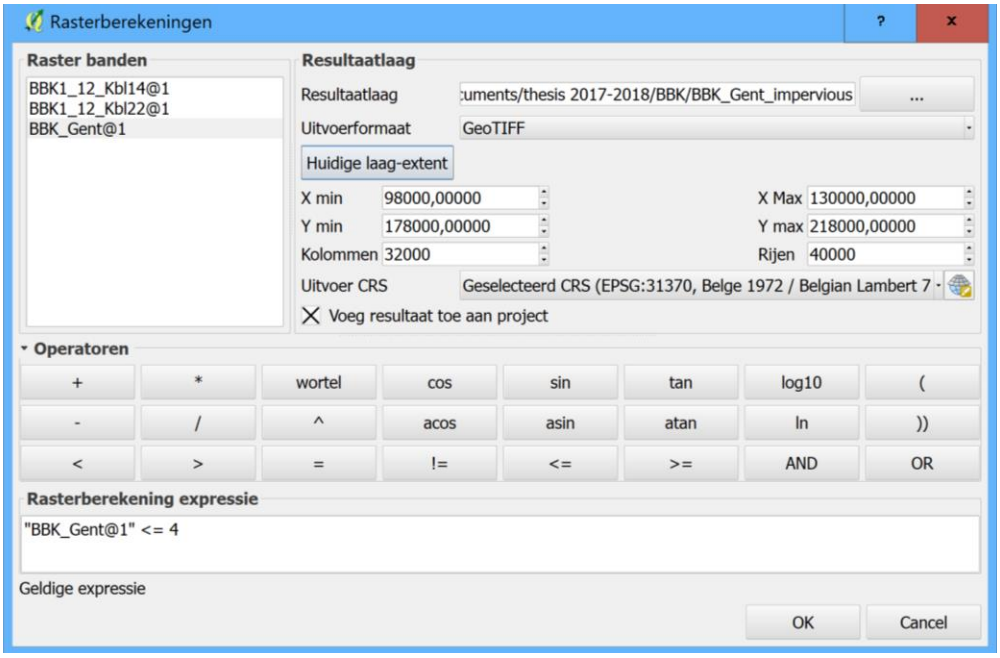

The resulting layer only contains values 1 and 0 by doing this.
If the result is a completely black field as shown below , then adapt the colours of the raster image. Go to layer properties, so the colour of the values can be changed.

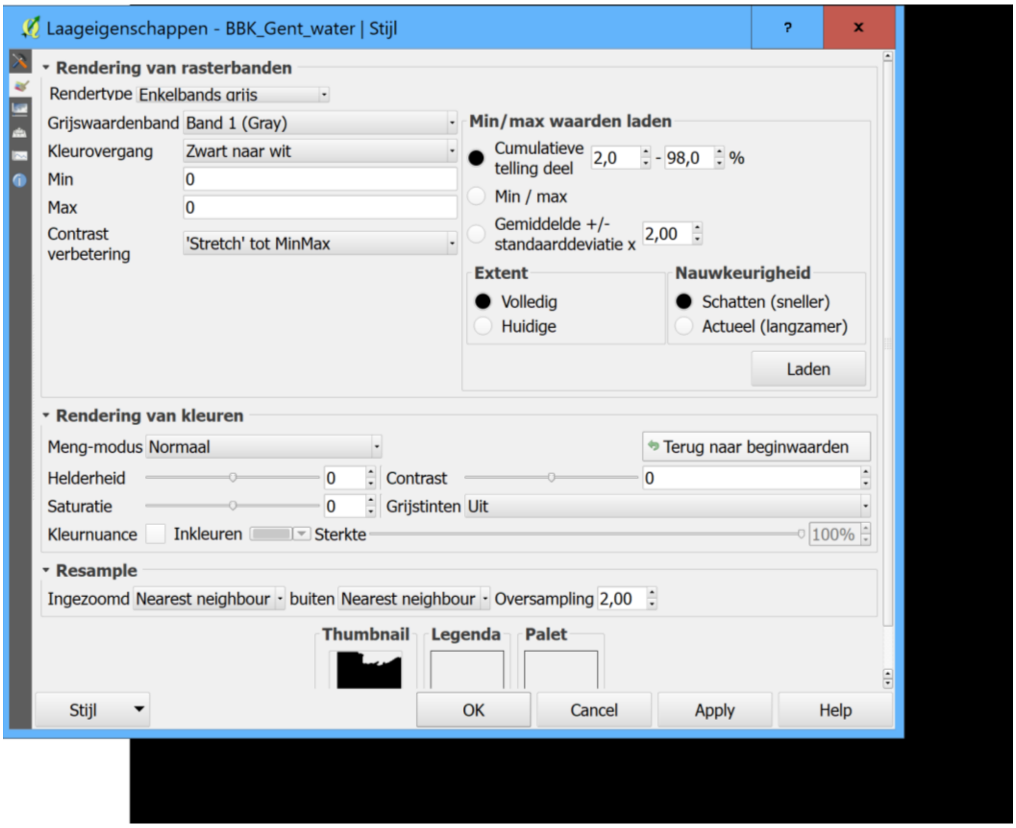

Tick ‘min/max’ instead of ‘Cumulative’ and click on the button ‘Load’. Min should have value 0 and max should have value 1.

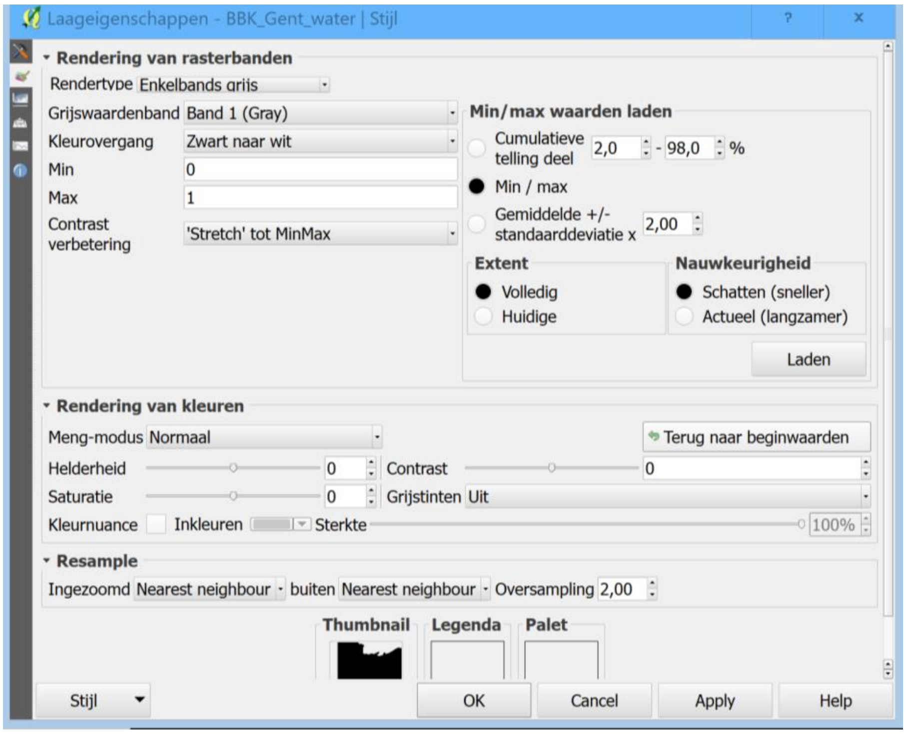

Click ‘ok’.

Value 1 (white) is the impervious land cover and value 0 (black) are the remaining classes.

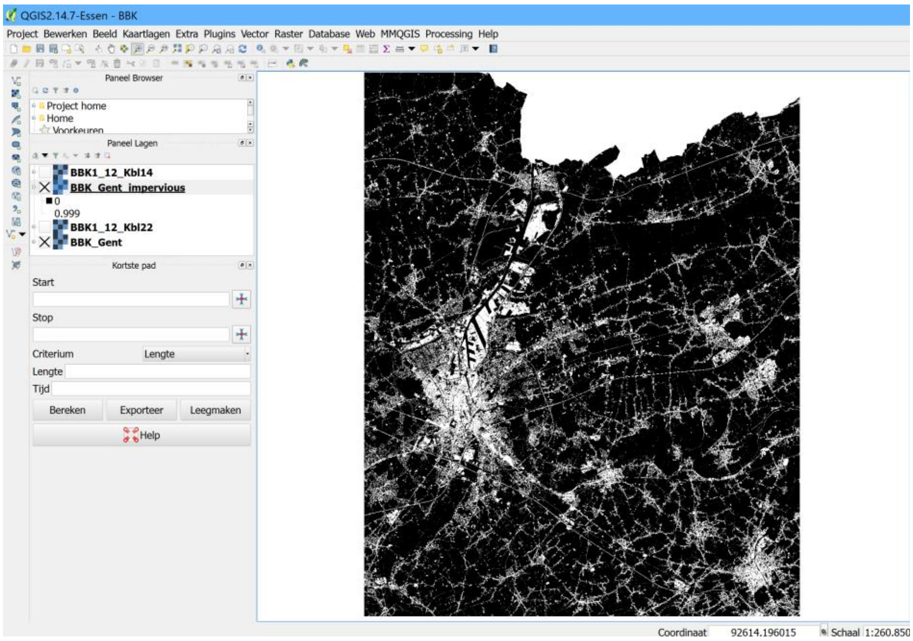

Right click on the layer and open the 'Layer properties' to change the colours of layer.

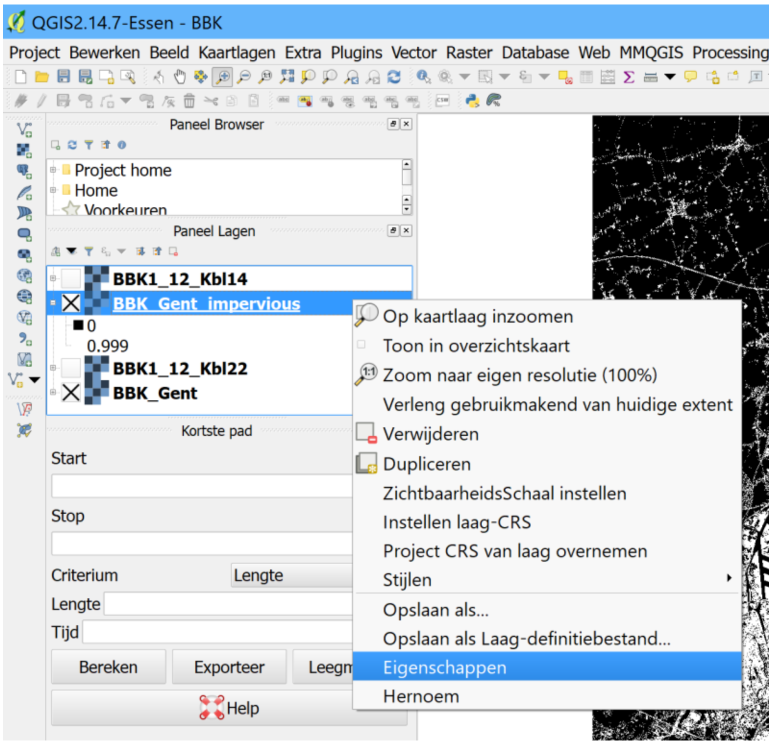

Press on the transparency tab and indicate the raster cells with value 0 as 'no data'.

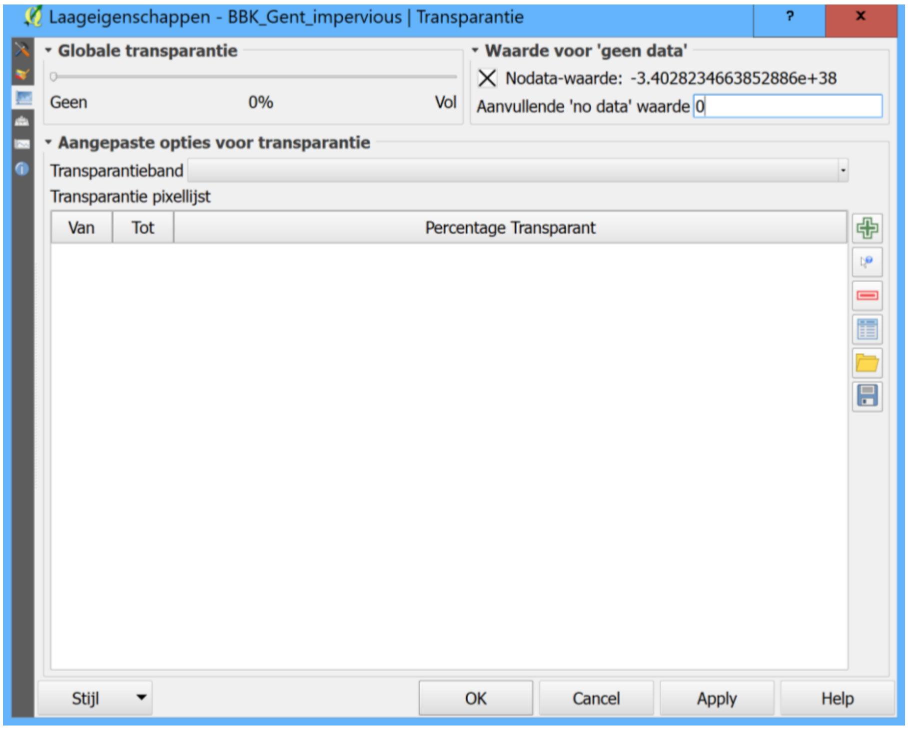

Result: The underlaying layer of BBK_Gent can be seen because the values 0 are represented as no data and are transparent. The raster cells with impervious land cover are coloured white and cover the underlaying BBK_Gent layer.

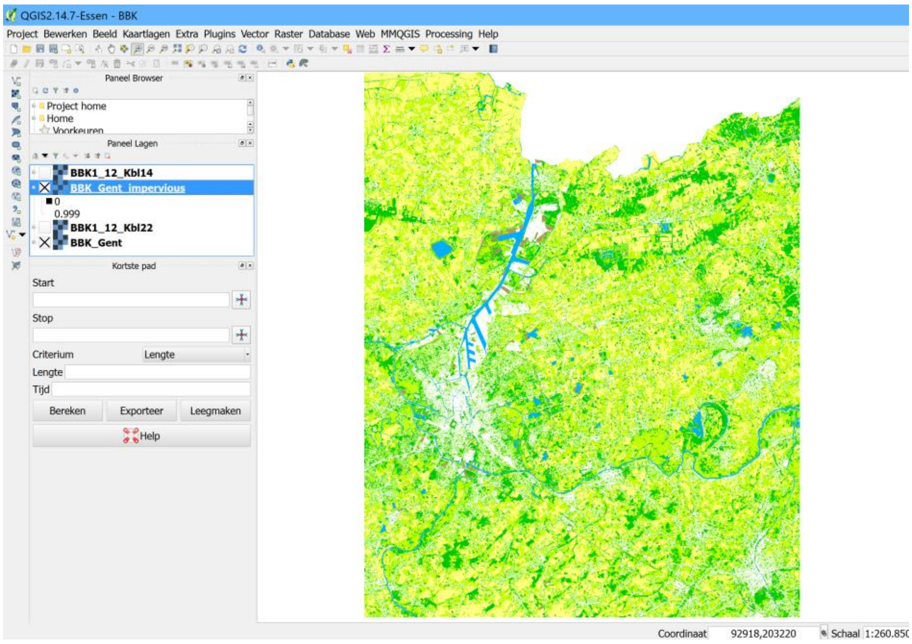

Load the shapefile with the buffers by using the ‘Add vector layer’ tool.

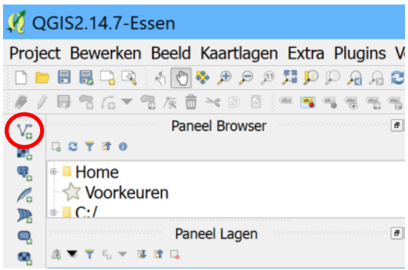

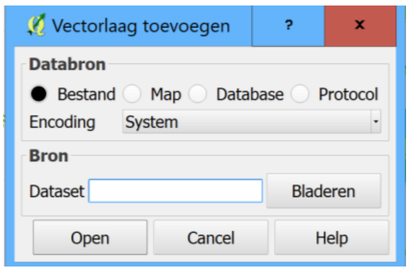

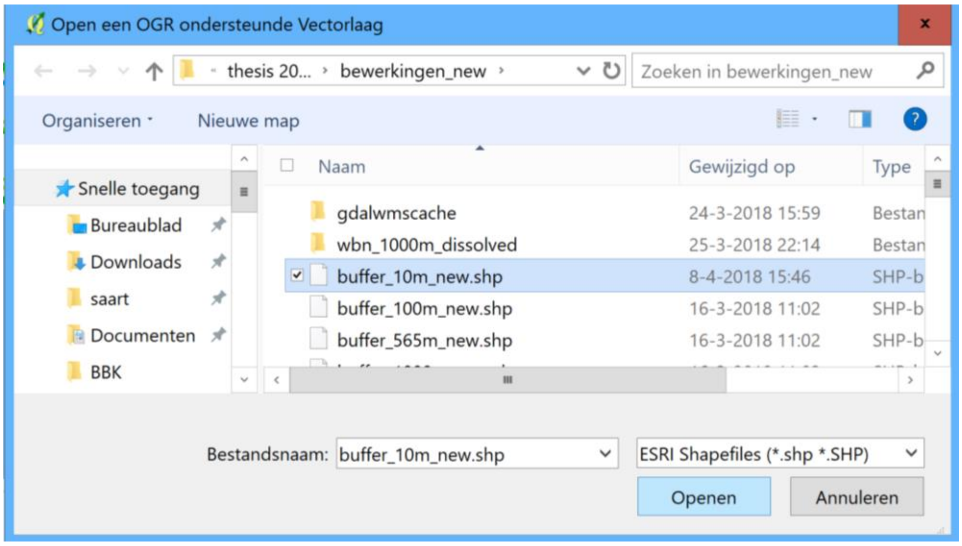

Click open and open the vector layer. Here the layer with buffers of 10 m radius around the stations are chosen. It is also possible to add all the layers of different buffer distances at once by selecting them all.

Zoom in on the layer of 10 m with the magnifying glass.

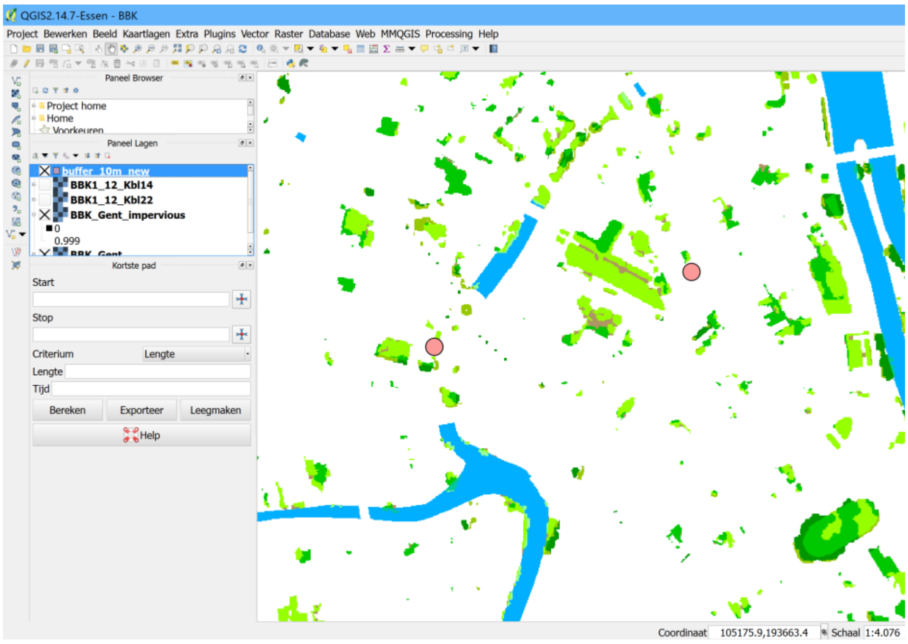

Open the ‘Zonal statistics’ tool.

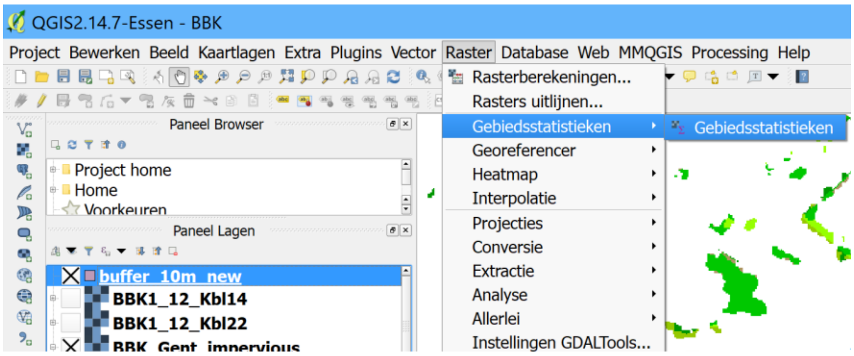

Choose the input raster layer and the vector layer were the statistics will be saved. Tick the statistics that are needed and click ok.

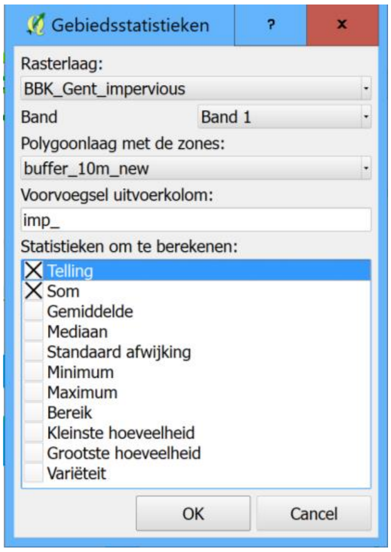

‘Count’ is used to determine the total area of the buffer and ‘Sum’ is used to know how many cells are indicated as impervious land cover. The ‘Sum’ function can be used since the value of the raster cells with impervious land cover is equal to 1.

Open the attribute table.

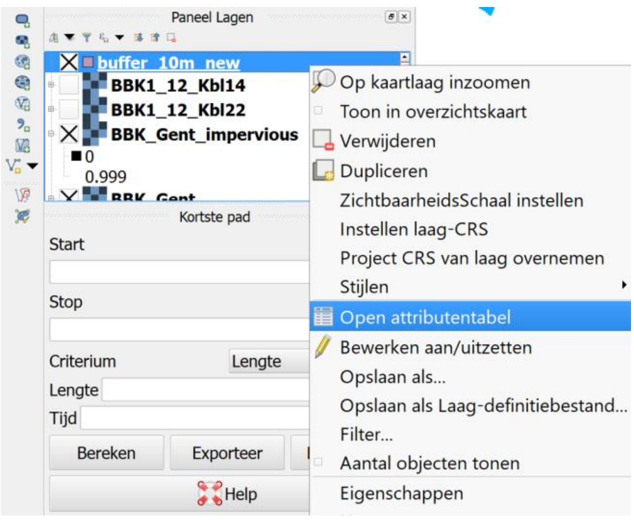

Result:

buffer_10m_new :: Features total: 6, filtered: 6, selected: 0

	oordW	oordW	ocatior	eaBuff	3K_cou	imp_count	imp_sum
0	3.728...	51.05...	Provi...	308	310.0...	310.000000000...	220.0000000000...
1	3.732...	51.05...	Sint-B...	308	311.0...	311.000000000...	235.0000000000...
2	3.749...	51.10...	Honda	308	312.0...	312.000000000...	129.0000000000...
3	3.722...	51.03...	Plant...	308	308.0...	308.000000000...	0.000000000000...
4	3.703...	51.08...	Wond...	308	310.0...	310.000000000...	130.0000000000...
5	3.816...	50.97...	Melle	308	310.0...	310.000000000...	0.000000000000...

Do the same for water, green space and surface occupied by buildings.

The formula used for water is:

"BBK_Gent@1" = 5

The formula used for green space is:

"BBK_Gent@1" > 5

The formula used for buildings is:

"BBK_Gent@1" = 1

The resulting land cover fractions in the buffer with a radius of 10 m for each station are (here without buildings):

buffer_10m_new :: Features total: 6, filtered: 6, selected: 0

	oordW	oordW	location	eaBuff	BBK_count	ıp_cou	imp_sum	wat_sum	gre_sum
0	3.728...	51.05...	Provinciehuis	308	310.00000...	310.0...	220.0000...	0.00000...	90.000...
1	3.732...	51.05...	Sint-Bavo	308	311.00000...	311.0...	235.0000...	0.00000...	76.000...
2	3.749...	51.10...	Honda	308	312.00000...	312.0...	129.0000...	0.00000...	183.00...
3	3.722...	51.03...	Plantentuin	308	308.00000...	308.0...	0.000000...	0.00000...	308.00...
4	3.703...	51.08...	Wondelgem	308	310.00000...	310.0...	130.0000...	0.00000...	180.00...
5	3.816...	50.97...	Melle	308	310.00000...	310.0...	0.000000...	0.00000...	310.00...

Convert to an Excel workbook. Right click on the shapefile layer and choose ‘Save as …’.

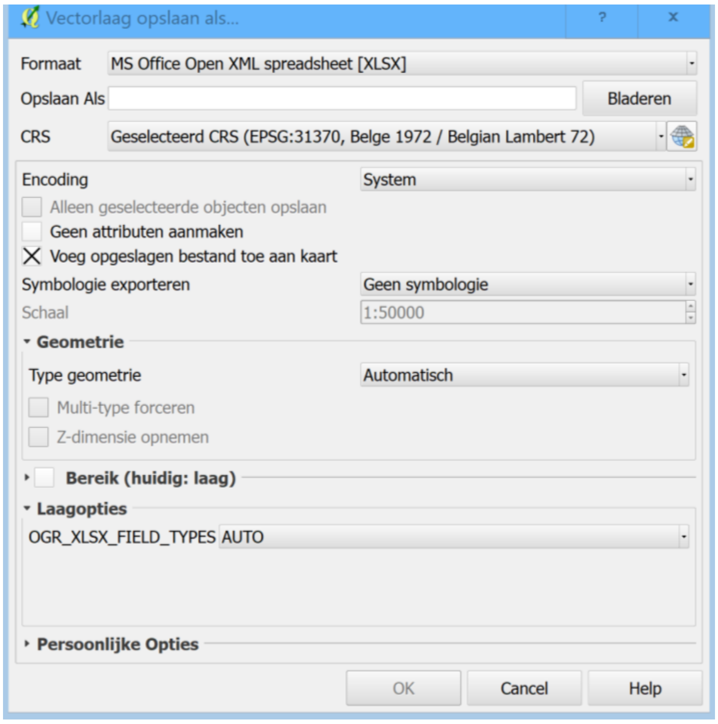

Make sure the file format is set to MS Office (or a CSV file is also possible for post processing the data).

Choose a location and a file name to save the file.

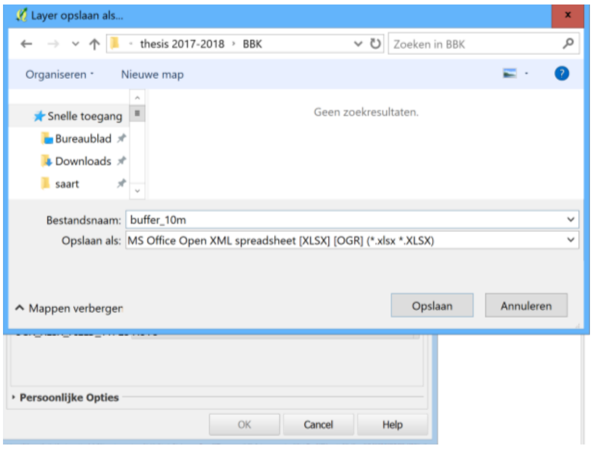

The layer should not be added to the interface of the QGIS project, thus do not tick that option.

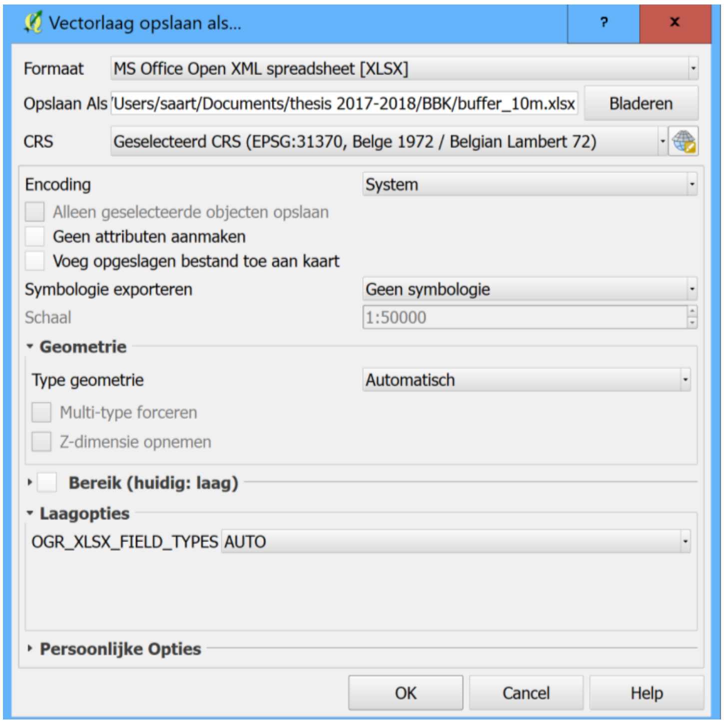

Click ‘ok’ and the task will be completed.

Open the Excel file by double click on the file name.

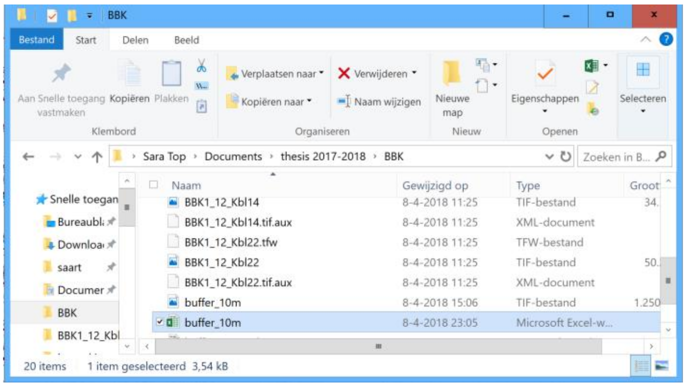

Result:

	A	B	C	D	E	F	G	H	I
1	XcoordWeb	YcoordWeb	location	areaBuffer	BBK_	imp_count	imp_sum	wat_sum	gre_sum
2	3,728	51,051	Provinciehuis	308	310	310	220	0.0000000000000	90
3	3,732	51,052	Sint-Bavo	308	311	311	235	0.0000000000000	76
4	3,749	51,109	Honda	308	312	312	129	0.0000000000000	183
5	3,722	51,036	Plantentuin	308	308	308	0.0000000000000	0.0000000000000	308
6	3,703	51,084	Wondelgem	308	310	310	130	0.0000000000000	180
7	3,816	50,98	Melle	308	310	310	0.0000000000000	0.0000000000000	310

Apply the same procedure with zonal statistics for the other buffer distances.

This is the resulting attribute table for the 100 m buffer land cover.

buffer_100m_new :: Features total: 6, filtered: 6, selected: 0

	oordW	oordW	location	eaBuff	imp_count	imp_sum	wat_count	wat_sum	gre_count	gre_sum
0	3.728...	51.05...	Provinciehuis	30816	30891.00...	28101.0...	30891.000...	540.0000...	30891.000...	2250.0000...
1	3.732...	51.05...	Sint-Bavo	30816	30925.00...	26094.0...	30925.000...	0.000000...	30925.000...	4831.0000...
2	3.749...	51.10...	Honda	30814	30883.00...	26597.0...	30883.000...	112.0000...	30883.000...	4174.0000...
3	3.722...	51.03...	Plantentuin	30816	30892.00...	11082.0...	30892.000...	463.0000...	30892.000...	19347.000...
4	3.703...	51.08...	Wondelgem	30815	30886.00...	7093.00...	30886.000...	837.0000...	30886.000...	22956.000...
5	3.816...	50.97...	Melle	30818	30885.00...	1550.00...	30885.000...	0.000000...	30885.000...	29335.000...

This is the attribute table for the 565 m buffer land cover.

buffer_565m_new :: Features total: 6, filtered: 6, selected: 0

	oordW	oordW	location	AMBpr	'LAMBpre	areaBuffer	imp-count	imp-sum	wat_count	wat_sum	gre_count	gre_sum
0	3.728...	51.05...	Provinciehuis	1050...	193642.88	995977	998751.0...	878521.00...	998751.000...	45207.00...	998751.0...	75023.00...
1	3.732...	51.05...	Sint-Bavo	1053...	193729.01	995977	998760.0...	798070.00...	998760.000...	73209.0...	998760.0...	127481.0...
2	3.749...	51.10...	Honda	1065...	200059.90	995930	998753.0...	760654.00...	998753.000...	198169....	998753.0...	39930.00...
3	3.722...	51.03...	Plantentuin	1046...	191921.71	995989	998759.0...	648698.00...	998759.000...	4398.00...	998759.0...	345663.0...
4	3.703...	51.08...	Wondelgem	1033...	197307.01	995951	998758.0...	395573.00...	998758.000...	1677.000...	998758.0...	601508.0...
5	3.816...	50.97...	Melle	1111...	185719.85	996032	998753.0...	93962.000...	998753.000...	726.000...	998753.0...	904065.0...

This is the attribute table for the 1000 m buffer land cover.

buffer_1000m_new :: Features total: 6, filtered: 6, selected: 0

	oordW	oordW	location	eaBuff	imp_count	imp_sum	wat_count	wat_sum	gre_count	gre_sum
0	3.728...	51.05...	Provinciehuis	3119...	3128710....	244632...	3128710....	173782....	3128710...	508600.0...
1	3.732...	51.05...	Sint-Bavo	3119...	3128686....	243543...	3128686....	178625....	3128686...	514628.0...
2	3.749...	51.10...	Honda	3119...	3128699....	186537...	3128699....	840640....	3128699...	422687.0...
3	3.722...	51.03...	Plantentuin	3120...	3128688....	216471...	3128688....	54722.0...	3128688...	909248.0...
4	3.703...	51.08...	Wondelgem	3119...	3128686....	127068...	3128686....	3298.00...	3128686...	1854707....
5	3.816...	50.97...	Melle	3120...	3128701....	295704...	3128701....	2418.00...	3128701...	2830579....

This information from the shapefiles is converted into Excel files.

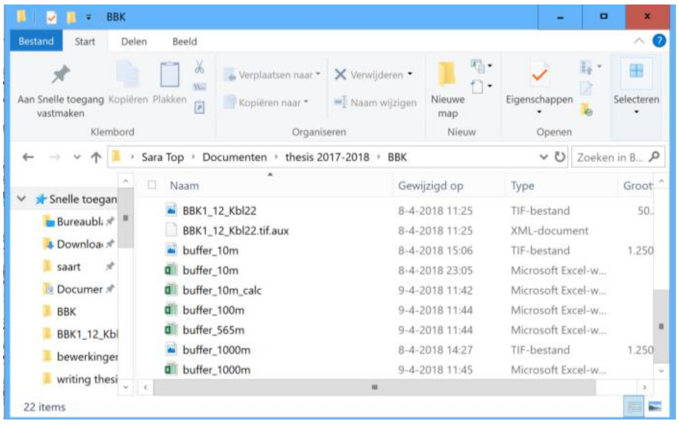

4. Calculating the average building height

Open a new project.

Open the vector layer ‘GRBGebL1D240000R500.shp’ of the 3D GRB.

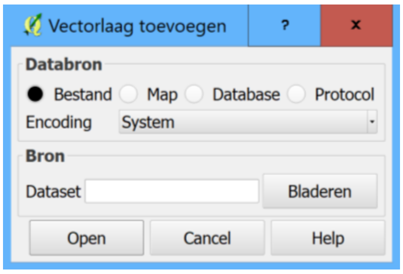

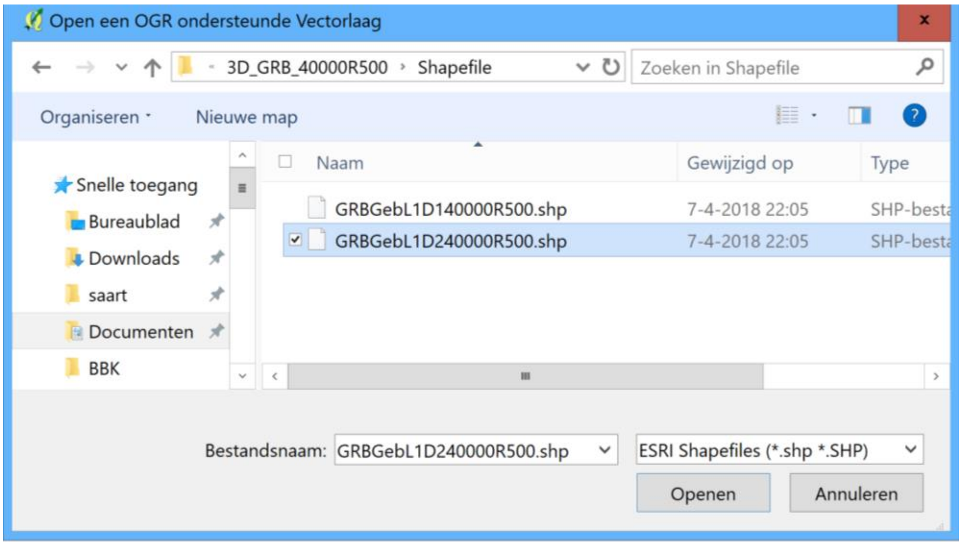

Open also the vector layers with the different buffers.

Save this as QGIS project.

Open the attribute table of the buffers and remove the land cover features.

Start editing by clicking on the ‘Edit’ button.

Then start removing the land cover features by activating the ‘Remove features’ tool.

Select the features that have to be deleted.

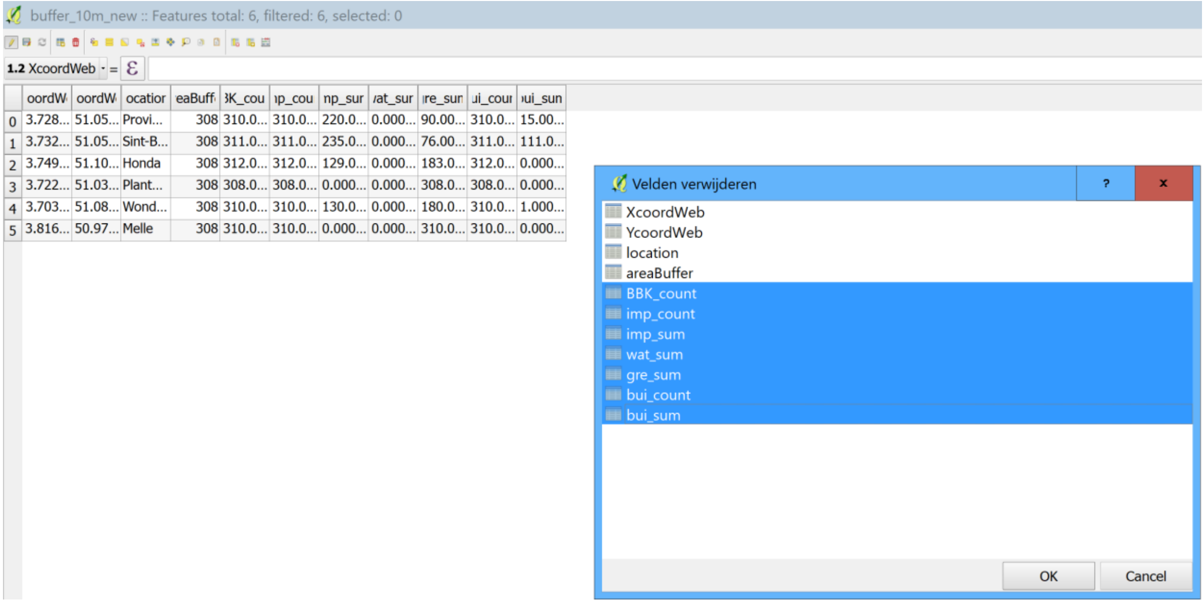

Result:

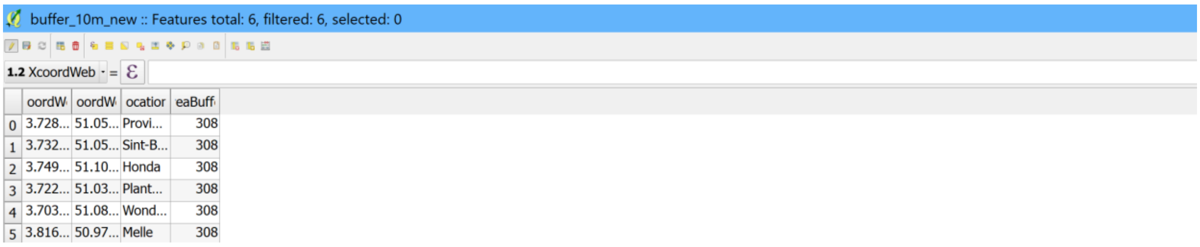

Once the results have been checked, click the ‘Save’ button followed by the ‘Edit’ button to stop editing.

Repeat this process for all the different buffer distances.

Use the ‘Intersection’ tool in order to select the information of the 3D GRB for a specific buffer area. With this tool the information of the 3D GRB is linked to a buffer area of one station (or more buffers if they overlap).

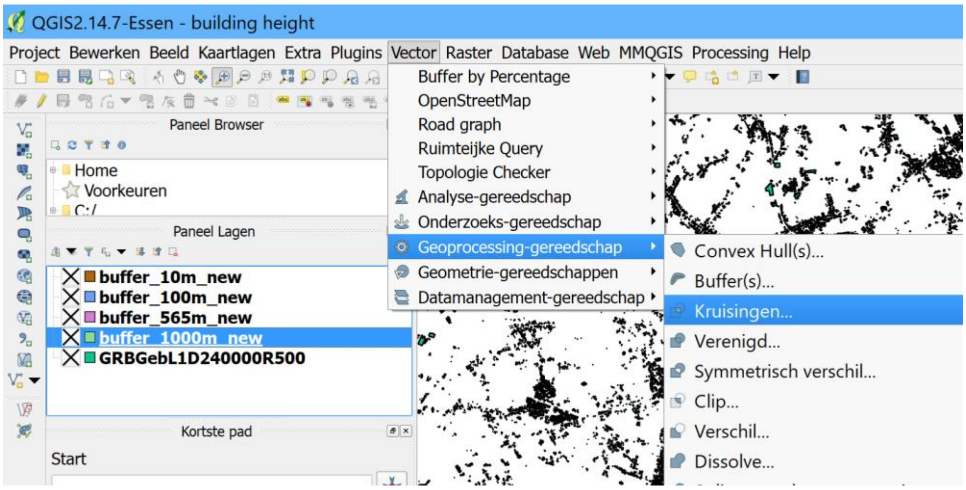

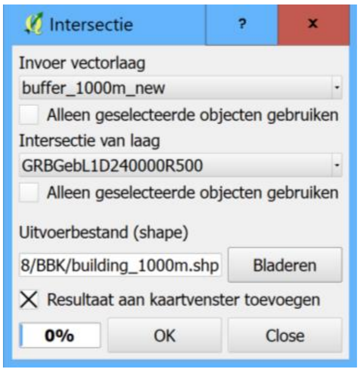

Choose a location and name it to save the new created file.

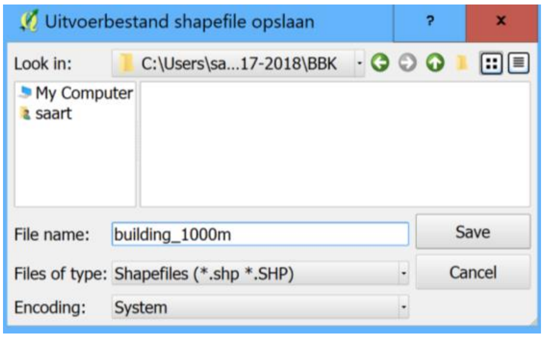

Click ‘ok’. This computation can take a while.

As result, the buffer layer contains the features of the buildings within the buffer distance.

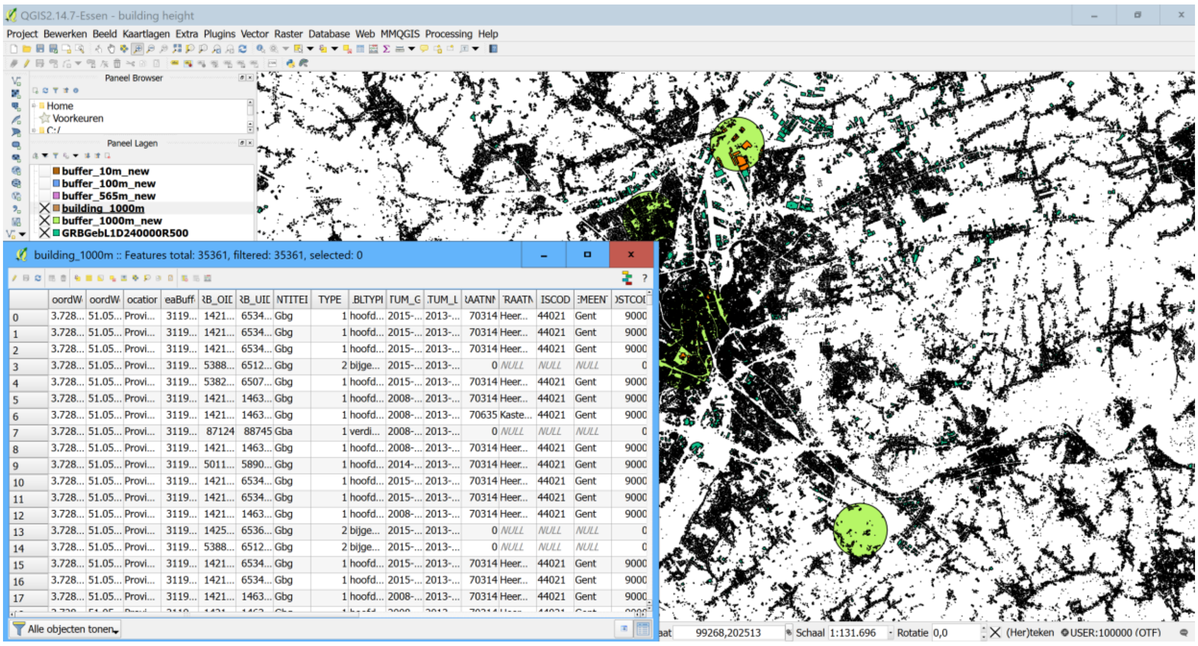

Do the same for the other buffer distances.

Remove in the attribute table of each layer with buffers the features with a bad quality label, namely the label *'slecht'*.

Open the attribute table and cick on 'Select by expression'.

Fill in the expression to remove the bad attributes and press 'Select'.

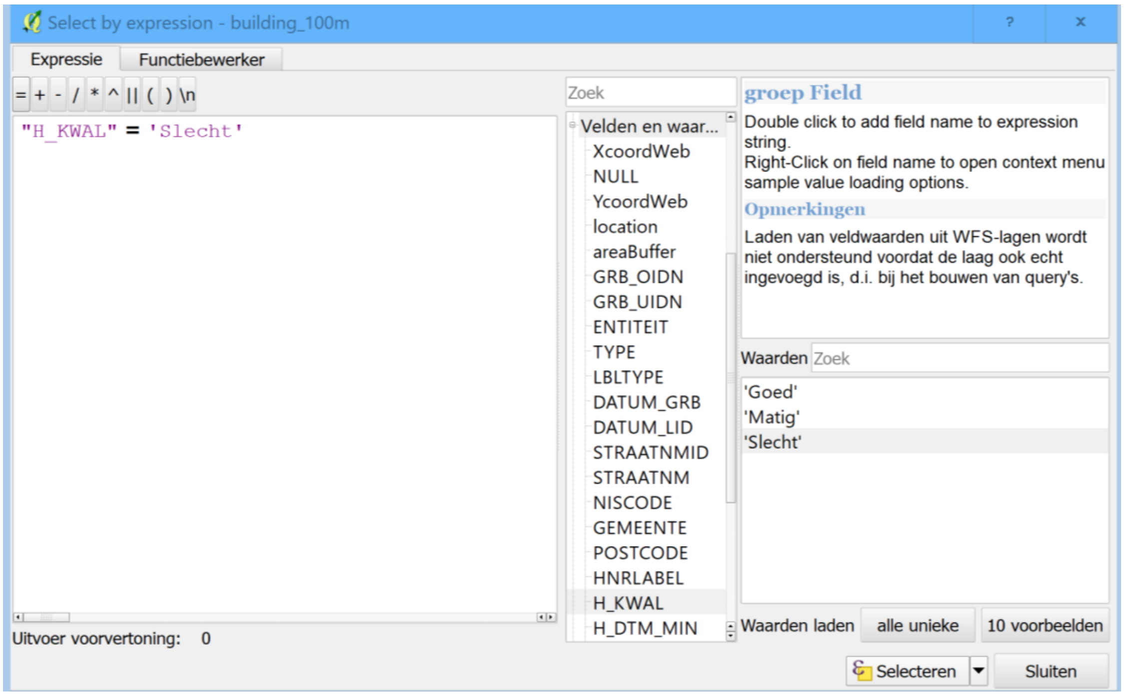

Show only the selected items in the attribute table to check the selection that was made.

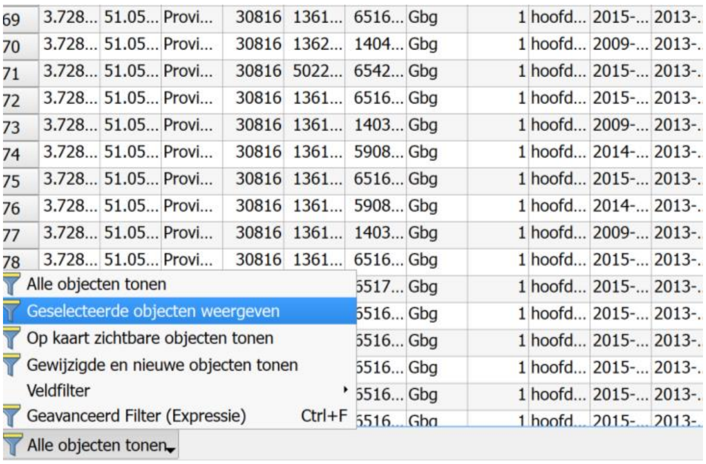

Click the ‘Edit’ button to start editing and remove the selected items.

Result:

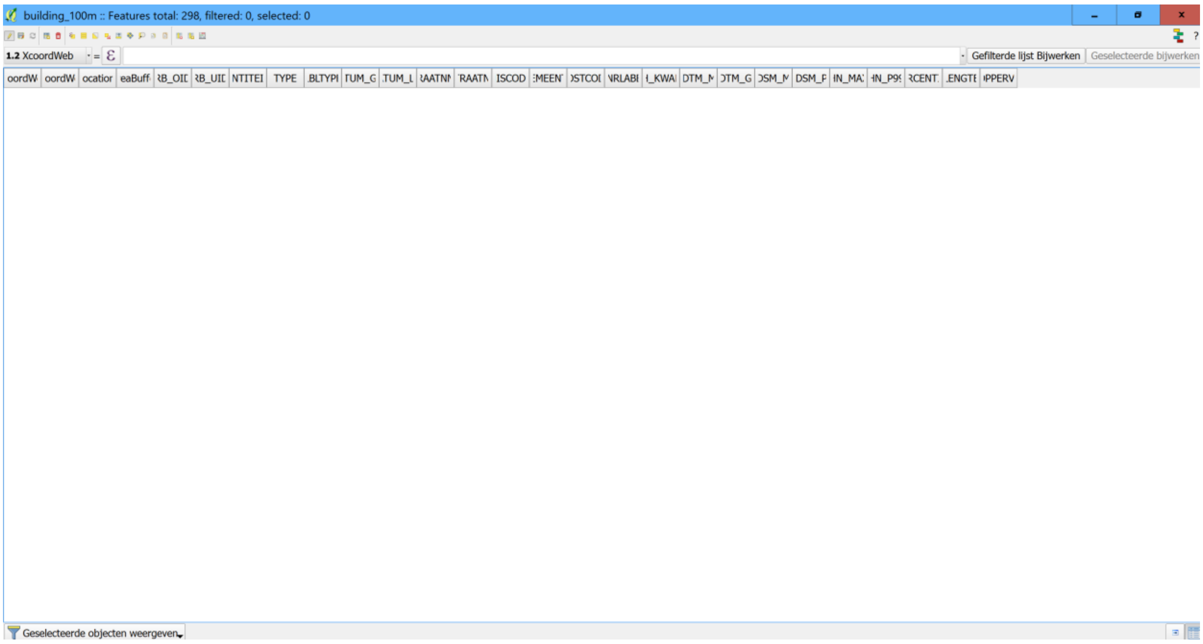

Not all the attributes are gone, but all the selected attributes are deleted.

Save.

Now, all the features are given again in the attribute table, but the attributes with the label '*slecht*' have been removed.

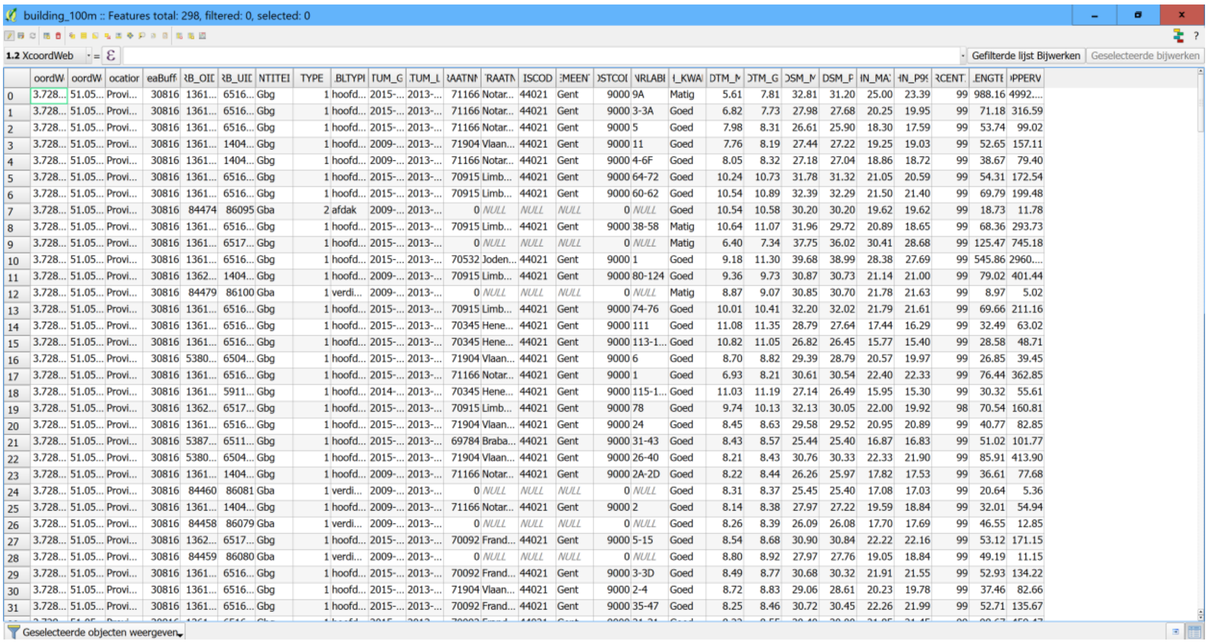

Add a new field with the field calculator to add the area that the buildings occupy within the buffer area.

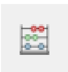

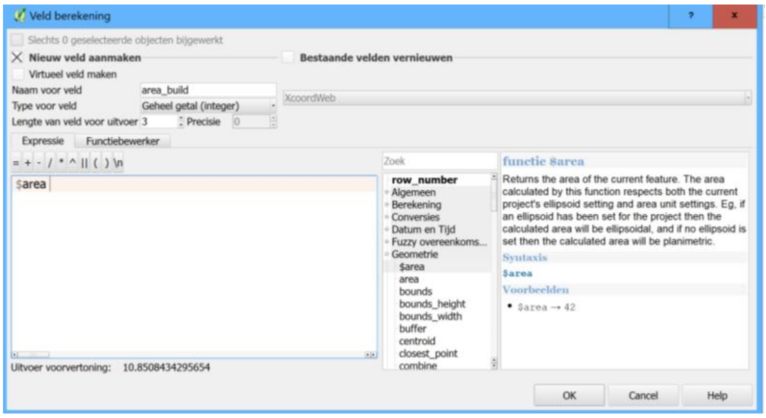

Result:

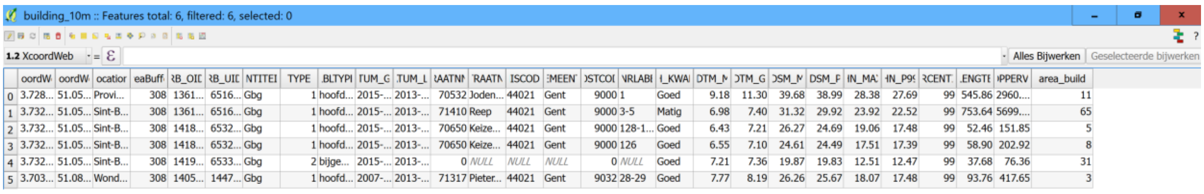

Click the 'Save' button, followed by the 'Edit' button to stop editing.

Convert this information to Excel.

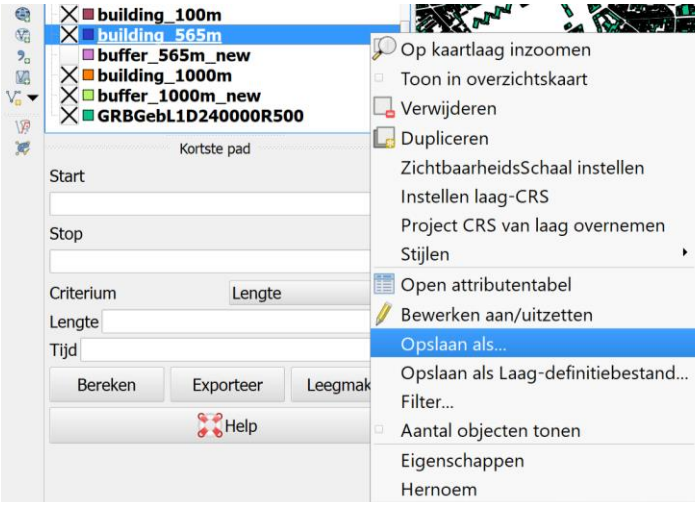

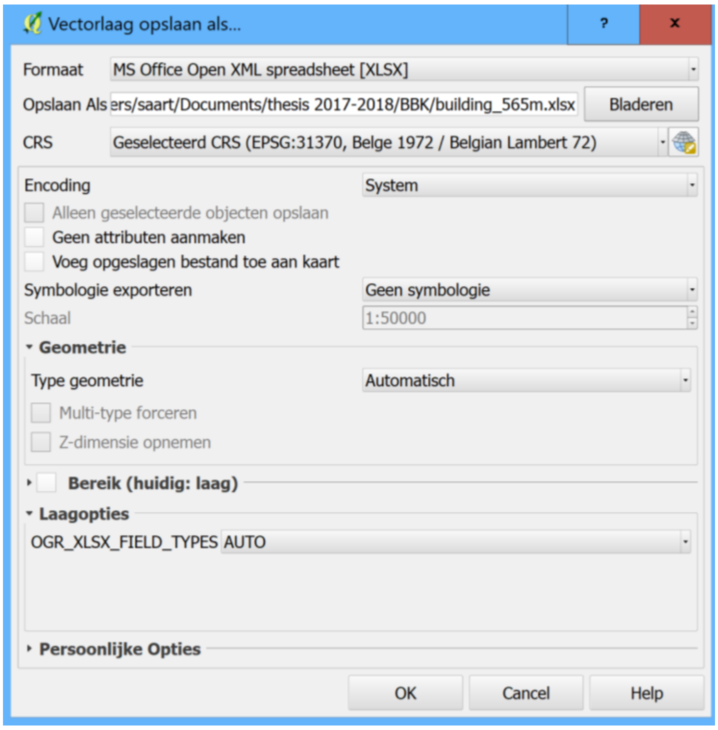

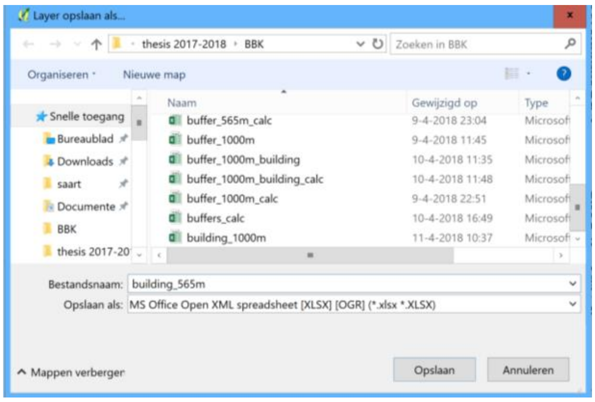

5. Splitting overlapping buffers

Press on the button ‘Select by’.

Press Ctrl and click in the editing field. Draw a rectangle over the buffer areas that must be selected.

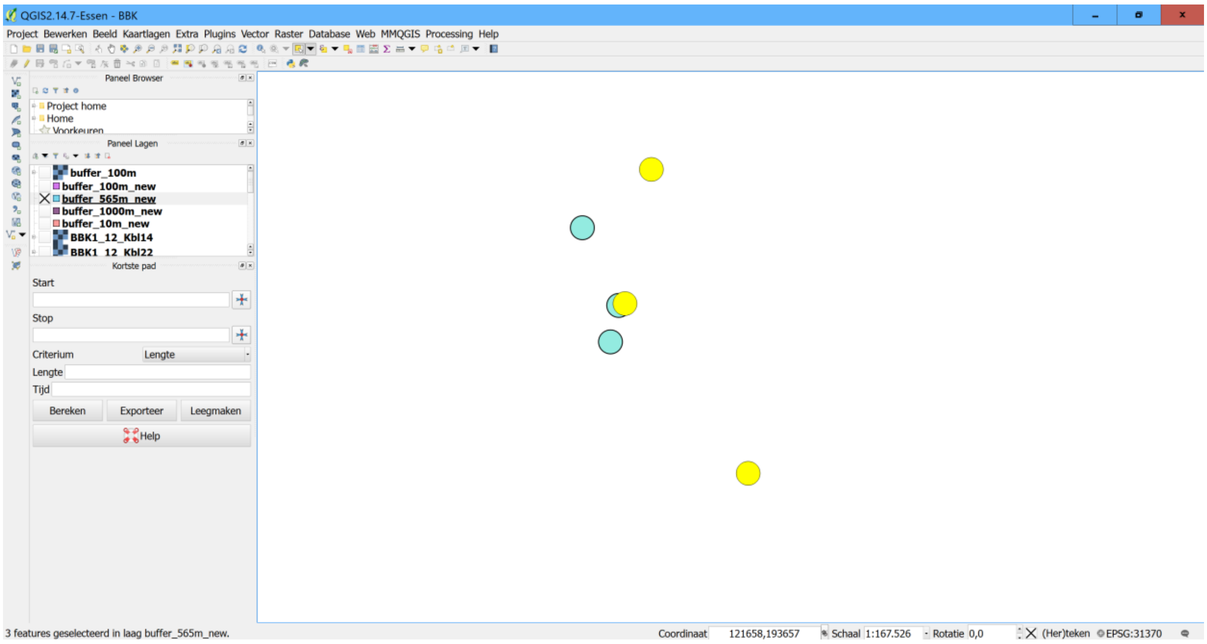

The selected buffer areas are indicated in yellow.

Save only these selected buffers in a new shapefile.

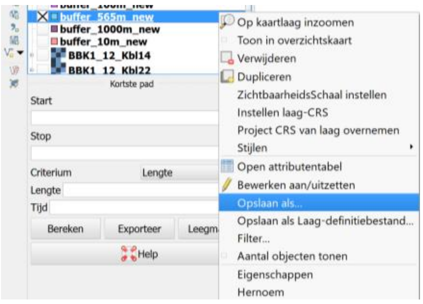

Make sure 'only selected items' is ticked.

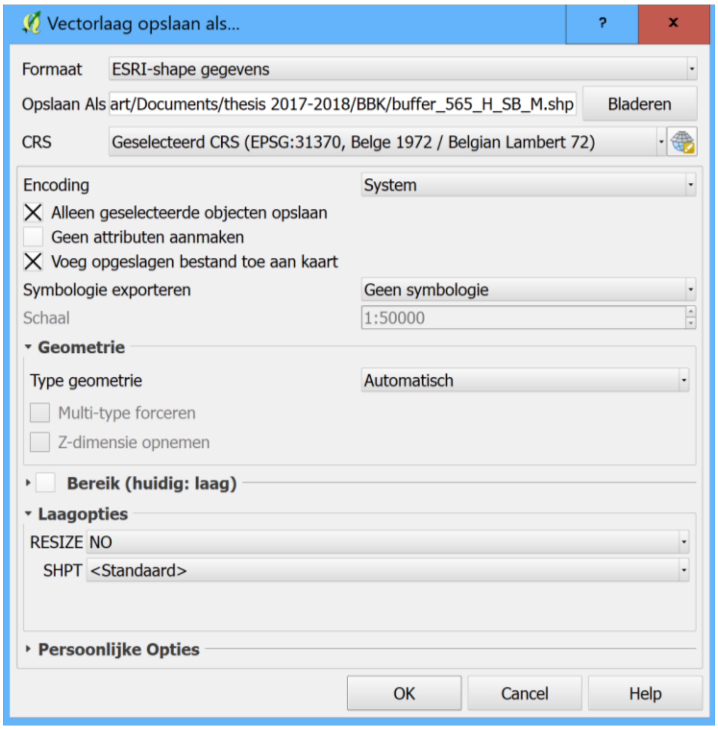

A new shapefile layer with the buffer areas that do not overlap is obtained as result. (The pink buffers are one layer and none of the buffers overlap.)

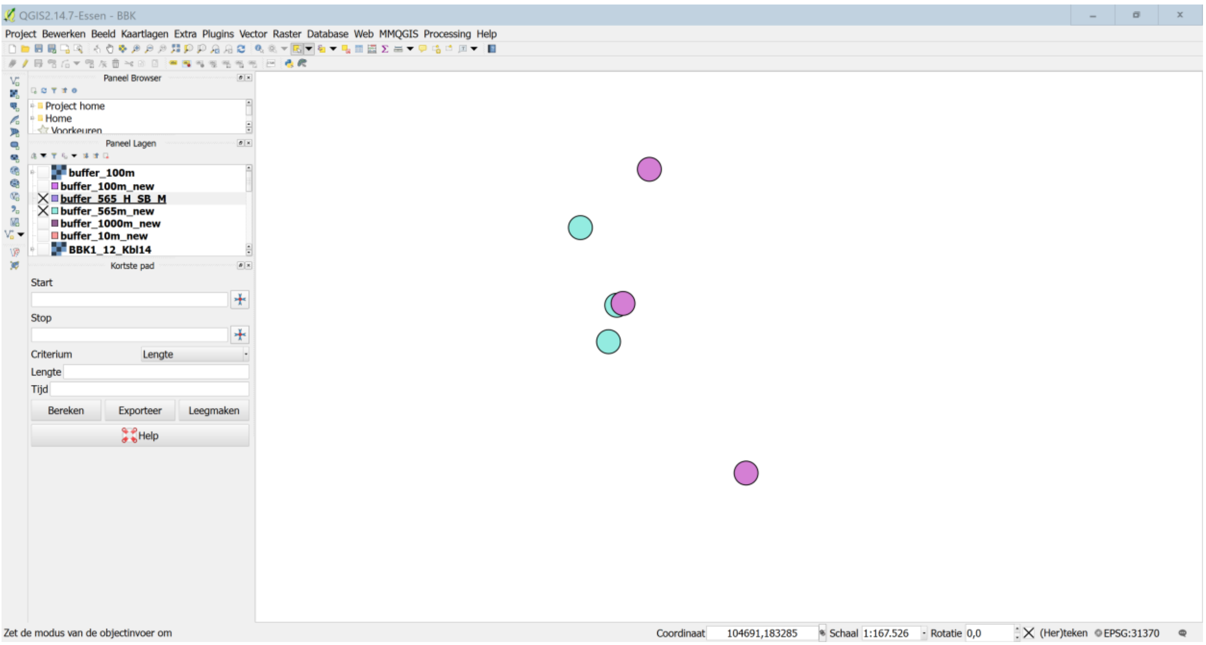

Do the same for the other three buffers in the buffer_100m layer as well as the buffer_1000m layer. Here the layer has to only be split into two different layers because only two buffers overlap. If for example three buffers overlap with each other then, three different layers have to be created.

Once this is done the layer BBK_Gent can be clipped with the new created layers.

6. Clipping for visualisation

For the visualisation, the buffers must be clipped out of the map to represent the buffers in a darker colour on top of the basemap.

The tool clip is opened via: Raster → Extraction → clip.

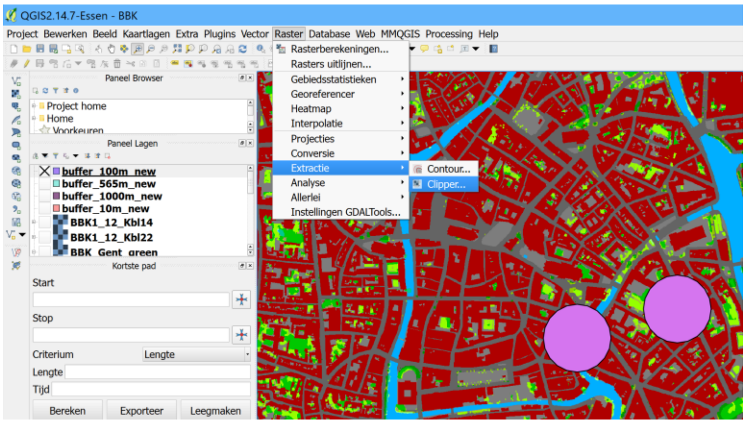

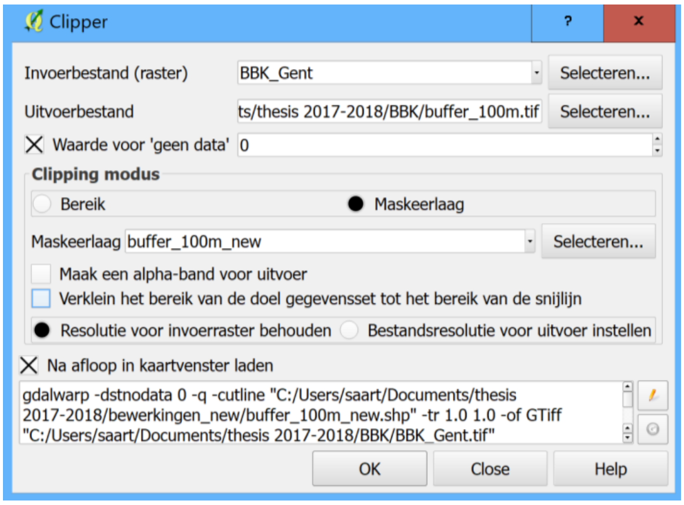

Click on ‘Select’ to choose a folder to save the resulting clipped raster layer.

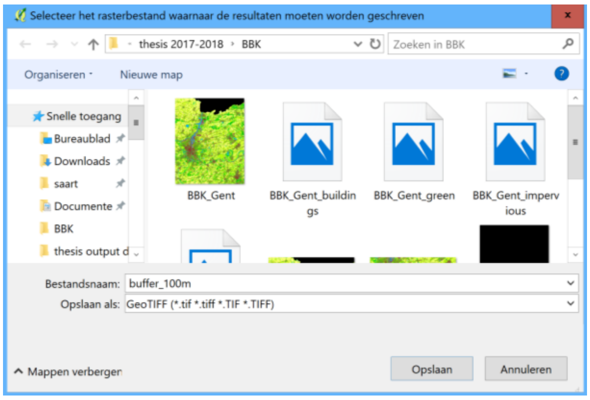

Fill in the name of the new raster layer that will be created.

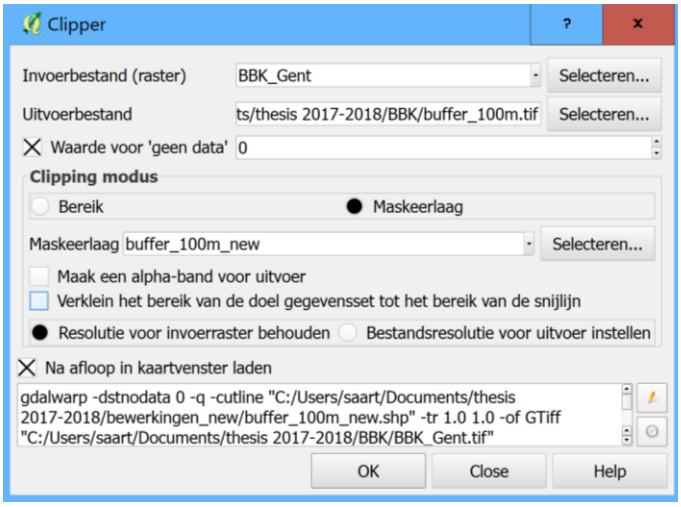

Click on ‘ok’. It might take a while before the task is completed.

Result:

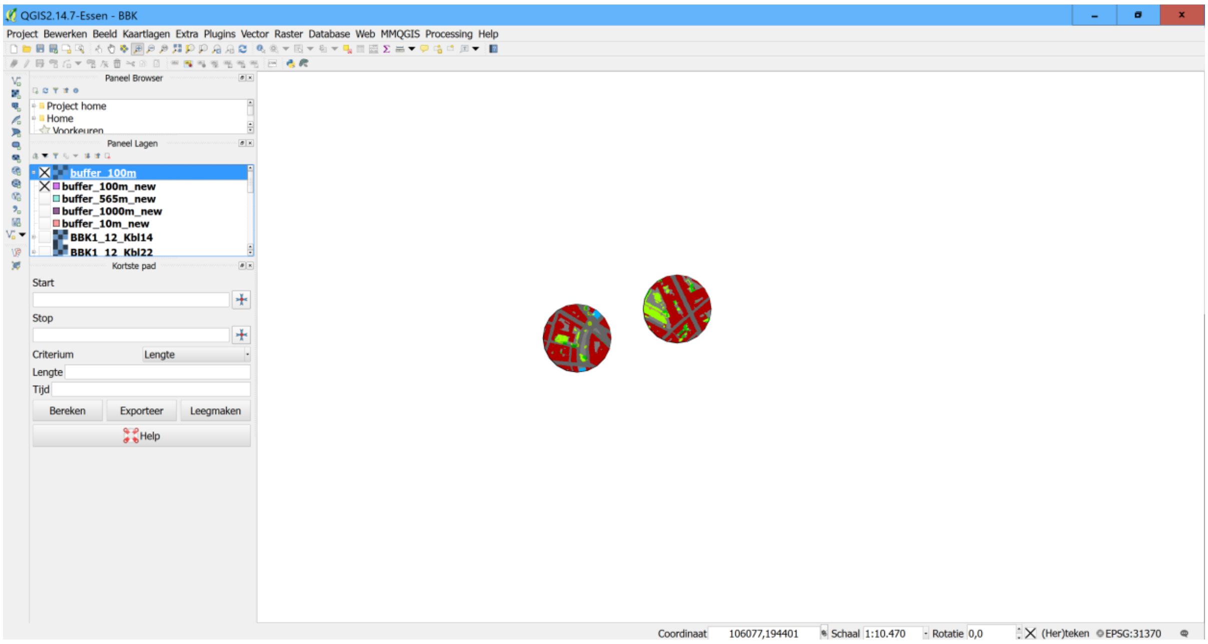

This can be done in a similar way for the layer buffer_10m, since the buffers do not overlap. The buffers that do overlap for the layers with buffer radii of 1000 m and 565 m have to be saved in different layers. Therfore, the layer of the buffer is split in two different layers as explained in the previous section.

Annex II: Ghent_extrac.R – code to extract the forcing data at 4 km resolution for the six MOCCA locations over a period from July till September

```
library(Rfa)

dir_alaro="/mnt/HDS_CLIMATE/CLIMATE/duchenef/GHENT_SUMMER/4km/TEB"
dir_output="/home/hamdi/THESIS_SARA/" #free to put any path

months=c(6:9)
day_month=c(31,28,31,30,31,30,31,31,30,31,30,31)
hours=c(11:35)

dom = attr(FAopen("/mnt/HDS_CLIMATE/CLIMATE/duchenef/GHENT_SUMMER/4km/TEB/20160629/ICMSHBE04+0009"),"domain") #domain

coord_1=lalopoint(dom,lon=3.816,lat=50.980) #------Convert coord to gridpoints (Melle)
coord_2=lalopoint(dom,lon=3.722,lat=51.036) #------Convert coord to gridpoints (Plantentuin)
coord_3=lalopoint(dom,lon=3.728,lat=51.051) #------Convert coord to gridpoints (Provinciehuis)
coord_4=lalopoint(dom,lon=3.732,lat=51.052) #------Convert coord to gridpoints (Sint-bavo)
coord_5=lalopoint(dom,lon=3.749,lat=51.109) #------Convert coord to gridpoints (Honda)
coord_6=lalopoint(dom,lon=3.703,lat=51.084) #------Convert coord to gridpoints (Wondelgem)

cat("",file=paste(dir_output,"Melle.dat",sep="")) #errase file first
cat("",file=paste(dir_output,"Plantentuin.dat",sep="")) #errase file first
cat("",file=paste(dir_output,"Provinciehuis.dat",sep="")) #errase file first
cat("",file=paste(dir_output,"Sint-bavo.dat",sep="")) #errase file first
cat("",file=paste(dir_output,"Honda.dat",sep="")) #errase file first
cat("",file=paste(dir_output,"Wondelgem.dat",sep="")) #errase file first

for (i_month in months)
{
        for (i_day in 1:day_month[i_month])
        {
                for (i_file in hours)
                {
                        check=file.exists(paste(dir_alaro,"/2016",i2a(i_month,2),i2a(i_day,2),"/pfBE04zzzz+00",i2a(i_file,2),sep=""))
                        if (check == TRUE)
                        {
                                cat(sprintf("Date : 2016%s%s h:%s\n...\n",i2a(i_month,2),i2a(i_day,2),i2a(i_file,2)))
                                #reading ICMSH files
                                file=FAopen(paste(dir_alaro,"/2016",i2a(i_month,2),i2a(i_day,2),"/pfBE04zzzz+00",i2a(i_file,2),sep=""))
```

```
t=FAdec(file,"H00050TEMPERATUR")
p=FAdec(file,"H00050PRESSURE")
u=FAdec(file,"H00050WIND.U.PHY")
v=FAdec(file,"H00050WIND.V.PHY")
q=FAdec(file,"H00050HUMI.SPECI")

swdir=FAdec(file,"SURFRAYT DIR SUR")
swtotal=FAdec(file,"SURFRAYT SOLA DE")
lw=FAdec(file,"SURFRAYT THER DE")
precwaterstrat=FAdec(file,"SURFPREC.EAU.GEC")
precwaterconv=FAdec(file,"SURFPREC.EAU.CON")
precsnowstrat=FAdec(file,"SURFPREC.NEI.GEC")
precsnowconv=FAdec(file,"SURFPREC.NEI.CON")


#Writing in files
#Melle
t_station1=t[coord_1$index[1],coord_1$index[2]]
p_station1=p[coord_1$index[1],coord_1$index[2]]
u_station1=u[coord_1$index[1],coord_1$index[2]]
v_station1=v[coord_1$index[1],coord_1$index[2]]
q_station1=q[coord_1$index[1],coord_1$index[2]]

swdir_station1=swdir[coord_1$index[1],coord_1$index[2]]
swtotal_station1=swtotal[coord_1$index[1],coord_1$index[2]]
lw_station1=lw[coord_1$index[1],coord_1$index[2]]
precwaterstrat_station1=precwaterstrat[coord_1$index[1],coord_1$index[2]]
precwaterconv_station1=precwaterconv[coord_1$index[1],coord_1$index[2]]
precsnowstrat_station1=precsnowstrat[coord_1$index[1],coord_1$index[2]]
precsnowconv_station1=precsnowconv[coord_1$index[1],coord_1$index[2]]

cat("2016", i2a(i_month,2), i2a(i_day,2), i2a(i_file,2) ,t_station1, p_station1,

u_station1,v_station1,q_station1,swdir_station1,swtotal_station1,lw_station1,precwaterstrat_station1,precwaterconv_station1,precsnowstrat_station1,precsnowconv_station1,
"\n",file=paste(dir_output,"Melle.dat",sep=""), append=TRUE)
```

```
#Plantentuin
t_station2=t[coord_2$index[1],coord_2$index[2]]
p_station2=p[coord_2$index[1],coord_2$index[2]]
u_station2=u[coord_2$index[1],coord_2$index[2]]
v_station2=v[coord_2$index[1],coord_2$index[2]]
q_station2=q[coord_2$index[1],coord_2$index[2]]

swdir_station2=swdir[coord_2$index[1],coord_2$index[2]]
swtotal_station2=swtotal[coord_2$index[1],coord_2$index[2]]
lw_station2=lw[coord_2$index[1],coord_2$index[2]]
precwaterstrat_station2=precwaterstrat[coord_2$index[1],coord_2$index[2]]
precwaterconv_station2=precwaterconv[coord_2$index[1],coord_2$index[2]]
precsnowstrat_station2=precsnowstrat[coord_2$index[1],coord_2$index[2]]
precsnowconv_station2=precsnowconv[coord_2$index[1],coord_2$index[2]]

cat("2016", i2a(i_month,2), i2a(i_day,2), i2a(i_file,2) ,t_station2, p_station2,

u_station2,v_station2,q_station2,swdir_station2,swtotal_station2,lw_station2,precwaterstrat_station2,precwaterconv_station2,precsnowstrat_station2,precsnowconv_station2,
"\n",file=paste(dir_output,"Plantentium.dat",sep=""), append=TRUE)


#Provinciehuis
t_station3=t[coord_3$index[1],coord_3$index[2]]
p_station3=p[coord_3$index[1],coord_3$index[2]]
u_station3=u[coord_3$index[1],coord_3$index[2]]
v_station3=v[coord_3$index[1],coord_3$index[2]]
q_station3=q[coord_3$index[1],coord_3$index[2]]

swdir_station3=swdir[coord_3$index[1],coord_3$index[2]]
swtotal_station3=swtotal[coord_3$index[1],coord_3$index[2]]
lw_station3=lw[coord_3$index[1],coord_3$index[2]]
precwaterstrat_station3=precwaterstrat[coord_3$index[1],coord_3$index[2]]
precwaterconv_station3=precwaterconv[coord_3$index[1],coord_3$index[2]]
precsnowstrat_station3=precsnowstrat[coord_3$index[1],coord_3$index[2]]
precsnowconv_station3=precsnowconv[coord_3$index[1],coord_3$index[2]]

cat("2016", i2a(i_month,2), i2a(i_day,2), i2a(i_file,2) ,t_station3, p_station3,
```

```
u_station3,v_station3,q_station3,swdir_station3,swtotal_station3,lw_station3,precwaterstrat_station3,precwaterconv_station3,precsnowstrat_station3,precsnowconv_station3,
"\n",file=paste(dir_output,"Provinciehuis.dat",sep=""), append=TRUE)


                                #Sint-bavo
                                t_station4=t[coord_4$index[1],coord_4$index[2]]
                                p_station4=p[coord_4$index[1],coord_4$index[2]]
                                u_station4=u[coord_4$index[1],coord_4$index[2]]
                                v_station4=v[coord_4$index[1],coord_4$index[2]]
                                q_station4=q[coord_4$index[1],coord_4$index[2]]

                                swdir_station4=swdir[coord_4$index[1],coord_4$index[2]]
                                swtotal_station4=swtotal[coord_4$index[1],coord_4$index[2]]
                                lw_station4=lw[coord_4$index[1],coord_4$index[2]]
                                precwaterstrat_station4=precwaterstrat[coord_4$index[1],coord_4$index[2]]
                                precwaterconv_station4=precwaterconv[coord_4$index[1],coord_4$index[2]]
                                precsnowstrat_station4=precsnowstrat[coord_4$index[1],coord_4$index[2]]
                                precsnowconv_station4=precsnowconv[coord_4$index[1],coord_4$index[2]]

                                cat("2016", i2a(i_month,2), i2a(i_day,2), i2a(i_file,2) ,t_station4, p_station4,

u_station4,v_station4,q_station4,swdir_station4,swtotal_station4,lw_station4,precwaterstrat_station4,precwaterconv_station4,precsnowstrat_station4,precsnowconv_station4,
"\n",file=paste(dir_output,"Sint-Bavo.dat",sep=""), append=TRUE)
```

```
#Honda
t_station5=t[coord_5$index[1],coord_5$index[2]]
p_station5=p[coord_5$index[1],coord_5$index[2]]
u_station5=u[coord_5$index[1],coord_5$index[2]]
v_station5=v[coord_5$index[1],coord_5$index[2]]
q_station5=q[coord_5$index[1],coord_5$index[2]]

swdir_station5=swdir[coord_5$index[1],coord_5$index[2]]
swtotal_station5=swtotal[coord_5$index[1],coord_5$index[2]]
lw_station5=lw[coord_5$index[1],coord_5$index[2]]
precwaterstrat_station5=precwaterstrat[coord_5$index[1],coord_5$index[2]]
precwaterconv_station5=precwaterconv[coord_5$index[1],coord_5$index[2]]
precsnowstrat_station5=precsnowstrat[coord_5$index[1],coord_5$index[2]]
precsnowconv_station5=precsnowconv[coord_5$index[1],coord_5$index[2]]

cat("2016", i2a(i_month,2), i2a(i_day,2), i2a(i_file,2) ,t_station5, p_station5,

u_station5,v_station5,q_station5,swdir_station5,swtotal_station5,lw_station5,precwaterstrat_station5,precwaterconv_station5,precsnowstrat_station5,precsnowconv_station5,
"\n",file=paste(dir_output,"Honda.dat",sep=""), append=TRUE)


#Wondelgem
t_station6=t[coord_6$index[1],coord_6$index[2]]
p_station6=p[coord_6$index[1],coord_6$index[2]]
u_station6=u[coord_6$index[1],coord_6$index[2]]
v_station6=v[coord_6$index[1],coord_6$index[2]]
q_station6=q[coord_6$index[1],coord_6$index[2]]

swdir_station6=swdir[coord_6$index[1],coord_6$index[2]]
swtotal_station6=swtotal[coord_6$index[1],coord_6$index[2]]
lw_station6=lw[coord_6$index[1],coord_6$index[2]]
precwaterstrat_station6=precwaterstrat[coord_6$index[1],coord_6$index[2]]
precwaterconv_station6=precwaterconv[coord_6$index[1],coord_6$index[2]]
precsnowstrat_station6=precsnowstrat[coord_6$index[1],coord_6$index[2]]
precsnowconv_station6=precsnowconv[coord_6$index[1],coord_6$index[2]]

cat("2016", i2a(i_month,2), i2a(i_day,2), i2a(i_file,2) ,t_station6, p_station6,

u_station6,v_station6,q_station6,swdir_station6,swtotal_station6,lw_station6,precwaterstrat_station6,precwaterconv_station6,precsnowstrat_station6,precsnowconv_station6,
"\n",file=paste(dir_output,"Wondelgem.dat",sep=""), append=TRUE)

        }
      }
    }
}
```

Annex III: Installation of SURFEX

The following explanation was provided by Dr. Steven Caluwaerts. More information can be found on the SURFEX website (http://www.umr-cnrm.fr/surfex/spip.php?rubrique17, consulted on November 13, 2017) and the user's guide (CNRM, *s.d.*).

1. Install ksh and work on ksh
2. Extract the tar-file
3. Add some lines to the .profile

```
export SURFEX_EXPORT="$HOME/Desktop/SODA_v8_tb"
. $SURFEX_EXPORT/conf/profile_surfex
export LD_LIBRARY_PATH=~/Desktop/SODA_v8_tb/src/LIB/grib_api-1.17.0-Source-LXgfortran/lib

export OMP_NUM_THREADS=1
```

and type on the command line:

export VER_MPI="NOMPI"

4. Run the .profile: . ./.profile
5. Go to the src directory and: ./compile_surfex.sh

Do a test:

1. Export VER_USER=FORC
2. In src: ./configure
3. Execute the file that you get back at the end of the configure:

   . ../conf/profile_surfex-LXgfortran-SFX-V8-0-0-FORC-NOMPI-OMP-O2
4. Sometimes appear some warnings. Follow the suggestions of the warnings and rerun the configure file till there are no remarks anymore.
5. Execute: make user
6. Execute: make installuser
7. Go to MY_RUN/FORCING and run ./prepare_forcing.bash hapex
8. Go to KTEST and run:

   ./pgd.exe

   ./prep.exe and

   ./offline.exe
9. You should have output now

Annex IV: Changing the ECOCLIMAP module

1. Go to the directory of ECOCLIMAP in SURFEX and look what is in this folder with the ls command.

```
satop@xps:~/SODA_v8_tb/MY_RUN$ cd ECOCLIMAP/
satop@xps:~/SODA_v8_tb/MY_RUN/ECOCLIMAP$ ls
a.out                      ecoclimapI_covers_param.bin    ecoclimapII_eu_covers_param.bin  gtopo30.dir        sand_
clay_fao.dir               ecoclimapI_covers_param.dat    ecoclimapII_eu_covers_param.dat  gtopo30.hdr        sand_
clay_fao.hdr               ecoclimapII_af_covers_param.bin  ecoclimats_v2.dir                job_ecoclimap_aix64  write
convert_ecoclimap_param.f90  ecoclimapII_af_covers_param.dat  ecoclimats_v2.hdr              job_ecoclimap_sx8
```

2. Copy the unzipped data folders of ECOCLIMAP-II from the Downloads folder to the ECOCLIMAP folder and check with the ls command if the folders are copied well.

```
satop@xps:~/SODA_v8_tb/MY_RUN/ECOCLIMAP$ cp ../../../Downloads/ECOCLIMAP_II_EUROP_V2.3.dir ECOCLIMAP_II_EUROP_V2.3.dir
satop@xps:~/SODA_v8_tb/MY_RUN/ECOCLIMAP$ cp ../../../Downloads/ECOCLIMAP_II_EUROP_V2.3.hdr ECOCLIMAP_II_EUROP_V2.3.hdr
satop@xps:~/SODA_v8_tb/MY_RUN/ECOCLIMAP$ ls
a.out                      ecoclimapI_covers_param.bin    ecoclimapII_eu_covers_param.bin  ecoclimats_v2.dir  job_ecc
clay_fao.dir               ecoclimapI_covers_param.dat    ecoclimapII_eu_covers_param.dat  ecoclimats_v2.hdr  job_ecc
clay_fao.hdr               ecoclimapII_af_covers_param.bin  ECOCLIMAP_II_EUROP_V2.3.dir    gtopo30.dir        sand_fa
convert_ecoclimap_param.f90  ecoclimapII_af_covers_param.dat  ECOCLIMAP_II_EUROP_V2.3.hdr  gtopo30.hdr        sand_fa
```

3. To save some memory the downloaded files in the Downloads directory can be removed.

```
satop@xps:~/SODA_v8_tb/MY_RUN/ECOCLIMAP$ cd ..
satop@xps:~/SODA_v8_tb/MY_RUN$ cd ..
satop@xps:~/SODA_v8_tb$ cd ..
satop@xps:~$ cd Downloads/
satop@xps:~/Downloads$ ls
ECOCLIMAP_II_EUROP_V2.3.dir     ECOCLIMAP_II_EUROP_V2.3.hdr     Honda.dat  MTO_CNRM_archive.zip  Plantentium.dat     Sint-
ECOCLIMAP_II_EUROP_V2.3.dir.gz  ECOCLIMAP_II_EUROP_V2.3.hdr.gz  Melle.dat  OPTIONS.nam           Provinciehuis.dat   SODA_
satop@xps:~/Downloads$ rm ECOCLIMAP_II_EUROP_V2.3.dir
satop@xps:~/Downloads$ ls
ECOCLIMAP_II_EUROP_V2.3.dir.gz  ECOCLIMAP_II_EUROP_V2.3.hdr.gz  Melle.dat             OPTIONS.nam      Provinciehuis.dat
ECOCLIMAP_II_EUROP_V2.3.hdr     Honda.dat                       MTO_CNRM_archive.zip  Plantentium.dat  Sint-Bavo.dat
satop@xps:~/Downloads$ rm ECOCLIMAP_II_EUROP_V2.3.hdr
satop@xps:~/Downloads$ ls
ECOCLIMAP_II_EUROP_V2.3.dir.gz  Honda.dat  MTO_CNRM_archive.zip  Plantentium.dat     Sint-Bavo.dat    THESIS_SARA      Wond
ECOCLIMAP_II_EUROP_V2.3.hdr.gz  Melle.dat  OPTIONS.nam           Provinciehuis.dat   SODA_v8_tb.tgz   THESIS_SARA.zip
```

4. Go to the folder KTEST of the station were the ECOCLIMAP-I module has to be changed in ECOCLIMAP-II and replace the links of ECOCLIMAP-I with those of ECOCLIMAP-II.

```
satop@xps:~/Downloads$ cd ..
satop@xps:~$ cd SODA_v8_tb/MY_RUN/KTEST/
satop@xps:~/SODA_v8_tb/MY_RUN/KTEST$ ls
1D_test_case  bavo1.zip  melle       melle1v3.zip  plantentuin       provincie         provincie1v1.zip  wondelgem         wondelgem (c
bavo          hapex      melle1v1.zip  melle1v4.zip  plantentuin1v1.zip  provincie1     provincie1.zip    wondelgem1v1.zip
bavo1v1.zip   honda      melle1v2.zip  melle1.zip    plantentuin1.zip  provincie1_1.zip  Sodankyla       wondelgem1.zip
```

```
satop@xps:~/SODA_v8_tb/MY_RUN/KTEST/wondelgem$ ls
ASN_RD.TXT                       Forc_SCA_SW.txt  H.TXT               log0                      RN.TXT          SAG_VEG9.TXT      TROAD5.TXT
ASN_RF.TXT                       Forc_SNOW.txt    HU2M_ISBA.TXT       MER10M_ISBA.TXT           RSN_RD1.TXT     sand_fao.dir      TROOF1.TXT
ASN_VEG.TXT                      Forc_TA.txt      HU2MMAX_ISBA.TXT    MER10M_TEB.TXT            RSN_RF1.TXT     sand_fao.hdr      TROOF2.TXT
class_cover_data.tex             Forc_WIND.txt    HU2MMAX_TEB.TXT     MER10M.TXT                RSN_VEG10.TXT   SFCO2_ISBA.TXT    TROOF3.TXT
clay_fao.dir                     FRAC_NATURE.TXT  HU2MMAX.TXT         offline.exe               RSN_VEG11.TXT   SFCO2_TEB.TXT     TROOF4.TXT
clay_fao.hdr                     FRAC_SEA.TXT     HU2MMIN_ISBA.TXT    OPTIONS.nam               RSN_VEG12.TXT   SFCO2.TXT         TROOF5.TXT
DRAIN_ISBA.TXT                   FRAC_TOWN.TXT    HU2MMIN_TEB.TXT     OPTIONS.nam_save.3330     RSN_VEG1.TXT    SNDRIF_ISBA.TXT   TSN_RD1.TXT
ecoclimapI_covers_param.bin      FRAC_WATER.TXT   HU2MMIN.TXT         OPTIONS.nam_save.3392     RSN_VEG2.TXT    SNOMLT_ISBA.TXT   TSN_RF1.TXT
ecoclimapII_eu_covers_param.bin  GFLUX_ISBA.TXT   HU2M_TEB.TXT        OPTIONS.nam_save.3465     RSN_VEG3.TXT    SUBL_ISBA.TXT     TSRAD_NAT.TXT
ecoclimats_v2.dir                GFLUX_TEB.TXT    HU2M.TXT            OPTIONS.nam_save.3535     RSN_VEG4.TXT    SUBL.TXT          TSRAD.TXT
ecoclimats_v2.hdr                GFLUX.TXT        LAI.TXT             OPTIONS.nam_save.3711     RSN_VEG5.TXT    T2M_ISBA.TXT      TS.TXT
EMIS_ISBA.TXT                    gtopo30.dir      LEGI_ISBA.TXT       OPTIONS.nam_save.3751     RSN_VEG6.TXT    T2MMAX_ISBA.TXT   TWALL1.TXT
EMIS.TXT                         gtopo30.hdr      LEG_ISBA.TXT        OPTIONS.nam_save.3793     RSN_VEG7.TXT    T2MMAX_TEB.TXT    TWALL2.TXT
EVAP_ISBA.TXT                    H_ISBA.TXT       LEI_ISBA.TXT        OPTIONS.nam_save.3836     RSN_VEG8.TXT    T2MMAX.TXT        TWALL3.TXT
EVAP.TXT                         HSN_VEG10.TXT    LE_ISBA.TXT         OPTIONS.nam_save.4053     RSN_VEG9.TXT    T2MMIN_ISBA.TXT   TWALL4.TXT
FMUNOSSO.TXT                     HSN_VEG11.TXT    LEI.TXT             OPTIONS.nam_save.5395     RUNOFF_ISBA.TXT T2MMIN_TEB.TXT    TWALL5.TXT
FMU.TXT                          HSN_VEG12.TXT    LER_ISBA.TXT        Params_config.txt         SAG_VEG10.TXT   T2MMIN.TXT        T_WIN1.TXT
FMVNOSSO.TXT                     HSN_VEG1.TXT     LES_ISBA.TXT        PATCH.TXT                 SAG_VEG11.TXT   T2M_TEB.TXT       VEG.TXT
FMV.TXT                          HSN_VEG2.TXT     LESL_ISBA.TXT       pgd.exe                   SAG_VEG12.TXT   T2M.TXT           W10M_ISBA.TXT
Forc_CO2.txt                     HSN_VEG3.TXT     LE_TEB.TXT          PGD.txt                   SAG_VEG1.TXT    TCANYON.TXT       W10MMAX_ISBA.
Forc_DIR_SW.txt                  HSN_VEG4.TXT     LETR_ISBA.TXT       prep.exe                  SAG_VEG2.TXT    TG1.TXT           W10MMAX_TEB.T
Forc_DIR.txt                     HSN_VEG5.TXT     LE.TXT              PREP.txt                  SAG_VEG3.TXT    TG2.TXT           W10MMAX.TXT
FORCING.nc                       HSN_VEG6.TXT     LEV_ISBA.TXT        Q2M.TXT                   SAG_VEG4.TXT    TI_BLD.TXT        W10M_TEB.TXT
Forc_LW.txt                      HSN_VEG7.TXT     LISTING_FORCING.txt QCANYON.TXT               SAG_VEG5.TXT    TROAD1.TXT        W10M.TXT
Forc_PS.txt                      HSN_VEG8.TXT     LISTING_OFFLINE0.txt RI.TXT                   SAG_VEG6.TXT    TROAD2.TXT        WG1.TXT
Forc_QA.txt                      HSN_VEG9.TXT     LISTING_PGD.txt     RN_ISBA.TXT               SAG_VEG7.TXT    TROAD3.TXT        WG2.TXT
Forc_RAIN.txt                    H_TEB.TXT        LISTING_PREP.txt    RN_TEB.TXT                SAG_VEG8.TXT    TROAD4.TXT        WGI1.TXT
```

```
satop@xps:~/SODA_v8_tb/MY_RUN/KTEST/wondelgem$ rm ecoclimats_v2.dir
satop@xps:~/SODA_v8_tb/MY_RUN/KTEST/wondelgem$ ls
ASN_RD.TXT                        Forc_SNOW.txt     HU2M_ISBA.TXT       MER10M_ISBA.TXT          RSN_RD1.TXT       sand_fao.dir      TROOF1.TXT
ASN_RF.TXT                        Forc_TA.txt       HU2MMAX_ISBA.TXT    MER10M_TEB.TXT           RSN_RF1.TXT       sand_fao.hdr      TROOF2.TXT
ASN_VEG.TXT                       Forc_WIND.txt     HU2MMAX_TEB.TXT     MER10M.TXT               RSN_VEG10.TXT     SFCO2_ISBA.TXT    TROOF3.TXT
class_cover_data.tex              FRAC_NATURE.TXT   HU2MMAX.TXT         offline.exe              RSN_VEG11.TXT     SFCO2_TEB.TXT     TROOF4.TXT
clay_fao.dir                      FRAC_SEA.TXT      HU2MMIN_ISBA.TXT    OPTIONS.nam              RSN_VEG12.TXT     SFCO2.TXT         TROOF5.TXT
clay_fao.hdr                      FRAC_TOWN.TXT     HU2MMIN_TEB.TXT     OPTIONS.nam_save.3330    RSN_VEG1.TXT      SNDRIF_ISBA.TXT   TSN_RD1.TXT
DRAIN_ISBA.TXT                    FRAC_WATER.TXT    HU2MMIN.TXT         OPTIONS.nam_save.3392    RSN_VEG2.TXT      SNOMLT_ISBA.TXT   TSN_RF1.TXT
ecoclimapI_covers_param.bin       GFLUX_ISBA.TXT    HU2M_TEB.TXT        OPTIONS.nam_save.3465    RSN_VEG3.TXT      SUBL_ISBA.TXT     TSRAD_NAT.TXT
ecoclimapII_eu_covers_param.bin   GFLUX_TEB.TXT     HU2M.TXT            OPTIONS.nam_save.3535    RSN_VEG4.TXT      SUBL.TXT          TSRAD.TXT
ecoclimats_v2.hdr                 GFLUX.TXT         LAI.TXT             OPTIONS.nam_save.3711    RSN_VEG5.TXT      T2M_ISBA.TXT      TS.TXT
EMIS_ISBA.TXT                     gtopo30.dir       LEGI_ISBA.TXT       OPTIONS.nam_save.3751    RSN_VEG6.TXT      T2MMAX_ISBA.TXT   TWALL1.TXT
EMIS.TXT                          gtopo30.hdr       LEG_ISBA.TXT        OPTIONS.nam_save.3793    RSN_VEG7.TXT      T2MMAX_TEB.TXT    TWALL2.TXT
EVAP_ISBA.TXT                     H_ISBA.TXT        LEI_ISBA.TXT        OPTIONS.nam_save.3836    RSN_VEG8.TXT      T2MMAX.TXT        TWALL3.TXT
EVAP.TXT                          HSN_VEG10.TXT     LE_ISBA.TXT         OPTIONS.nam_save.4053    RSN_VEG9.TXT      T2MMIN_ISBA.TXT   TWALL4.TXT
FMUNOSSO.TXT                      HSN_VEG11.TXT     LEI.TXT             OPTIONS.nam_save.5395    RUNOFF_ISBA.TXT   T2MMIN_TEB.TXT    TWALL5.TXT
FMU.TXT                           HSN_VEG12.TXT     LER_ISBA.TXT        Params_config.txt        SAG_VEG10.TXT     T2MMIN.TXT        T_WIN1.TXT
FMVNOSSO.TXT                      HSN_VEG1.TXT      LES_ISBA.TXT        PATCH.TXT                SAG_VEG11.TXT     T2M_TEB.TXT       VEG.TXT
FMV.TXT                           HSN_VEG2.TXT      LESL_ISBA.TXT       pgd.exe                  SAG_VEG12.TXT     T2M.TXT           W10M_ISBA.TXT
Forc_CO2.txt                      HSN_VEG3.TXT      LE_TEB.TXT          PGD.txt                  SAG_VEG1.TXT      TCANYON.TXT       W10MMAX_ISBA.
Forc_DIR_SW.txt                   HSN_VEG4.TXT      LETR_ISBA.TXT       prep.exe                 SAG_VEG2.TXT      TG1.TXT           W10MMAX_TEB.T
Forc_DIR.txt                      HSN_VEG5.TXT      LE.TXT              PREP.txt                 SAG_VEG3.TXT      TG2.TXT           W10MMAX.TXT
FORCING.nc                        HSN_VEG6.TXT      LEV_ISBA.TXT        Q2M.TXT                  SAG_VEG4.TXT      TI_BLD.TXT        W10M_TEB.TXT
Forc_LW.txt                       HSN_VEG7.TXT      LISTING_FORCING.txt QCANYON.TXT              SAG_VEG5.TXT      TROAD1.TXT        W10M.TXT
Forc_PS.txt                       HSN_VEG8.TXT      LISTING_OFFLINE0.txt RI.TXT                  SAG_VEG6.TXT      TROAD2.TXT        WG1.TXT
Forc_QA.txt                       HSN_VEG9.TXT      LISTING_PGD.txt     RN_ISBA.TXT              SAG_VEG7.TXT      TROAD3.TXT        WG2.TXT
Forc_RAIN.txt                     H_TEB.TXT         LISTING_PREP.txt    RN_TEB.TXT               SAG_VEG8.TXT      TROAD4.TXT        WGI1.TXT
Forc_SCA_SW.txt                   H.TXT             log0                RN.TXT                   SAG_VEG9.TXT      TROAD5.TXT        WGI2.TXT
```

```
satop@xps:~/SODA_v8_tb/MY_RUN/KTEST/wondelgem$ rm ecoclimats_v2.hdr
satop@xps:~/SODA_v8_tb/MY_RUN/KTEST/wondelgem$ ls
ASN_RD.TXT                        Forc_SNOW.txt     H.TXT               LISTING_PREP.txt         RN_ISBA.TXT       SAG_VEG6.TXT      TROAD1.TXT
ASN_RF.TXT                        Forc_TA.txt       HU2M_ISBA.TXT       log0                     RN_TEB.TXT        SAG_VEG7.TXT      TROAD2.TXT
ASN_VEG.TXT                       Forc_WIND.txt     HU2MMAX_ISBA.TXT    MER10M_ISBA.TXT          RN.TXT            SAG_VEG8.TXT      TROAD3.TXT
class_cover_data.tex              FRAC_NATURE.TXT   HU2MMAX_TEB.TXT     MER10M_TEB.TXT           RSN_RD1.TXT       SAG_VEG9.TXT      TROAD4.TXT
clay_fao.dir                      FRAC_SEA.TXT      HU2MMAX.TXT         MER10M.TXT               RSN_RF1.TXT       sand_fao.dir      TROAD5.TXT
clay_fao.hdr                      FRAC_TOWN.TXT     HU2MMIN_ISBA.TXT    offline.exe              RSN_VEG10.TXT     sand_fao.hdr      TROOF1.TXT
DRAIN_ISBA.TXT                    FRAC_WATER.TXT    HU2MMIN_TEB.TXT     OPTIONS.nam              RSN_VEG11.TXT     SFCO2_ISBA.TXT    TROOF2.TXT
ecoclimapI_covers_param.bin       GFLUX_ISBA.TXT    HU2MMIN.TXT         OPTIONS.nam_save.3330    RSN_VEG12.TXT     SFCO2_TEB.TXT     TROOF3.TXT
ecoclimapII_eu_covers_param.bin   GFLUX_TEB.TXT     HU2M_TEB.TXT        OPTIONS.nam_save.3392    RSN_VEG1.TXT      SFCO2.TXT         TROOF4.TXT
EMIS_ISBA.TXT                     GFLUX.TXT         HU2M.TXT            OPTIONS.nam_save.3465    RSN_VEG2.TXT      SNDRIF_ISBA.TXT   TROOF5.TXT
EMIS.TXT                          gtopo30.dir       LAI.TXT             OPTIONS.nam_save.3535    RSN_VEG3.TXT      SNOMLT_ISBA.TXT   TSN_RD1.TXT
EVAP_ISBA.TXT                     gtopo30.hdr       LEGI_ISBA.TXT       OPTIONS.nam_save.3711    RSN_VEG4.TXT      SUBL_ISBA.TXT     TSN_RF1.TXT
EVAP.TXT                          H_ISBA.TXT        LEG_ISBA.TXT        OPTIONS.nam_save.3751    RSN_VEG5.TXT      SUBL.TXT          TSRAD_NAT.TXT
FMUNOSSO.TXT                      HSN_VEG10.TXT     LEI_ISBA.TXT        OPTIONS.nam_save.3793    RSN_VEG6.TXT      T2M_ISBA.TXT      TSRAD.TXT
FMU.TXT                           HSN_VEG11.TXT     LE_ISBA.TXT         OPTIONS.nam_save.3836    RSN_VEG7.TXT      T2MMAX_ISBA.TXT   TS.TXT
FMVNOSSO.TXT                      HSN_VEG12.TXT     LEI.TXT             OPTIONS.nam_save.4053    RSN_VEG8.TXT      T2MMAX_TEB.TXT    TWALL1.TXT
FMV.TXT                           HSN_VEG1.TXT      LER_ISBA.TXT        OPTIONS.nam_save.5395    RSN_VEG9.TXT      T2MMAX.TXT        TWALL2.TXT
Forc_CO2.txt                      HSN_VEG2.TXT      LES_ISBA.TXT        Params_config.txt        RUNOFF_ISBA.TXT   T2MMIN_ISBA.TXT   TWALL3.TXT
Forc_DIR_SW.txt                   HSN_VEG3.TXT      LESL_ISBA.TXT       PATCH.TXT                SAG_VEG10.TXT     T2MMIN_TEB.TXT    TWALL4.TXT
Forc_DIR.txt                      HSN_VEG4.TXT      LE_TEB.TXT          pgd.exe                  SAG_VEG11.TXT     T2MMIN.TXT        TWALL5.TXT
FORCING.nc                        HSN_VEG5.TXT      LETR_ISBA.TXT       PGD.txt                  SAG_VEG12.TXT     T2M_TEB.TXT       T_WIN1.TXT
Forc_LW.txt                       HSN_VEG6.TXT      LE.TXT              prep.exe                 SAG_VEG1.TXT      T2M.TXT           VEG.TXT
Forc_PS.txt                       HSN_VEG7.TXT      LEV_ISBA.TXT        PREP.txt                 SAG_VEG2.TXT      TCANYON.TXT       W10M_ISBA.TXT
Forc_QA.txt                       HSN_VEG8.TXT      LISTING_FORCING.txt Q2M.TXT                  SAG_VEG3.TXT      TG1.TXT           W10MMAX_ISBA.
Forc_RAIN.txt                     HSN_VEG9.TXT      LISTING_OFFLINE0.txt QCANYON.TXT             SAG_VEG4.TXT      TG2.TXT           W10MMAX_TEB.T
Forc_SCA_SW.txt                   H_TEB.TXT         LISTING_PGD.txt     RI.TXT                   SAG_VEG5.TXT      TI_BLD.TXT        W10MMAX.TXT
satop@xps:~/SODA_v8_tb/MY_RUN/KTEST/wondelgem$ ln -s ../../ECOCLIMAP/ECOCLIMAP_II_EUROP_V2.3.dir ECOCLIMAP_II_EUROP_V2.3.dir
satop@xps:~/SODA_v8_tb/MY_RUN/KTEST/wondelgem$ ln -s ../../ECOCLIMAP/ECOCLIMAP_II_EUROP_V2.3.hdr ECOCLIMAP_II_EUROP_V2.3.hdr
```

```
satop@xps:~/SODA_v8_tb/MY_RUN/KTEST/wondelgem$ ls
ASN_RD.TXT                        Forc_SCA_SW.txt   H.TXT               log0                     RN.TXT            SAG_VEG9.TXT      TROAD5.TXT
ASN_RF.TXT                        Forc_SNOW.txt     HU2M_ISBA.TXT       MER10M_ISBA.TXT          RSN_RD1.TXT       sand_fao.dir      TROOF1.TXT
ASN_VEG.TXT                       Forc_TA.txt       HU2MMAX_ISBA.TXT    MER10M_TEB.TXT           RSN_RF1.TXT       sand_fao.hdr      TROOF2.TXT
class_cover_data.tex              Forc_WIND.txt     HU2MMAX_TEB.TXT     MER10M.TXT               RSN_VEG10.TXT     SFCO2_ISBA.TXT    TROOF3.TXT
clay_fao.dir                      FRAC_NATURE.TXT   HU2MMAX.TXT         offline.exe              RSN_VEG11.TXT     SFCO2_TEB.TXT     TROOF4.TXT
clay_fao.hdr                      FRAC_SEA.TXT      HU2MMIN_ISBA.TXT    OPTIONS.nam              RSN_VEG12.TXT     SFCO2.TXT         TROOF5.TXT
DRAIN_ISBA.TXT                    FRAC_TOWN.TXT     HU2MMIN_TEB.TXT     OPTIONS.nam_save.3330    RSN_VEG1.TXT      SNDRIF_ISBA.TXT   TSN_RD1.TXT
ecoclimapI_covers_param.bin       FRAC_WATER.TXT    HU2MMIN.TXT         OPTIONS.nam_save.3392    RSN_VEG2.TXT      SNOMLT_ISBA.TXT   TSN_RF1.TXT
ecoclimapII_eu_covers_param.bin   GFLUX_ISBA.TXT    HU2M_TEB.TXT        OPTIONS.nam_save.3465    RSN_VEG3.TXT      SUBL_ISBA.TXT     TSRAD_NAT.TXT
ECOCLIMAP_II_EUROP_V2.3.dir       GFLUX_TEB.TXT     HU2M.TXT            OPTIONS.nam_save.3535    RSN_VEG4.TXT      SUBL.TXT          TSRAD.TXT
ECOCLIMAP_II_EUROP_V2.3.hdr       GFLUX.TXT         LAI.TXT             OPTIONS.nam_save.3711    RSN_VEG5.TXT      T2M_ISBA.TXT      TS.TXT
EMIS_ISBA.TXT                     gtopo30.dir       LEGI_ISBA.TXT       OPTIONS.nam_save.3751    RSN_VEG6.TXT      T2MMAX_ISBA.TXT   TWALL1.TXT
EMIS.TXT                          gtopo30.hdr       LEG_ISBA.TXT        OPTIONS.nam_save.3793    RSN_VEG7.TXT      T2MMAX_TEB.TXT    TWALL2.TXT
EVAP_ISBA.TXT                     H_ISBA.TXT        LEI_ISBA.TXT        OPTIONS.nam_save.3836    RSN_VEG8.TXT      T2MMAX.TXT        TWALL3.TXT
EVAP.TXT                          HSN_VEG10.TXT     LE_ISBA.TXT         OPTIONS.nam_save.4053    RSN_VEG9.TXT      T2MMIN_ISBA.TXT   TWALL4.TXT
FMUNOSSO.TXT                      HSN_VEG11.TXT     LEI.TXT             OPTIONS.nam_save.5395    RUNOFF_ISBA.TXT   T2MMIN_TEB.TXT    TWALL5.TXT
FMU.TXT                           HSN_VEG12.TXT     LER_ISBA.TXT        Params_config.txt        SAG_VEG10.TXT     T2MMIN.TXT        T_WIN1.TXT
FMVNOSSO.TXT                      HSN_VEG1.TXT      LES_ISBA.TXT        PATCH.TXT                SAG_VEG11.TXT     T2M_TEB.TXT       VEG.TXT
FMV.TXT                           HSN_VEG2.TXT      LESL_ISBA.TXT       pgd.exe                  SAG_VEG12.TXT     T2M.TXT           W10M_ISBA.TXT
Forc_CO2.txt                      HSN_VEG3.TXT      LE_TEB.TXT          PGD.txt                  SAG_VEG1.TXT      TCANYON.TXT       W10MMAX_ISBA.
Forc_DIR_SW.txt                   HSN_VEG4.TXT      LETR_ISBA.TXT       prep.exe                 SAG_VEG2.TXT      TG1.TXT           W10MMAX_TEB.T
Forc_DIR.txt                      HSN_VEG5.TXT      LE.TXT              PREP.txt                 SAG_VEG3.TXT      TG2.TXT           W10MMAX.TXT
FORCING.nc                        HSN_VEG6.TXT      LEV_ISBA.TXT        Q2M.TXT                  SAG_VEG4.TXT      TI_BLD.TXT        W10M_TEB.TXT
Forc_LW.txt                       HSN_VEG7.TXT      LISTING_FORCING.txt QCANYON.TXT              SAG_VEG5.TXT      TROAD1.TXT        W10M.TXT
Forc_PS.txt                       HSN_VEG8.TXT      LISTING_OFFLINE0.txt RI.TXT                  SAG_VEG6.TXT      TROAD2.TXT        WG1.TXT
Forc_QA.txt                       HSN_VEG9.TXT      LISTING_PGD.txt     RN_ISBA.TXT              SAG_VEG7.TXT      TROAD3.TXT        WG2.TXT
Forc_RAIN.txt                     H_TEB.TXT         LISTING_PREP.txt    RN_TEB.TXT               SAG_VEG8.TXT      TROAD4.TXT        WGI1.TXT
```

5. Change OPTIONS.nam

```
satop@xps:~/SODA_v8_tb/MY_RUN/KTEST/wondelgem$ gedit OPTIONS.nam
&NAM_FRAC               LECOCLIMAP = T,
/
&NAM_PGD_ARRANGE_COVER
                        LTOWN_TO_ROCK=.FALSE.
/
&NAM_COVER              YCOVER     = 'ECOCLIMAP_II_EUROP_V2.3',
                        YCOVERFILETYPE = 'DIRECT'
/
&NAM_PGD_GRID           CGRID = 'LONLAT REG'
/
&NAM_LONLAT_REG         XLONMIN = 3.699       ,
                        XLONMAX = 3.707        ,
                        XLATMIN = 51.080       ,
                        XLATMAX = 51.088       ,
                        NLON    = 1          ,
                        NLAT    = 1
 ,
```

Change the name to the filename of ECOCLMAP-II

6. Run pgd.exe, prep.exe and offline.exe

```
satop@xps:~/SODA_v8_tb/MY_RUN/KTEST/wondelgem$ ./pgd.exe

     ----------------------
     | PGD ENDS CORRECTLY |
     ----------------------
satop@xps:~/SODA_v8_tb/MY_RUN/KTEST/wondelgem$ ./prep.exe

     -----------------------
     | PREP ENDS CORRECTLY |
     -----------------------
satop@xps:~/SODA_v8_tb/MY_RUN/KTEST/wondelgem$ ./offline.exe
 CAUTION: DID YOU THINK TO SET OMP_NUM_THREADS=1?
 PLEASE VERIFY OMP_NUM_THREADS IS INITIALIZED : TYPE ECHO $OMP_NUM_THREADS IN A TERMINAL
SFX  DAY :     1 /    57
SFX  DAY :     2 /    57
SFX  DAY :     3 /    57
SFX  DAY :     4 /    57
SFX  DAY :     5 /    57
SFX  DAY :     6 /    57
SFX  DAY :     7 /    57
SFX  DAY :     8 /    57
SFX  DAY :     9 /    57
SFX  DAY :    10 /    57
SFX  DAY :    11 /    57
SFX  DAY :    12 /    57
SFX  DAY :    13 /    57
SFX  DAY :    14 /    57
SFX  DAY :    15 /    57
SFX  DAY :    16 /    57
SFX  DAY :    17 /    57
SFX  DAY :    18 /    57
SFX  DAY :    19 /    57
SFX  DAY :    20 /    57
SFX  DAY :    21 /    57
SFX  DAY :    22 /    57
SFX  DAY :    23 /    57
SFX  DAY :    24 /    57
SFX  DAY :    25 /    57
SFX  DAY :    26 /    57
SFX  DAY :    27 /    57
SFX  DAY :    28 /    57
```

```
SFX  DAY :    50 /    57
SFX  DAY :    51 /    57
SFX  DAY :    52 /    57
SFX  DAY :    53 /    57
SFX  DAY :    54 /    57
SFX  DAY :    55 /    57
SFX  DAY :    56 /    57
SFX  DAY :    57 /    57

     --------------------------
     | OFFLINE ENDS CORRECTLY |
     --------------------------

satop@xps:~/SODA_v8_tb/MY_RUN/KTEST/wondelgem$
```

Annex V: OPTIONS.nam code

Standard setting of the OPTIONS.nam file when SURFEX is downloaded:

```
&NAM_DATA_ISBA          NTIME = 12 ,
                        XUNIF_VEGTYPE(1)     = 0.,
                        XUNIF_VEGTYPE(2)     = 0.,
                        XUNIF_VEGTYPE(3)     = 0.,
                        XUNIF_VEGTYPE(4)     = 0.,
                        XUNIF_VEGTYPE(5)     = 0.,
                        XUNIF_VEGTYPE(6)     = 0.,
                        XUNIF_VEGTYPE(7)     = 1.,
                        XUNIF_VEGTYPE(8)     = 0.,
                        XUNIF_VEGTYPE(9)     = 0.,
                        XUNIF_VEGTYPE(10)    = 0.,
                        XUNIF_VEGTYPE(11)    = 0.,
                        XUNIF_VEGTYPE(12)    = 0.,
                        XUNIF_VEGTYPE(13)    = 0.,
                        XUNIF_VEGTYPE(14)    = 0.,
                        XUNIF_VEGTYPE(15)    = 0.,
                        XUNIF_VEGTYPE(16)    = 0.,
                        XUNIF_VEGTYPE(17)    = 0.,
                        XUNIF_VEGTYPE(18)    = 0.,
                        XUNIF_VEGTYPE(19)    = 0.,
                        XUNIF_VEG(1,1)       = 0.,
                        XUNIF_VEG(1,2)       = 0.,
                        XUNIF_VEG(1,3)       = 0.,
                        XUNIF_VEG(1,4)       = 0.,
                        XUNIF_VEG(1,5)       = 0.5,
                        XUNIF_VEG(1,6)       = 0.9,
                        XUNIF_VEG(1,7)       = 0.9,
                        XUNIF_VEG(1,8)       = 0.9,
                        XUNIF_VEG(1,9)       = 0.9,
                        XUNIF_VEG(1,10)      = 0.,
                        XUNIF_VEG(1,11)      = 0.,
                        XUNIF_VEG(1,12)      = 0.,
                        XUNIF_LAI(1,1)       = 0.,
                        XUNIF_LAI(1,2)       = 0.,
                        XUNIF_LAI(1,3)       = 0.,
                        XUNIF_LAI(1,4)       = 0.,
                        XUNIF_LAI(1,5)       = 1.,
                        XUNIF_LAI(1,6)       = 3.,
                        XUNIF_LAI(1,7)       = 3.,
                        XUNIF_LAI(1,8)       = 3.,
                        XUNIF_LAI(1,9)       = 3.,
                        XUNIF_LAI(1,10)      = 0.,
                        XUNIF_LAI(1,11)      = 0.,
                        XUNIF_LAI(1,12)      = 0.,
                        XUNIF_Z0(1,1)        = 0.01,
                        XUNIF_Z0(1,2)        = 0.01,
                        XUNIF_Z0(1,3)        = 0.01,
                        XUNIF_Z0(1,4)        = 0.01,
                        XUNIF_Z0(1,5)        = 0.05,
                        XUNIF_Z0(1,6)        = 0.15,
                        XUNIF_Z0(1,7)        = 0.15,
                        XUNIF_Z0(1,8)        = 0.15,
                        XUNIF_Z0(1,9)        = 0.15,
                        XUNIF_Z0(1,10)       = 0.01,
                        XUNIF_Z0(1,11)       = 0.01,
                        XUNIF_Z0(1,12)       = 0.01,
                        XUNIF_EMIS(1,1)      = 0.98,
                        XUNIF_EMIS(1,2)      = 0.98,
                        XUNIF_EMIS(1,3)      = 0.98,
                        XUNIF_EMIS(1,4)      = 0.98,
                        XUNIF_EMIS(1,5)      = 0.98,
                        XUNIF_EMIS(1,6)      = 0.98,
                        XUNIF_EMIS(1,7)      = 0.98,
                        XUNIF_EMIS(1,8)      = 0.98,
                        XUNIF_EMIS(1,9)      = 0.98,
                        XUNIF_EMIS(1,10)     = 0.98,
                        XUNIF_EMIS(1,11)     = 0.98,
                        XUNIF_EMIS(1,12)     = 0.98,
                        XUNIF_DG(1,1)        = 0.01,
                        XUNIF_DG(1,2)        = 1.60,
                        XUNIF_DG(1,3)        = 1.60,
                        XUNIF_ROOTFRAC(1,1)  = -999.,
                        XUNIF_ROOTFRAC(1,2)  = -999.,
                        XUNIF_ROOTFRAC(1,3)  = -999.,
                        XUNIF_RSMIN(1)       = 40.,
                        XUNIF_GAMMA(1)       = 0.,
```

```
                       XUNIF_WRMAX_CF(1)    = 0.2,
                       XUNIF_RGL(1)         = 100.,
                       XUNIF_CV(1)          = 0.00002,
                       XUNIF_Z0_O_Z0H(1)    = 10.,
                       XUNIF_ALBNIR_VEG(1)  = 0.3,
                       XUNIF_ALBVIS_VEG(1)  = 0.1,
                       XUNIF_ALBUV_VEG(1)   = 0.0425,
                       XUNIF_ALBNIR_SOIL(1) = 0.3,
                       XUNIF_ALBVIS_SOIL(1) = 0.1,
                       XUNIF_ALBUV_SOIL(1)  = 0.06,
                       XUNIF_GMES(1)        = 0.003,
                       XUNIF_RE25(1)        = 0.0000003,
                       XUNIF_BSLAI(1)       = 0.06,
                       XUNIF_LAIMIN(1)      = 0.3,
                       XUNIF_SEFOLD(1)      = 5184000.,
                       XUNIF_GC(1)          = 0.00025,
                       XUNIF_DMAX(1)        = 0.1,
                       XUNIF_F2I(1)         = 0.3,
                       XUNIF_H_TREE(1)      = 20.,
                       XUNIF_CE_NITRO(1)    = 3.79,
                       XUNIF_CF_NITRO(1)    = 9.84,
                       XUNIF_CNA_NITRO(1)   = 1.3,
/
&NAM_DATA_TEB          NROOF_LAYER      = 3,
                       XUNIF_ALB_ROOF   = 0.2,
                       XUNIF_EMIS_ROOF  = 0.97,
                       XUNIF_HC_ROOF(1) = 2110000.,
                       XUNIF_HC_ROOF(2) = 2800000.,
                       XUNIF_HC_ROOF(3) = 2900000.,
                       XUNIF_TC_ROOF(1) = 1.51,
                       XUNIF_TC_ROOF(2) = 0.08,
                       XUNIF_TC_ROOF(3) = 0.05,
                       XUNIF_D_ROOF(1)  = 0.05,
                       XUNIF_D_ROOF(2)  = 0.4,
                       XUNIF_D_ROOF(3)  = 0.1,
                       NROAD_LAYER      = 3,
                       XUNIF_ALB_ROAD   = 0.2,
                      XUNIF_ALB_ROAD   = 0.2,
                      XUNIF_EMIS_ROAD  = 0.97,
                      XUNIF_HC_ROAD(1) = 2110000.,
                      XUNIF_HC_ROAD(2) = 2800000.,
                      XUNIF_HC_ROAD(3) = 2900000.,
                      XUNIF_TC_ROAD(1) = 1.51,
                      XUNIF_TC_ROAD(2) = 0.08,
                      XUNIF_TC_ROAD(3) = 0.05,
                      XUNIF_D_ROAD(1)  = 0.05,
                      XUNIF_D_ROAD(2)  = 0.4,
                      XUNIF_D_ROAD(3)  = 0.1,
                      NWALL_LAYER      = 3,
                      XUNIF_ALB_WALL   = 0.2,
                      XUNIF_EMIS_WALL  = 0.97,
                      XUNIF_HC_WALL(1) = 2110000.,
                      XUNIF_HC_WALL(2) = 2800000.,
                      XUNIF_HC_WALL(3) = 2900000.,
                      XUNIF_TC_WALL(1) = 1.51,
                      XUNIF_TC_WALL(2) = 0.08,
                      XUNIF_TC_WALL(3) = 0.05,
                      XUNIF_D_WALL(1)  = 0.05,
                      XUNIF_D_WALL(2)  = 0.4,
                      XUNIF_D_WALL(3)  = 0.1,
```

```
                       XUNIF_Z0_TOWN    = 1.,
                       XUNIF_BLD        = 0.5,
                       XUNIF_BLD_HEIGHT = 10.,
                       XUNIF_WALL_O_HOR = 0.5,
                       XUNIF_H_TRAFFIC  = 10.,
                       XUNIF_LE_TRAFFIC = 0.,
                       XUNIF_H_INDUSTRY = 5.,
                       XUNIF_LE_INDUSTRY= 0.
/
&NAM_FRAC              LECOCLIMAP = F,
                       XUNIF_SEA    = 0.,
                       XUNIF_WATER  = 0.,
                       XUNIF_TOWN   = 0.,
                       XUNIF_NATURE = 1.
/
&NAM_PGD_GRID          CGRID = 'LONLAT REG'
/
&NAM_LONLAT_REG        XLONMIN = 0.           ,
                       XLONMAX = 0.           ,
                       XLATMIN = 0.          ,
                       XLATMAX = 0.          ,
                       NLON    = 1            ,
                       NLAT    = 1
/
&NAM_PGD_SCHEMES       CNATURE = 'ISBA  '    ,
                       CSEA    = 'SEAFLX'    ,
                       CTOWN   = 'TEB   '    ,
                       CWATER  = 'WATFLX'
/
&NAM_ZS                XUNIF_ZS  = 113.
/
&NAM_ISBA              XUNIF_CLAY    = 0.37          ,
                       XUNIF_SAND    = 0.37          ,
                       XUNIF_RUNOFFB = 0.5           ,
                       CISBA         = '2-L'         ,
                       CPHOTO        = 'NON'         ,
                       NPATCH        = 1             ,
                       NGROUND_LAYER = 2
/

&NAM_PREP_SURF_ATM NYEAR  = 1986,
                   NMONTH = 1,
                   NDAY   = 1,
                   XTIME  = 0.
/
&NAM_PREP_SEAFLUX  XSST_UNIF = 285.,
                   NYEAR  = 1986,
                   NMONTH = 1,
                   NDAY   = 1,
                   XTIME  = 0.
/
&NAM_PREP_WATFLUX  XTS_WATER_UNIF = 285.,
                   NYEAR  = 1986,
                   NMONTH = 1,
                   NDAY   = 1,
                   XTIME  = 0.
/
&NAM_PREP_TEB      XTI_ROAD= 285.,
                   XTI_BLD = 285.
                   XTS_ROAD= 285.
                   XTS_ROOF= 285.,
                   XTS_WALL= 285.,
                   XWS_ROAD= 0.,
                   XWS_ROOF= 0.,
                   NYEAR  = 1986,
                   NMONTH = 1,
                   NDAY   = 1,
                   XTIME  = 0.
```

```
/
&NAM_PREP_ISBA      XHUG_SURF = 1.,
                    XHUG_ROOT = 1.,
                    XHUG_DEEP = 1.,
                    XTG_SURF  = 276.16,
                    XTG_ROOT  = 276.16,
                    XTG_DEEP  = 276.16,
                    NYEAR  = 1986,
                    NMONTH = 1,
                    NDAY   = 1,
                    XTIME  = 0.
/
&NAM_PREP_ISBA_SNOW    CSNOW = '3-L'
/


&NAM_IO_OFFLINE        LPRINT  = T                          ,
                       CFORCING_FILETYPE =    'NETCDF'    ,
                       CSURF_FILETYPE =       'ASCII '    ,
                       CTIMESERIES_FILETYPE = 'TEXTE '    ,
                       XTSTEP_OUTPUT = 86400.
/


&NAM_DIAG_SURFn        LSURF_BUDGET = T      ,
                       N2M          = 2      ,
                       LCOEF        = F      ,
                       LSURF_VARS   = F      ,
                       LSURF_BUDGETC = F
/
&NAM_DIAG_SURF_ATMn    LFRAC        = F
/
&NAM_DIAG_ISBAn        LPGD              = T ,
                       LSURF_EVAP_BUDGET = T ,
                       LSURF_MISC_BUDGET = F
/
&NAM_DIAG_SURF_ATMn    LFRAC        = F
/
&NAM_DIAG_ISBAn        LPGD              = T ,
                       LSURF_EVAP_BUDGET = T ,
                       LSURF_MISC_BUDGET = F
/
&NAM_DIAG_TEBn         LSURF_MISC_BUDGET = F
/
&NAM_SGH_ISBAn         CRUNOFF    = "WSAT"
/
&NAM_ISBAn             CROUGH     = "Z04D"     ,
                       CSCOND     = "NP89"     ,
                       CALBEDO    = "DRY"      ,
                       CC1DRY     = 'DEF '     ,
                       CSOILFRZ   = 'DEF'      ,
                       CDIFSFCOND = 'DEF '     ,
                       CSNOWRES   = 'DEF'      ,
                       CCPSURF    = 'DRY'
/
&NAM_CH_ISBAn          CCH_DRY_DEP = "WES89 "
/
&NAM_SEAFLUXn          CSEA_ALB = "TA96"
/
&NAM_CH_SEAFLUXn       CCH_DRY_DEP = "WES89 "
/
&NAM_CH_WATFLUXn       CCH_DRY_DEP = "WES89 "
/
&NAM_CH_TEBn           CCH_DRY_DEP = "WES89 "
/
```

Adaptations that can be made in the OPTIONS.nam file to use ECOCLIMAP data:

OPTIONS.nam ×

```
&NAM_FRAC               LECOCLIMAP = T,
/
&NAM_PGD_ARRANGE_COVER
                        LTOWN_TO_ROCK=.FALSE.
/
&NAM_COVER              YCOVER     = 'ecoclimats_v2',
                        YCOVERFILETYPE = 'DIRECT'
/
&NAM_PGD_GRID           CGRID = 'LONLAT REG'
/
&NAM_LONLAT_REG         XLONMIN = 3.70
                        XLONMAX = 3.9
                        XLATMIN = 51.0          ,
                        XLATMAX = 52.14          ,
                        NLON    = 1             ,
                        NLAT    = 1
/
&NAM_PGD_SCHEMES
/
&NAM_ZS                 YZS='gtopo30',
                        YZSFILETYPE='DIRECT'
/
&NAM_ISBA
                        YCLAY='clay_fao',
                        YCLAYFILETYPE='DIRECT',
                        YSAND='sand_fao',
                        YSANDFILETYPE='DIRECT',
                        CISBA='2-L',
/
&NAM_PREP_SURF_ATM  NYEAR  = 2016,
                    NMONTH = 7,
                    NDAY   = 1,
                    XTIME  = 0.
/
&NAM_PREP_SEAFLUX   XSST_UNIF = 285.,
                    NYEAR  = 2016,
                    NMONTH = 7,
                    NDAY   = 1,
                    XTIME  = 0.

/
&NAM_PREP_SEAFLUX   XSST_UNIF = 285.,
                    NYEAR  = 2016,
                    NMONTH = 7,
                    NDAY   = 1,
                    XTIME  = 0.
/
&NAM_PREP_WATFLUX   XTS_WATER_UNIF = 285.,
                    NYEAR  = 2016,
                    NMONTH = 7,
                    NDAY   = 1,
                    XTIME  = 0.
/
&NAM_PREP_TEB       XTI_ROAD= 285.,
                    XTI_BLD = 285.
                    XTS_ROAD= 285.
                    XTS_ROOF= 285.,
                    XTS_WALL= 285.,
                    XWS_ROAD= 0.,
                    XWS_ROOF= 0.,
                    NYEAR  = 2016,
                    NMONTH = 7,
                    NDAY   = 1,
                    XTIME  = 0.
/
&NAM_PREP_ISBA      XHUG_SURF = 1.,
                    XHUG_ROOT = 1.,
                    XHUG_DEEP = 1.,
                    XTG_SURF  = 276.16,
                    XTG_ROOT  = 276.16,
                    XTG_DEEP  = 276.16,
                    NYEAR  = 2016,
                    NMONTH = 7,
                    NDAY   = 1,
```

Town to rock is false, so cities are taken into account

Change the name to the name of the ECOCLMAP file

Minimum and maximum coordinates. The coordinates were changed a bit because a minimum area is needed.

There is only one grid point

The PGD schemes were deleted and therefore the default values are taken

Date when the experiment starts

```
                   XTIME  = 0.
/
&NAM_PREP_ISBA_SNOW    CSNOW = '3-L'
/



&NAM_IO_OFFLINE        LPRINT  = T                              ,
                       CFORCING_FILETYPE =    'NETCDF'    ,
                       CSURF_FILETYPE =       'ASCII '    ,
                       CTIMESERIES_FILETYPE = 'TEXTE '    ,
                       XTSTEP_OUTPUT = 86400.             ,
                       NHALO=2                            ,
                       LWRITE_COORD = T
/



&NAM_DIAG_SURFn        LSURF_BUDGET = T       ,
                       N2M          = 1       ,
                       LCOEF        = F       ,
                       LSURF_VARS   = F       ,
                       LSURF_BUDGETC = F
/
&NAM_DIAG_SURF_ATMn    LFRAC        = T
/
&NAM_DIAG_ISBAn        LPGD              = T ,
                       LSURF_EVAP_BUDGET = T ,
                       LSURF_MISC_BUDGET = F
/
&NAM_DIAG_TEBn         LSURF_MISC_BUDGET = F
/
&NAM_SGH_ISBAn         CRUNOFF    = "WSAT"

    _   _
/
&NAM_ISBAn             CROUGH     = "Z04D"     ,
                       CSCOND     = "NP89"     ,
                       CALBEDO    = "DRY"      ,
                       CC1DRY     = 'DEF '     ,
                       CSOILFRZ   = 'DEF'      ,
                       CDIFSFCOND = 'DEF '     ,
                       CSNOWRES   = 'DEF'      ,
                       CCPSURF    = 'DRY'
/
&NAM_CH_ISBAn          CCH_DRY_DEP = "WES89 "
/
&NAM_SEAFLUXn          CSEA_ALB = "TA96"
/
&NAM_CH_SEAFLUXn       CCH_DRY_DEP = "WES89 "
/
&NAM_CH_WATFLUXn       CCH_DRY_DEP = "WES89 "
/
&NAM_CH_TEBn           CCH_DRY_DEP = "WES89 "
/
```

Adaptations that can be made to the standard settings of the OPTIONS.nam file to implement land cover data and city geometry data that was obtained with the GIS-analysis:

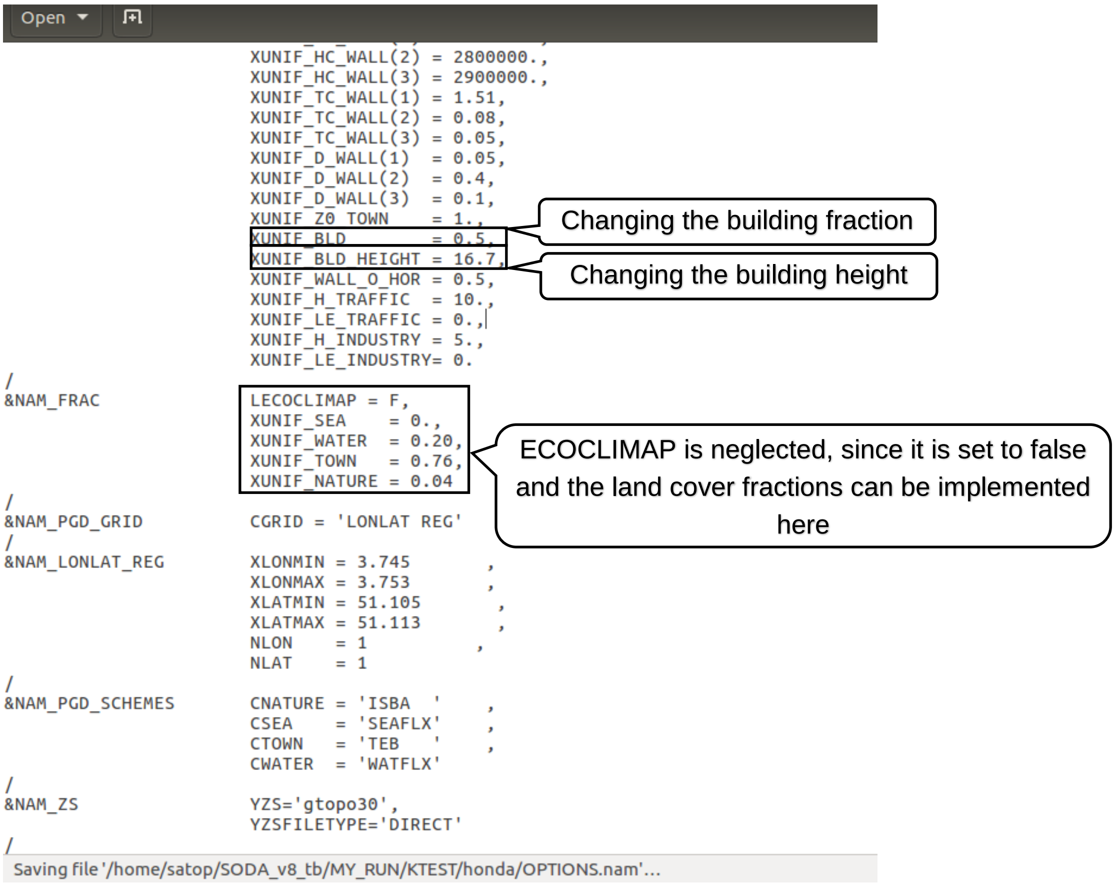

```
                      XUNIF_HC_WALL(2) = 2800000.,
                      XUNIF_HC_WALL(3) = 2900000.,
                      XUNIF_TC_WALL(1) = 1.51,
                      XUNIF_TC_WALL(2) = 0.08,
                      XUNIF_TC_WALL(3) = 0.05,
                      XUNIF_D_WALL(1)  = 0.05,
                      XUNIF_D_WALL(2)  = 0.4,
                      XUNIF_D_WALL(3)  = 0.1,
                      XUNIF_Z0_TOWN    = 1.,
                      XUNIF_BLD        = 0.5,
                      XUNIF_BLD_HEIGHT = 16.7,
                      XUNIF_WALL_O_HOR = 0.5,
                      XUNIF_H_TRAFFIC  = 10.,
                      XUNIF_LE_TRAFFIC = 0.,
                      XUNIF_H_INDUSTRY = 5.,
                      XUNIF_LE_INDUSTRY= 0.
/
&NAM_FRAC             LECOCLIMAP = F,
                      XUNIF_SEA    = 0.,
                      XUNIF_WATER  = 0.20,
                      XUNIF_TOWN   = 0.76,
                      XUNIF_NATURE = 0.04
/
&NAM_PGD_GRID         CGRID = 'LONLAT REG'
/
&NAM_LONLAT_REG       XLONMIN = 3.745        ,
                      XLONMAX = 3.753        ,
                      XLATMIN = 51.105        ,
                      XLATMAX = 51.113        ,
                      NLON    = 1           ,
                      NLAT    = 1
/
&NAM_PGD_SCHEMES      CNATURE = 'ISBA  '     ,
                      CSEA    = 'SEAFLX'     ,
                      CTOWN   = 'TEB   '     ,
                      CWATER  = 'WATFLX'
/
&NAM_ZS               YZS='gtopo30',
                      YZSFILETYPE='DIRECT'
/
```

ANNEX VIII: R Code of the statistical computations

Code to calculate the bias, index of agreement, p-value, RMSE and systematic and unsystematic RMSE of the different runs can be found in the files 'sysRMSEscores2.R' and 'sysRMSEunsysUHI3.R'.

Code to calculate the T-test between the different runs can be found in the files 't_test.R' and 'UHIt_test'. Here, the code of the UHIt_test file is given:

```
##### Reading the files #####
### ECOCLIMAP-I
BavoI=read.csv("C:/Users/saart/Documents/thesis_scores/Bavo_compare_rmse_run7_1_August.csv",header=TRUE,sep=";",dec=",")
HondaI=read.csv("C:/Users/saart/Documents/thesis_scores/Honda_compare_rmse_run7_august.csv",header=TRUE,sep=";",dec=",")
MelleI=read.csv("C:/Users/saart/Documents/thesis_scores/Melle_compare_rmse_run7_1_august.csv",header=TRUE,sep=";",dec=",")
PlantenI=read.csv("C:/Users/saart/Documents/thesis_scores/Plantentuin_compare_rmse_run7_August.csv",header=TRUE,sep=";",dec=",")
ProvincieI=read.csv("C:/Users/saart/Documents/thesis_scores/Provincie_compare_rmse_run7_August.csv",header=TRUE,sep=";",dec=",")
WondelI=read.csv("C:/Users/saart/Documents/thesis_scores/Wondelgem_compare_rmse_run7_August.csv",header=TRUE,sep=";",dec=",")

### ECOCLIMAP-II
BavoII=read.csv("C:/Users/saart/Documents/thesis_scores/Bavo_compare_rmse_2v7_august.csv",header=TRUE,sep=";",dec=",")
HondaII=read.csv("C:/Users/saart/Documents/thesis_scores/Honda_compare_rmse_2v7_august.csv",header=TRUE,sep=";",dec=",")
MelleII=read.csv("C:/Users/saart/Documents/thesis_scores/Melle_compare_rmse_2v7_August.csv",header=TRUE,sep=";",dec=",")
PlantenII=read.csv("C:/Users/saart/Documents/thesis_scores/Plantentuin_compare_rmse_2v7_august.csv",header=TRUE,sep=";",dec=",")
ProvincieII=read.csv("C:/Users/saart/Documents/thesis_scores/Provincie_compare_rmse_2v7_august.csv",header=TRUE,sep=";",dec=",")
WondelII=read.csv("C:/Users/saart/Documents/thesis_scores/Wondelgem_compare_rmse_2v7_august.csv",header=TRUE,sep=";",dec=",")

### ECOCLIMAP-I 100 m
Bavo100=read.csv("C:/Users/saart/Documents/thesis_scores/Bavo_compare_rmse_3v1_100_august.csv",header=TRUE,sep=";",dec=",")
Honda100=read.csv("C:/Users/saart/Documents/thesis_scores/Honda_compare_rmse_3v1_100_august.csv",header=TRUE,sep=";",dec=",")
Melle100=read.csv("C:/Users/saart/Documents/thesis_scores/Melle_compare_rmse_3v1_100_august.csv",header=TRUE,sep=";",dec=",")
Planten100=read.csv("C:/Users/saart/Documents/thesis_scores/Plantentuin_compare_rmse_3v1_100_august.csv",header=TRUE,sep=";",dec=",")
Provincie100=read.csv("C:/Users/saart/Documents/thesis_scores/Provincie_compare_rmse_3v1_100_august.csv",header=TRUE,sep=";",dec=",")
Wondel100=read.csv("C:/Users/saart/Documents/thesis_scores/Wondelgem_compare_rmse_3v1_100_august.csv",header=TRUE,sep=";",dec=",")

### ECOCLIMAP-I 565 m
Bavo565=read.csv("C:/Users/saart/Documents/thesis_scores/Bavo_compare_rmse_3v1_0_august.csv",header=TRUE,sep=";",dec=",")
Honda565=read.csv("C:/Users/saart/Documents/thesis_scores/Honda_compare_rmse_3v1_0_August.csv",header=TRUE,sep=";",dec=",")
Melle565=read.csv("C:/Users/saart/Documents/thesis_scores/Melle_compare_rmse_3v1_0_august.csv",header=TRUE,sep=";",dec=",")
Planten565=read.csv("C:/Users/saart/Documents/thesis_scores/Plantentuin_compare_rmse_3v1_0_august.csv",header=TRUE,sep=";",dec=",")
Provincie565=read.csv("C:/Users/saart/Documents/thesis_scores/Provincie_compare_rmse_3v1_0_august.csv",header=TRUE,sep=";",dec=",")
Wondel565=read.csv("C:/Users/saart/Documents/thesis_scores/Wondelgem_compare_rmse_3v1_0_august.csv",header=TRUE,sep=";",dec=",")

### ECOCLIMAP-I 1000 m
Bavo1000=read.csv("C:/Users/saart/Documents/thesis_scores/Bavo_compare_rmse_3v1_1000_august.csv",header=TRUE,sep=";",dec=",")
Honda1000=read.csv("C:/Users/saart/Documents/thesis_scores/Honda_compare_rmse_3v1_1000_august.csv",header=TRUE,sep=";",dec=",")
Melle1000=read.csv("C:/Users/saart/Documents/thesis_scores/Melle_compare_rmse_3v1_1000_august.csv",header=TRUE,sep=";",dec=",")
Planten1000=read.csv("C:/Users/saart/Documents/thesis_scores/Plantentuin_compare_rmse_3v1_1000_august.csv",header=TRUE,sep=";",dec=",")
Provincie1000=read.csv("C:/Users/saart/Documents/thesis_scores/Provincie_compare_rmse_3v1_1000_august.csv",header=TRUE,sep=";",dec=",")
Wondel1000=read.csv("C:/Users/saart/Documents/thesis_scores/Wondelgem_compare_rmse_3v1_1000_august.csv",header=TRUE,sep=";",dec=",")
```

```
### ECOCLIMAP-I 565 m building fraction
BavoB=read.csv("C:/Users/saart/Documents/thesis_scores/Bavo_compare_rmse_3v1_0B_august.csv",header=TRUE,sep=";",dec=",")
HondaB=read.csv("C:/Users/saart/Documents/thesis_scores/Honda_compare_rmse_3v1_0B_august.csv",header=TRUE,sep=";",dec=",")
MelleB=read.csv("C:/Users/saart/Documents/thesis_scores/Melle_compare_rmse_3v1_0B_august.csv",header=TRUE,sep=";",dec=",")
PlantenB=read.csv("C:/Users/saart/Documents/thesis_scores/Plantentuin_compare_rmse_3v1_0B_august.csv",header=TRUE,sep=";",dec=",")
ProvincieB=read.csv("C:/Users/saart/Documents/thesis_scores/Provincie_compare_rmse_3v1_0B_august.csv",header=TRUE,sep=";",dec=",")
WondelB=read.csv("C:/Users/saart/Documents/thesis_scores/Wondelgem_compare_rmse_3v1_0B_august.csv",header=TRUE,sep=";",dec=",")

### ECOCLIMAP-I 565 m building height
BavoH=read.csv("C:/Users/saart/Documents/thesis_scores/Bavo_compare_rmse_3v1_0H_august.csv",header=TRUE,sep=";",dec=",")
HondaH=read.csv("C:/Users/saart/Documents/thesis_scores/Honda_compare_rmse_3v1_0H_august.csv",header=TRUE,sep=";",dec=",")
MelleH=read.csv("C:/Users/saart/Documents/thesis_scores/Melle_compare_rmse_3v1_0H_august.csv",header=TRUE,sep=";",dec=",")
PlantenH=read.csv("C:/Users/saart/Documents/thesis_scores/Plantentuin_compare_rmse_3v1_0H_august.csv",header=TRUE,sep=";",dec=",")
ProvincieH=read.csv("C:/Users/saart/Documents/thesis_scores/Provincie_compare_rmse_3v1_0H_august.csv",header=TRUE,sep=";",dec=",")
WondelH=read.csv("C:/Users/saart/Documents/thesis_scores/Wondelgem_compare_rmse_3v1_0H_august.csv",header=TRUE,sep=";",dec=",")


##### Extract columns and calculation UHI #####


### ECOCLIMAP-I

BavoISURFEX <- BavoI[ ,c("model")]
BavoISURFEX=BavoISURFEX[1:648]
BavoIOBS <- BavoI[ ,c("obs")]
BavoIOBS=BavoIOBS[1:648]

HondaISURFEX <- HondaI[ ,c("model")]
HondaISURFEX=HondaISURFEX[1:648]
HondaIOBS <- HondaI[ ,c("obs")]
HondaIOBS=HondaIOBS[1:648]

MelleISURFEX <- MelleI[ ,c("model")]
MelleISURFEX=MelleISURFEX[1:648]
MelleIOBS <- MelleI[ ,c("obs")]
MelleIOBS=MelleIOBS[1:648]

PlantenISURFEX <- PlantenI[ ,c("model")]
```

```
PlantenISURFEX=PlantenISURFEX[1:648]
PlantenIOBS <- PlantenI[ ,c("obs")]
PlantenIOBS=PlantenIOBS[1:648]

ProvincieISURFEX <- ProvincieI[ ,c("model")]
ProvincieISURFEX=ProvincieISURFEX[1:648]
ProvincieIOBS <- ProvincieI[ ,c("obs")]
ProvincieIOBS=ProvincieIOBS[1:648]

WondelISURFEX <- WondelI[ ,c("model")]
WondelISURFEX=WondelISURFEX[1:648]
WondelIOBS <- WondelI[ ,c("obs")]
WondelIOBS=WondelIOBS[1:648]

# calculation UHI

BavoISURFEX=BavoISURFEX-MelleISURFEX
BavoIOBS=BavoIOBS-MelleIOBS

HondaISURFEX=HondaISURFEX-MelleISURFEX
HondaIOBS=HondaIOBS-MelleIOBS

PlantenISURFEX=PlantenISURFEX-MelleISURFEX
PlantenIOBS=PlantenIOBS-MelleIOBS

ProvincieISURFEX=ProvincieISURFEX-MelleISURFEX
ProvincieIOBS=ProvincieIOBS-MelleIOBS

WondelISURFEX=WondelISURFEX-MelleISURFEX
WondelIOBS=WondelIOBS-MelleIOBS

### ECOCLIMAP-II

BavoIISURFEX <- BavoII[ ,c("model")]
BavoIISURFEX=BavoIISURFEX[1:648]
BavoIIOBS <- BavoII[ ,c("obs")]
BavoIIOBS=BavoIIOBS[1:648]
```

```
HondaIISURFEX <- HondaII[ ,c("model")]
HondaIISURFEX=HondaIISURFEX[1:648]
HondaIIOBS <- HondaII[ ,c("obs")]
HondaIIOBS=HondaIIOBS[1:648]

MelleIISURFEX <- MelleII[ ,c("model")]
MelleIISURFEX=MelleIISURFEX[1:648]
MelleIIOBS <- MelleII[ ,c("obs")]
MelleIIOBS=MelleIIOBS[1:648]

PlantenIISURFEX <- PlantenII[ ,c("model")]
PlantenIISURFEX=PlantenIISURFEX[1:648]
PlantenIIOBS <- PlantenII[ ,c("obs")]
PlantenIIOBS=PlantenIIOBS[1:648]

ProvincieIISURFEX <- ProvincieII[ ,c("model")]
ProvincieIISURFEX=ProvincieIISURFEX[1:648]
ProvincieIIOBS <- ProvincieII[ ,c("obs")]
ProvincieIIOBS=ProvincieIIOBS[1:648]

WondelIISURFEX <- WondelII[ ,c("model")]
WondelIISURFEX=WondelIISURFEX[1:648]
WondelIIOBS <- WondelII[ ,c("obs")]
WondelIIOBS=WondelIIOBS[1:648]

# calculation UHI

BavoIISURFEX=BavoIISURFEX-MelleIISURFEX
BavoIIOBS=BavoIIOBS-MelleIIOBS

HondaIISURFEX=HondaIISURFEX-MelleIISURFEX
HondaIIOBS=HondaIIOBS-MelleIIOBS

PlantenIISURFEX=PlantenIISURFEX-MelleIISURFEX
PlantenIIOBS=PlantenIIOBS-MelleIIOBS

ProvincieIISURFEX=ProvincieIISURFEX-MelleIISURFEX
ProvincieIIOBS=ProvincieIIOBS-MelleIIOBS
```

```
WondelIISURFEX=WondelIISURFEX-MelleIISURFEX
WondelIIOBS=WondelIIOBS-MelleIIOBS

### ECOCLIMAP-I 100 m

Bavo100SURFEX <- Bavo100[ ,c("model")]
Bavo100SURFEX=Bavo100SURFEX[1:648]
Bavo100OBS <- Bavo100[ ,c("obs")]
Bavo100OBS=Bavo100OBS[1:648]

Honda100SURFEX <- Honda100[ ,c("model")]
Honda100SURFEX=Honda100SURFEX[1:648]
Honda100OBS <- Honda100[ ,c("obs")]
Honda100OBS=Honda100OBS[1:648]

Melle100SURFEX <- Melle100[ ,c("model")]
Melle100SURFEX=Melle100SURFEX[1:648]
Melle100OBS <- Melle100[ ,c("obs")]
Melle100OBS=Melle100OBS[1:648]

Planten100SURFEX <- Planten100[ ,c("model")]
Planten100SURFEX=Planten100SURFEX[1:648]
Planten100OBS <- Planten100[ ,c("obs")]
Planten100OBS=Planten100OBS[1:648]

Provincie100SURFEX <- Provincie100[ ,c("model")]
Provincie100SURFEX=Provincie100SURFEX[1:648]
Provincie100OBS <- Provincie100[ ,c("obs")]
Provincie100OBS=Provincie100OBS[1:648]

Wondel100SURFEX <- Wondel100[ ,c("model")]
Wondel100SURFEX=Wondel100SURFEX[1:648]
Wondel100OBS <- Wondel100[ ,c("obs")]
Wondel100OBS=Wondel100OBS[1:648]

# calculation UHI

Bavo100SURFEX=Bavo100SURFEX-Melle100SURFEX
Bavo100OBS=Bavo100OBS-Melle100OBS
```

```
Honda100SURFEX=Honda100SURFEX-Melle100SURFEX
Honda100OBS=Honda100OBS-Melle100OBS

Planten100SURFEX=Planten100SURFEX-Melle100SURFEX
Planten100OBS=Planten100OBS-Melle100OBS

Provincie100SURFEX=Provincie100SURFEX-Melle100SURFEX
Provincie100OBS=Provincie100OBS-Melle100OBS

Wondel100SURFEX=Wondel100SURFEX-Melle100SURFEX
Wondel100OBS=Wondel100OBS-Melle100OBS

### ECOCLIMAP-I 565 m

Bavo565SURFEX <- Bavo565[ ,c("model")]
Bavo565SURFEX=Bavo565SURFEX[1:648]
Bavo565OBS <- Bavo565[ ,c("obs")]
Bavo565OBS=Bavo565OBS[1:648]

Honda565SURFEX <- Honda565[ ,c("model")]
Honda565SURFEX=Honda565SURFEX[1:648]
Honda565OBS <- Honda565[ ,c("obs")]
Honda565OBS=Honda565OBS[1:648]

Melle565SURFEX <- Melle565[ ,c("model")]
Melle565SURFEX=Melle565SURFEX[1:648]
Melle565OBS <- Melle565[ ,c("obs")]
Melle565OBS=Melle565OBS[1:648]

Planten565SURFEX <- Planten565[ ,c("model")]
Planten565SURFEX=Planten565SURFEX[1:648]
Planten565OBS <- Planten565[ ,c("obs")]
Planten565OBS=Planten565OBS[1:648]
```

```
Provincie565SURFEX <- Provincie565[ ,c("model")]
Provincie565SURFEX=Provincie565SURFEX[1:648]
Provincie565OBS <- Provincie565[ ,c("obs")]
Provincie565OBS=Provincie565OBS[1:648]

Wondel565SURFEX <- Wondel565[ ,c("model")]
Wondel565SURFEX=Wondel565SURFEX[1:648]
Wondel565OBS <- Wondel565[ ,c("obs")]
Wondel565OBS=Wondel565OBS[1:648]

# calculation UHI

Bavo565SURFEX=Bavo565SURFEX-Melle565SURFEX
Bavo565OBS=Bavo565OBS-Melle565OBS

Honda565SURFEX=Honda565SURFEX-Melle565SURFEX
Honda565OBS=Honda565OBS-Melle565OBS

Planten565SURFEX=Planten565SURFEX-Melle565SURFEX
Planten565OBS=Planten565OBS-Melle565OBS

Provincie565SURFEX=Provincie565SURFEX-Melle565SURFEX
Provincie565OBS=Provincie565OBS-Melle565OBS

Wondel565SURFEX=Wondel565SURFEX-Melle565SURFEX
Wondel565OBS=Wondel565OBS-Melle565OBS

### ECOCLIMAP-I 1000 m

Bavo1000SURFEX <- Bavo1000[ ,c("model")]
Bavo1000SURFEX=Bavo1000SURFEX[1:648]
Bavo1000OBS <- Bavo1000[ ,c("obs")]
Bavo1000OBS=Bavo1000OBS[1:648]

Honda1000SURFEX <- Honda1000[ ,c("model")]
Honda1000SURFEX=Honda1000SURFEX[1:648]
Honda1000OBS <- Honda1000[ ,c("obs")]
Honda1000OBS=Honda1000OBS[1:648]
```

```
Melle1000SURFEX <- Melle1000[ ,c("model")]
Melle1000SURFEX=Melle1000SURFEX[1:648]
Melle1000OBS <- Melle1000[ ,c("obs")]
Melle1000OBS=Melle1000OBS[1:648]

Planten1000SURFEX <- Planten1000[ ,c("model")]
Planten1000SURFEX=Planten1000SURFEX[1:648]
Planten1000OBS <- Planten1000[ ,c("obs")]
Planten1000OBS=Planten1000OBS[1:648]

Provincie1000SURFEX <- Provincie1000[ ,c("model")]
Provincie1000SURFEX=Provincie1000SURFEX[1:648]
Provincie1000OBS <- Provincie1000[ ,c("obs")]
Provincie1000OBS=Provincie1000OBS[1:648]

Wondel1000SURFEX <- Wondel1000[ ,c("model")]
Wondel1000SURFEX=Wondel1000SURFEX[1:648]
Wondel1000OBS <- Wondel1000[ ,c("obs")]
Wondel1000OBS=Wondel1000OBS[1:648]

# calculation UHI

Bavo1000SURFEX=Bavo1000SURFEX-Melle1000SURFEX
Bavo1000OBS=Bavo1000OBS-Melle1000OBS

Honda1000SURFEX=Honda1000SURFEX-Melle1000SURFEX
Honda1000OBS=Honda1000OBS-Melle1000OBS

Planten1000SURFEX=Planten1000SURFEX-Melle1000SURFEX
Planten1000OBS=Planten1000OBS-Melle1000OBS

Provincie1000SURFEX=Provincie1000SURFEX-Melle1000SURFEX
Provincie1000OBS=Provincie1000OBS-Melle1000OBS

Wondel1000SURFEX=Wondel1000SURFEX-Melle1000SURFEX
Wondel1000OBS=Wondel1000OBS-Melle1000OBS
```

```
### ECOCLIMAP-I 565 m building fraction

BavoBSURFEX <- BavoB[ ,c("model")]
BavoBSURFEX=BavoBSURFEX[1:648]
BavoBOBS <- BavoB[ ,c("obs")]
BavoBOBS=BavoBOBS[1:648]

HondaBSURFEX <- HondaB[ ,c("model")]
HondaBSURFEX=HondaBSURFEX[1:648]
HondaBOBS <- HondaB[ ,c("obs")]
HondaBOBS=HondaBOBS[1:648]

MelleBSURFEX <- MelleB[ ,c("model")]
MelleBSURFEX=MelleBSURFEX[1:648]
MelleBOBS <- MelleB[ ,c("obs")]
MelleBOBS=MelleBOBS[1:648]

PlantenBSURFEX <- PlantenB[ ,c("model")]
PlantenBSURFEX=PlantenBSURFEX[1:648]
PlantenBOBS <- PlantenB[ ,c("obs")]
PlantenBOBS=PlantenBOBS[1:648]

ProvincieBSURFEX <- ProvincieB[ ,c("model")]
ProvincieBSURFEX=ProvincieBSURFEX[1:648]
ProvincieBOBS <- ProvincieB[ ,c("obs")]
ProvincieBOBS=ProvincieBOBS[1:648]

WondelBSURFEX <- WondelB[ ,c("model")]
WondelBSURFEX=WondelBSURFEX[1:648]
WondelBOBS <- WondelB[ ,c("obs")]
WondelBOBS=WondelBOBS[1:648]

# calculation UHI

BavoBSURFEX=BavoBSURFEX-MelleBSURFEX
BavoBOBS=BavoBOBS-MelleBOBS

HondaBSURFEX=HondaBSURFEX-MelleBSURFEX
HondaBOBS=HondaBOBS-MelleBOBS
```

```
PlantenBSURFEX=PlantenBSURFEX-MelleBSURFEX
PlantenBOBS=PlantenBOBS-MelleBOBS

ProvincieBSURFEX=ProvincieBSURFEX-MelleBSURFEX
ProvincieBOBS=ProvincieBOBS-MelleBOBS

WondelBSURFEX=WondelBSURFEX-MelleBSURFEX
WondelBOBS=WondelBOBS-MelleBOBS



### ECOCLIMAP-I 565 m building height

BavoHSURFEX <- BavoH[ ,c("model")]
BavoHSURFEX=BavoHSURFEX[1:648]
BavoHOBS <- BavoH[ ,c("obs")]
BavoHOBS=BavoHOBS[1:648]

HondaHSURFEX <- HondaH[ ,c("model")]
HondaHSURFEX=HondaHSURFEX[1:648]
HondaHOBS <- HondaH[ ,c("obs")]
HondaHOBS=HondaHOBS[1:648]

MelleHSURFEX <- MelleH[ ,c("model")]
MelleHSURFEX=MelleHSURFEX[1:648]
MelleHOBS <- MelleH[ ,c("obs")]
MelleHOBS=MelleHOBS[1:648]

PlantenHSURFEX <- PlantenH[ ,c("model")]
PlantenHSURFEX=PlantenHSURFEX[1:648]
PlantenHOBS <- PlantenH[ ,c("obs")]
PlantenHOBS=PlantenHOBS[1:648]

ProvincieHSURFEX <- ProvincieH[ ,c("model")]
ProvincieHSURFEX=ProvincieHSURFEX[1:648]
ProvincieHOBS <- ProvincieH[ ,c("obs")]
ProvincieHOBS=ProvincieHOBS[1:648]
```

```
WondelHSURFEX <- WondelH[ ,c("model")]
WondelHSURFEX=WondelHSURFEX[1:648]
WondelHOBS <- WondelH[ ,c("obs")]
WondelHOBS=WondelHOBS[1:648]

# calculation UHI

BavoHSURFEX=BavoHSURFEX-MelleHSURFEX
BavoHOBS=BavoHOBS-MelleHOBS

HondaHSURFEX=HondaHSURFEX-MelleHSURFEX
HondaHOBS=HondaHOBS-MelleHOBS

PlantenHSURFEX=PlantenHSURFEX-MelleHSURFEX
PlantenHOBS=PlantenHOBS-MelleHOBS

ProvincieHSURFEX=ProvincieHSURFEX-MelleHSURFEX
ProvincieHOBS=ProvincieHOBS-MelleHOBS

WondelHSURFEX=WondelHSURFEX-MelleHSURFEX
WondelHOBS=WondelHOBS-MelleHOBS



##### T-Test #####

#Bavo
TI=t.test(BavoIOBS,BavoISURFEX,paired=TRUE)
print("result T_Test ECOCLIMAP-I:")
print(TI)
TII=t.test(BavoIIOBS,BavoIISURFEX,paired=TRUE)
T100=t.test(Bavo100OBS,Bavo100SURFEX,paired=TRUE)
T565=t.test(Bavo565OBS,Bavo565SURFEX,paired=TRUE)
T1000=t.test(Bavo1000OBS,Bavo1000SURFEX,paired=TRUE)
TB=t.test(BavoBOBS,BavoBSURFEX,paired=TRUE)
TH=t.test(BavoHOBS,BavoHSURFEX,paired=TRUE)
```

```
write.table(TI[["p.value"]], file="C:/Users/saart/Documents/thesis_scores/UHIBavo_OBSTtest.csv", sep=";", dec=",", append=TRUE,
row.names="IOBS_SURFEX_p-value", col.names=FALSE)
write.table(TII[["p.value"]], file="C:/Users/saart/Documents/thesis_scores/UHIBavo_OBSTtest.csv", sep=";", dec=",", append=TRUE,
 row.names="IIOBS_SURFEX_p-value", col.names=FALSE)
write.table(T100[["p.value"]], file="C:/Users/saart/Documents/thesis_scores/UHIBavo_OBSTtest.csv", sep=";", dec=",", append=TRUE,
 row.names="100OBS_SURFEX_p-value", col.names=FALSE)
write.table(T565[["p.value"]], file="C:/Users/saart/Documents/thesis_scores/UHIBavo_OBSTtest.csv", sep=";", dec=",", append=TRUE,
 row.names="565OBS_SURFEX_p-value", col.names=FALSE)
write.table(T1000[["p.value"]], file="C:/Users/saart/Documents/thesis_scores/UHIBavo_OBSTtest.csv", sep=";", dec=",", append=TRUE,
 row.names="1000OBS_SURFEX_p-value", col.names=FALSE)
write.table(TB[["p.value"]], file="C:/Users/saart/Documents/thesis_scores/UHIBavo_OBSTtest.csv", sep=";", dec=",", append=TRUE,
 row.names="BOBS_SURFEX_p-value", col.names=FALSE)
write.table(TH[["p.value"]], file="C:/Users/saart/Documents/thesis_scores/UHIBavo_OBSTtest.csv", sep=";", dec=",", append=TRUE,
 row.names="HOBS_SURFEX_p-value", col.names=FALSE)

## T-Test between model runs
TI_II=t.test(BavoISURFEX, BavoIISURFEX, paired=TRUE)
TI_100=t.test(BavoISURFEX, Bavo100SURFEX, paired=TRUE)
TI_565=t.test(BavoISURFEX, Bavo565SURFEX, paired=TRUE)
TI_1000=t.test(BavoISURFEX, Bavo1000SURFEX, paired=TRUE)
#TI_B=t.test(BavoISURFEX, BavoBSURFEX, paired=TRUE)
#TI_H=t.test(BavoISURFEX, BavoHSURFEX, paired=TRUE)
TII_100=t.test(BavoIISURFEX, Bavo100SURFEX, paired=TRUE)
TII_565=t.test(BavoIISURFEX, Bavo565SURFEX, paired=TRUE)
TII_1000=t.test(BavoIISURFEX, Bavo1000SURFEX, paired=TRUE)
#TII_B=t.test(BavoIISURFEX, BavoBSURFEX, paired=TRUE)
#TII_H=t.test(BavoIISURFEX, BavoHSURFEX, paired=TRUE)
T565_100=t.test(Bavo565SURFEX, Bavo100SURFEX, paired=TRUE)
T565_1000=t.test(Bavo565SURFEX, Bavo1000SURFEX, paired=TRUE)
T100_1000=t.test(Bavo100SURFEX, Bavo1000SURFEX, paired=TRUE)

T565_B=t.test(Bavo565SURFEX, BavoBSURFEX, paired=TRUE)
T565_H=t.test(Bavo565SURFEX, BavoHSURFEX, paired=TRUE)
TB_H=t.test(BavoBSURFEX, BavoHSURFEX, paired=TRUE)
```

```
write.table(TI_II[["p.value"]], file="C:/Users/saart/Documents/thesis_scores/UHIBavo_SURFEXTtest.csv", sep=";", dec=",",
 append=TRUE, row.names="I_II_p-value", col.names=FALSE)
write.table(TI_100[["p.value"]], file="C:/Users/saart/Documents/thesis_scores/UHIBavo_SURFEXTtest.csv", sep=";", dec=",",
 append=TRUE, row.names="I_100_p-value", col.names=FALSE)
write.table(TI_565[["p.value"]], file="C:/Users/saart/Documents/thesis_scores/UHIBavo_SURFEXTtest.csv", sep=";", dec=",",
 append=TRUE, row.names="I_565_p-value", col.names=FALSE)
write.table(TI_1000[["p.value"]], file="C:/Users/saart/Documents/thesis_scores/UHIBavo_SURFEXTtest.csv", sep=";", dec=",",
 append=TRUE, row.names="I_1000_p-value", col.names=FALSE)
#write.table(TI_B[["p.value"]], file="C:/Users/saart/Documents/thesis_scores/UHIBavo_SURFEXTtest.csv", sep=";", dec=",",
 append=TRUE, row.names="I_B_p-value", col.names=FALSE)
#write.table(TI_H[["p.value"]], file="C:/Users/saart/Documents/thesis_scores/UHIBavo_SURFEXTtest.csv", sep=";", dec=",",
 append=TRUE, row.names="I_H_p-value", col.names=FALSE)
write.table(TII_100[["p.value"]], file="C:/Users/saart/Documents/thesis_scores/UHIBavo_SURFEXTtest.csv", sep=";", dec=",",
 append=TRUE, row.names="II_100_p-value", col.names=FALSE)
write.table(TII_565[["p.value"]], file="C:/Users/saart/Documents/thesis_scores/UHIBavo_SURFEXTtest.csv", sep=";", dec=",",
 append=TRUE, row.names="II_565_p-value", col.names=FALSE)
write.table(TII_1000[["p.value"]], file="C:/Users/saart/Documents/thesis_scores/UHIBavo_SURFEXTtest.csv", sep=";", dec=",",
 append=TRUE, row.names="II_1000_p-value", col.names=FALSE)
#write.table(TII_B[["p.value"]], file="C:/Users/saart/Documents/thesis_scores/UHIBavo_SURFEXTtest.csv", sep=";", dec=",",
 append=TRUE, row.names="II_B_p-value", col.names=FALSE)
#write.table(TII_H[["p.value"]], file="C:/Users/saart/Documents/thesis_scores/UHIBavo_SURFEXTtest.csv", sep=";", dec=",",
 append=TRUE, row.names="II_H_p-value", col.names=FALSE)
write.table(T565_100[["p.value"]], file="C:/Users/saart/Documents/thesis_scores/UHIBavo_SURFEXTtest.csv", sep=";", dec=",",
 append=TRUE, row.names="565_100_p-value", col.names=FALSE)
write.table(T565_1000[["p.value"]], file="C:/Users/saart/Documents/thesis_scores/UHIBavo_SURFEXTtest.csv", sep=";", dec=",",
 append=TRUE, row.names="565_1000_p-value", col.names=FALSE)
write.table(T100_1000[["p.value"]], file="C:/Users/saart/Documents/thesis_scores/UHIBavo_SURFEXTtest.csv", sep=";", dec=",",
 append=TRUE, row.names="100_1000_p-value", col.names=FALSE)

write.table(T565_B[["p.value"]], file="C:/Users/saart/Documents/thesis_scores/UHIBavo_SURFEXTtest.csv", sep=";", dec=",",
 append=TRUE, row.names="565_B_p-value", col.names=FALSE)
write.table(T565_H[["p.value"]], file="C:/Users/saart/Documents/thesis_scores/UHIBavo_SURFEXTtest.csv", sep=";", dec=",",
 append=TRUE, row.names="565_H_p-value", col.names=FALSE)
write.table(TB_H[["p.value"]], file="C:/Users/saart/Documents/thesis_scores/UHIBavo_SURFEXTtest.csv", sep=";", dec=",",
 append=TRUE, row.names="B_H_p-value", col.names=FALSE)
```

```
#Honda
TI=t.test(HondaIOBS,HondaISURFEX,paired=TRUE)
print("result T_Test ECOCLIMAP-I:")
print(TI)
TII=t.test(HondaIIOBS,HondaIISURFEX,paired=TRUE)
T100=t.test(Honda100OBS,Honda100SURFEX,paired=TRUE)
T565=t.test(Honda565OBS,Honda565SURFEX,paired=TRUE)
T1000=t.test(Honda1000OBS,Honda1000SURFEX,paired=TRUE)
TB=t.test(HondaBOBS,HondaBSURFEX,paired=TRUE)
TH=t.test(HondaHOBS,HondaHSURFEX,paired=TRUE)

write.table(TI[["p.value"]], file="C:/Users/saart/Documents/thesis_scores/UHIHonda_OBSTtest.csv", sep=";", dec=",",
 append=TRUE, row.names="IOBS_SURFEX_p-value", col.names=FALSE)
write.table(TII[["p.value"]], file="C:/Users/saart/Documents/thesis_scores/UHIHonda_OBSTtest.csv", sep=";", dec=",",
 append=TRUE, row.names="IIOBS_SURFEX_p-value", col.names=FALSE)
write.table(T100[["p.value"]], file="C:/Users/saart/Documents/thesis_scores/UHIHonda_OBSTtest.csv", sep=";", dec=",",
 append=TRUE, row.names="100OBS_SURFEX_p-value", col.names=FALSE)
write.table(T565[["p.value"]], file="C:/Users/saart/Documents/thesis_scores/UHIHonda_OBSTtest.csv", sep=";", dec=",",
 append=TRUE, row.names="565OBS_SURFEX_p-value", col.names=FALSE)
write.table(T1000[["p.value"]], file="C:/Users/saart/Documents/thesis_scores/UHIHonda_OBSTtest.csv", sep=";", dec=",",
 append=TRUE, row.names="1000OBS_SURFEX_p-value", col.names=FALSE)
write.table(TB[["p.value"]], file="C:/Users/saart/Documents/thesis_scores/UHIHonda_OBSTtest.csv", sep=";", dec=",",
 append=TRUE, row.names="BOBS_SURFEX_p-value", col.names=FALSE)
write.table(TH[["p.value"]], file="C:/Users/saart/Documents/thesis_scores/UHIHonda_OBSTtest.csv", sep=";", dec=",",
 append=TRUE, row.names="HOBS_SURFEX_p-value", col.names=FALSE)

## T-Test between model runs
TI_II=t.test(HondaISURFEX, HondaIISURFEX, paired=TRUE)
TI_100=t.test(HondaISURFEX, Honda100SURFEX, paired=TRUE)
TI_565=t.test(HondaISURFEX, Honda565SURFEX, paired=TRUE)
TI_1000=t.test(HondaISURFEX, Honda1000SURFEX, paired=TRUE)
#TI_B=t.test(HondaISURFEX, HondaBSURFEX, paired=TRUE)
#TI_H=t.test(HondaISURFEX, HondaHSURFEX, paired=TRUE)
TII_100=t.test(HondaIISURFEX, Honda100SURFEX, paired=TRUE)
TII_565=t.test(HondaIISURFEX, Honda565SURFEX, paired=TRUE)
TII_1000=t.test(HondaIISURFEX, Honda1000SURFEX, paired=TRUE)
#TII_B=t.test(HondaIISURFEX, HondaBSURFEX, paired=TRUE)
```

```
#TII_H=t.test(HondaIISURFEX, HondaHSURFEX, paired=TRUE)
T565_100=t.test(Honda565SURFEX, Honda100SURFEX, paired=TRUE)
T565_1000=t.test(Honda565SURFEX, Honda1000SURFEX, paired=TRUE)
T100_1000=t.test(Honda100SURFEX, Honda1000SURFEX, paired=TRUE)

T565_B=t.test(Honda565SURFEX, HondaBSURFEX, paired=TRUE)
T565_H=t.test(Honda565SURFEX, HondaHSURFEX, paired=TRUE)
TB_H=t.test(HondaBSURFEX, HondaHSURFEX, paired=TRUE)

write.table(TI_II[["p.value"]], file="C:/Users/saart/Documents/thesis_scores/UHIHonda_SURFEXTtest.csv", sep=";", dec=",",
 append=TRUE, row.names="I_II_p-value", col.names=FALSE)
write.table(TI_100[["p.value"]], file="C:/Users/saart/Documents/thesis_scores/UHIHonda_SURFEXTtest.csv", sep=";", dec=",",
 append=TRUE, row.names="I_100_p-value", col.names=FALSE)
write.table(TI_565[["p.value"]], file="C:/Users/saart/Documents/thesis_scores/UHIHonda_SURFEXTtest.csv", sep=";", dec=",",
 append=TRUE, row.names="I_565_p-value", col.names=FALSE)
write.table(TI_1000[["p.value"]], file="C:/Users/saart/Documents/thesis_scores/UHIHonda_SURFEXTtest.csv", sep=";", dec=",",
 append=TRUE, row.names="I_1000_p-value", col.names=FALSE)
#write.table(TI_B[["p.value"]], file="C:/Users/saart/Documents/thesis_scores/UHIHonda_SURFEXTtest.csv", sep=";", dec=",",
 append=TRUE, row.names="I_B_p-value", col.names=FALSE)
#write.table(TI_H[["p.value"]], file="C:/Users/saart/Documents/thesis_scores/UHIHonda_SURFEXTtest.csv", sep=";", dec=",",
 append=TRUE, row.names="I_H_p-value", col.names=FALSE)
write.table(TII_100[["p.value"]], file="C:/Users/saart/Documents/thesis_scores/UHIHonda_SURFEXTtest.csv", sep=";", dec=",",
 append=TRUE, row.names="II_100_p-value", col.names=FALSE)
write.table(TII_565[["p.value"]], file="C:/Users/saart/Documents/thesis_scores/UHIHonda_SURFEXTtest.csv", sep=";", dec=",",
 append=TRUE, row.names="II_565_p-value", col.names=FALSE)
write.table(TII_1000[["p.value"]], file="C:/Users/saart/Documents/thesis_scores/UHIHonda_SURFEXTtest.csv", sep=";", dec=",",
 append=TRUE, row.names="II_1000_p-value", col.names=FALSE)
#write.table(TII_B[["p.value"]], file="C:/Users/saart/Documents/thesis_scores/UHIHonda_SURFEXTtest.csv", sep=";", dec=",",
 append=TRUE, row.names="II_B_p-value", col.names=FALSE)
#write.table(TII_H[["p.value"]], file="C:/Users/saart/Documents/thesis_scores/UHIHonda_SURFEXTtest.csv", sep=";", dec=",",
 append=TRUE, row.names="II_H_p-value", col.names=FALSE)
write.table(T565_100[["p.value"]], file="C:/Users/saart/Documents/thesis_scores/UHIHonda_SURFEXTtest.csv", sep=";", dec=",",
 append=TRUE, row.names="565_100_p-value", col.names=FALSE)
write.table(T565_1000[["p.value"]], file="C:/Users/saart/Documents/thesis_scores/UHIHonda_SURFEXTtest.csv", sep=";", dec=",",
 append=TRUE, row.names="565_1000_p-value", col.names=FALSE)
write.table(T100_1000[["p.value"]], file="C:/Users/saart/Documents/thesis_scores/UHIHonda_SURFEXTtest.csv", sep=";", dec=",",
 append=TRUE, row.names="100_1000_p-value", col.names=FALSE)
```

```
write.table(T565_B[["p.value"]], file="C:/Users/saart/Documents/thesis_scores/UHIHonda_SURFEXTtest.csv", sep=";", dec=",",
 append=TRUE, row.names="565_B_p-value", col.names=FALSE)
write.table(T565_H[["p.value"]], file="C:/Users/saart/Documents/thesis_scores/UHIHonda_SURFEXTtest.csv", sep=";", dec=",",
 append=TRUE, row.names="565_H_p-value", col.names=FALSE)
write.table(TB_H[["p.value"]], file="C:/Users/saart/Documents/thesis_scores/UHIHonda_SURFEXTtest.csv", sep=";", dec=",",
 append=TRUE, row.names="B_H_p-value", col.names=FALSE)


#Melle


#Planten
TI=t.test(PlantenIOBS,PlantenISURFEX,paired=TRUE)
print("result T_Test ECOCLIMAP-I:")
print(TI)
TII=t.test(PlantenIIOBS,PlantenIISURFEX,paired=TRUE)
T100=t.test(Planten100OBS,Planten100SURFEX,paired=TRUE)
T565=t.test(Planten565OBS,Planten565SURFEX,paired=TRUE)
T1000=t.test(Planten1000OBS,Planten1000SURFEX,paired=TRUE)
TB=t.test(PlantenBOBS,PlantenBSURFEX,paired=TRUE)
TH=t.test(PlantenHOBS,PlantenHSURFEX,paired=TRUE)

write.table(TI[["p.value"]], file="C:/Users/saart/Documents/thesis_scores/UHIPlanten_OBSTtest.csv", sep=";", dec=",",
 append=TRUE, row.names="IOBS_SURFEX_p-value", col.names=FALSE)
write.table(TII[["p.value"]], file="C:/Users/saart/Documents/thesis_scores/UHIPlanten_OBSTtest.csv", sep=";", dec=",",
 append=TRUE, row.names="IIOBS_SURFEX_p-value", col.names=FALSE)
write.table(T100[["p.value"]], file="C:/Users/saart/Documents/thesis_scores/UHIPlanten_OBSTtest.csv", sep=";", dec=",",
 append=TRUE, row.names="100OBS_SURFEX_p-value", col.names=FALSE)
write.table(T565[["p.value"]], file="C:/Users/saart/Documents/thesis_scores/UHIPlanten_OBSTtest.csv", sep=";", dec=",",
 append=TRUE, row.names="565OBS_SURFEX_p-value", col.names=FALSE)
write.table(T1000[["p.value"]], file="C:/Users/saart/Documents/thesis_scores/UHIPlanten_OBSTtest.csv", sep=";", dec=",",
 append=TRUE, row.names="1000OBS_SURFEX_p-value", col.names=FALSE)
write.table(TB[["p.value"]], file="C:/Users/saart/Documents/thesis_scores/UHIPlanten_OBSTtest.csv", sep=";", dec=",",
 append=TRUE, row.names="BOBS_SURFEX_p-value", col.names=FALSE)
write.table(TH[["p.value"]], file="C:/Users/saart/Documents/thesis_scores/UHIPlanten_OBSTtest.csv", sep=";", dec=",",
 append=TRUE, row.names="HOBS_SURFEX_p-value", col.names=FALSE)
```

```
## T-Test between model runs
TI_II=t.test(PlantenISURFEX, PlantenIISURFEX, paired=TRUE)
TI_100=t.test(PlantenISURFEX, Planten100SURFEX, paired=TRUE)
TI_565=t.test(PlantenISURFEX, Planten565SURFEX, paired=TRUE)
TI_1000=t.test(PlantenISURFEX, Planten1000SURFEX, paired=TRUE)
#TI_B=t.test(PlantenISURFEX, PlantenBSURFEX, paired=TRUE)
#TI_H=t.test(PlantenISURFEX, PlantenHSURFEX, paired=TRUE)
TII_100=t.test(PlantenIISURFEX, Planten100SURFEX, paired=TRUE)
TII_565=t.test(PlantenIISURFEX, Planten565SURFEX, paired=TRUE)
TII_1000=t.test(PlantenIISURFEX, Planten1000SURFEX, paired=TRUE)
#TII_B=t.test(PlantenIISURFEX, PlantenBSURFEX, paired=TRUE)
#TII_H=t.test(PlantenIISURFEX, PlantenHSURFEX, paired=TRUE)
T565_100=t.test(Planten565SURFEX, Planten100SURFEX, paired=TRUE)
T565_1000=t.test(Planten565SURFEX, Planten1000SURFEX, paired=TRUE)
T100_1000=t.test(Planten100SURFEX, Planten1000SURFEX, paired=TRUE)

T565_B=t.test(Planten565SURFEX, PlantenBSURFEX, paired=TRUE)
T565_H=t.test(Planten565SURFEX, PlantenHSURFEX, paired=TRUE)
TB_H=t.test(PlantenBSURFEX, PlantenHSURFEX, paired=TRUE)

write.table(TI_II[["p.value"]], file="C:/Users/saart/Documents/thesis_scores/UHIPlanten_SURFEXTtest.csv", sep=";", dec=",",
 append=TRUE, row.names="I_II_p-value", col.names=FALSE)
write.table(TI_100[["p.value"]], file="C:/Users/saart/Documents/thesis_scores/UHIPlanten_SURFEXTtest.csv", sep=";", dec=",",
 append=TRUE, row.names="I_100_p-value", col.names=FALSE)
write.table(TI_565[["p.value"]], file="C:/Users/saart/Documents/thesis_scores/UHIPlanten_SURFEXTtest.csv", sep=";", dec=",",
 append=TRUE, row.names="I_565_p-value", col.names=FALSE)
write.table(TI_1000[["p.value"]], file="C:/Users/saart/Documents/thesis_scores/UHIPlanten_SURFEXTtest.csv", sep=";", dec=",",
 append=TRUE, row.names="I_1000_p-value", col.names=FALSE)
#write.table(TI_B[["p.value"]], file="C:/Users/saart/Documents/thesis_scores/UHIPlanten_SURFEXTtest.csv", sep=";", dec=",",
 append=TRUE, row.names="I_B_p-value", col.names=FALSE)
#write.table(TI_H[["p.value"]], file="C:/Users/saart/Documents/thesis_scores/UHIPlanten_SURFEXTtest.csv", sep=";", dec=",",
 append=TRUE, row.names="I_H_p-value", col.names=FALSE)
write.table(TII_100[["p.value"]], file="C:/Users/saart/Documents/thesis_scores/UHIPlanten_SURFEXTtest.csv", sep=";", dec=",",
 append=TRUE, row.names="II_100_p-value", col.names=FALSE)
write.table(TII_565[["p.value"]], file="C:/Users/saart/Documents/thesis_scores/UHIPlanten_SURFEXTtest.csv", sep=";", dec=",",
 append=TRUE, row.names="II_565_p-value", col.names=FALSE)
write.table(TII_1000[["p.value"]], file="C:/Users/saart/Documents/thesis_scores/UHIPlanten_SURFEXTtest.csv", sep=";", dec=",",
```

```
 append=TRUE, row.names="II_1000_p-value", col.names=FALSE)
#write.table(TII_B[["p.value"]], file="C:/Users/saart/Documents/thesis_scores/UHIPlanten_SURFEXTtest.csv", sep=";", dec=",",
 append=TRUE, row.names="II_B_p-value", col.names=FALSE)
#write.table(TII_H[["p.value"]], file="C:/Users/saart/Documents/thesis_scores/UHIPlanten_SURFEXTtest.csv", sep=";", dec=",",
 append=TRUE, row.names="II_H_p-value", col.names=FALSE)
write.table(T565_100[["p.value"]], file="C:/Users/saart/Documents/thesis_scores/UHIPlanten_SURFEXTtest.csv", sep=";", dec=",",
 append=TRUE, row.names="565_100_p-value", col.names=FALSE)
write.table(T565_1000[["p.value"]], file="C:/Users/saart/Documents/thesis_scores/UHIPlanten_SURFEXTtest.csv", sep=";", dec=",",
 append=TRUE, row.names="565_1000_p-value", col.names=FALSE)
write.table(T100_1000[["p.value"]], file="C:/Users/saart/Documents/thesis_scores/UHIPlanten_SURFEXTtest.csv", sep=";", dec=",",
 append=TRUE, row.names="100_1000_p-value", col.names=FALSE)

write.table(T565_B[["p.value"]], file="C:/Users/saart/Documents/thesis_scores/UHIPlanten_SURFEXTtest.csv", sep=";", dec=",",
 append=TRUE, row.names="565_B_p-value", col.names=FALSE)
write.table(T565_H[["p.value"]], file="C:/Users/saart/Documents/thesis_scores/UHIPlanten_SURFEXTtest.csv", sep=";", dec=",",
 append=TRUE, row.names="565_H_p-value", col.names=FALSE)
write.table(TB_H[["p.value"]], file="C:/Users/saart/Documents/thesis_scores/UHIPlanten_SURFEXTtest.csv", sep=";", dec=",",
 append=TRUE, row.names="B_H_p-value", col.names=FALSE)



#Provincie
TI=t.test(ProvincieIOBS,ProvincieISURFEX,paired=TRUE)
print("result T_Test ECOCLIMAP-I:")
print(TI)
TII=t.test(ProvincieIIOBS,ProvincieIISURFEX,paired=TRUE)
T100=t.test(Provincie100OBS,Provincie100SURFEX,paired=TRUE)
T565=t.test(Provincie565OBS,Provincie565SURFEX,paired=TRUE)
T1000=t.test(Provincie1000OBS,Provincie1000SURFEX,paired=TRUE)
TB=t.test(ProvincieBOBS,ProvincieBSURFEX,paired=TRUE)
TH=t.test(ProvincieHOBS,ProvincieHSURFEX,paired=TRUE)

write.table(TI[["p.value"]], file="C:/Users/saart/Documents/thesis_scores/UHIProvincie_OBSTtest.csv", sep=";", dec=",",
 append=TRUE, row.names="IOBS_SURFEX_p-value", col.names=FALSE)
write.table(TII[["p.value"]], file="C:/Users/saart/Documents/thesis_scores/UHIProvincie_OBSTtest.csv", sep=";", dec=",",
 append=TRUE, row.names="IIOBS_SURFEX_p-value", col.names=FALSE)
write.table(T100[["p.value"]], file="C:/Users/saart/Documents/thesis_scores/UHIProvincie_OBSTtest.csv", sep=";", dec=",",
 append=TRUE, row.names="100OBS_SURFEX_p-value", col.names=FALSE)
write.table(T565[["p.value"]], file="C:/Users/saart/Documents/thesis_scores/UHIProvincie_OBSTtest.csv", sep=";", dec=",",
```

```
 append=TRUE, row.names="565OBS_SURFEX_p-value", col.names=FALSE)
write.table(T1000[["p.value"]], file="C:/Users/saart/Documents/thesis_scores/UHIProvincie_OBSTtest.csv", sep=";", dec=",",
 append=TRUE, row.names="1000OBS_SURFEX_p-value", col.names=FALSE)
write.table(TB[["p.value"]], file="C:/Users/saart/Documents/thesis_scores/UHIProvincie_OBSTtest.csv", sep=";", dec=",",
 append=TRUE, row.names="BOBS_SURFEX_p-value", col.names=FALSE)
write.table(TH[["p.value"]], file="C:/Users/saart/Documents/thesis_scores/UHIProvincie_OBSTtest.csv", sep=";", dec=",",
 append=TRUE, row.names="HOBS_SURFEX_p-value", col.names=FALSE)

## T-Test between model runs
TI_II=t.test(ProvincieISURFEX, ProvincieIISURFEX, paired=TRUE)
TI_100=t.test(ProvincieISURFEX, Provincie100SURFEX, paired=TRUE)
TI_565=t.test(ProvincieISURFEX, Provincie565SURFEX, paired=TRUE)
TI_1000=t.test(ProvincieISURFEX, Provincie1000SURFEX, paired=TRUE)
#TI_B=t.test(ProvincieISURFEX, ProvincieBSURFEX, paired=TRUE)
#TI_H=t.test(ProvincieISURFEX, ProvincieHSURFEX, paired=TRUE)
TII_100=t.test(ProvincieIISURFEX, Provincie100SURFEX, paired=TRUE)
TII_565=t.test(ProvincieIISURFEX, Provincie565SURFEX, paired=TRUE)
TII_1000=t.test(ProvincieIISURFEX, Provincie1000SURFEX, paired=TRUE)
#TII_B=t.test(ProvincieIISURFEX, ProvincieBSURFEX, paired=TRUE)
#TII_H=t.test(ProvincieIISURFEX, ProvincieHSURFEX, paired=TRUE)
T565_100=t.test(Provincie565SURFEX, Provincie100SURFEX, paired=TRUE)
T565_1000=t.test(Provincie565SURFEX, Provincie1000SURFEX, paired=TRUE)
T100_1000=t.test(Provincie100SURFEX, Provincie1000SURFEX, paired=TRUE)

T565_B=t.test(Provincie565SURFEX, ProvincieBSURFEX, paired=TRUE)
T565_H=t.test(Provincie565SURFEX, ProvincieHSURFEX, paired=TRUE)
TB_H=t.test(ProvincieBSURFEX, ProvincieHSURFEX, paired=TRUE)

write.table(TI_II[["p.value"]], file="C:/Users/saart/Documents/thesis_scores/UHIProvincie_SURFEXTtest.csv", sep=";", dec=",",
 append=TRUE, row.names="I_II_p-value", col.names=FALSE)
write.table(TI_100[["p.value"]], file="C:/Users/saart/Documents/thesis_scores/UHIProvincie_SURFEXTtest.csv", sep=";", dec=",",
 append=TRUE, row.names="I_100_p-value", col.names=FALSE)
write.table(TI_565[["p.value"]], file="C:/Users/saart/Documents/thesis_scores/UHIProvincie_SURFEXTtest.csv", sep=";", dec=",",
 append=TRUE, row.names="I_565_p-value", col.names=FALSE)
write.table(TI_1000[["p.value"]], file="C:/Users/saart/Documents/thesis_scores/UHIProvincie_SURFEXTtest.csv", sep=";", dec=",",
 append=TRUE, row.names="I_1000_p-value", col.names=FALSE)
#write.table(TI_B[["p.value"]], file="C:/Users/saart/Documents/thesis_scores/UHIProvincie_SURFEXTtest.csv", sep=";", dec=",",
```

```
 append=TRUE, row.names="I_B_p-value", col.names=FALSE)
#write.table(TI_H[["p.value"]], file="C:/Users/saart/Documents/thesis_scores/UHIProvincie_SURFEXTtest.csv", sep=";", dec=",",
 append=TRUE, row.names="I_H_p-value", col.names=FALSE)
write.table(TII_100[["p.value"]], file="C:/Users/saart/Documents/thesis_scores/UHIProvincie_SURFEXTtest.csv", sep=";", dec=",",
 append=TRUE, row.names="II_100_p-value", col.names=FALSE)
write.table(TII_565[["p.value"]], file="C:/Users/saart/Documents/thesis_scores/UHIProvincie_SURFEXTtest.csv", sep=";", dec=",",
 append=TRUE, row.names="II_565_p-value", col.names=FALSE)
write.table(TII_1000[["p.value"]], file="C:/Users/saart/Documents/thesis_scores/UHIProvincie_SURFEXTtest.csv", sep=";", dec=",",
 append=TRUE, row.names="II_1000_p-value", col.names=FALSE)
#write.table(TII_B[["p.value"]], file="C:/Users/saart/Documents/thesis_scores/UHIProvincie_SURFEXTtest.csv", sep=";", dec=",",
 append=TRUE, row.names="II_B_p-value", col.names=FALSE)
#write.table(TII_H[["p.value"]], file="C:/Users/saart/Documents/thesis_scores/UHIProvincie_SURFEXTtest.csv", sep=";", dec=",",
 append=TRUE, row.names="II_H_p-value", col.names=FALSE)
write.table(T565_100[["p.value"]], file="C:/Users/saart/Documents/thesis_scores/UHIProvincie_SURFEXTtest.csv", sep=";", dec=",",
 append=TRUE, row.names="565_100_p-value", col.names=FALSE)
write.table(T565_1000[["p.value"]], file="C:/Users/saart/Documents/thesis_scores/UHIProvincie_SURFEXTtest.csv", sep=";", dec=",",
 append=TRUE, row.names="565_1000_p-value", col.names=FALSE)
write.table(T100_1000[["p.value"]], file="C:/Users/saart/Documents/thesis_scores/UHIProvincie_SURFEXTtest.csv", sep=";", dec=",",
 append=TRUE, row.names="100_1000_p-value", col.names=FALSE)

write.table(T565_B[["p.value"]], file="C:/Users/saart/Documents/thesis_scores/UHIProvincie_SURFEXTtest.csv", sep=";", dec=",",
 append=TRUE, row.names="565_B_p-value", col.names=FALSE)
write.table(T565_H[["p.value"]], file="C:/Users/saart/Documents/thesis_scores/UHIProvincie_SURFEXTtest.csv", sep=";", dec=",",
 append=TRUE, row.names="565_H_p-value", col.names=FALSE)
write.table(TB_H[["p.value"]], file="C:/Users/saart/Documents/thesis_scores/UHIProvincie_SURFEXTtest.csv", sep=";", dec=",",
 append=TRUE, row.names="B_H_p-value", col.names=FALSE)



#Wondel
TI=t.test(WondelIOBS,WondelISURFEX,paired=TRUE)
print("result T_Test ECOCLIMAP-I:")
print(TI)
TII=t.test(WondelIIOBS,WondelIISURFEX,paired=TRUE)
T100=t.test(Wondel100OBS,Wondel100SURFEX,paired=TRUE)
T565=t.test(Wondel565OBS,Wondel565SURFEX,paired=TRUE)
T1000=t.test(Wondel1000OBS,Wondel1000SURFEX,paired=TRUE)
TB=t.test(WondelBOBS,WondelBSURFEX,paired=TRUE)
TH=t.test(WondelHOBS,WondelHSURFEX,paired=TRUE)
```

```
write.table(TI[["p.value"]], file="C:/Users/saart/Documents/thesis_scores/UHIWondel_OBSTtest.csv", sep=";", dec=",",
 append=TRUE, row.names="IOBS_SURFEX_p-value", col.names=FALSE)
write.table(TII[["p.value"]], file="C:/Users/saart/Documents/thesis_scores/UHIWondel_OBSTtest.csv", sep=";", dec=",",
 append=TRUE, row.names="IIOBS_SURFEX_p-value", col.names=FALSE)
write.table(T100[["p.value"]], file="C:/Users/saart/Documents/thesis_scores/UHIWondel_OBSTtest.csv", sep=";", dec=",",
 append=TRUE, row.names="100OBS_SURFEX_p-value", col.names=FALSE)
write.table(T565[["p.value"]], file="C:/Users/saart/Documents/thesis_scores/UHIWondel_OBSTtest.csv", sep=";", dec=",",
 append=TRUE, row.names="565OBS_SURFEX_p-value", col.names=FALSE)
write.table(T1000[["p.value"]], file="C:/Users/saart/Documents/thesis_scores/UHIWondel_OBSTtest.csv", sep=";", dec=",",
 append=TRUE, row.names="1000OBS_SURFEX_p-value", col.names=FALSE)
write.table(TB[["p.value"]], file="C:/Users/saart/Documents/thesis_scores/UHIWondel_OBSTtest.csv", sep=";", dec=",",
 append=TRUE, row.names="BOBS_SURFEX_p-value", col.names=FALSE)
write.table(TH[["p.value"]], file="C:/Users/saart/Documents/thesis_scores/UHIWondel_OBSTtest.csv", sep=";", dec=",",
 append=TRUE, row.names="HOBS_SURFEX_p-value", col.names=FALSE)

## T-Test between model runs
TI_II=t.test(WondelISURFEX, WondelIISURFEX, paired=TRUE)
TI_100=t.test(WondelISURFEX, Wondel100SURFEX, paired=TRUE)
TI_565=t.test(WondelISURFEX, Wondel565SURFEX, paired=TRUE)
TI_1000=t.test(WondelISURFEX, Wondel1000SURFEX, paired=TRUE)
#TI_B=t.test(WondelISURFEX, WondelBSURFEX, paired=TRUE)
#TI_H=t.test(WondelISURFEX, WondelHSURFEX, paired=TRUE)
TII_100=t.test(WondelIISURFEX, Wondel100SURFEX, paired=TRUE)
TII_565=t.test(WondelIISURFEX, Wondel565SURFEX, paired=TRUE)
TII_1000=t.test(WondelIISURFEX, Wondel1000SURFEX, paired=TRUE)
#TII_B=t.test(WondelIISURFEX, WondelBSURFEX, paired=TRUE)
#TII_H=t.test(WondelIISURFEX, WondelHSURFEX, paired=TRUE)
T565_100=t.test(Wondel565SURFEX, Wondel100SURFEX, paired=TRUE)
T565_1000=t.test(Wondel565SURFEX, Wondel1000SURFEX, paired=TRUE)
T100_1000=t.test(Wondel100SURFEX, Wondel1000SURFEX, paired=TRUE)

T565_B=t.test(Wondel565SURFEX, WondelBSURFEX, paired=TRUE)
T565_H=t.test(Wondel565SURFEX, WondelHSURFEX, paired=TRUE)
TB_H=t.test(WondelBSURFEX, WondelHSURFEX, paired=TRUE)
```

```
write.table(TI_II[["p.value"]], file="C:/Users/saart/Documents/thesis_scores/UHIWondel_SURFEXTtest.csv", sep=";", dec=",",
 append=TRUE, row.names="I_II_p-value", col.names=FALSE)
write.table(TI_100[["p.value"]], file="C:/Users/saart/Documents/thesis_scores/UHIWondel_SURFEXTtest.csv", sep=";", dec=",",
 append=TRUE, row.names="I_100_p-value", col.names=FALSE)
write.table(TI_565[["p.value"]], file="C:/Users/saart/Documents/thesis_scores/UHIWondel_SURFEXTtest.csv", sep=";", dec=",",
 append=TRUE, row.names="I_565_p-value", col.names=FALSE)
write.table(TI_1000[["p.value"]], file="C:/Users/saart/Documents/thesis_scores/UHIWondel_SURFEXTtest.csv", sep=";", dec=",",
 append=TRUE, row.names="I_1000_p-value", col.names=FALSE)
#write.table(TI_B[["p.value"]], file="C:/Users/saart/Documents/thesis_scores/UHIWondel_SURFEXTtest.csv", sep=";", dec=",",
 append=TRUE, row.names="I_B_p-value", col.names=FALSE)
#write.table(TI_H[["p.value"]], file="C:/Users/saart/Documents/thesis_scores/UHIWondel_SURFEXTtest.csv", sep=";", dec=",",
 append=TRUE, row.names="I_H_p-value", col.names=FALSE)
write.table(TII_100[["p.value"]], file="C:/Users/saart/Documents/thesis_scores/UHIWondel_SURFEXTtest.csv", sep=";", dec=",",
 append=TRUE, row.names="II_100_p-value", col.names=FALSE)
write.table(TII_565[["p.value"]], file="C:/Users/saart/Documents/thesis_scores/UHIWondel_SURFEXTtest.csv", sep=";", dec=",",
 append=TRUE, row.names="II_565_p-value", col.names=FALSE)
write.table(TII_1000[["p.value"]], file="C:/Users/saart/Documents/thesis_scores/UHIWondel_SURFEXTtest.csv", sep=";", dec=",",
 append=TRUE, row.names="II_1000_p-value", col.names=FALSE)
#write.table(TII_B[["p.value"]], file="C:/Users/saart/Documents/thesis_scores/UHIWondel_SURFEXTtest.csv", sep=";", dec=",",
 append=TRUE, row.names="II_B_p-value", col.names=FALSE)
#write.table(TII_H[["p.value"]], file="C:/Users/saart/Documents/thesis_scores/UHIWondel_SURFEXTtest.csv", sep=";", dec=",",
 append=TRUE, row.names="II_H_p-value", col.names=FALSE)
write.table(T565_100[["p.value"]], file="C:/Users/saart/Documents/thesis_scores/UHIWondel_SURFEXTtest.csv", sep=";", dec=",",
 append=TRUE, row.names="565_100_p-value", col.names=FALSE)
write.table(T565_1000[["p.value"]], file="C:/Users/saart/Documents/thesis_scores/UHIWondel_SURFEXTtest.csv", sep=";", dec=",",
 append=TRUE, row.names="565_1000_p-value", col.names=FALSE)
write.table(T100_1000[["p.value"]], file="C:/Users/saart/Documents/thesis_scores/UHIWondel_SURFEXTtest.csv", sep=";", dec=",",
 append=TRUE, row.names="100_1000_p-value", col.names=FALSE)

write.table(T565_B[["p.value"]], file="C:/Users/saart/Documents/thesis_scores/UHIWondel_SURFEXTtest.csv", sep=";", dec=",",
 append=TRUE, row.names="565_B_p-value", col.names=FALSE)
write.table(T565_H[["p.value"]], file="C:/Users/saart/Documents/thesis_scores/UHIWondel_SURFEXTtest.csv", sep=";", dec=",",
 append=TRUE, row.names="565_H_p-value", col.names=FALSE)
write.table(TB_H[["p.value"]], file="C:/Users/saart/Documents/thesis_scores/UHIWondel_SURFEXTtest.csv", sep=";", dec=",",
 append=TRUE, row.names="B_H_p-value", col.names=FALSE)


###### END ######
```

Annex VII: Observed temperatures and UHI averaged over daytime and nighttime

Table 1: Average temperature during the months July and August of 2016. Day time is defined form 5 UTC till 19 UTC, night time is defined form 20 UTC till 4 UTC, according to Caluwaerts *et al*. (2018).

	HONDA	MELLE	PLANTEN-TUIN	PROVINCIE-HUIS	SINT-BAVO	WONDELGEM
TEMPERATURE DURING DAY TIME (°C)	20,7	20,3	20,1	21,3	20,9	20,6
TEMPERATURE DURING NIGHT TIME (°C)	17,65	15,85	16,97	17,80	17,80	16,61

Table 2: Average UHI during the months July and August of 2016. Day time is defined form 5 UTC till 19 UTC, night time is defined form 20 UTC till 4 UTC, according to Caluwaerts *et al*. (2018).

	HONDA	PLANTENTUIN	PROVINCIEHUIS	SINT-BAVO	WONDELGEM
UHI DURING DAY TIME (°C)	0,4	-0,2	0,9	0,6	0,2
UHI DURING NIGHT TIME (°C)	1,8	1,1	1,9	1,9	0,8

ANNEX VIII: Model errors for different tuning parameters

Table 1: Model errors on temperatures of Melle for different values of the parameter XHUG_ROOT

XHUG_ROOT	1,00 (default)	0,50	0,25	0,10	0,01
INDEX OF AGREEMENT (%)	0,85	0,86	0,86	0,86	0,86
RMSE (°C)	3,38	3,25	3,24	3,23	3,23
BIAS (°C)	-1,58	-1,17	-1,10	-1,09	-1,08

Table 2: Error on modelled UHI of Sint-Bavo for different values of the parameter XHUG_ROOT

XHUG_ROOT	1,00 (default)	0,50	0,01
INDEX OF AGREEMENT (%)	0,49	0,51	0,52
RMSE (°C)	2,86	2,70	2,68
BIAS (°C)	1,72	1,35	1,28

ANNEX IX: T-tests between different model runs

Table 1: P-values of T-tests between the temperatures of model runs with a different parameterisation. Non-coloured values indicate that the temperatures series differ significantly from each other at a significance level of 99%. Red coloured values indicate they do not. The value 'NA' is obtained when two identical temperatures series are compared.

	SINT-BAVO	HONDA	MELLE	PLANTENTUIN	PROVINCIEHUIS	WONDELGEM
ECOCLIMAP-I & ECOCLIMAP-II	NA	3,37E-73	1,20E-56	5,23E-06	NA	3,59E-95
ECOCLIMAP-I & 100 m buffer	1,72E-12	1,10E-14	4,80E-16	1,83E-95	7,22E-12	1,00E-116
ECOCLIMAP-I & 565 m buffer	6,78E-73	2,64E-181	1,91E-46	7,62E-28	2,35E-40	1,85E-80
ECOCLIMAP-I & 1000 m buffer	1,79E-66	1,14E-204	1,91E-46	1,06E-41	1,36E-66	1,70E-79
ECOCLIMAP-II & 100 m buffer	1,72E-12	8,35E-99	1,03E-60	5,89E-103	7,22E-12	2,23E-117
ECOCLIMAP-II & 565 m buffer	6,78E-73	0,000275	2,19E-41	2,53E-26	2,35E-40	4,58E-75
ECOCLIMAP-II & 1000 m buffer	1,79E-66	1,95E-11	2,19E-41	7,76E-37	1,36E-66	9,49E-74
565 m buffer & 100 m buffer	6,03E-192	9,52E-190	8,88E-115	1,54E-132	7,63E-224	1,38E-193
565 m buffer & 1000 m buffer	0,002066	4,15E-248	NA	0,002108	3,80E-165	3,53E-111
100 m buffer & 1000 m buffer	6,50E-224	1,83E-224	8,88E-115	1,04E-99	3,41E-235	9,33E-190
565 m buffer & built fraction	1,81E-47	0,059163	0,60468	6,76E-44	3,02E-48	0,121439
565 m buffer & building height	5,68E-09	6,40E-09	5,24E-10	5,24E-09	5,24E-09	1,29E-10
built fraction & building height	1,04E-25	0,159467	4,35E-07	7,63E-14	7,12E-27	1,51E-48

Table 2: P-values of T-tests between the bias of the temperatures obtained from model runs with a different parameterisation. Non-coloured values indicate that the temperatures series differ significantly from each other at a significance level of 99%. Red coloured values indicate they do not. The value 'NA' is obtained when two identical temperatures series are compared.

	SINT-BAVO	HONDA	MELLE	PLANTENTUIN	PROVINCIEHUIS	WONDELGEM
ECOCLIMAP-I & ECOCLIMAP-II	NA	5,75E-204	7,41E-176	3,92E-238	NA	3,81E-199
ECOCLIMAP-I & 100 m buffer	1,38E-207	3,90E-175	5,52E-251	9,30E-190	6,04E-192	2,34E-187
ECOCLIMAP-I & 565 m buffer	7,64E-185	6,03E-172	3,62E-225	3,13E-169	2,55E-183	1,10E-181
ECOCLIMAP-I & 1000 m buffer	2,27E-187	3,99E-175	3,62E-225	5,52E-154	2,42E-187	5,02E-187
ECOCLIMAP-II & 100 m buffer	1,38E-207	4,98E-208	1,20E-153	2,02E-186	6,04E-192	9,75E-186
ECOCLIMAP-II & 565 m buffer	7,64E-185	3,31E-260	4,30E-136	1,55E-145	2,55E-183	6,41E-175
ECOCLIMAP-II & 1000 m buffer	2,27E-187	1,14E-31	4,30E-136	4,23E-127	2,42E-187	8,95E-184
565 m buffer & 100 m buffer	2,75E-170	6,74E-171	6,69E-195	1,77E-195	2,39E-174	1,85E-190
565 m buffer & 1000 m buffer	1,16E-22	1,54E-181	NA	9,54E-23	5,36E-192	1,64E-182
100 m buffer & 1000 m buffer	2,33E-174	6,96E-175	6,69E-195	1,15E-199	1,33E-184	1,08E-187
565 m buffer & built fraction	1,11E-212	1,86E-189	3,18E-133	4,35E-212	5,14E-213	7,25E-187
565 m buffer & building height	3,01E-202	1,34E-202	1,92E-230	1,32E-204	1,65E-200	6,80E-184
built fraction & building height	3,49E-211	0,066689	5,61E-205	2,62E-209	1,39E-210	4,70E-215

Table 3: P-values of T-tests between the RMSE of the temperatures obtained from model runs with a different parameterisation. Non-coloured values indicate that the temperatures series differ significantly from each other at a significance level of 99%. Red coloured values indicate they do not. The value 'NA' is obtained when two identical temperatures series are compared.

	SINT-BAVO	HONDA	MELLE	PLANTENTUIN	PROVINCIEHUIS	WONDELGEM
ECOCLIMAP-I & ECOCLIMAP-II	NA	1,17E-30	3,94E-159	4,03E-237	NA	5,37E-164
ECOCLIMAP-I & 100 m buffer	3,53E-184	4,59E-123	1,11E-205	5,78E-15	2,52E-191	1,38E-23
ECOCLIMAP-I & 565 m buffer	1,28E-181	6,17E-17	6,06E-213	4,11E-06	6,97E-190	1,63E-181
ECOCLIMAP-I & 1000 m buffer	1,68E-182	5,92E-71	6,06E-213	3,79E-08	1,20E-189	1,91E-77
ECOCLIMAP-II & 100 m buffer	3,53E-184	5,03E-185	6,65E-143	0,000138	2,52E-191	8,34E-61
ECOCLIMAP-II & 565 m buffer	1,28E-181	1,60E-84	2,62E-124	3,08E-53	6,97E-190	1,38E-195
ECOCLIMAP-II & 1000 m buffer	1,68E-182	1,94E-26	2,62E-124	4,35E-80	1,20E-189	9,29E-28
565 m buffer & 100 m buffer	3,84E-08	2,56E-64	6,28E-203	2,33E-21	4,21E-31	1,02E-217
565 m buffer & 1000 m buffer	3,82E-142	2,08E-136	NA	0,289029	3,36E-123	3,24E-238
100 m buffer & 1000 m buffer	5,64E-27	1,39E-115	6,28E-203	8,84E-17	6,10E-83	4,61E-163
565 m buffer & built fraction	4,50E-60	9,34E-205	1,25E-64	8,80E-127	5,51E-66	7,13E-237
565 m buffer & building height	3,63E-206	1,08E-210	9,59E-161	5,43E-167	4,62E-222	1,16E-237
built fraction & building height	1,30E-198	4,46E-210	7,51E-05	2,08E-207	1,91E-205	3,13E-56

Table 4: T-tests between the index of agreement of the temperatures obtained from model runs with a different parameterisation. Red indicates that the runs do not differ significantly from each other and non-coloured values indicate that they do differ significantly from each other with a significance level of 99%. The value 'NA' is obtained when all the values in the indexes of agreement are the same and thus when the two runs produce completely the same indexes of agreement.

	SINT-BAVO	HONDA	MELLE	PLANTENTUIN	PROVINCIEHUIS	WONDELGEM
ECOCLIMAP-I & ECOCLIMAP-II	NA	3,87E-198	2,32E-176	4,70E-257	NA	4,70E-196
ECOCLIMAP-I & 100 m buffer	3,00E-211	2,05E-171	1,59E-268	4,18E-183	1,88E-180	1,20E-179
ECOCLIMAP-I & 565 m buffer	1,23E-174	2,37E-160	3,48E-232	2,43E-164	5,66E-172	1,51E-216
ECOCLIMAP-I & 1000 m buffer	4,85E-178	7,86E-164	3,48E-232	1,55E-144	9,50E-178	2,01E-181
ECOCLIMAP-II & 100 m buffer	3,00E-211	3,76E-201	1,98E-150	2,45E-178	1,88E-180	2,10E-177
ECOCLIMAP-II & 565 m buffer	1,23E-174	3,59E-240	2,82E-132	1,08E-134	5,66E-172	5,82E-214
ECOCLIMAP-II & 1000 m buffer	4,85E-178	2,15E-60	2,82E-132	5,96E-116	9,50E-178	2,20E-177
565 m buffer & 100 m buffer	5,93E-157	4,91E-158	1,06E-189	7,52E-188	9,36E-162	1,03E-195
565 m buffer & 1000 m buffer	3,21E-14	4,31E-171	NA	2,85E-20	8,71E-184	9,09E-202
100 m buffer & 1000 m buffer	1,99E-161	1,16E-162	1,06E-189	2,34E-194	6,00E-174	2,94E-177
565 m buffer & built fraction	9,43E-208	8,87E-176	8,60E-160	1,51E-206	1,92E-208	1,35E-201
565 m buffer & building height	1,09E-202	2,10E-202	3,57E-239	1,59E-204	1,10E-199	1,69E-201
built fraction & building height	4,00E-213	7,13E-39	3,54E-198	4,10E-212	2,78E-212	2,30E-213

Table 5: T-tests between the UHI intensities from model runs with a different parameterisation. Red indicates that the runs do not differ significantly from each other and non-coloured values indicate that they do differ significantly from each other with a significance level of 99%.

	SINT-BAVO	HONDA	PLANTENTUIN	PROVINCIEHUIS	WONDELGEM
ECOCLIMAP-I & ECOCLIMAP-II	1,20E-56	3,65E-73	4,00E-43	1,20E-56	3,78E-68
ECOCLIMAP-I & 100 m buffer	2,33E-14	5,75E-17	3,55E-87	2,48E-14	5,16E-108
ECOCLIMAP-I & 565 m buffer	2,11E-73	8,48E-179	4,95E-41	7,56E-47	1,74E-77
ECOCLIMAP-I & 1000 m buffer	1,70E-67	5,30E-201	3,38E-58	1,35E-67	1,04E-76
ECOCLIMAP-II & 100 m buffer	0,458959	1,19E-101	6,70E-96	0,001538	1,68E-120
ECOCLIMAP-II & 565 m buffer	1,27E-60	1,21E-08	0,182748	7,76E-22	1,08E-67
ECOCLIMAP-II & 1000 m buffer	4,55E-55	0,000412	0,970381	3,30E-55	1,94E-65
565 m buffer & 100 m buffer	4,91E-231	7,20E-207	4,11E-135	4,91E-248	3,02E-210
565 m buffer & 1000 m buffer	0,002066	4,15E-248	0,002108	3,80E-165	3,53E-111
100 m buffer & 1000 m buffer	1,68E-247	1,25E-232	1,74E-97	8,35E-218	3,90E-205
565 m buffer & built fraction	3,31E-27	0,03533	1,51E-06	3,68E-31	0,001716
565 m buffer & building height	3,13E-09	3,95E-09	2,30E-09	3,16E-09	3,75E-10
built fraction & building height	1,04E-30	0,071828	2,61E-20	4,37E-31	8,62E-21

Table 6: T-tests between the bias of UHI intensities from model runs with a different parameterisation. Red indicates that the runs do not differ significantly from each other and non-coloured values indicate that they do differ significantly from each other with a significance level of 99%.

	SINT-BAVO	HONDA	PLANTENTUIN	PROVINCIEHUIS	WONDELGEM
ECOCLIMAP-I & ECOCLIMAP-II	7,41E-176	3,20E-199	7,60E-184	7,41E-176	1,28E-182
ECOCLIMAP-I & 100 m buffer	3,27E-221	1,24E-197	1,43E-195	1,34E-215	7,95E-192
ECOCLIMAP-I & 565 m buffer	8,00E-194	4,10E-178	3,39E-195	1,84E-197	4,18E-192
ECOCLIMAP-I & 1000 m buffer	8,83E-196	3,60E-179	3,40E-187	9,49E-196	1,62E-194
ECOCLIMAP-II & 100 m buffer	9,34E-12	2,49E-199	2,46E-203	6,27E-95	2,41E-197
ECOCLIMAP-II & 565 m buffer	2,51E-206	1,15E-234	6,76E-87	3,77E-229	2,93E-201
ECOCLIMAP-II & 1000 m buffer	2,92E-210	0,000642	2,82E-115	3,47E-210	1,61E-210
565 m buffer & 100 m buffer	6,03E-175	9,28E-173	1,47E-195	6,71E-181	1,12E-189
565 m buffer & 1000 m buffer	1,16E-22	1,54E-181	9,54E-23	5,36E-192	1,64E-182
100 m buffer & 1000 m buffer	3,02E-178	6,90E-176	2,33E-200	2,64E-186	3,57E-186
565 m buffer & built fraction	5,64E-209	2,41E-195	1,55E-195	4,17E-210	8,51E-187
565 m buffer & building height	1,05E-204	2,01E-205	6,11E-208	1,09E-202	9,53E-185
built fraction & building height	1,22E-211	9,32E-26	1,77E-211	5,53E-211	3,03E-214

Table 7: T-tests between the RMSE of UHI intensities from model runs with a different parameterisation. Red indicates that the runs do not differ significantly from each other and non-coloured values indicate that they do differ significantly from each other with a significance level of 99%.

	SINT-BAVO	HONDA	PLANTENTUIN	PROVINCIEHUIS	WONDELGEM
ECOCLIMAP-I & ECOCLIMAP-II	1,34E-196	6,63E-205	5,22E-206	6,09E-199	5,26E-199
ECOCLIMAP-I & 100 m buffer	7,04E-200	6,13E-185	3,31E-216	1,49E-202	1,20E-211
ECOCLIMAP-I & 565 m buffer	7,05E-208	5,64E-222	1,53E-208	2,12E-206	4,18E-215
ECOCLIMAP-I & 1000 m buffer	4,46E-207	1,31E-235	8,97E-206	5,68E-209	1,59E-204
ECOCLIMAP-II & 100 m buffer	1,84E-203	2,78E-223	1,62E-227	1,22E-205	5,48E-230
ECOCLIMAP-II & 565 m buffer	2,02E-219	9,49E-116	2,53E-68	3,92E-216	5,21E-150
ECOCLIMAP-II & 1000 m buffer	3,44E-217	1,14E-55	9,30E-80	1,07E-218	2,08E-215
565 m buffer & 100 m buffer	2,79E-238	6,99E-222	2,01E-224	9,03E-222	1,89E-206
565 m buffer & 1000 m buffer	2,58E-180	2,16E-09	5,26E-220	3,31E-219	1,74E-192
100 m buffer & 1000 m buffer	4,82E-231	1,22E-82	6,40E-225	1,36E-220	3,79E-247
565 m buffer & built fraction	3,74E-223	7,00E-164	9,68E-155	7,25E-203	2,88E-193
565 m buffer & building height	8,83E-203	2,17E-199	1,70E-219	3,19E-207	8,83E-193
built fraction & building height	1,53E-213	2,28E-183	7,05E-223	1,71E-212	5,76E-225

Table 8: T-tests between the index of agreement of UHI intensities from model runs with a different parameterisation. Red indicates that the runs do not differ significantly from each other and non-coloured values indicate that they do differ significantly from each other with a significance level of 99%.

	SINT-BAVO	HONDA	PLANTENTUIN	PROVINCIEHUIS	WONDELGEM
ECOCLIMAP-I & ECOCLIMAP-II	1,20E-177	7,66E-171	1,50E-169	1,85E-178	7,89E-176
ECOCLIMAP-I & 100 m buffer	2,15E-184	1,10E-173	3,82E-177	1,34E-182	3,90E-178
ECOCLIMAP-I & 565 m buffer	8,15E-183	1,83E-185	2,40E-177	1,84E-182	1,12E-133
ECOCLIMAP-I & 1000 m buffer	7,68E-183	1,57E-197	1,12E-174	2,01E-182	6,35E-180
ECOCLIMAP-II & 100 m buffer	8,10E-192	1,59E-166	4,01E-184	2,10E-183	1,09E-179
ECOCLIMAP-II & 565 m buffer	1,38E-185	8,53E-151	1,38E-13	1,87E-183	1,05E-177
ECOCLIMAP-II & 1000 m buffer	6,98E-186	1,22E-139	2,84E-105	4,42E-184	3,33E-186
565 m buffer & 100 m buffer	4,05E-161	1,39E-05	9,20E-177	8,98E-181	2,33E-179
565 m buffer & 1000 m buffer	2,17E-180	1,17E-55	2,46E-191	8,03E-182	1,64E-181
100 m buffer & 1000 m buffer	8,19E-171	2,32E-32	5,63E-179	1,10E-181	3,12E-163
565 m buffer & built fraction	3,48E-132	2,76E-184	0,999439	7,16E-46	1,89E-181
565 m buffer & building height	2,09E-191	1,82E-188	4,15E-187	1,39E-189	2,13E-181
built fraction & building height	1,86E-190	5,79E-187	4,84E-193	7,00E-191	2,69E-185